STUDY OF SOLAR ABSORPTION

COOLING SYSTEMS

AUTHOR : PRADEEP KUMAR

THESIS SUBMITTED FOR THE DEGREE
OF DOCTOR OF PHILOSOPHY

DEPARTMENT OF CHEMICAL & GAS ENGINEERING
UNIVERSITY OF SALFORD
ENGLAND (U.K.)

1984

T O

MY PARENTS

ABSTRACT

Solar energy is a vast and inexhaustible source of energy. However, solar radiation approaching the earth's surface is variable. Efficient use of this radiation is complicated by this variable nature. The work described in this thesis deals mainly with the use of solar energy for absorption cooling systems.

Basic cooling and heat pump systems are described in brief. A literature survey of the absorption cooling systems is given and the scope for research work in this area is discussed.

The effect of variations of the parameters in the closed cycle and open cycle absorption cooling systems has been analysed in order to optimise the performance of the systems. Experimental verification of the above analysis for a closed cycle system using water-lithium bromide as a working pair is presented along with some typical characteristic performance data for certain conditions. These conditions are lower generator temperatures, which lead to more efficient solar energy collection systems and higher absorber/condenser temperatures providing the feasibility of air cooling. Computer programs for the above analyses are given.

A closed cycle absorption system using water-lithium bromide has also been theoretically analysed for simultaneous cooling and heating. A computer program developed for the above analysis is presented.

A modification in the practical cycle to achieve high temperature lifts for simultaneous heating and cooling appears to be

very attractive. An expression for coefficient of performance of an ideal absorption cycle system, when condensing temperature is not equal to absorber temperature, has been derived. Experimental verification of the above concept in a single stage cycle is also reported.

An experimental unit to generate design data for a solar generator of an open cycle absorption cooling system has been designed and installed. This unit is described in detail. Solar simulation has been done in two ways. The first way is by a radiation source consisting of CSI lamps and the second way is by providing an equivalent electrical heat flux. The relationship between the two is discussed. Based on the experimental data obtained, correlations in conventional forms for heat and mass transfer operations in the generator are presented.

A mathematical model of the solar generator incorporating the above correlations is discussed. A computer program for the prediction of the performance of the generator is presented. The experimental results are compared with the predicted results and optimum conditions for various situations are discussed.

ACKNOWLEDGEMENT

I wish to express my sincere gratitude to Professor F A Holland, Chairman of the Department of Chemical and Gas Engineering, University of Salford, U.K., for his valuable guidance and continued encouragement throughout the work.

I am thankful to Mr F A Watson, Senior Lecturer (retired) for his guidance during the first year of the present work and to Dr S Devotta, Research Fellow, for some very useful discussions and suggestions.

My thanks also go to Mr P J Diggory, Chief Scientific Officer, and the staff of the departmental workshop for their assistance in the construction and modification of the experimental systems.

During the later part of the present work, the help and useful discussions forthcoming from Mr M G Sane, Scientist, National Chemical Laboratory, Pune, India, are much appreciated.

My special thanks are due to the Government of India for nominating me for the Commonwealth Scholarship and to the Government of the United Kingdom for financial support.

I extend my thanks to the members of the Heat Pump Research Group whose comments and views have been most helpful and to Mrs B Price for her diligent typing of the thesis.

NOMENCLATURE

A	area,	m^2
c	current,	amp
(COP)	coefficient of performance,	dimensionless
(COP)'	coefficient of performance without economiser heat exchanger,	dimensionless
C_p	heat capacity,	kJ kg^{-1} K^{-1}
D	diffusivity,	m^2 h^{-1}
e	voltage,	volt
E	thermodynamic effectiveness,	dimensionless
f	fanning friction factor,	dimensionless
(FR)	flow ratio,	dimensionless
g	acceleration due to gravity,	m s^{-2}
h_C	convective heat transfer coefficient,	kW m^{-2} K^{-1}
h_{COND}	conductive heat transfer coefficient,	kW m^{-2} K^{-1}
h_R	radiative heat transfer coefficient,	kW m^{-2} K^{-1}
h_y	local heat transfer coefficient	kW m^{-2} K^{-1}

		v
H	enthalpy per unit weight of solution,	kW kg^{-1}
I	total solar insolation,	kW m^{-2}
k	thermal conductivity,	kW m^{-1} K^{-1}
K_p	mass transfer coefficient,	kg m^{-2} h^{-1} mbar^{-1}
L	length of generator,	m
m	mass flow rate,	kg h^{-1} m^{-2}
M	mass flow rate per unit width,	kg h^{-1} m^{-1}
p	partial pressure or vapour pressure,	mbar
P	pressure,	mbar
q	heat flux,	kW m^{-2}
Q	heat load,	kW
Q´	heat load without economiser heat exchanger,	kW
R	reflux ratio,	dimensionless
RH	relative humidity,	per cent
T	temperature,	^{o}C or K
TU	air temperature	^{o}C
U	overall heat transfer coefficient,	kW m^{-2} K^{-1}
v	air velocity,	m s^{-1}

V	specific volume,	$m^3\ kg^{-1}$
w	width,	m
W	mechanical energy,	kW
X	absorbent concentration,	wt fraction
y	length,	m

Dimensionless groups

j	j-factor for mass or heat transfer
N_{NU}	Nusselt number
N_{PR}	Prandtl number
N_{RE}	Reynolds number
N_{SC}	Schmidt number
N_{SH}	Sherwood number
N_{ST}	Stanton number

Greek leters

α	absorptance of the generator surface and liquid film,	dimensionless
ρ	density,	$kg\ m^{-3}$
λ	latent heat of vaporisation,	$kW\ h\ kg^{-1}$
ε	emissivity,	dimensionless
ν	kinematic viscosity,	$m^2\ h^{-1}$

σ	Stefan-Boltzman constant,	$kW\ m^{-2}\ K^{-4}$
Δ	difference,	-
η	efficiency or effectiveness,	dimensionless
μ	viscosity,	$kg\ m^{-1}\ h^{-1}$

Subscripts

A	absorbent
AB	absorber
ACL	actual cooling
AH	actual heating
AM	ambient
AOV	actual overall
AV	average
C	Carnot
CCL	Carnot cooling
CH	Carnot heating
CL	cooling
CO	condenser
COND	conduction
CONV	convection
COV	Carnot overall
CS	cooling source
D	mass transfer or dry bulb
ES	evaporator source
EX	economiser heat exchanger
EV	evaporator or evaporation
F	final
GE	generator

GS	generator source
H	heating or heat transfer
I	initial or inlet
INS	insulation
MH	modified heating
OV	overall
P	pump
R	radiation
S	solution
SC	solar collector
SEN	sensible
W	water or wet bulb
Y	local
1-14	state points in the figures

LIST OF TABLES

LIST OF FIGURES

CONTENTS

APPENDICES

CHAPTER 1

INTRODUCTION

INTRODUCTION

1.1 ENERGY

The fossil fuel supplies of the world are limited and the fuel reserves are getting depleted. It is difficult to predict exact quantities of recoverable reserves of fossil fuels in the world. Primary energy consumption worldwide has increased by 23 per cent from 2.4 Gigatons of coal equivalent (Gtce) (85.2 EJ) in 1972 to 9.1 Gtce (323.1 EJ) in 1982, but the share of the developing countries, in the total consumption for the same period has increased from 8 to 10 per cent of the total consumption (Ref. 24). In Western Europe since 1980, there is a declining trend in energy consumption. However, the rate of decline in energy consumption has reduced. This is largely due to some slight recovery in economic activity and falling energy costs (Fells 1984).

It is not envisaged that the type of energy sources, to meet the anticipated energy demand, will alter greatly by the year 2000. Modern technologies, to extract energy from sources such as solar or wind/wave energy, are not expected to give a significant contribution in this century. However, research in these areas is required to reduce the dependence on fossil fuels.

Various estimates have been made of the time available before the reserves of fossil fuels are depleted. These estimates are all based on assumptions as to how industrial and domestic energy trends will vary with time and are all doubtful. What is certain is that, at whatever level the industrial and domestic energy demands might be, changes in the method of using that energy have been re-examined. It is possible to

increase the efficiencies of conversion processes e.g., the efficiencies of power producing equipment.

A better alternative is to reduce the amount of energy wasted. The conversion of energy should include reuse wherever possible. One way is to reuse the thermal waste heat streams from industrial sources, such as power stations, rather than to discharge them as thermal pollutant to air and water. This means that the temperatures of the waste streams should be high enough to be useful. In some cases a heat pump may be used to raise the temperature of low grade heat energy to a more useful level by using a relatively small amount of high grade energy.

1.2 ENERGY SOURCES

It is clear that at some time alternative energy sources will replace the fossil fuels. All such sources depend upon either nuclear energy generation by fission or fusion, or on the sun.

Nuclear energy generation by fission has a number of disadvantages. In brief, the main disadvantages are the problem of safe waste disposal and the danger of serious accidents. Nuclear energy generation by fusion is still at a very elementary state. Fusion has not yet been maintained in the laboratory for significant times. Even if sustained fusion is ever attained, its economics as a main energy supply is in doubt, partly because of the energy needed to extract sufficient deuterium from the sea.

Some of the various alternative energy sources are considered briefly below.

1.2.1 Wind and wave power

The heating and cooling of the various parts of the earth's surface by the sun induces wind with varying speeds in different parts of the world. The wind speed at a given location is also a function of the topology of the area.

Wind power has been used from prehistoric times. Until relatively recently, the assemblies of equipment used for extracting power from the wind were known as windmills. Additional names like wind-turbine generators, aerogenerators etc. are being used nowadays. Small windmills of several kilowatts capacity for farm and rural power needs are in use. There are some well proved designs, which are commercially available. However, considerable research work is still required in this area.

Wave power is variable from one part of the ocean to another. The amount of wave power which could be harnessed for use depends on the coastline of a particular country. For example, the U.K. has a coastline of approximately 1500 km. This could be used for the location of a practical wavepower system. The potential for the generation of electrical energy is of the order of 30,000 MW or about 50 per cent of the current installed capacity of the C.E.G.B. (Reay 1977). The experimental work at the University of Edinburgh and other places have demonstrated that there is a great scope to extract energy from tidal waves using a specially contoured rocking device (Salter 1974).

1.2.2 Geothermal energy

Geothermal energy can be utilized in many ways. In some regions wet, or even superheated, steam can be obtained by drilling in suitable areas such as those where geysers occur naturally. In other regions

hot water can be obtained naturally, as from thermal springs, or by pumping water into hot rocks. All these methods are likely to require expensive materials of construction to withstand the corrosive effects of hot solutions of minerals present in the rocks. Hot water and wet steam are often produced under conditions of high geothermal pressure in deeply buried sedimentary rocks. Under these circumstances the hot water can also contain significant quantities of dissolved natural gas which is flashed off at the surface and could be collected for use as a fuel.

1.2.3 Ocean thermal energy gradient

Oceans cover 71 per cent of the earth's surface and receive the majority of the solar energy incident on the earth. In tropical and semitropical oceans, the available temperature difference is sufficient for Ocean Thermal Energy Conversion (OTEC) operations. It is available 24 hours a day. The vast potential for OTEC implementation can be appreciated by noting that electrical power equal to the entire projected U.S. demand in the year 2000 (about 7×10^5 MW) could be obtained by extracting from the ocean, in the $\pm 10^{o}$ latitude band near the equator, an amount of energy equal to only 0.004 per cent of the incident solar energy (Kreider et al 1981).

However, the overall thermal efficiency of an OTEC plant is low. Therefore, large seawater pumps and large heat exchangers are required. Typically, the ideal Carnot cycle efficiency would be about 7.5 per cent with a typical available temperature difference of 22K and hot water temperature of 295K. In an actual power plant, after deducting for temperature differences in heat exchangers and pumping etc., the efficiency would be less than 3 per cent (Kreider et al 1981).

1.2.4 Solar energy

Solar energy is a nonpolluting inexhaustible energy source. The surface of the sun is at an effective temperature of about 6000 K. The sun is effectively a continuous fusion reactor. Its constituents are gases retained by gravitational forces. The energy is produced in the interior of the sun, at estimated temperatures of 8×10^6 to 40×10^6 K.

The total energy intensity of extraterrestrial solar radiation, measured just outside the earth's atmosphere and integrated over the entire solar spectrum, is called the solar constant. The value of this solar constant has been estimated to be 1.37 kW m^{-2} (Kreider et al 1981). Solar radiation covers a wide band of wavelengths and the peak intensity occurs in the interval of visible light at a wavelength of about 0.6 μm. Types of solar radiation and their approximate wavelengths are given in the following table (Kreider et al 1981).

radiation type		wavelength interval (μm)
Gamma rays		10^{-4}
X-rays		5×10^{-2} to 5×10^{-6}
Ultraviolet		0.005 to 0.35
Visible light		0.35 to 0.75
Infrared		0.75 to 300
Radio waves	short	1×10^2 to 1×10^8
	long	1×10^8

Solar radiation is considerably altered in its passage through the earth's atmosphere by absorption and scattering. The factors which affect the availability of solar energy are given below ;

1) geographic location,

2) time of the day,

3) time of the year,

and 4) atmospheric conditions.

Solar energy, in the form of electromagnetic radiation, is transmitted through space to earth. This energy is relatively dilute when it reaches the earth. Therefore, the size of a system used to convert it to heat must be relatively large.

The devices used to convert the solar radiation to heat are called solar energy collectors. They usually consist of surfaces that absorb radiation and convert the incident flux to heat. This raises the temperature of the absorbing material. A part of this energy is then removed from the absorbing surface by heat transfer to a fluid. The solar thermal energy collectors could be classified into the following categories:

1) non-concentrating solar collectors

2) concentrating solar collectors

and 3) non-convecting solar ponds.

The non-concentrating solar collectors are usually either flat plate collectors or tubular solar energy collectors. A basic flat plate collector is shown in Figure 1.1. It consists of one or more transparent flat front plates and an absorbing rear plate. The front plates provide insulating zones bounded by these plates. Heat is removed from the rear plate by a fluid such as water or air. Thermal insulation is usually used behind the absorber plate to prevent heat losses. The front plates or covers are generally glass which is transparent to incoming solar radiation and relatively opaque to the infrared reradiation from

from the absorber plate. The glass covers also act as convection shields to reduce heat losses. The absorber plate which incorporates water channels can be metal or other suitable materials such as certain plastics. The space above or below the absorber plate serves as the conduit for air systems. The surface finish of the absorber plate may be a matt black paint with an appropriate primer. For round the year operation of a flat plate solar collector, an optimum inclination to the horizontal lies in the range from about (latitude) to (latitude + 15^{o}). However, the variation of the collector performance for the whole range is marginal (Lof et al 1973). A variety of well-proved designs of flat plate collectors are commercially available. The collector efficiencies are a function of the difference between the temperature of the absorber plate and the ambient temperature. It is desirable to keep the absorber plate temperature low to obtain high efficiency. However, this temperature depends on a particular application. Flat plate collectors can generally be used up to a temperature of about $100^{o}C$. However, the collector efficiency, at about $100^{o}C$, could vary in the range of about 10 per cent to 40 per cent depending upon the number of glass plates, type of surface finish, ambient temperature and the incident flux etc. (Meinel et al 1977).

A basic tubular collector is also shown in Figure 1.1. In a tubular collector, convection losses are completely eliminated by surrounding the absorber surface with a vacuum of the order of 10^{-4} mm Hg. This results in improving the performance significantly compared to a flat platecollector. These tubular collectors can also be used to achieve a small level of concentration by forming a mirror from part of the internal concave surface of the glass tube. Various designs of tubular solar energy collectors are available. Some of these can be used in the range

of 200°C to 600°C. The efficiency of extraction of absorbed energy could vary in the range of 10 per cent to 90 per cent depending upon various factors such as operating temperature, design of the collector, quality of absorber surface, etc. (Meinel et al 1977).

Generally, concentration of solar radiation is done when higher temperatures than those which can be obtained by a flat plate collector are desired. The concentrating solar collectors or concentrators are of various types. These types utilize a wide variety of means for increasing the flux of radiation on receivers. They can be classified as lenses or reflectors by the type of mounting and orienting systems, by the concentration of radiation they are able to accomplish, by material of construction or by application.

The focussing systems can use either cylindrical reflectors or refractors, focussing radiation more or less sharply on a line, or they can be circular reflectors or refractors which form radiation on a point receiver. Concentration ratios for the latter can be much higher than their cylindrical counterparts. A cylindrical parabolic collector is shown in Figure 1.2. The cylindrical systems usually require orientation change seasonally. However, circular reflectors or refractors usually require continuous tracking as shown in Figure 1.2. These types of collectors could be operated in the range of 200°C to 2000°C depending upon various factors such as one axis or two axis tracking, design of the collector etc. Another interesting type of collector is the compound parabolic collector which may or may not require any orientation change for round the year operation. These can be operated in the range of 100°C to 180°C (Kreider et al 1981). In general, the efficiency of a concentrating collector is higher than a flat plate collector. Peak noon efficiency of a concentrating collector

could range from about 40 per cent to 65 per cent depending upon the operating temperature, the type of collector etc. (Kreider et al 1981).

A pond, lake, or ocean, is a potential horizontal collector of large area. Therefore, several attempts have been made in the past to use black-bottomed ponds as solar collectors. Evaporation, convection and radiation from an uncovered pond results in surface temperatures close to ambient. Attempts have been made to reduce the evaporative loss by the use of an oil layer or monomolecular layer. This was not successful because of the wind which removed the layer. Covering a pond with a transparent window leads to the problems of limited size, removal of dirt, etc. The stability of a solar pond warmed by solar radiation could be maintained by means of a sufficiently steep salt concentration gradient. This concept of a non-convecting pond has been found to be particularly attractive. Elevated temperatures at the bottom are feasible because water acts as its own insulator. The solar pond allows thermal energy collection with negligible transport losses. There is sufficient built-in storage to smooth out diurnal and weekly fluctuations of output. Operating temperatures of about $90^{o}C$ can usually be obtained at a depth of about 1.5 m in a solar pond (Meinel et al 1977).

Generally, the amount of source energy consumed by an industrial system is easily controlled to produce a desired effect. Using traditional energy sources such as coal, oil, gas or electricity, such control is relatively simply achieved. Solar energy is a variable source of energy and is consequently more difficult to control. This leads to another important aspect of solar energy applications, i.e. energy storage. Storage is essential to any system that depends

entirely on solar energy or that needs such energy at specific times. It is required to adjust mismatches between the load and an intermittant or variable energy source. The operation of a system can also be improved by a small amount of buffer storage for transient smoothing. The storage can not only shift the period of energy delivery to the period of greater demand but can also extend the period of solar energy utilization. Such control is only possible if the solar energy collecting system is oversized. Unfortunately, the overdesign of the solar energy systems is impractical because of the high cost.

1.3 UTILIZATION OF SOLAR ENERGY

In tropical countries such as India, solar energy is reliably available for long periods each day for much of the year, so that direct solar energy collection could be an attractive and cheap source of thermal energy.

The direct use of solar energy has many advantages over the conventional use of fossil fuels. It does not produce by-products which can harm the environment by direct pollution or by the greenhouse effect which may result from an excess of carbon dioxide in the atmosphere. The latter is made more likely by deforestation caused by cutting of trees or by damage caused to trees by sulphur dioxide, etc., formed by combustion of oil or coal.

There is a great scope for the exploitation of solar energy in countries such as India where it is most widely available. It could be utilized for various purposes. One of the important uses could be to produce cooling for air-conditioning and other purposes. An indoor

temperature of 24°C with a wet bulb temperature of 18°C, is considered a comfortable optimum for both commercial and residential cooling applications (Kreider et al 1981). It has been found that controlled thermal environments can greatly influence human performance (Ref. 5). There are many requirements even in industry apart from human considerations.

There exists a dynamic relationship between any cooling system, the building it cools, the users of the building and the ambient conditions to which the building is exposed. There are additional variables of timing and temperature when the cooling system is energised by solar energy. The efficiency of a cooling system itself depends on the cooling load of the building at the desired temperature and humidity conditions, the temperature at which heat is received by the system, the temperature at which heat is supplied to energize the system and the temperature level at which the heat is rejected. All these factors are time dependent and can be out of phase. An understanding of these factors with a cooling system can result in the improvement of the efficiency of the system.

The performance of a cooling system is critically influenced by the temperature at which the spent heat and the heat taken from the conditioned space is rejected. In most installations this heat is rejected through a cooling tower to ambient air. The water temperature in the cooling tower approaches the ambient wet bulb temperature to within a few degrees when it is operated at the usual design conditions. As the ambient wet bulb temperature drops, the approach increases for the same conditions of the cooling system. However, at any wet bulb temperature the approach is reduced by a reduction in the temperature of the circulating water due to a decrease in the cooling load.

The total energy required for a refrigeration unit to maintain the desired temperature and humidity conditions in a given building is usually reduced by modulation of cooling capacity. In modulation, the temperature at which the refrigerant evaporates is raised at reduced loads, and the temperature of the heat rejected as in condensers and absorbers is lowered. Therefore, the efficiency of the cycle is increased because the cycle becomes more compact thermodynamically. However, the hours of operation of auxiliary equipment such as pumps and fans are increased by modulation. For example, when operating in a modulated mode at half capacity the hours of operation for the same heat removal will be approximately doubled. It is therefore, generally necessary to reduce the speed of auxiliaries to avoid the energy of auxiliaries becoming large enough to offset significant savings in the operation of the main refrigeration unit.

The most effecient collector arrays are associated with cooling systems which can make use of thermal energy at the lowest temperatures. Only the direct beam component of solar energy is collected by concentrating collectors whereas a flat plate collector uses the diffuse component as well. This must also be considered before designing collector arrays for a particular geographical location. In the case of the cooling of buildings, the total energy requirement could be minimised by the selection of equipment to operate efficiently over the entire range of conditions to which the system is exposed. The part load capabilities of the cooling unit, and the use of the lowest possible energizing temperature should be utilized in order to increase the amount of useful energy received from any given collector array.

The cooling load is defined as the rate of heat removal from the space to maintain the air in the space at the designed temperature and humidity conditions. The heat gain in the space could be from solar radiation, latent heat additions which add water vapour to air and from sensible heat additions. There is always a time lag with the radiative part of the heat gains. The radiation raises the temperature of walls, floor, and furniture on which it falls. This heat is then transferred to air in the space.

The above discussions indicate that the variables affecting cooling load calculations are intricately related. Therefore, it is important to determine the entire range of loads and the length of time they exist. Accurate cooling load and heat gain calculations could be done by methods given in ASHRAE handbook of fundamentals (Ref. 5).

Unfortunately, cooling is expensive to produce in energy terms. A typical refrigeration or air-conditioning system uses 0.25-0.50 kW of electrical energy to produce 1 kW of cooling (Ward 1979). In many developing countries the necessary amount of energy which conventional systems require in the form of electricity, is not available. Consequently, either the cooling has to be foregone or some alternative electricity user has to be deprived of supply. There is a great need to utilize alternative energy sources like solar energy.

Cooling is the basis of the large and well developed refrigeration and air conditioning industries. Generally, refrigeration systems use electricity driven compressors. Some designs use gas or diesel engines as the power source but only a few use absorption systems in which the compressor is replaced by a heat driven unit. It is worthy

of note that in terms of the primary heat source, considering the most modern thermal power plants, electricity generation is only about 35 per cent efficient (Ref. 26). The conventional unit, therefore, requires about 0.7-1.4 kW of primary energy to produce 1 kW of cooling, based on the most modern power plants. This value should be compared with the 1.2-2.0 kW of heat energy required to produce 1 kW of cooling in a typical absorption cooling unit. Absorption cooling systems and vapour compression systems were compared by Gosling (Gosling 1980). The following table is adapted from this reference.

POWER REQUIREMENTS PER UNIT REFRIGERATION EFFECT

	absorption refrigeration	centrifugal compressor
condenser water pump	0.012	0.007
cooling tower fan	0.041	0.021
solutions and refrigerant pumps	0.003	-
compressor	-	0.222
sub total, electrical power	0.056	0.250
steam or hot water	1.430	-
total power	1.486	0.250
total heat rejected	2.486	1.250

If everything including the generation and transmission losses etc. is taken into account, the vapour compression system has little thermodynamic superiority over the absorption system. However, there are certain disadvantages of the absorption system. The heat rejection rate from the absorption system is considerably higher than that from a compressor driven system. Therefore, a larger cooling tower would be required for an equivalent absorption system. The capital cost of the absorption system would be higher because of the increased number of items of equipment.

This will lead to a higher payback period. However, payback period should not be the only criterion. A system with higher payback period could still be advantageous if the operating cost is low. It obviously requires a detailed economic analysis for a particular situation. Kreider et al (Kreider et al 1981) have given an excellent account of guidelines for economic analysis of solar energy assisted systems. An absorption system driven with solar energy has the further disadvantage of either requiring a very large energy storage system or of having to operate the system intermittently. All these considerations indicate the scope of improvement and work required in this area.

If an absorption cooling unit could be operated efficiently by solar energy then cooling might become cheaply and readily available in those parts of the world where it is most needed.

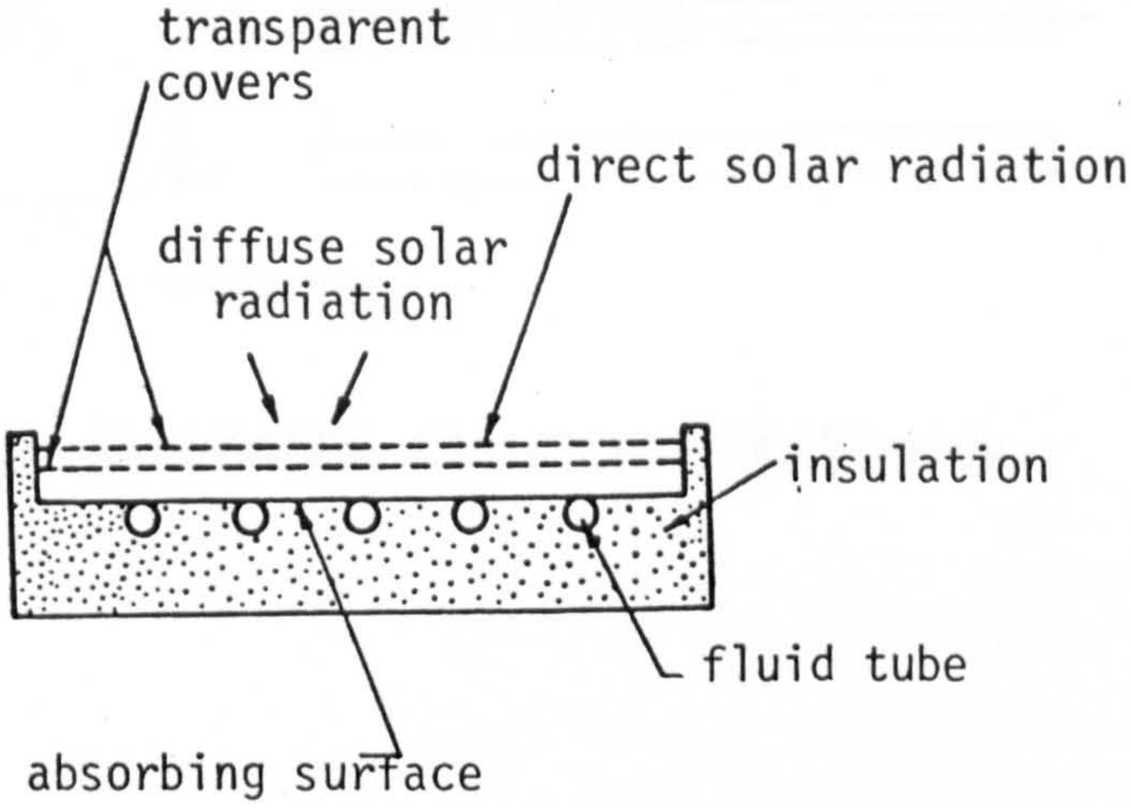

(A) BASIC FLAT PLATE COLLECTOR

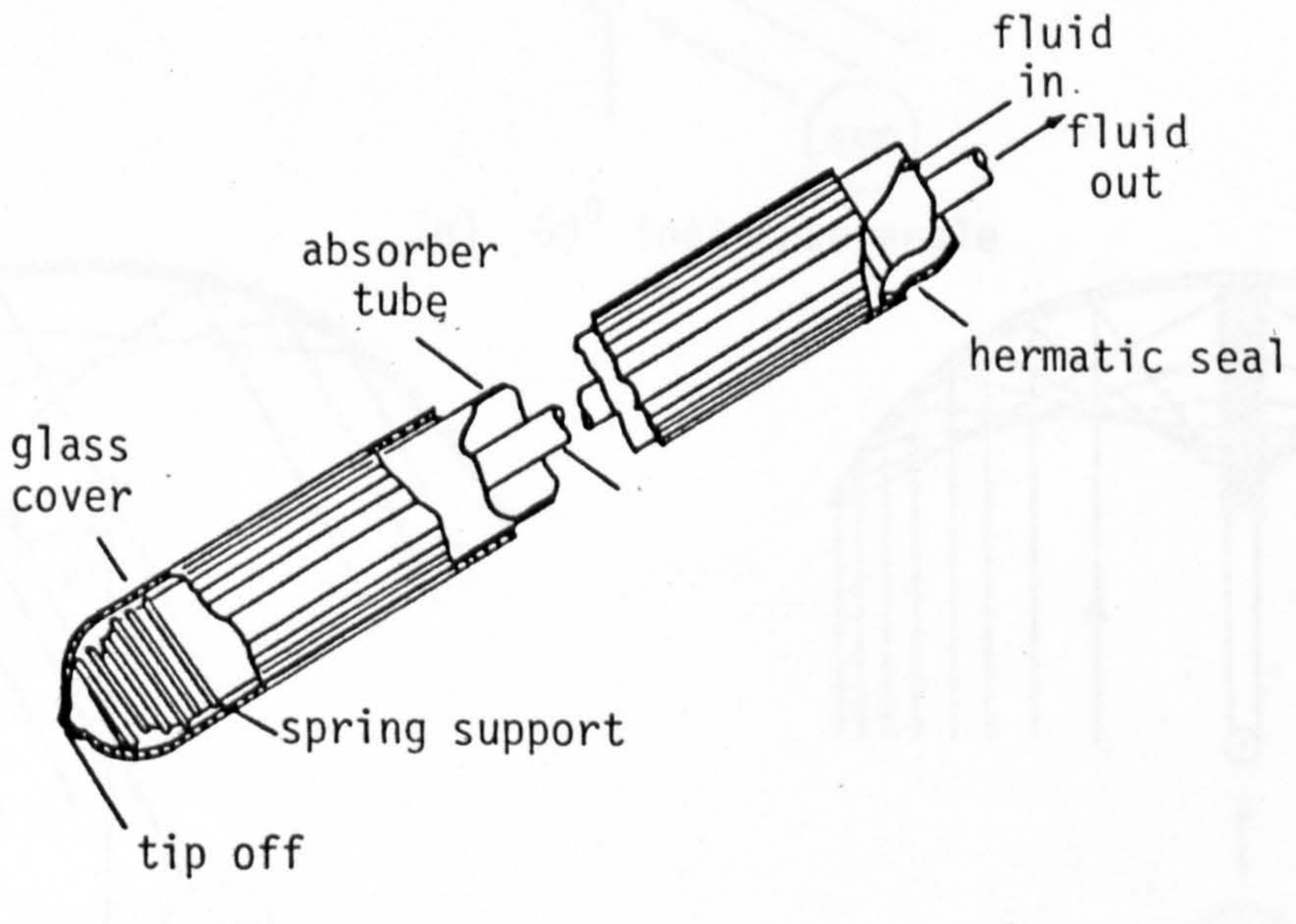

(B) TUBULAR SOLAR COLLECTOR

FIGURE 1.1 NON-CONCENTRATING COLLECTORS

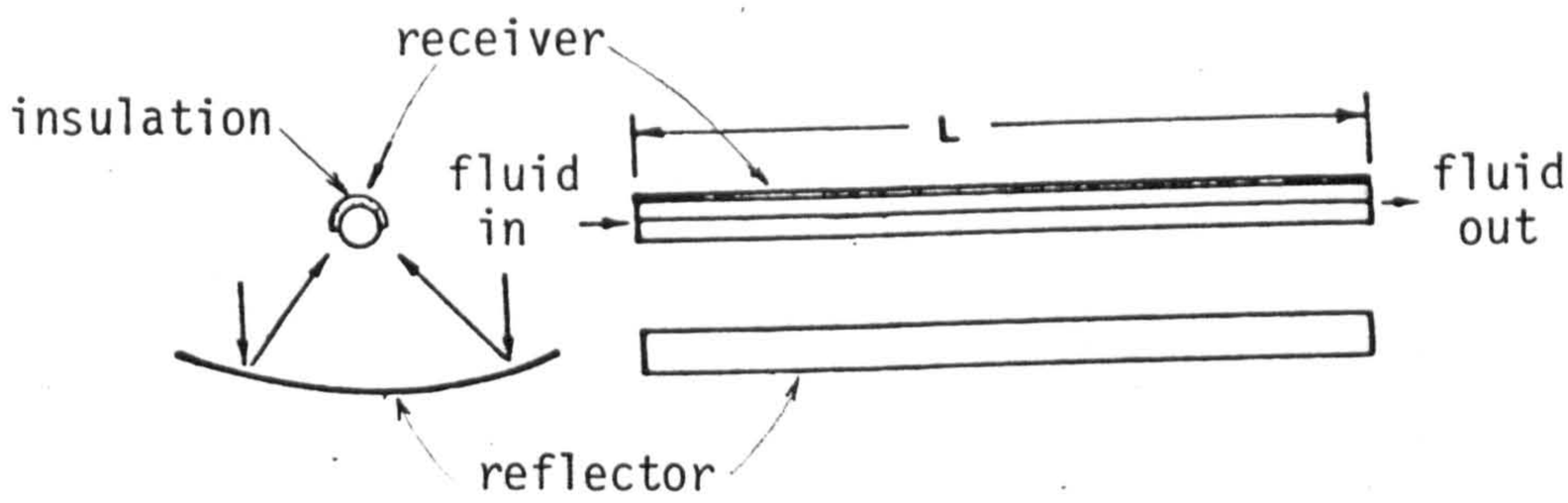

(A) CYLINDRICAL PARABOLIC CONCENTRATOR

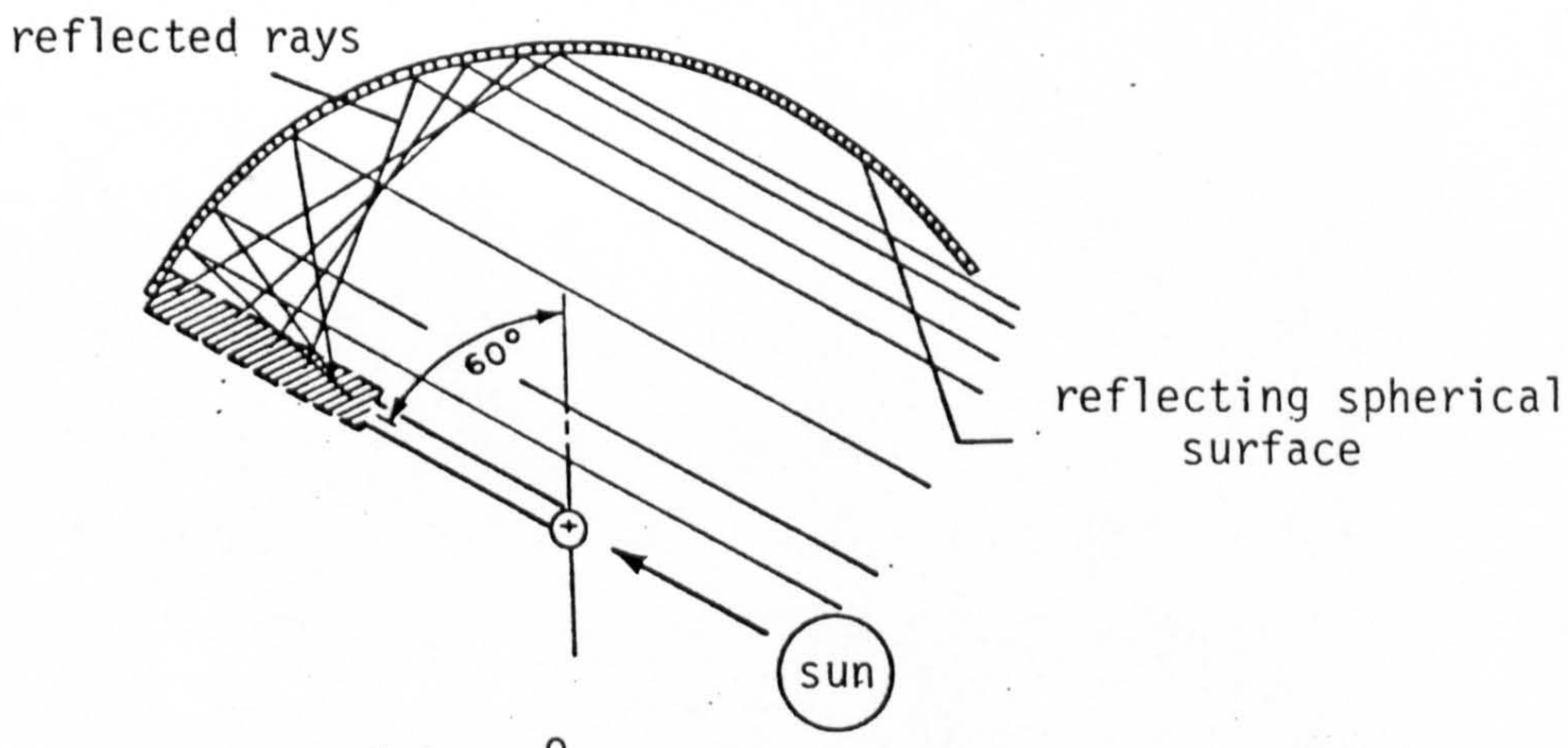

(a) 60^{o} incidence angle

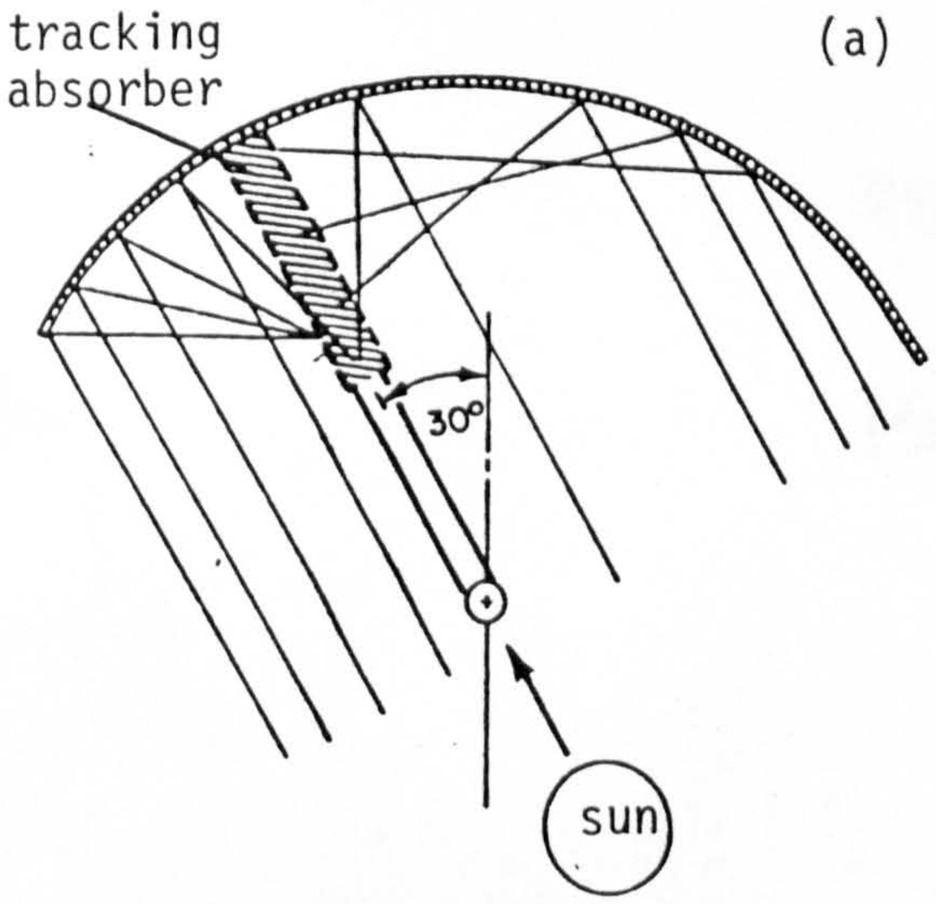

(b) 30^{o} incidence angle

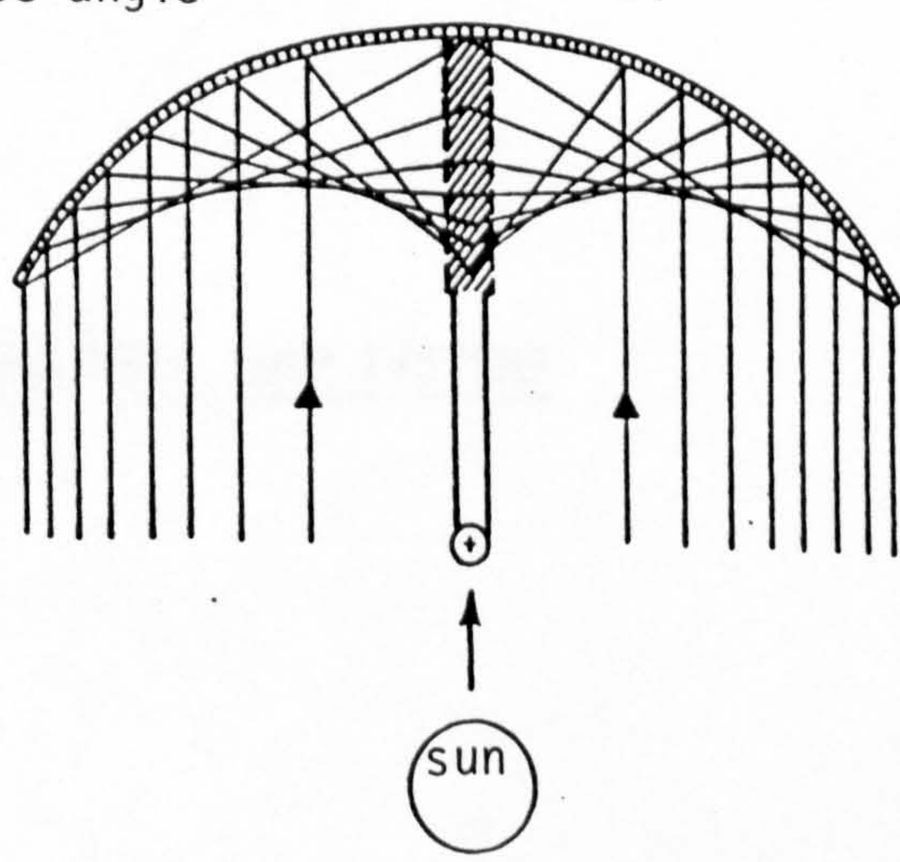

(c) normal incidence

(B) SPHERICAL STATIONARY REFLECTOR/TRACKING ABSORBER CONCENTRATOR

FIGURE 1.2 CONCENTRATING COLLECTORS

CHAPTER 2

BASIC COOLING AND HEAT PUMP SYSTEMS

BASIC COOLING AND HEAT PUMP SYSTEMS

2.1 VAPOUR COMPRESSION CYCLE

A schematic representation of a typical vapour compression cycle is shown in Figure 2.1. A working fluid, usually called refrigerant, is vaporised in the evaporator thereby extracting heat from the solid, liquid, or gas to be cooled. Refrigerant vapour from the evaporator is compressed to a suitable higher pressure which permits the latent heat to be removed in the condenser. Condensation must take place at a temperature higher than the temperature of available water or air used to remove the heat. The condensed refrigerant is then expanded to the evaporator pressure through an expansion valve or other restriction. The liquid is partially vaporised in doing so. The system is considered to be a cooling system when removal of heat Q_{EV} at the evaporator temperature T_{EV} is the main purpose. The system is considered to be a heat pump if the supply of heat Q_{CO} at the condenser temperature T_{CO} is the main purpose. Coefficients of performance for this system can be defined by Equations (2.1) and (2.2) respectively.

$$\text{For cooling systems, } (COP)_{CL} = Q_{EV}/W \qquad (2.1)$$

$$\text{For heat pumps, } (COP)_{H} = Q_{CO}/W \qquad (2.2)$$

where W is the energy absorbed at the shaft of the compressor. Equations (2.1) and (2.2) are related by the temperature difference $(T_{CO} - T_{EV})$. Specifying this gross temperature lift and either T_{EV} or T_{CO} determines the compression ratio and theoretical power input when a given working fluid is used (Holland et al 1982).

2.2 CLOSED CYCLE SYSTEMS

2.2.1 Absorption systems

The principle of the closed cycle absorption system is shown schematically in Figure 2.2. Three components of the conventional vapour compression cycle, condenser, expansion valve and evaporator are retained. The compressor and compressor drive have been replaced by a circuit comprising of an absorber, solution pump, economiser heat exchanger, generator and an expansion valve.

After vaporisation in the evaporator, the refrigerant is absorbed by the absorbent in the absorber. The process of absorption is accompanied by a rejection of heat Q_{AB} to the surroundings. This heat could be removed by cooling water or any other cooling medium. The solution, enriched with refrigerant is called weak solution. The weak solution is transferred by a pump into the generator which operates at a higher pressure. The weak solution is heated to a temperature T_{GE}, by a heat source, e.g., solar energy. The refrigerant vapours are obtained in the generator which are passed on to the condenser. The solution, depleted by refrigerant, is reduced to the pressure of the absorber by passing it through an expansion valve.

The refrigerant vapour from the generator is condensed in a water or air cooled condenser and the liquid refrigerant returns to the evaporator through another expansion valve.

An economiser heat exchanger is usually used to heat the weak solution by cooling the strong solution before weak solution enters the generator. This reduces the amount of heat required in the generator directly.

Like the vapour compression system, an absorption system is considered to be a cooling system when the removal of heat Q_{EV} at the evaporator temperature T_{EV} is the main purpose. The system is considered to be a heat pump if the supply of heat $(Q_{CO} + Q_{AB})$ at a temperature $(T_{CO} = T_{AB})$ is the main purpose. The coefficient of performance for this system can be defined as follows :

For cooling system, $(COP)_{CL} = Q_{EV}/Q_{GE}$ (2.3)

For heat pump, $(COP)_{H} = (Q_{AB} + Q_{CO})/Q_{GE}$ (2.4)

2.2.2 Derivatives of the vapour compression and the absorption heat pumps

Three derivatives of the vapour compression and the absorption heat pumps are the reversed absorption heat pump, the resorption heat pump and the absorption-resorption heat pump. Simplified diagrams of the reversed absorption heat pump, the resorption heat pump and the absorption-resorption heat pump are presented in Figures 2.3a, 2.3b and 2.3c respectively.

In the reversed absorption heat pump system, the direction of flow of liquids through the system and the relative pressure levels in the heat exchangers are reversed compared with the conventional absorption heat pump system. Thus, in the reversed absorption heat pump $T_{AB} > T_{GE} = T_{EV} > T_{CO}$.

The resorption heat pump system consists of a solution circuit which is equivalent to the solution circuit of the reversed absorption heat pump system in the concentrations and pressure and temperature levels.

The refrigerant circuit is completed through a compressor as in the vapour compression heat pump. The compressed vapour is then absorbed by strong absorbent solution in the resorber. Heat is removed from the resorber at a temperature T_{RE}. The absorbent solution from the resorber after absorption passes through an expansion valve into the desorber. It takes in heat to generate refrigerant vapour at a temperature T_{DE}. Strong absorbent solution is pumped into the resorber and the refrigerant vapour passes to the compressor to complete the cycle.

The absorption-resorption heat pump consists of the equivalent of the generator-absorber solution circuit of the conventional absorption heat pump system in conjunction with the equivalent of the resorber-desorber solution circuit of the resorption heat pump system. The abscrption-resorption cycle makes it possible to operate at higher temperatures compared to the conventional absorption cycle.

2.3 INTERMITTENT SYSTEM

An intermittent absorption system alternates between two modes as shown schematically in Figure 2.4. In the cooling mode the refrigerant is allowed to vaporise in the evaporator, thereby extracting heat from the solid, liquid or gas to be cooled. The refrigerant vapour is then absorbed by the absorbent in the absorber. The heat of absorption is removed by water or air. The alternate mode is the regeneration mode. In this mode the evaporator and the condenser and the absorber and the generator exchange functions. Heat is supplied to the generator to produce refrigerant vapour. This vapour is condensed by water or air cooling in the condenser.

The intermittent system cannot be compared directly with the vapour compression system. Although the units alternate in function and the heat is released in the absorber and in the condenser, these are out of phase.

The coefficient of performance of this system can also be defined by Equations (2.3) and (2.4).

2.4 OPEN CYCLE COOLING SYSTEMS

2.4.1 Solar absorption cooling system

An open cycle solar absorption cooling system is shown schematically in Figure 2.5. In the open cycle system, water is always used as refrigerant and water-lithium chloride is the most commonly recommended absorbent. This system differs from the standard closed cycle absorption system in that the condenser is omitted and the generator is open to the atmosphere. Consequently, makeup water must be supplied to the evaporator.

The generator is the heart of the system. It concentrates the weak solution from the absorber to the strong solution for reusing the solution in the absorption cycle system. A thin film of solution flows over a flat surface of a shallow tray generator, painted matt-black for maximum absorption of the incident solar radiation. Interception of solar radiation is improved by tilting the surface to a suitable angle. The weak solution is pumped to a distributor at the top end of the generator. The weak solution is distributed over the generator surface in the form of a thin film. The solar radiation falling on the generator is partially absorbed by the solution,

which is heated up. The water vapour from the solution starts to evaporate as soon as the vapour pressure of water over the solution exceeds the partial pressure of water in the ambient air. Because of evaporation the solution is more concentrated by the time it reaches the bottom end of the generator. The water vapour is lost in the environment. The strong solution from the generator returns to the absorber through an economiser heat exchanger and an expansion valve as shown in Figure 2.5. The coefficient of performance for this system, which can only be used as a cooler, is given by the Equation (2.5).

$$(COP)_{ACL} = Q_{EV}/Q_{GE} \qquad (2.5)$$

2.4.2 Liquid desiccant evaporative cooling system

The liquid desiccant cooling system is shown schematically in Figure 2.6. The air to be cooled is first dehumidified in an absorber. A strong absorbent solution is sprayed over a bundle of tubes. The air enters at the bottom end of the absorber and flows countercurrent to the strong solution. The heat of absorption is removed by water flowing inside the tubes. The dehumidified air is sent to a water spray chamber where it is humidified and cooled. This air is used for air conditioning and similar cooling purposes. The strong solution in the absorber is weakened by absorbing moisture from the air. The weak solution is concentrated in a generator by the application of heat, which may be supplied by solar energy. The regenerated strong solution is then sent back to the absorber.

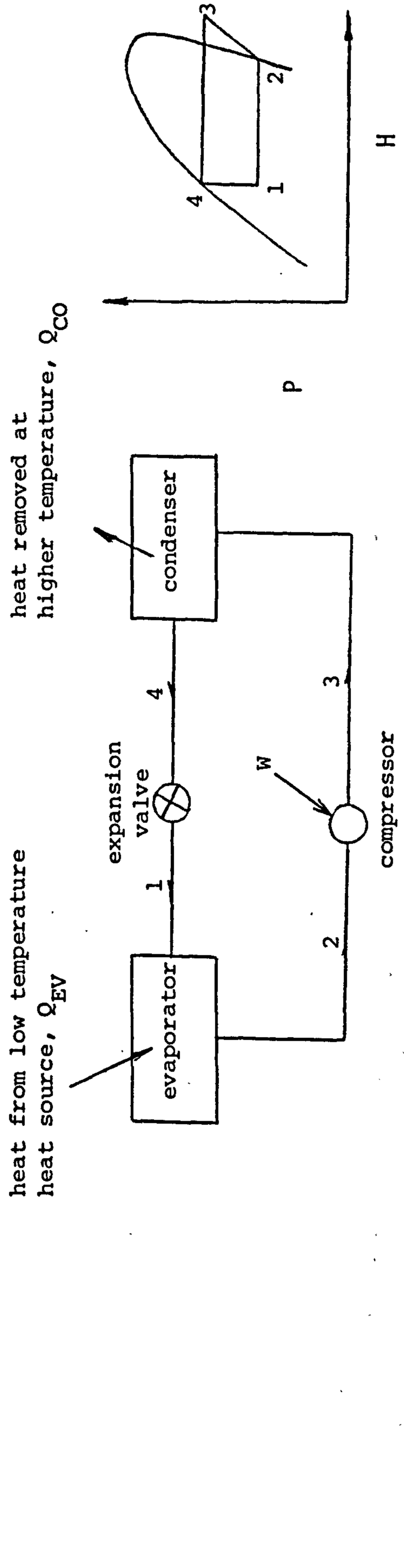

FIGURE 2.1 VAPOUR COMPRESSION CYCLE

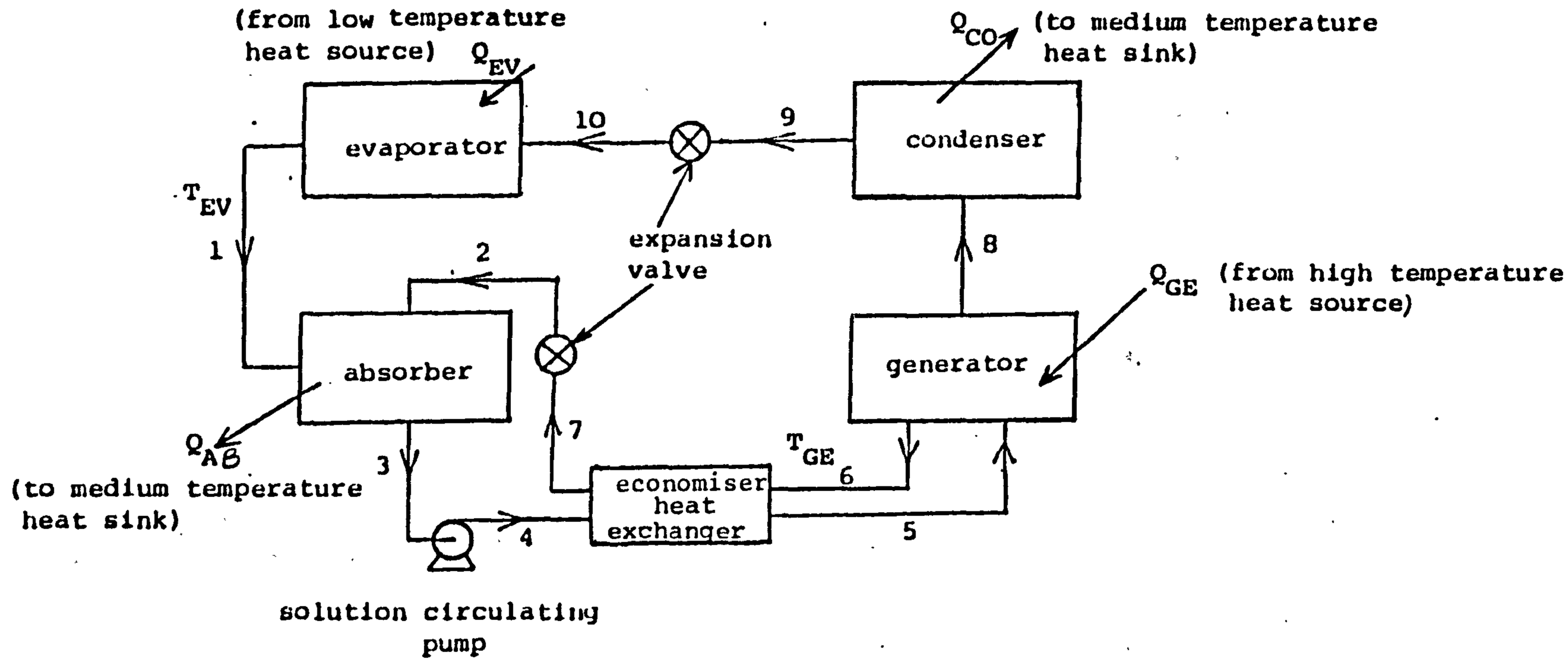

FIGURE 2.2 CLOSED CYCLE ABSORPTION COOLING SYSTEM

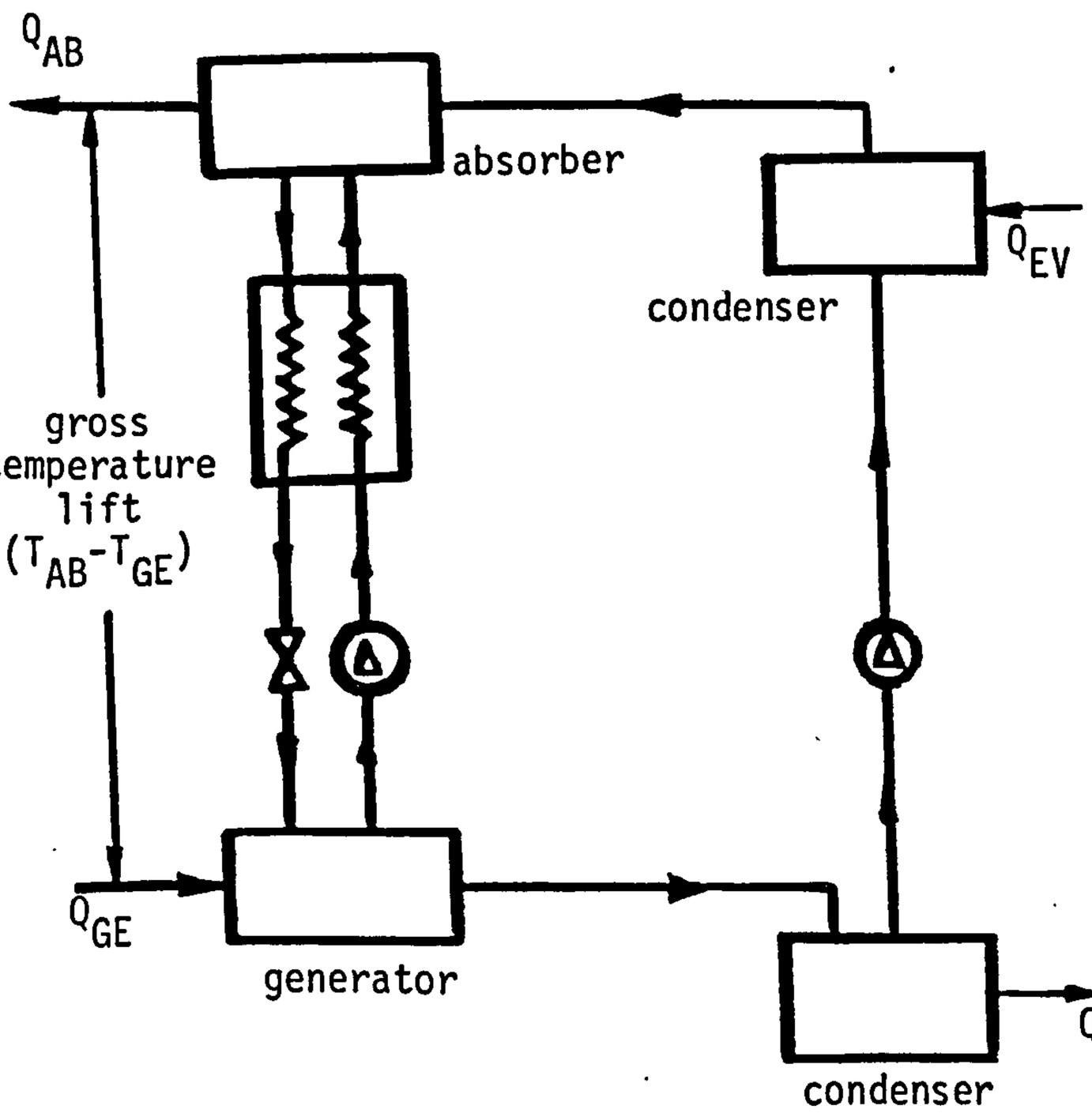

FIGURE 2.3a REVERSED ABSORPTION HEAT PUMP

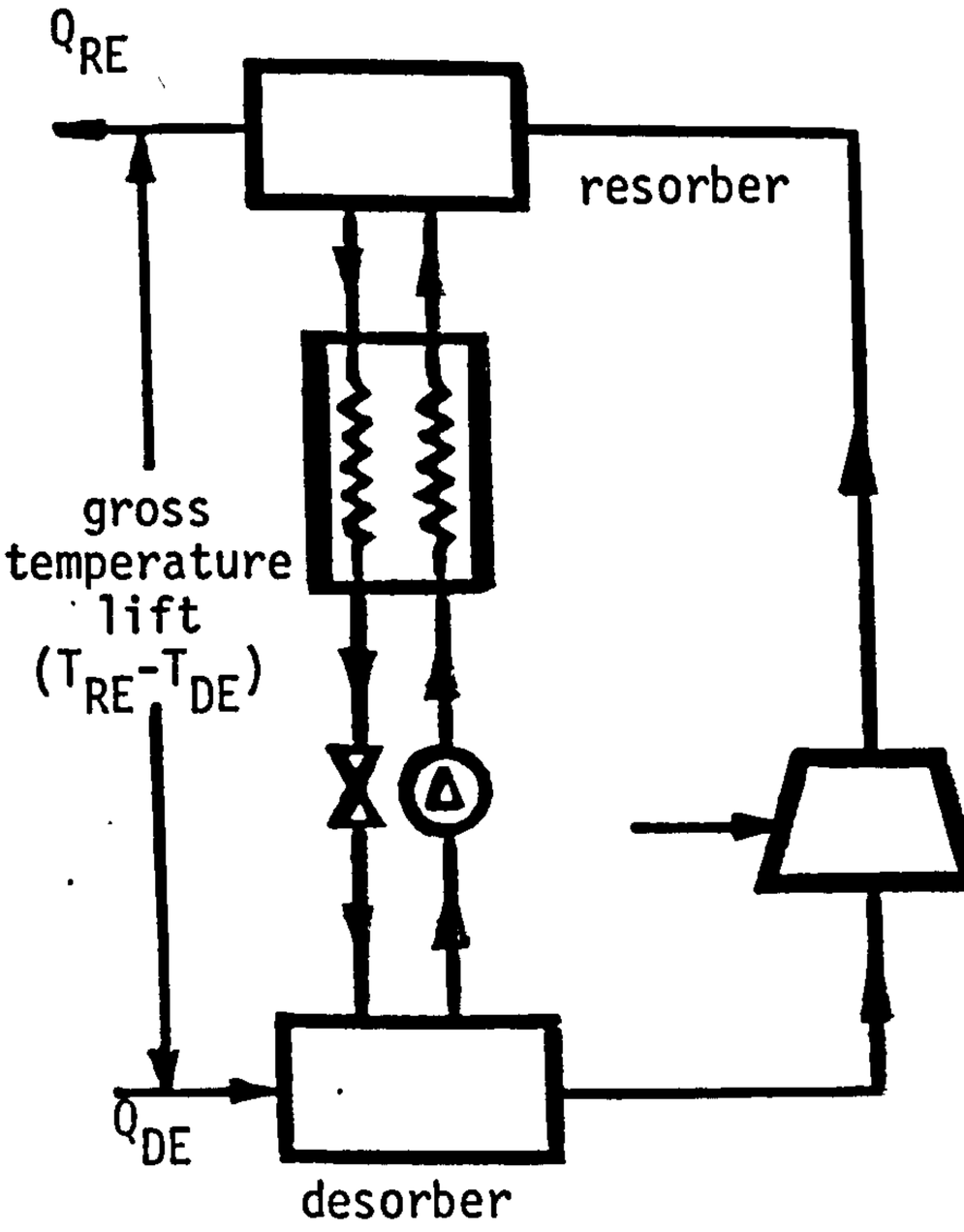

FIGURE 2.3b RESORPTION HEAT PUMP

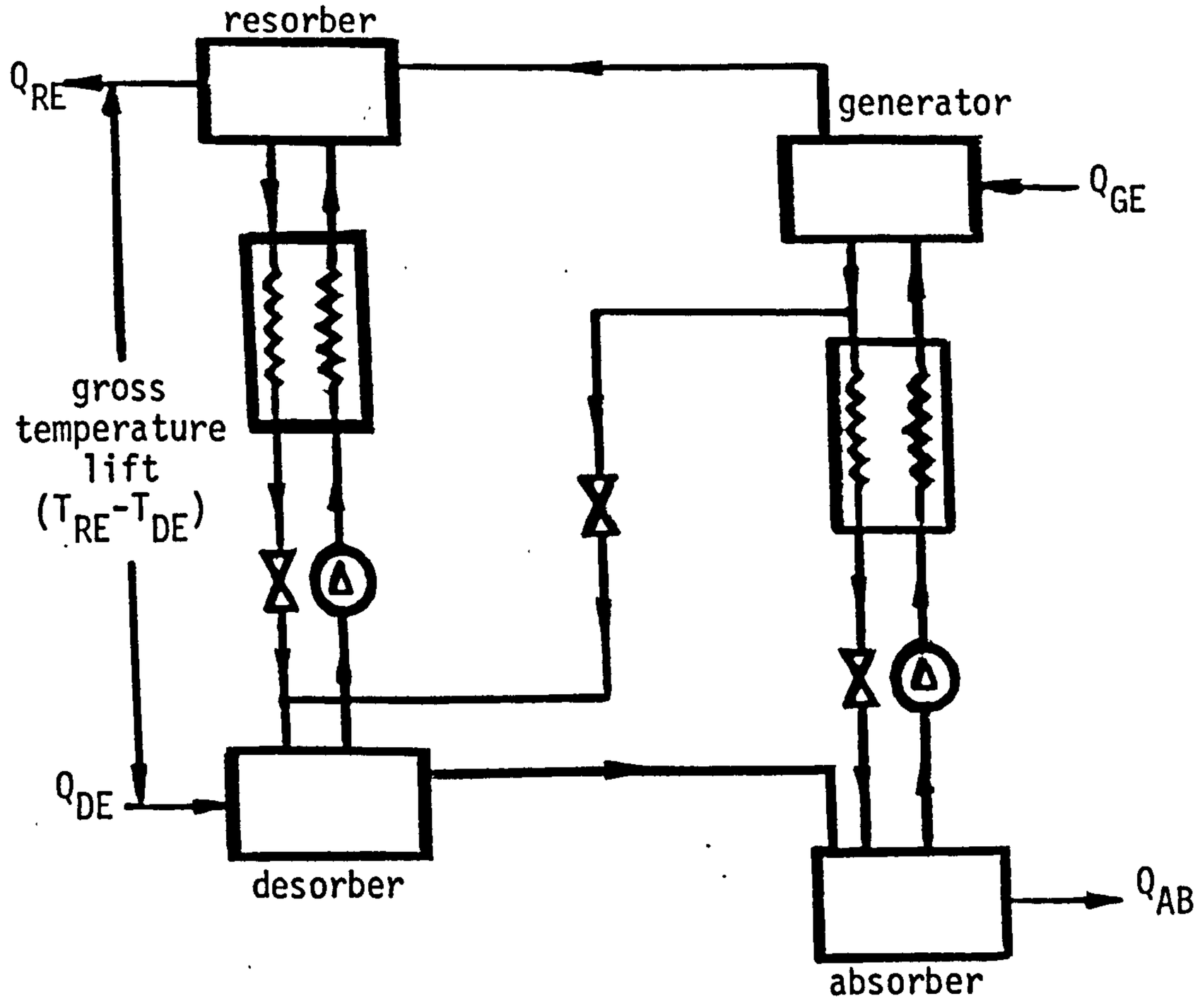

FIGURE 2.3c ABSORPTION-RESORPTION HEAT PUMP

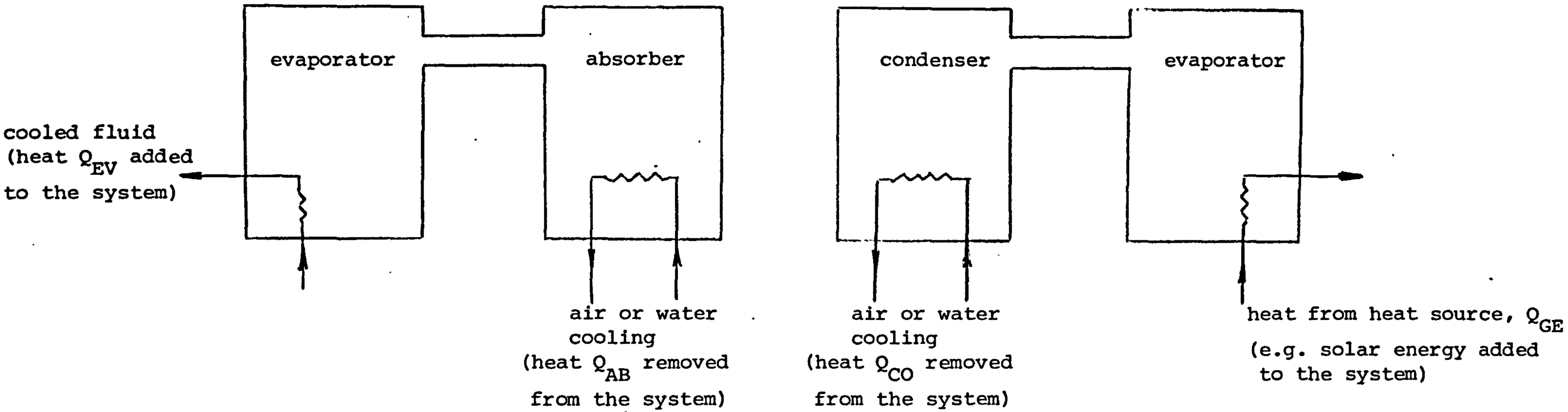

a. Cooling mode

b. Regeneration mode

FIGURE 2.4 INTERMITTENT ABSORPTION COOLING SYSTEM

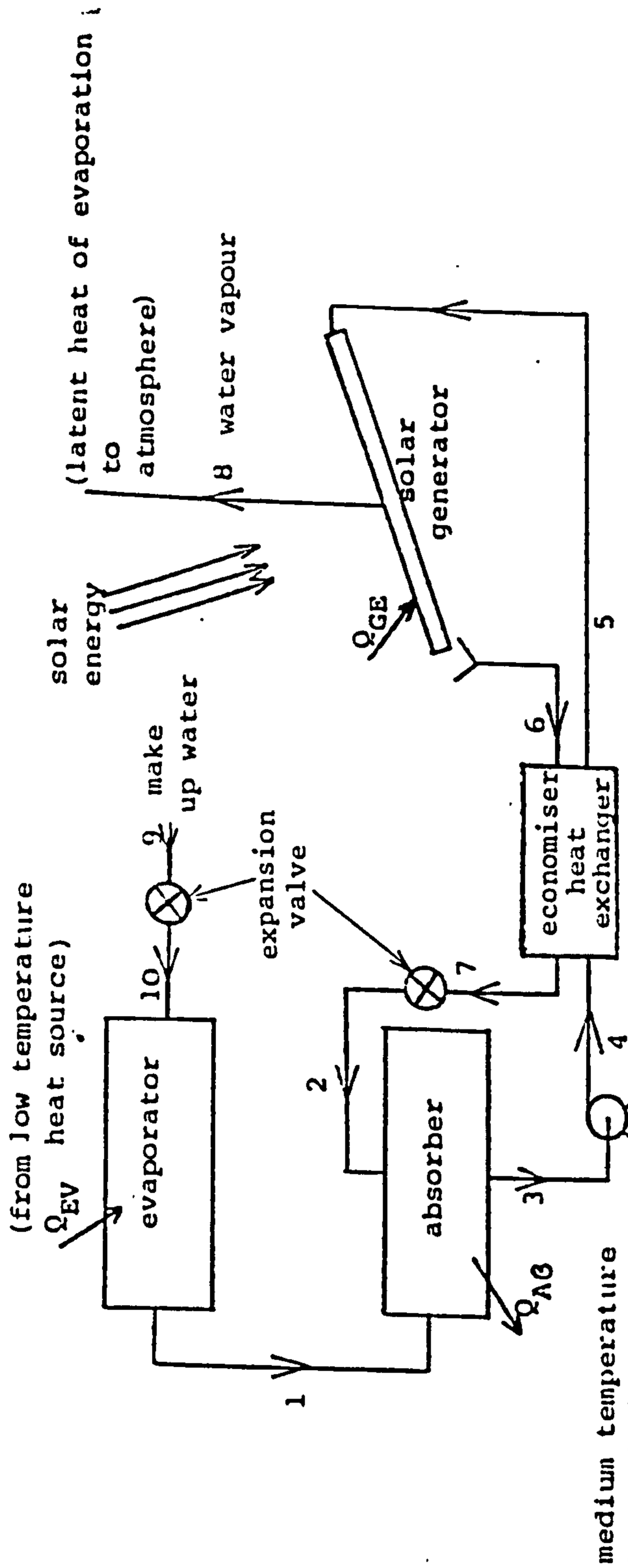

FIGURE 2.5 OPEN CYCLE ABSORPTION COOLING SYSTEM

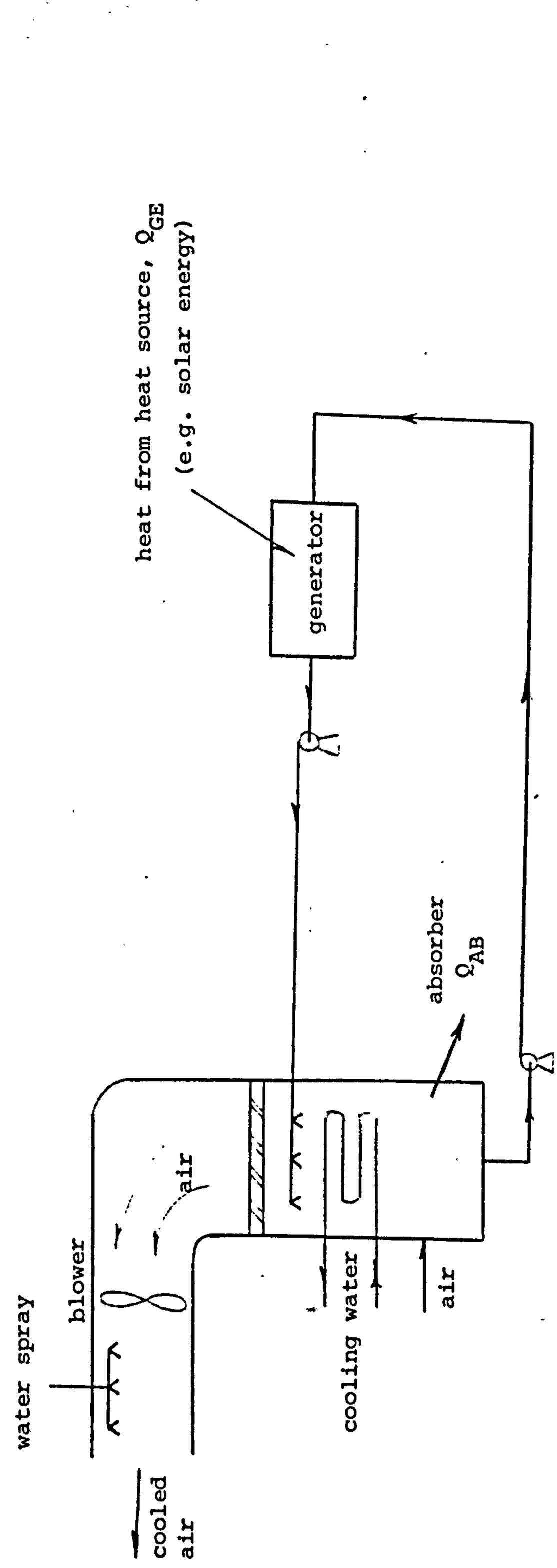

FIGURE 2.6 LIQUID DESICCANT EVAPORATIVE COOLING SYSTEM

CHAPTER 3

LITERATURE REVIEW OF ABSORPTION COOLING SYSTEMS

LITERATURE REVIEW OF ABSORPTION COOLING SYSTEMS

Numerous research papers have been published on absorption cooling systems. Utilization of solar energy in these systems has also been reported by a number of researchers. Most of these papers demonstrate the ability of solar energy flat-plate collectors to collect heat at the required temperatures necessary for operating absorption cooling systems. In addition to systems testing, continuing efforts have been directed towards computer simulations of absorption cooling systems.

A brief literature review in the following pages has been done based on the classification of refrigerant-absorbent pair.

3.1 SYSTEMS USING GAS-LIQUID WORKING FLUIDS

3.1.1. Systems using ammonia-water

A practical ammonia-water absorption cooling system is slightly different from the absorption cooling system discussed in Chapter 2. The generator in this case consists of a reboiler and a distillation column. This is required for getting almost pure ammonia in the condenser. There is usually a heat exchanger for cooling the liquid ammonia from the condenser by the ammonia vapour from the evaporator. Inclusion of this heat exchanger causes a decrease in the generator heat requirement by about 10 per cent, while the economiser heat exchanger decreases this amount by about 40 per cent (Whitlow 1971).

Absorption cooling systems using ammonia-water have been used in industry (Briley 1976). These systems operate with a coefficient of performance of about 0.5 to 0.7. Air cooling can be used whenever

generator temperatures of 120°C to 180°C are available (Ward 1979). Ammonia-water can be developed comparatively easily for air cooling (Simmons et al 1975), (Best et al 1976). Jacob et al studied factors affecting the coefficient of performance of the system (Jacob et al 1969). Whitlow studied the same with a view to using solar energy (Whitlow 1976). Dao et al carried out experimental and theoretical analyses of the system for using solar energy effectively (Dao et al 1976). They operated the system with a flow ratio of 27 kg of absorbent per kg of refrigerant so as to decrease the required generator temperature. The unit, in conjunction with a gas fired unit, was operated at a capacity of 6kW for generator temperature of about 77°C, condenser temperature of 30°C and evaporator temperature of 6°C. The coefficient of performance of the system with the above condition was 0.65. Holldorf suggested the use of multistage systems to get higher coefficient of performance (Holldorf 1979). Best et al operated an intermittant cycle system which could produce 25 kg of ice during continuous daily periods of 14 hours (Best et al 1976). Stoecker et al analysed and compared Carnot, basic aqua ammonia and refined aqua ammonia cycles (Stoecker et al 1971). Johnston analysed ammonia-water absorption cycles with relatively high generator temperatures with a view to using evacuated tubular solar collectors (Johnston 1980).

A comparison of systems using ammonia-water with other systems is given in Section 3.3 of this Chapter.

3.1.2 Systems using working fluids other than ammonia-water

Relatively few attempts have been made using gas-liquid working pairs other than ammonia-water. Jacob et al studied theoretically ammonia and sulphur dioxide combined with different organic solvents (Jacob et al 1969). They predicted an ideal coefficient of performance of 0.8 for ammonia and 0.7 for sulphur dioxide. Pechatnikov et al carried

out an experimental investigation using hydrocarbons as refrigerant-absorbent pairs (Pechatnikov et al 1968). They concluded that the best refrigerant is C_4H_{10} or C_4H_8 with C_6H_{14} or C_7H_{16} as the absorbent. Difluorochloromethane-perchloroethylene as the refrigerent-absorbent pair for absorption cooling was studied by Mosteza (Mosteza 1970). Freezing temperatures down to -60^{o}C were obtained. Usyukin et al suggested the use of methylamine-water (Usyukin et al 1971). The advantages discussed are the use of low grade heat, low pressures and less toxicity than ammonia-water. Orekhov et al used monoethylamine as refrigerant and glycerine as absorbent (Orekhov et al 1973). It was found that a coefficient of performance of 0.9 can be obtained by a mixture of 50 per cent of glycerine. Usyukin et al studied a solution of methylamine in DMETEG (dimethylether of tetraethylene glycol) and suggested the use with air cooling (Usyukin et al 1977).

3.2 SYSTEMS USING LIQUID-SOLID WORKING FLUIDS

3.2.1 Closed cycle systems

3.2.1.1 Systems using water-lithium bromide

Water-lithium bromide is the most extensively used refrigerant-absorbent pair. Refrigeration systems operating on this pair are available commercially. Smaller types of systems are normally gas fired whereas larger systems are steam operated (Ishida 1979). A number of experimental water-lithium bromide systems have been reported working with solar energy. Early experiments on solar energy operated water-lithium bromide absorption cooling systems used commercially available 3 to 5 ton machines without significant modifications (Chung et al 1963), (Sheridan 1962). A number of solar experimental cooling systems are reported to have been designed and fabricated, but published performance data are not yet

available. Ward et al, Namkoong and Bierman have reported successful experimental investigations (Ward et al 1975a, 1975b, 1977), (Ward 1975), (Namkoong 1976), (Bierman 1979).

Several simulation studies have been reported to study the effect of parameter variation, to explore the long-term performance, to assist in developing design, and to provide a basis for economic studies. Löf et al dealt with the cost of solar heating and cooling systems and concluded that combined functions of solar heating and cooling were more economical than either heating or cooling alone (Löf et al 1974). Another simulation study showed monthly performance of a system on a building (Butz et al 1974). A follow-up study applied these techniques to design an experimental facility (Oonk et al 1975). A simplified water-lithium bromide absorption system was simulated for steady state operation (Allen et al 1976). Modelling of a solar operated air-conditioner system with refrigerant storage was done by Grassie (Grassie et al 1976). The model included a solar collector and cooling tower. System temperatures, energy flows and coefficients of performance were predicted for different ambient wet and dry bulb temperatures and different solar radiations. Sheridan analysed the water-lithium bromide cooling cycle with implications for solar operations (Sheridan 1974). It was shown that the system should operate satisfactorily over a range of generator temperatures such as would be available from a solar collector. Temperatures of $90^{o}C$ to $100^{o}C$ from the solar collector were shown to be enough for operating the system satisfactorily. Besseler et al modelled a cooling system with water-lithium bromide using solar energy (Besseler et al 1975). They investigated various ways of improving the economics and performance of a solar system by varying the pertinent parameters. Alizadah et al carried out a general theoretical study on the design and optimisation of water-lithium bromide and ammonia-water absorption cooling cycles (Alizadah 1979). They concluded

that a water-lithium bromide system is much simpler than the ammonia-water system and that it operates with higher coefficients of performance and smaller heat exchange surfaces for same conditions. Ward et al carried out a performance study and analysis on the integration of evacuated tubular solar collectors with the lithium bromide absorption cooling cycle (Ward et al 1979). The study deals with two types of evacuated tubular solar collectors integrated with two solar heating and cooling systems.

Landauro et al reported the operation of an absorption cooling unit with relatively high abosrber and condenser temperatures. The working pair used in this study was water-lithium bromide (Landauro et al 1983). In a follow on study, Kumar et al reported the significance of the flow ratio for the utilization of solar energy (Kumar et al 1984). Lazzarin studied steady and transient behaviour of water-lithium bromide chillers of 4.5 kW and 25 kW capacity (Lazzarin 1980).

3.2.1.2 Systems using working fluids other than water-lithium bromide

When using water as a refrigerant, temperatures below $0^{o}C$ cannot be reached in the evaporator. Efforts have been made to find a suitable replacement for water to overcome this limitation. Aker et al evaluated alcohol-salt mixtures as the refrigerant-absorbent pair (Aker et al 1965). Grosman et al designed and carried out experiments with methanol and lithium bromide. They could operate the system with $-15^{o}C$ evaporator temperature. The solution was found to be very corrosive. This was attributed to the presence of free hydrogen bromide (Grosman et al 1968). Grosman found that viscosities of the methanol-lithium bromide solutions are significantly greater than those of water-lithium bromide solutions. (Grosman 1971). Vemura studied methanol-zinc bromide and methanol-

lithium bromide-zinc bromide absorption refrigeration machines (Vemura 1975, 1976, 1977). He found that the system using methanol-lithium bromide-zinc bromide has a greater coefficient of performance than the methanol-zinc bromide. In practical systems the coefficient of performance when using methanol-lithium bromide-zinc bromide was close to 0.75. He also worked with methanol-lithium iodide-zinc bromide and ethanol-lithium bromide and got similar results. This study provided physical and thermal properties of the mixtures along with the system performance. The above mixtures are quite corrosive. However, the addition of small quantities of arsenic trioxide and ethylene diamine tetra acetic acid can markedly inhibit the corrosion of ferrous metals (Krueger 1977).

An ammonia-salt mixture was also used as the refrigerant-absorbent pair (Mansoori et al 1979), (Jacob et al 1969). Properties of sodium thiocynate, which was used as the absorbent with ammonia as refrigerant by Mansoori et al, were presented by Blytas et al (Blytas et 1962). Macriss et al used mixtures of monomethylamine and sodium thiocyanate and mixtures in which part of the sodium thiocyanate was replaced with other thiocyanates of group I, II, and III in the Mendeleef periodic table, metals and related mixtures (Macriss et al 1969). A reduced economiser heat exchanger area in the absorption cycle and a high coefficient of performance were claimed for an air cooled absorption cooling system. It was reported that an ideal coefficient of performance of 0.92 could be obtained for methylamine-sodiumthiocyanate when the generator temperature was 121^{o}C and the evaporator temperature was 5^{o}C. Values of the coefficient of performance for similar conditions for the sytems ammonia-water and ammonia-sodiumthiocyanate were 0.84 and 0.87 respectively.

3.2.2 Open cycle cooling systems

3.2.2.1 Liquid desiccant evaporative cooling system

Liquid desiccant evaporative cooling systems have been studied by a number of researchers. Collier analysed the possibility of using a liquid desiccant evaporative cooling system and an absorption cooling system operating in series to both dry and cool air (Collier 1978). It was proposed to use a generator open to atmosphere for both the systems. It was concluded in the paper that the performance of the combined systems was better than individual system , especially in humid and windy climates. An open cycle solar absorption cooling system combined with a spray chamber was described by Kakabaev (Kakabaev et al 1971). The use of air cooled by partial humidification plus the cooling effect of an open cycle absorption cooling system was proposed. He suggested that at night such a system could function as an evaporative cooler. This sort of system was found particularly useful in hot, dry climates.

Hollands studied the regeneration of lithium chloride solution in a batch type solar still with the idea of using regenerated brine for cooling (Hollands 1962). Another type of solar generator was analysed by Kakabaev (Kakabaev et al 1972). In this type of generator, a glass plate was used over the solution to minimise contamination of the solution. However, the glass plate reduced the amount of solar radiation reaching the solution. Air was blown through the channel formed by the glass and the generator surface to remove water vapour. Similar work was also done with water-calcium chloride solution (Mullick et al 1974), (Gandhidasan, et al 1976, 1981).

3.2.2.2 Solar absorption cooling system

Kakabaev theoretically analysed the generator of an open cycle solar absorption cooling system (Kakabaev et al 1969). The generator was open to atmosphere. A thin film of water-lithium chloride solution was considered to flow over a blackened surface. The solution was heated up by solar radiation falling directly on the generator. The use of water-lithium chloride as the refrigerant-absorbent was recommended for open cycle absorption cooling systems instead of water-lithium bromide, which was extensively used for closed cycle absorption cooling systems. It is because lithium chloride is less corrosive to metals and more stable in the presence of air (Kakabaev et al 1969), (Ref.45). It was shown that a pressure of 9.2 mm Hg, which corresponds to $10^{o}C$ in the evaporator can be sustained in the absorber at a temperature of $35^{o}C$ and lithium chloride concentration of 38 per cent at the absorber outlet. Later, a simplified analysis of the generator was presented by Baum et al valid for situations when the liquid flow rate over the generator was sufficiently high (Baum et al 1972). In this analysis, solution flow rates of 8 to 15 kg m^{-2} h^{-1} were recommended for the generator. Prasad and Kumar analysed the regeneration of lithium chloride brine in a generator where free convection flow of ambient air removed the water (Prasad et al 1981). They also studied the possibility of using a continuous solar still type generator (Prasad et al 1981). The generator design based on the solar still was considered to eliminate the contamination of brine by the environment and to make the system's performance independent of the ambient humidity. A steady state analysis of the system was presented.

A solar absorption cooling system based on evaporation from a lithium chloride solution flowing on the roof of a building was described and the test results were reported under summer conditions in central Asia (Kakabaev et al 1976). The pilot plant was reported to have

operated satisfactorily with a relative humidity of about 25 per cent, a wind velocity of about 2 ms^{-1} and solar insolation values varying between 0.4 kW m^{-2} to 1.0 kW m^{-2}. The temperature achieved in the evaporator was about 13.5^{o}C. The concentration of lithium chloride solution varied between 29.5 per cent and 32.0 per cent.

Collier used the analysis of Kakabaev to predict the performance of an open cycle absorption cooling system in different cities of the USA (Collier 1979), (Kakabaev et al 1969). It was concluded in this analysis that more experimental verification was required in order to design systems with confidence.

3.3 SYSTEMS USING LIQUID-LIQUID WORKING FLUIDS

Liquid-liquid working fluids are advantageous when low-grade heat sources are used as the driving energy. Liquid-liquid refrigerant-absorbent pairs, which have been studied are mostly organic compounds. Halogenated organic compounds such as R22 (CHF_2Cl) have been tried as refrigerants with the dimethyl ether of tetraethylene glycol (DMETEG), a mixture of DMETEG and dimethyl formamide (DMF), and dimethyl formamide as absorbents.

There have been efforts to find a suitable absorbent-refrigerant combination. The use of R22 was illustrated by Eiseman (Eiseman et al 1959). R22 - DMETEG was recommended for use as refrigerant-absorbent pair. The relative merits of the pair were compared with water-lithium bromide and ammonia-water. These are shown in Table 3.1.

Usyukin and Chumachenko also used the same pair to discover the practical limits of its application (Usyukin et al 1971). Borde et al

Characteristic	H_2O - LiBr	NH_3 - H_2O	R22 - DMETEG
can be air cooled	no	yes	yes
can be used for refrigeration	no	yes	yes
refrigerant non-flammable	yes	no	yes
refrigerant non-toxic	yes	no	yes
absorbent non-flammable	yes	yes	no
absorbent non-toxic	yes	yes	yes
component non-corrosive	no	yes*	yes
non-volatility of absorbent	excellent	poor	good
latent heat of refrigerant	excellent	good	fair
operating pressure	extremely low	high	high

* copper and its alloys must be excluded because of corrosion

TABLE 3.1 RELATIVE MERITS OF THE WORKING FLUIDS

also studied the mixture of R22 with DMETEG and DMF (Borde et al 1977). They found that if the required evaporator temperature was above -5°C, and means of cooling the absorber and the condenser were available below 30°C, a system operating on R22 - DMF was economically more feasible. If the required temperature was below -5°C and the low grade heat source was in the range of 60°C to 90°C, the pair R22 - DMF was not suitable; alternatively, the use of R22 - DMETEG was recommended. A number of suitable pairs of refrigerant-absorbent combinations for absorption were presented by Johan et al (Johan et al 1979). It was proposed to use water as the refrigerant and glycol ether, polyoxyalkylene glycol, polyoxyalkylene polyglycol ether as absorbents in some of the pairs.

Unfortunately, organic fluids are generally susceptible to thermal instability after a long period of continuous use. There is considerable scope for work to be done in this area.

An account of possible new working fluid pairs has been edited by Raldow (Raldow, 1982). This publication also deals with the latest state of technology of absorption systems in Europe. A significant contribution for multistaging was given by Alefeld (Alefeld 1982). He suggested that by using absorption and desorption processes, new schemes for heat transformation with improved coefficients of performance can be designed. He also proposed a combination of compressor systems with absorption systems. He discussed various possibilities for these combinations.

3.4 CONCLUSIONS

On the basis of the above literature review, the following work programme was proposed.

1) Design data have been published for only a very limited range of applications for absorption cooling systems. These applications require operation in very limited temperature ranges. The actual temperature range depends on whether the application is for deep freezing, refrigeration, or for use in air conditioning systems. These systems should be tested to the extreme conditions appropriate to the type. One extreme is the highest achievable absorber and condenser temperatures. Another extreme is the minimum generator temperature which will allow the possibility of using low grade thermal energy from waste heat or solar sources. This study is required to be done in two steps:

(a) A theoretical analysis should be carried out to study the effect of parameter variations. This will indicate the relative sensitivity of the parameters and will help in planning the experiments.

(b) An experimental investigation should be planned and conducted based on the above theoretical analysis.

2) It is interesting to note that there is a possibility of cooling by the evaporator and simultaneous heating by the absorber and the condenser in continuous closed cycle absorption systems. This can be done if it is possible to maintain pressures corresponding to the required temperatures in the evaporator and the condenser. Generally, this might not be economical for vapour

compression systems because of increased compression ratios and therefore increased power consumption. A detailed theoretical analysis is required to be done to find out the limits of this possibility. Experimental verification of the conclusions drawn from the theoretical analysis is also required.

3) The open cycle solar absorption cooling system needs theoretical and experimental study as there are a number of parameters affecting the performance of the system. Apart from the usual parameters of the absorption system such as temperature, pressure, and solution concentration at different points in the cycle, the generator performance itself depends on the number of parameters. The variation of solar insolation, wind velocity and environmental humidity can affect the performance drastically. Simultaneous variation of the above parameters makes the heat and mass transfer processes complicated. Therefore, it was proposed to study this as follows:

(a) Experimental design data for the generator of the open cycle absorption cooling system are to be generated indoors because of the continuous variation of pertinent parameters outdoors.

(b) A theoretical simulation study of the generator is also necessary. This would not only help in predicting the performance, but would also be a helpful tool in the analysis of the experimental results. The latter can be done by incorporating the heat and mass transfer correlations in the mathematical model.

CHAPTER 4

ANALYSIS OF SOLAR ABSORPTION COOLING SYSTEMS FOR LOW GENERATOR TEMPERATURES

ANALYSIS OF ABSORPTION COOLING SYSTEMS WITH LOW GENERATOR TEMPERATURES

4.1 INTRODUCTION

The flow diagram of the closed cycle absorption cooling systems using water-lithium bromide and ammonia-water as working fluid pairs are shown in Figures 4.1 and 4.2 respectively. In the present analysis of closed cycle systems, solar energy has been considered as the heat source to the generator. However, the results are valid for any equivalent heat source. The open cycle solar absorption cooling system is shown schematically in Figure 4.3. This analysis deals with the efficient utilization of variable thermal energy sources like solar energy.

Solar energy may be used to provide the heat required in the generator using either flat plate or concentrating collectors. Although the latter may be used to produce high generator temperatures, concentrating collectors are complex, expensive and less efficient compared to flat plate collectors. It is known that flat plate collectors perform more efficiently at relatively low temperature. To take advantage of this aspect the temperature in the generator should be reduced which can be achieved in either of two ways. The first way is to operate at high flow ratios, i.e., the ratio of mass flow rates of absorbent to the refrigerant (Kumar et al 1984), (Dao et al 1976).

The second way is to use an open cycle which is only feasible when water is used as the refrigerant. Some experimental investigation using open cycle solar absorption cooling systems for relatively dry and high temperature ambient conditions have been reported by Kakabayev and co-workers (Kakabayev et al 1969), (Baum et al 1978).

Some theoretical analysis by Prasad et al and Collier have shown the feasibility of such systems for a wide range of conditions (Prasad et al 1981), (Collier 1979).

4.2 THEORETICAL CONSIDERATIONS

For the purpose of analysis the following assumptions have been made :

1.0 kg h^{-1} of refrigerant is vaporised in the evaporator.

The streams at state points 1, 3, 6, 8 and 9 in Figures 4.1, 4.2 and 4.3 are in equilibrium.

The evaporating temperature T_{EV}, the ambient temperature T_{AM} and the temperature at state point 3 are $4^{o}C$, $35^{o}C$ and $35^{o}C$, respectively. These conditions have been chosen for tropical conditions where cooling requirement is high. The condensing temperature T_{CO}, for the closed cycle systems is $35^{o}C$.

The generator temperature T_{GE}, in all the cases is taken to be the temperature of strong solution at the generator outlet. In the closed cycle systems, T_{GE} will be very close to the bulk temperature in the generator since the liquid is boiling. It has been reported that in the case of the open cycle, the temperature across the collector-generator unit remains nearly constant (Mullick et al 1974).

While using water-lithium bromide in the system, the energy required to pump liquid from the low to the high pressure side of the system is so small that the difference in enthalpy between states 3 and 4 is insignificant. Pressure drops and the heat losses in the systems are negligible.

The coefficient of performance of a cooling system is defined as

$$(COP)_{CL} = Q_{EV}/Q_{GE} \qquad (4.1)$$

The mass balance for the absorber is given by Equation (4.2).

$$(FR) = (X_1 - X_3)/(X_3 - X_2) \qquad (4.2)$$

A heat balance over the absorber gives the amount of heat Q_{AB} removed by cooling water in the absorber

$$Q_{AB} = H_1 + (FR)H_7 - H_3 \left[(FR) + 1\right] \qquad (4.3)$$

The effectiveness for countercurrent flow heat exchanger is defined as

$$\eta_{EX} = (T_6 - T_2)/(T_6 - T_3) \qquad (4.4)$$

Therefore, the heat exchanged in the economiser heat exchanger is

$$Q_{EX} = (FR)\ (C_p)_2\ \eta_{EX}\ (T_6 - T_3)\ . \qquad (4.5)$$

The work done by the pump W_p is given by Equation (4.6).

$$W_p = (P_{CO} - P_{EV})\ V_3 \qquad (4.6)$$

The enthalpies per unit mass of solution at state points 4, 5 and 7 can be written as follows

$$H_4 = H_3 + W_P \qquad (4.7)$$

$$H_5 = H_4 + Q_{EX} \Big/ \left[(FR) + 1\right] \qquad (4.8)$$

$$H_7 = H_6 - Q_{EX}/(FR) \qquad (4.9)$$

The function of the expansion valve in the cycle is merely to dissipate the pressure head through an isenthalpic process. Therefore, the following equations can be written for the two expansion valves in the cycle

$$H_9 = H_{10} \qquad (4.10)$$

$$H_7 = H_2 \qquad (4.11)$$

The heat removed in the evaporator is given by the heat balance

$$Q_{EV} = H_1 - H_{10} \qquad (4.12)$$

Similarly, the heat balance around the generator for the systems using water-lithium bromide is given by Equation (4.13).

$$Q_{GE} = (H_8 - H_5) + (FR)\ (H_6 - H_5) \qquad (4.13)$$

In the case of the closed cycle system using ammonia-water the heat balance equation is

$$Q_{GE} = (H_8 - H_5) + (FR)\ (H_6 - H_5) + R(H_8 - H_9) \qquad (4.14)$$

The Equation (4.14) is different from Equation (4.13) because the system operating with ammonia-water is provided with a distillation column. A part of liquid ammonia from the condenser is fed back to the distillation column to increase the distillation efficiency. The ratio of mass flow rates of liquid ammonia from the condenser to the distillation column and liquid ammonia from the condenser to the evaporator is called the reflux ratio R. In the present analysis, the value of reflux ratio is taken to be 0.2 (Stoecker et al 1971).

In the case of closed cycle systems the simplest type of flat plate solar collector is considered with a single glass cover over a matt black painted surface behind which a liquid flows in tubes. The performance of this type of collector can be predicted by Equation (4.15) •

$$\eta_{SC} = 0.77 - 7.0\,(T_{IN} - T_{AM})/I \qquad (4.15)$$

where I is the solar insolation (Beckmann et al 1977).

The temperature T_{IN} at the generator outlet or the solar collector inlet is given by

$$T_{IN} = T_{GE} + \Delta T_{GE} \qquad (4.16)$$

The temperature approach at the generator outlet T_{GE} is taken to be $5^{o}C$ in the present analysis.

The solar collector area required is calculated from

$$A = Q_{GE} \Big/ (\eta_{SC} I) \quad . \qquad (4.17)$$

The equilibrium properties for water-lithium bromide and ammonia-water systems are taken from published papers (Besseler et al 1976), (Jain et al 1971).

In the case of the open cycle system the analysis is done for partial pressures of water vapour of 0.013, 0.020, 0.027 and 0.034 bar (10.0, 15.0, 20.0 and 25.0 mm Hg respectively) in ambient air.

4.3 RESULTS AND DISCUSSION

Figure 4.4 is a plot of generator temperature T_{GE} against flow ratio (FR) for the closed and open cycle systems using water-lithium bromide. This plot shows that increasing the flow ratio (FR) leads to a significant reduction in the generator temperature T_{GE}. However, this rate of reduction in T_{GE} decreases as (FR) is increased. The curves tend to become flat after (FR) value of about 30.0. A higher flow ratio at constant absorber concentration implies lower concentration in the generator and therefore lower generator temperature. It can also be seen from Figure 4.4 that in an open cycle system, generator temperatures are considerably lower than in a closed cycle system and that T_{GE} is progressively reduced with increasing dryness of ambient air as implied by decreasing partial pressure p_W. In the case of an open cycle system the lower generator temperature leads to higher efficiency of the solar collector–generator unit.

The coefficient of performance values for the systems using water-lithium bromide have been plotted against (FR) in Figure 4.5. The $(COP)_{CL}$ values for closed cycle systems decrease as (FR) increases. Figure 4.5 also shows that $(COP)_{CL}$ values for open cycle system also

decrease with increase in flow ratio except for relatively dry ambient air. For a given flow ratio the $(COP)_{CL}$ values progressively increase with increasing dryness of ambient air. The $(COP)_{CL}$ values have been plotted for two different cases of with and without economiser heat exchanger. The effectiveness of this heat exchanger is included. These plots show that the open cycle system is better than a closed cycle system.

Figure 4.6 is a similar plot for the closed cycle system using ammonia-water. Both T_{GE} and $(COP)_{CL}$ curves show the same trend. In this case, the T_{GE} curves tend to become flat after a flow ratio value of about 15.0. These plots show that systems using water-lithium bromide offer higher $(COP)_{CL}$ values than the system using ammonia-water, but the limitation of systems using water-lithium bromide is that the evaporator cannot be operated at sub-zero temperatures. In all the cases, the inclusion of the economiser heat exchanger is advantageous.

In the case of the closed cycle system using ammonia-water the power requirement by the solution pump at a flow ratio of 10.0, as given by Equation (4.6), is 0.0034 kW. It becomes an important constraint for higher flow ratio values when using ammonia-water as the working fluid pair. In the case of water-lithium bromide this power requirement is negligible because of relatively low pressure differential across the generator and the absorber.

Figure 4.7 is a plot of open cycle system operating with a flow ratio of 14.0 using water-lithium bromide. It shows the variation of the $(COP)_{CL}$ against partial pressure of water vapour p_W in ambient air for various values of economiser heat exchanger effectiveness.

It can be seen that an ideal heat exchanger is required to make the performance of the open cycle system almost independent of the ambient humidity. However, this effect can be reasonably achieved by including an economiser heat exchanger with a fairly high effectiveness.

Figure 4.8 and Figure 4.9 respectively show that both absorber and generator heat loads are relatively independent of flow ratio for the open cycle system operating in relatively dry environment. In the case of closed cycle system the economiser heat exchanger reduces the absorber and generator heat loads more than in open cycle. Figure 4.10 shows the heat loads for closed cycle system using ammonia-water. In this case also, the economiser heat exchanger provides a definite advantage. For all the above cases, the evaporator conditions are kept constant including the heat load. The condenser conditions are nearly the same but for some change in the superheat of the condenser vapour.

In the case of the closed cycle systems with flat plate solar collectors, the solar energy collection efficiency η_{SC} increases with the decrease in the generator temperature as shown in Figure 4.11. It is worth noting that the η_{SC} becomes more sensitive to the generator temperature when the solar insolation values decrease.

Figures 4.12 and 4.13 are plots of the solar collector area required against flow ratio for closed cycle cooling systems, with various solar insolation levels, for water-lithium bromide and ammonia-water respectively. It can be seen from these figures that as the solar insolation decreases the minima of the curves shift towards a higher value of flow ratio. The economiser heat exchanger in the system reduces the area requirement and makes the system independent of flow ratio for a range of values. Therefore, it can be concluded that a closed cycle

system operating with a given solar collector area will work for a longer time when a relatively high flow ratio is used. In the present particular case, if we consider 0.6 kW as the minimum solar insolation, the optimum (FR) value would be about 25.0 for the system using water-lithium bromide and about 10.0 for the system using ammonia-water.

Computer progrms for this chapter are given in Appendix A.

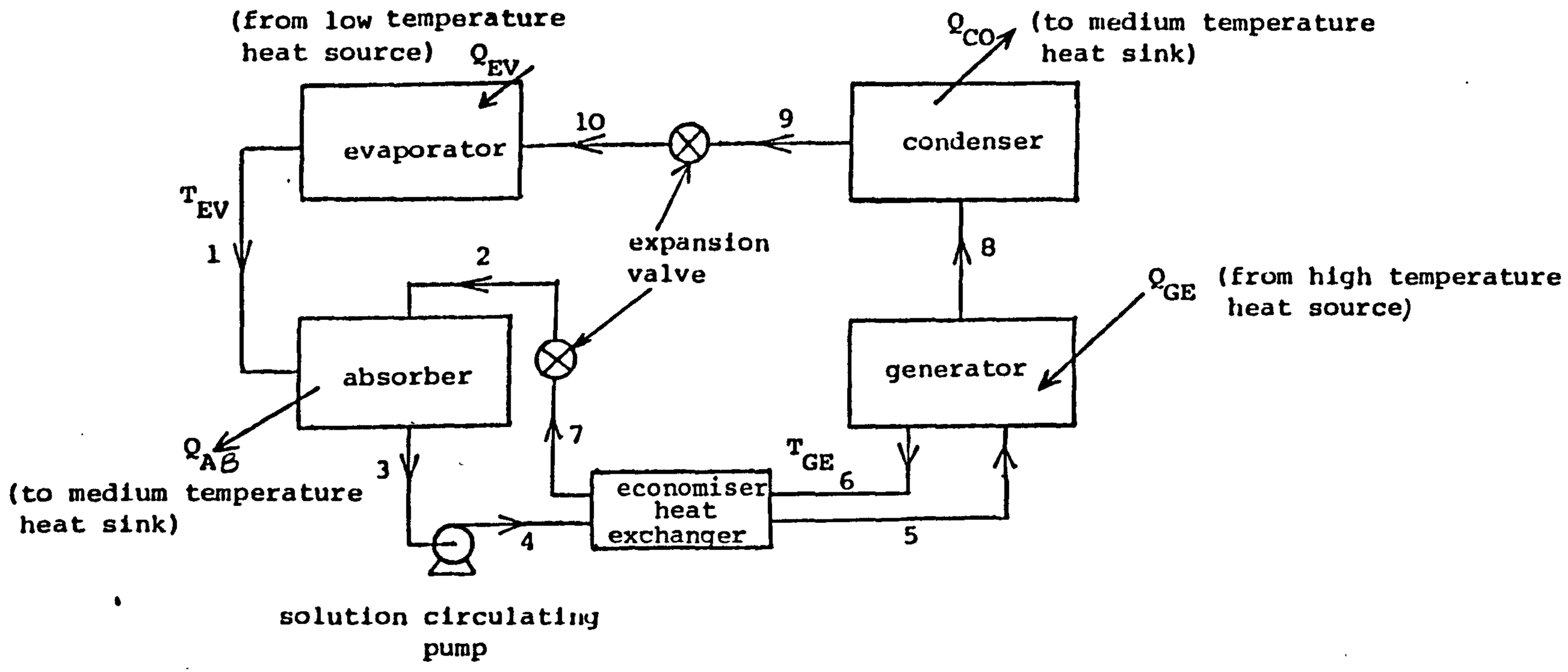

FIGURE 4.1 CLOSED CYCLE ABSORPTION COOLING SYSTEM USING WATER-LITHIUM BROMIDE

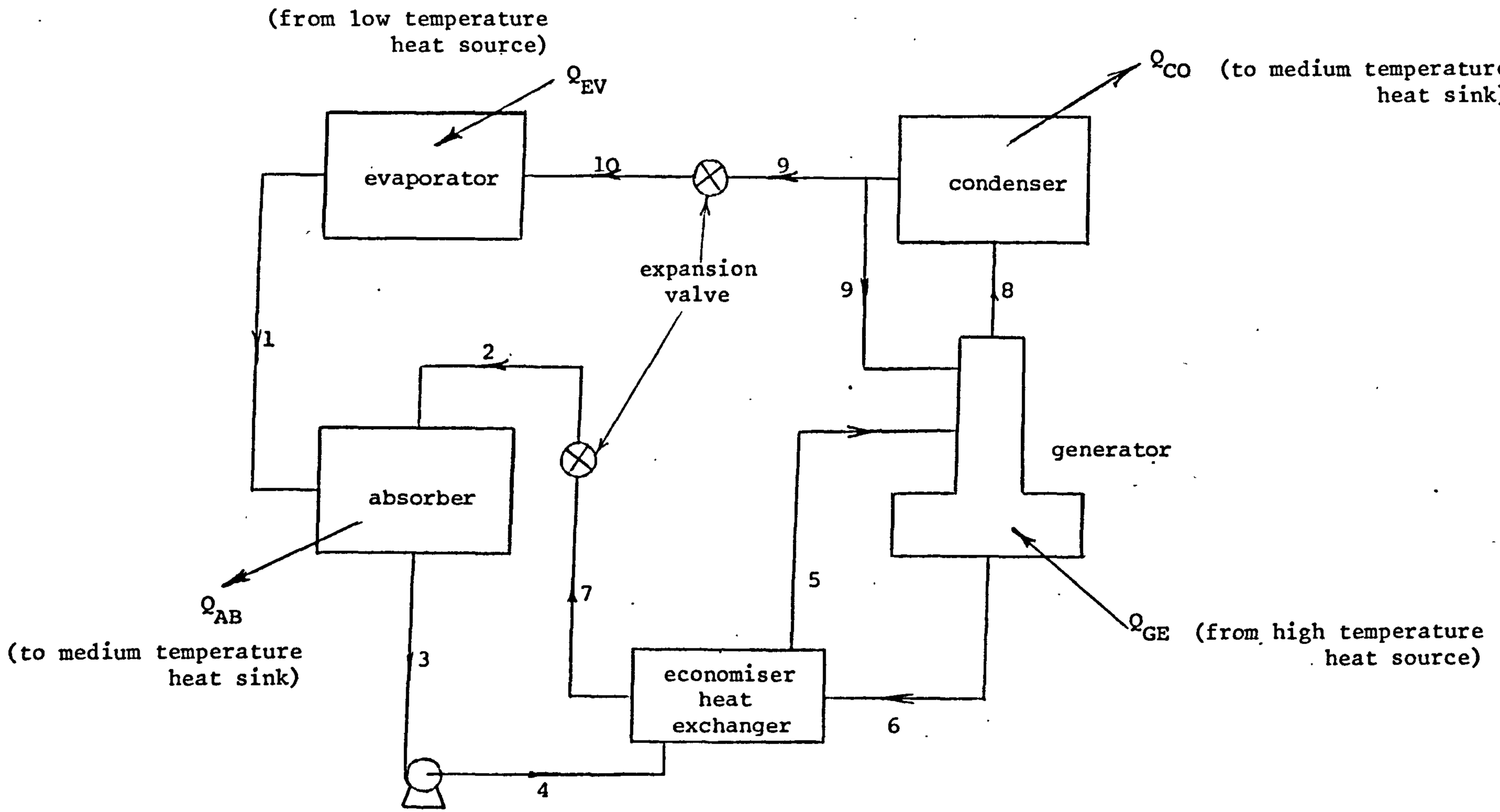

FIGURE 4.2 CLOSED CYCLE ABSORPTION COOLING SYSTEM USING AMMONIA-WATER

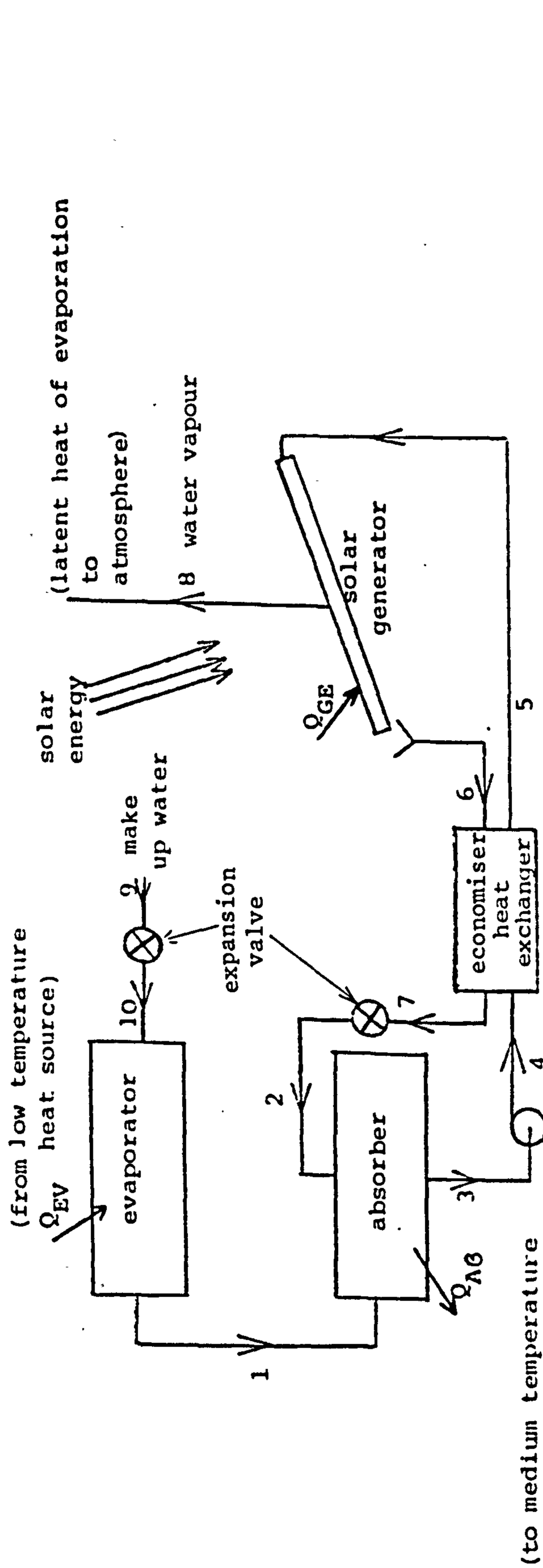

FIGURE 4.3 OPEN CYCLE ABSORPTION COOLING SYSTEM USING WATER-LITHIUM BROMIDE

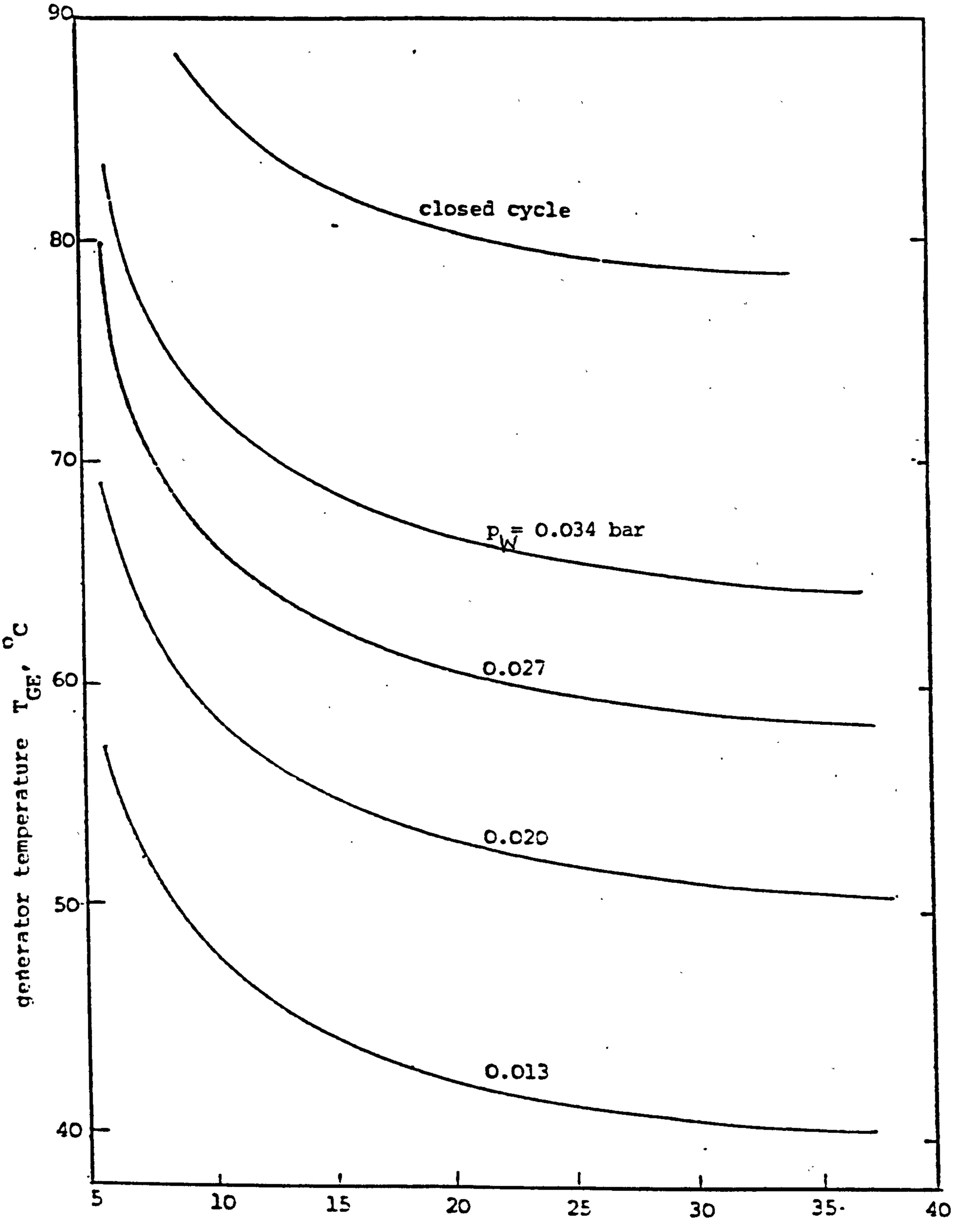

FIGURE 4.4 GENERATOR TEMPERATURE AGAINST FLOW RATIO FOR CLOSED AND OPEN CYCLE COOLING SYSTEMS USING WATER-LITHIUM BROMIDE

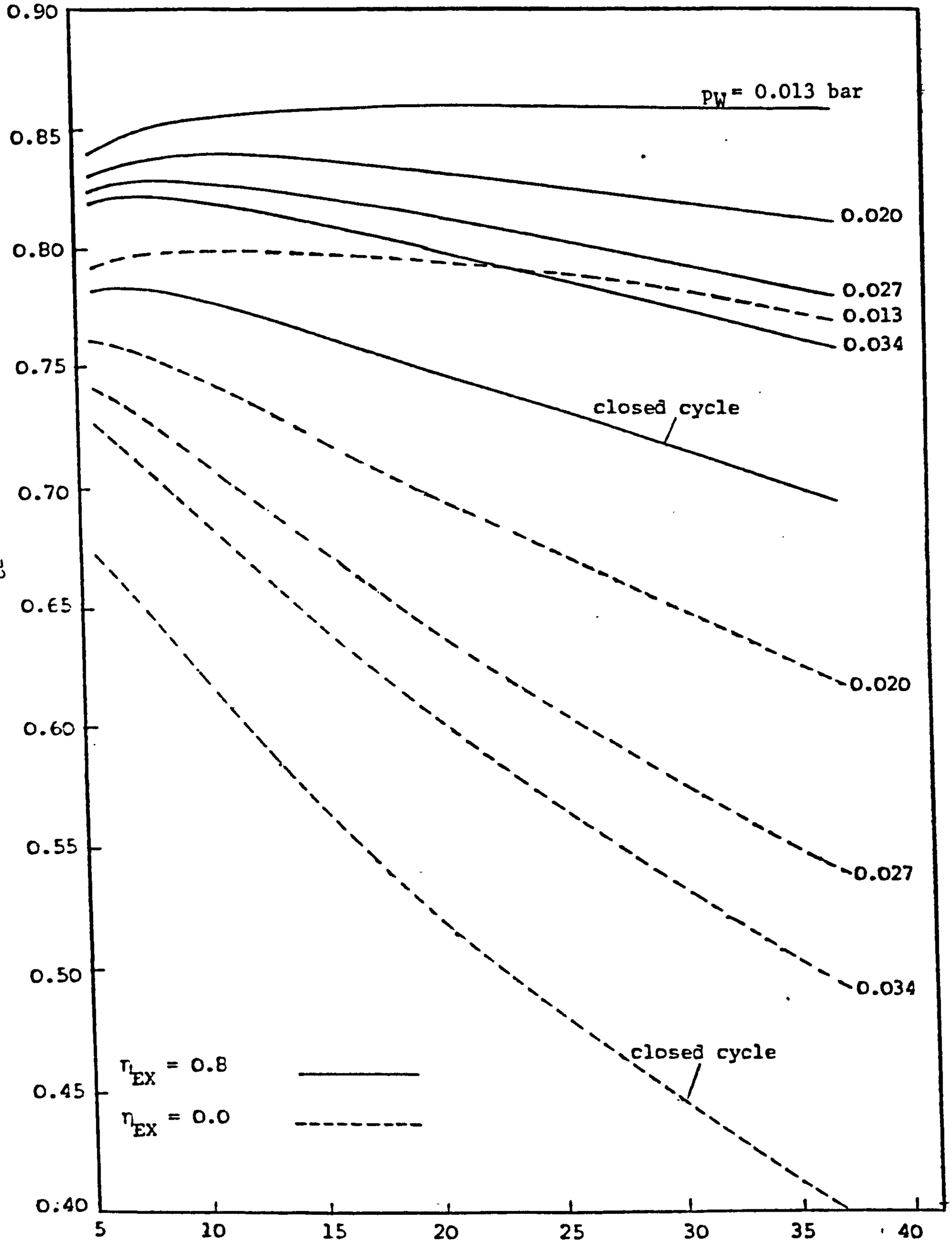

FIGURE 4.5 COEFFICIENT OF PERFORMANCE AGAINST FLOW RATIO FOR CLOSED CYCLE AND OPEN CYCLE COOLING SYSTEMS USING WATER-LITHIUM BROMIDE

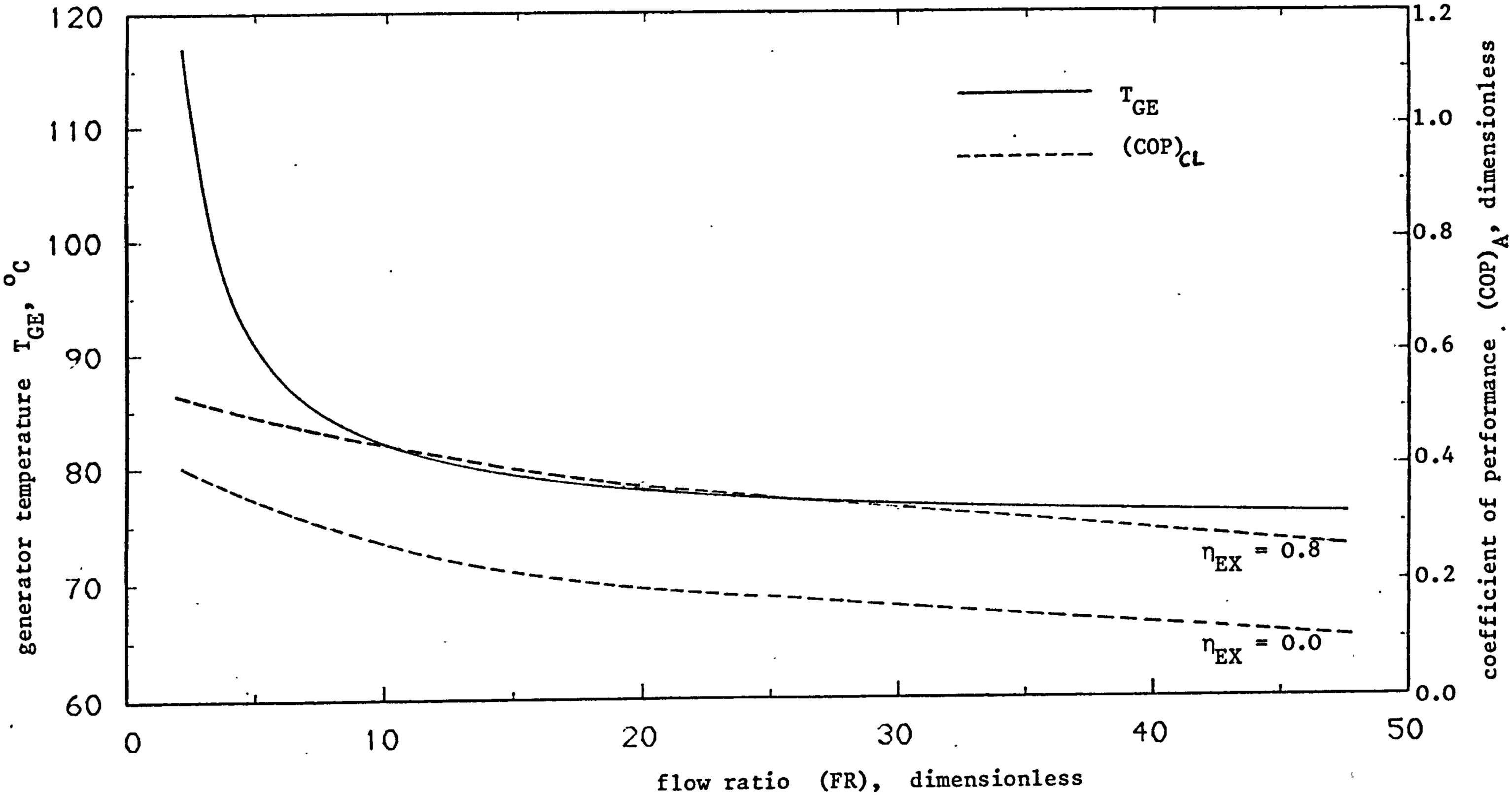

FIGURE 4.6 GENERATOR TEMPERATURE AGAINST FLOW RATIO FOR CLOSED CYCLE COOLING SYSTEM USING AMMONIA-WATER

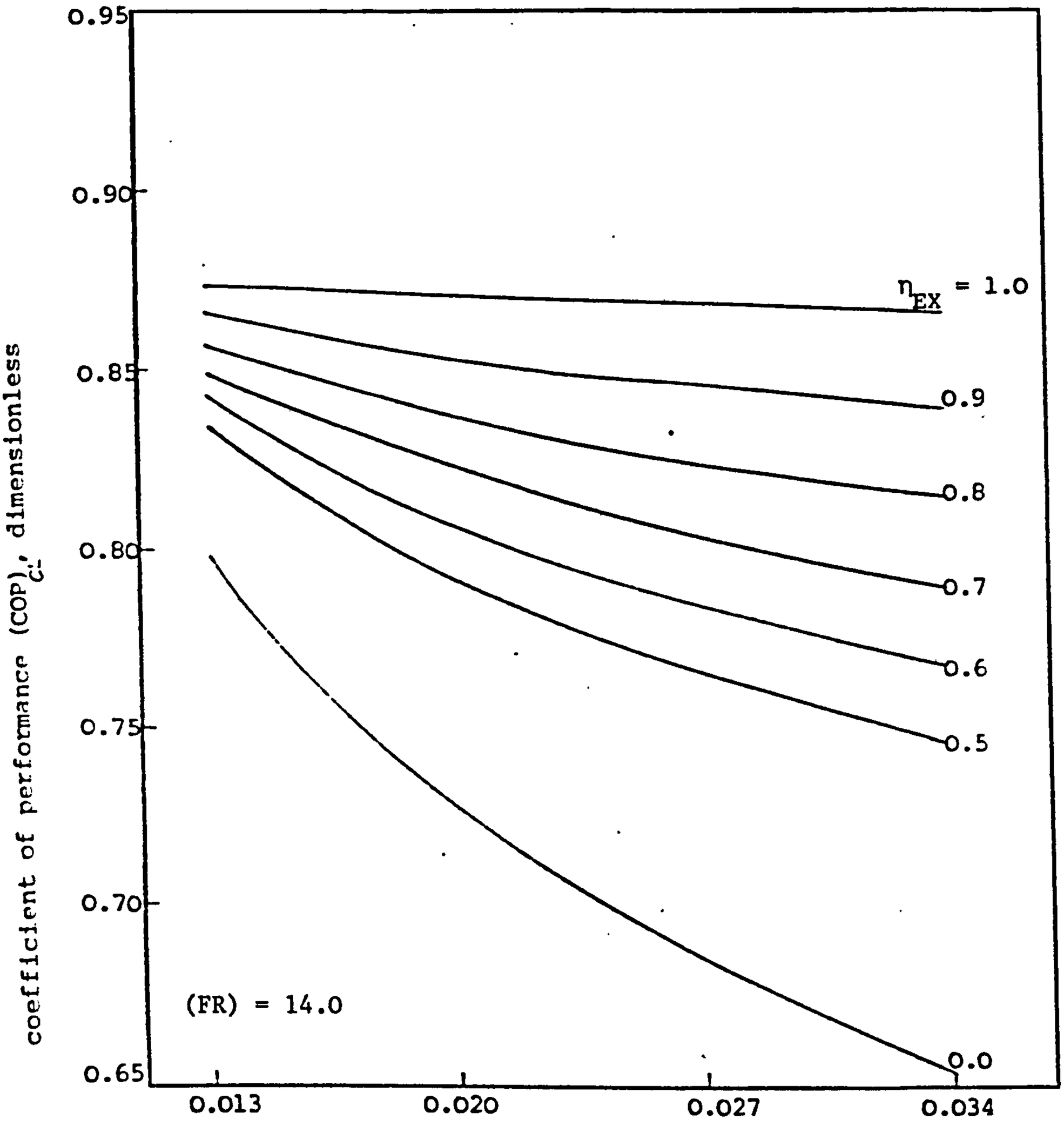

FIGURE 4.7 COEFFICIENT OF PERFORMANCE AGAINST PARTIAL PRESSURE OF WATER VAPOUR IN AMBIENT AIR WITH ECONOMISER HEAT EXCHANGER EFFECTIVENESS AS PARAMETER FOR OPEN CYCLE COOLING SYSTEM

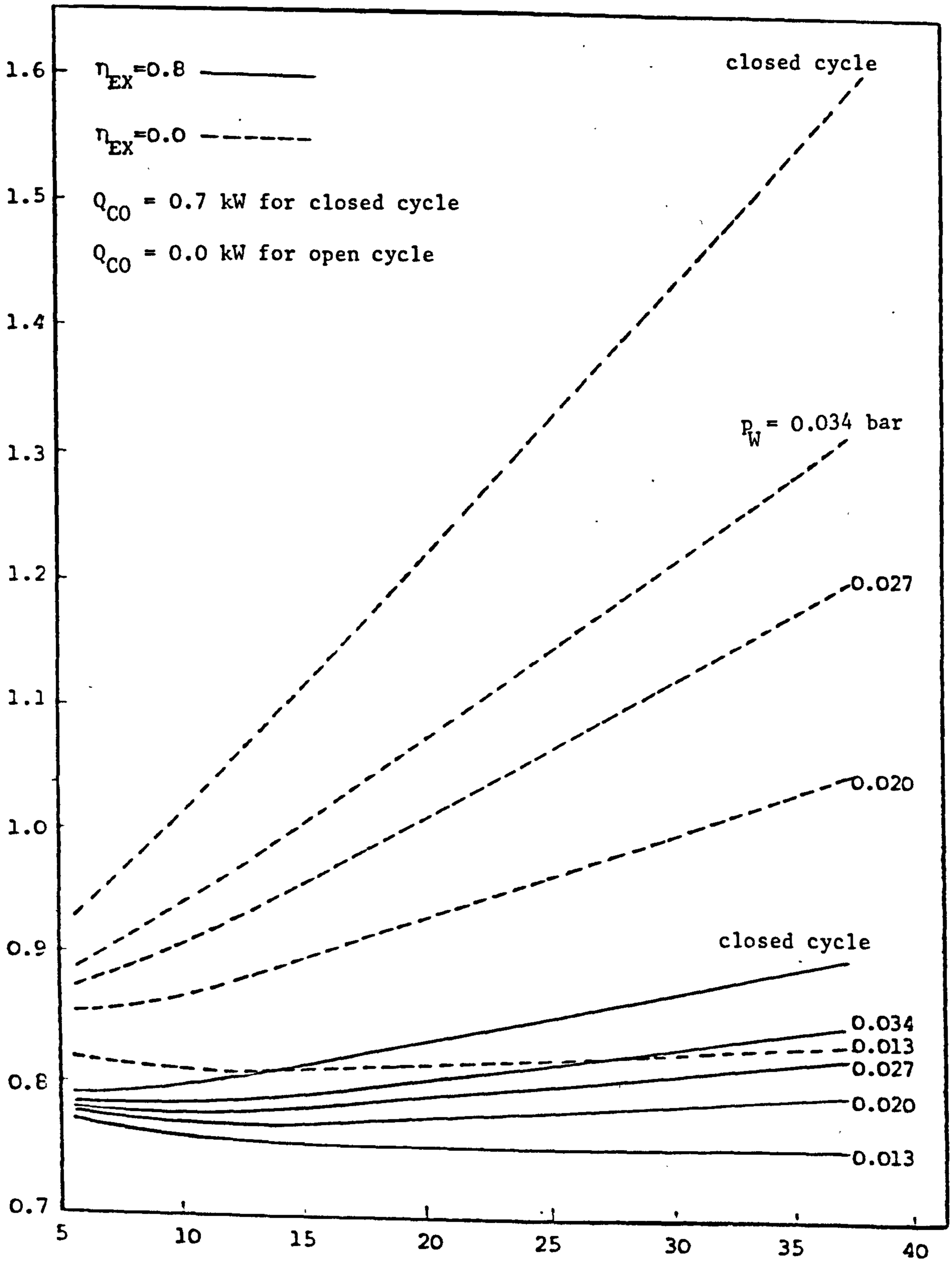

FIGURE 4.8 ABSORBER HEAT LOAD AGAINST FLOW RATIO FOR CLOSED CYCLE AND OPEN CYCLE COOLING SYSTEMS USING WATER-LITHIUM BROMIDE

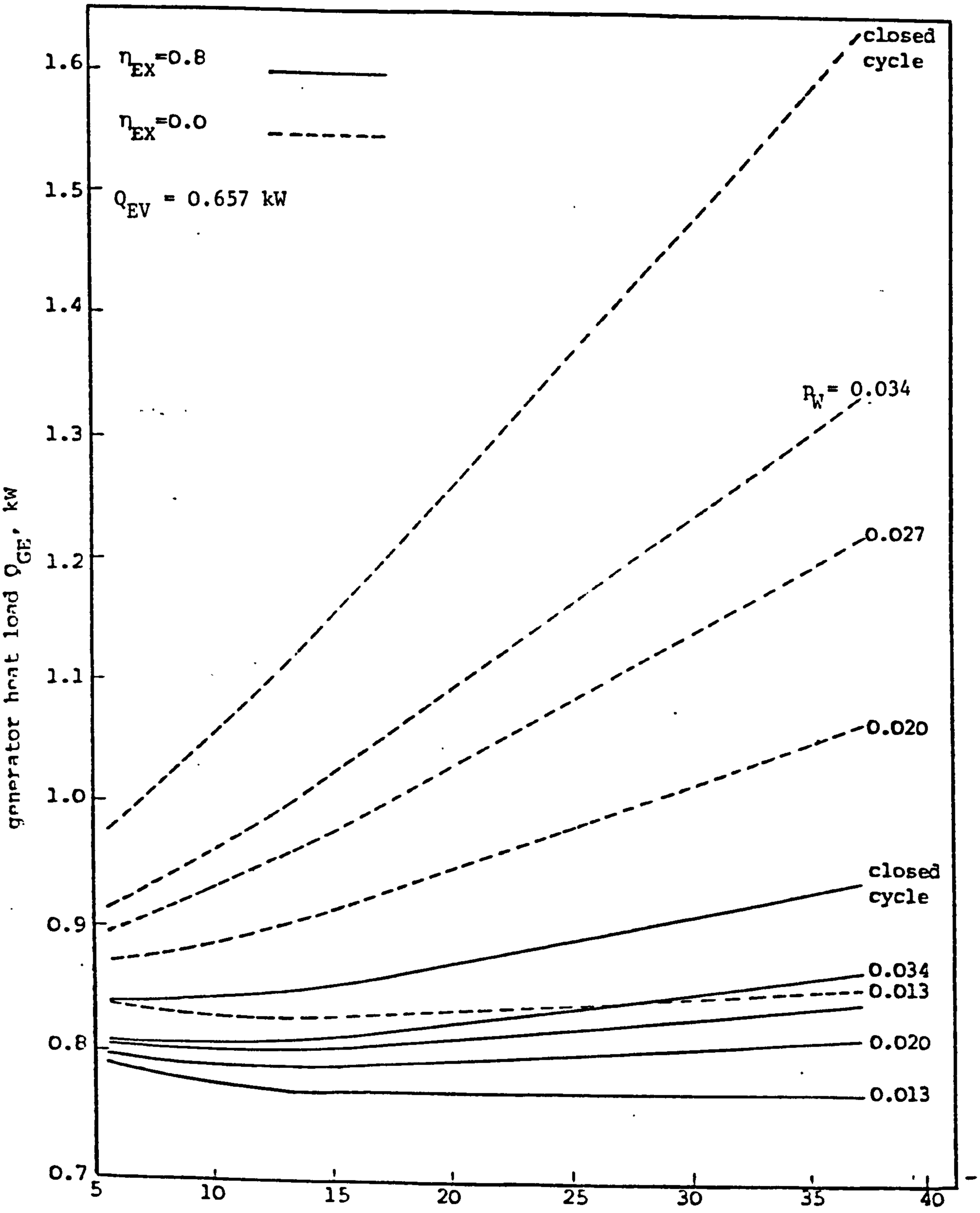

FIGURE 4.9 GENERATOR HEAT LOAD AGAINST FLOW RATIO FOR CLOSED AND OPEN CYCLE COOLING SYSTEMS USING WATER-LITHIUM BROMIDE

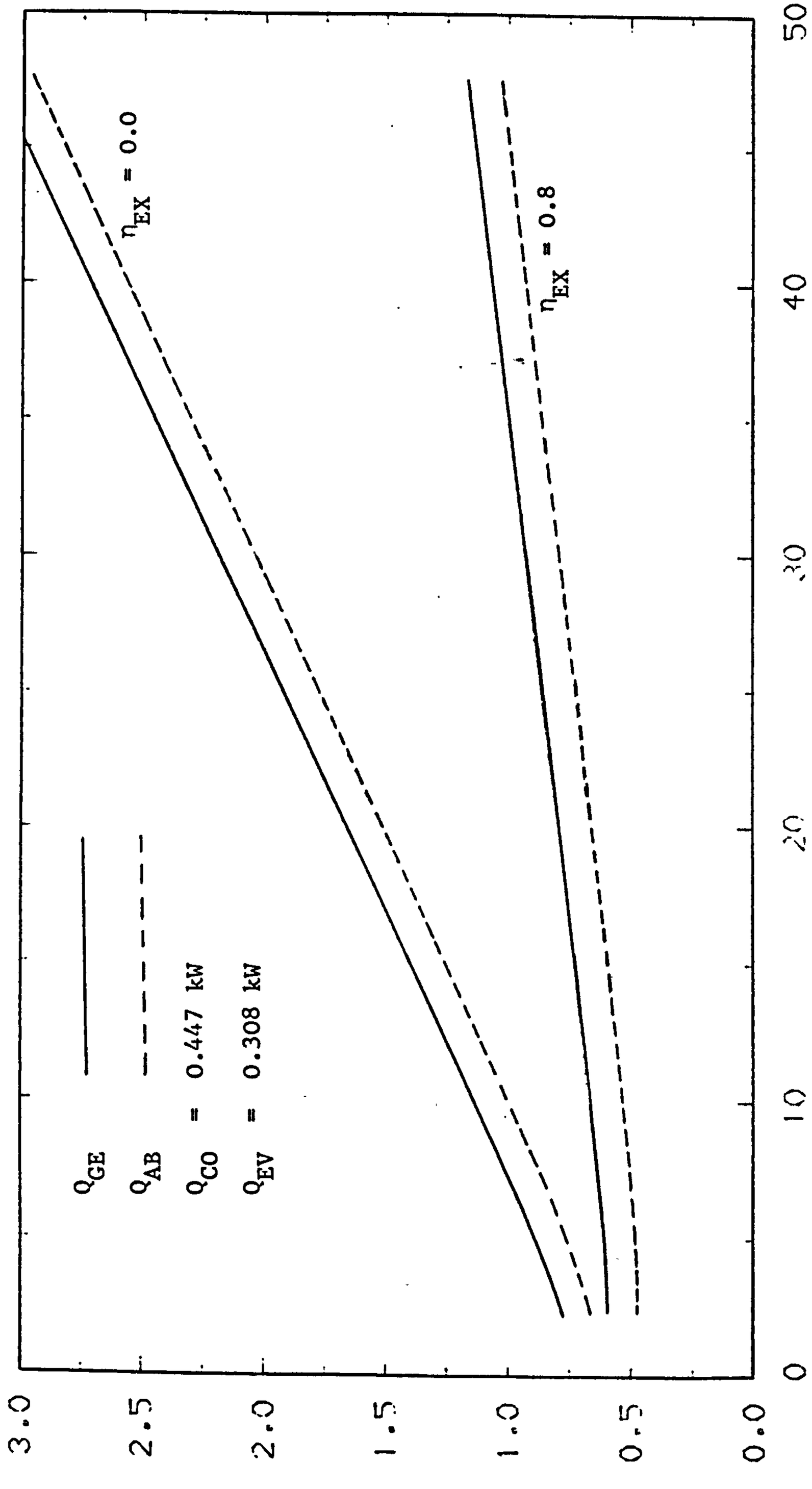

FIGURE 4.10 HEAT LOADS AGAINST FLOW RATIO WITH HEAT EXCHANGER EFFECTIVENESS AS PARAMETER FOR CLOSED CYCLE ABSORPTION COOLING SYSTEM USING AMMONIA-WATER

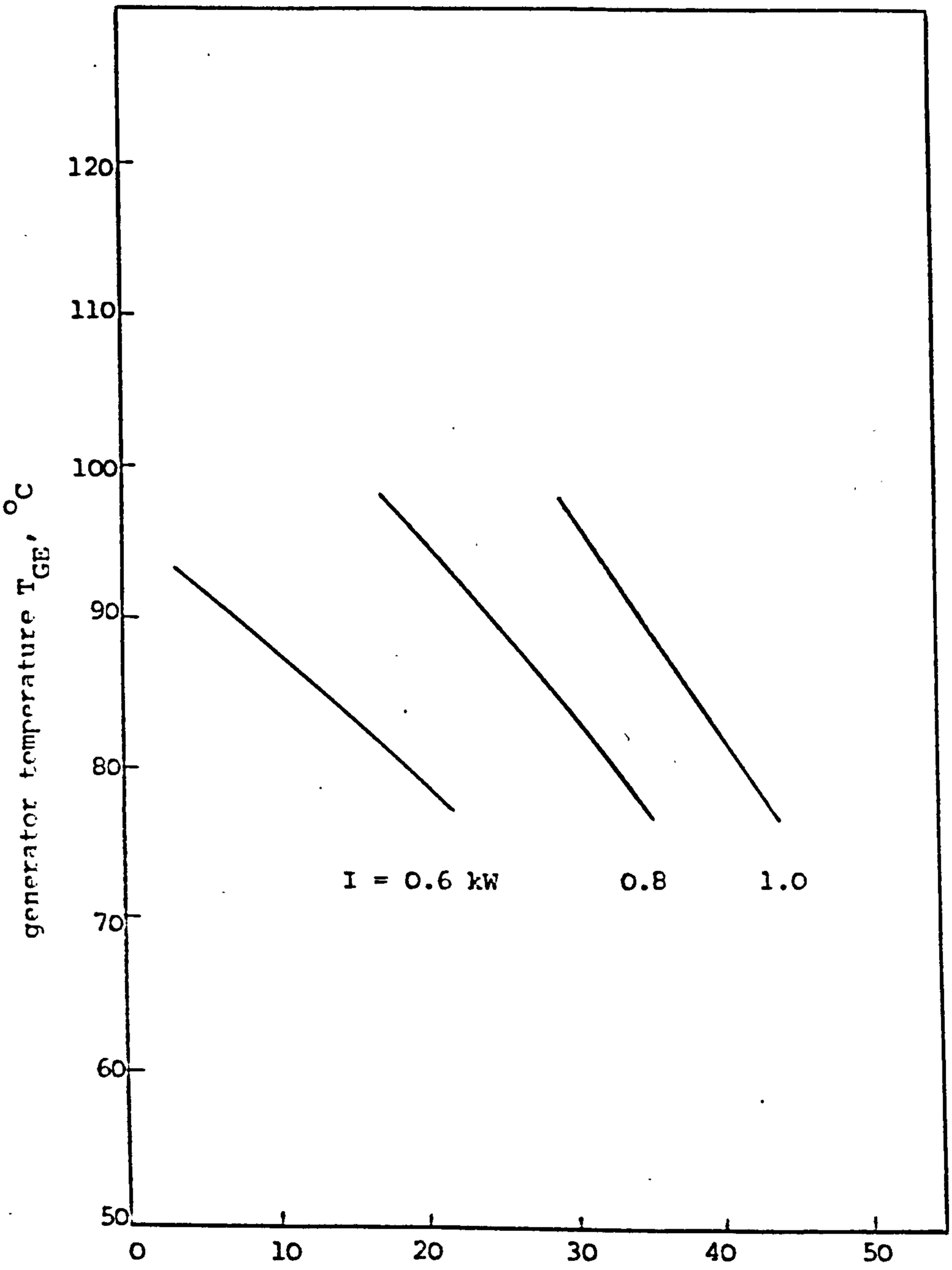

FIGURE 4.11 GENERATOR TEMPERATURE AGAINST SOLAR ENERGY COLLECTION EFFICIENCY WITH VARIOUS SOLAR INSOLATION LEVELS

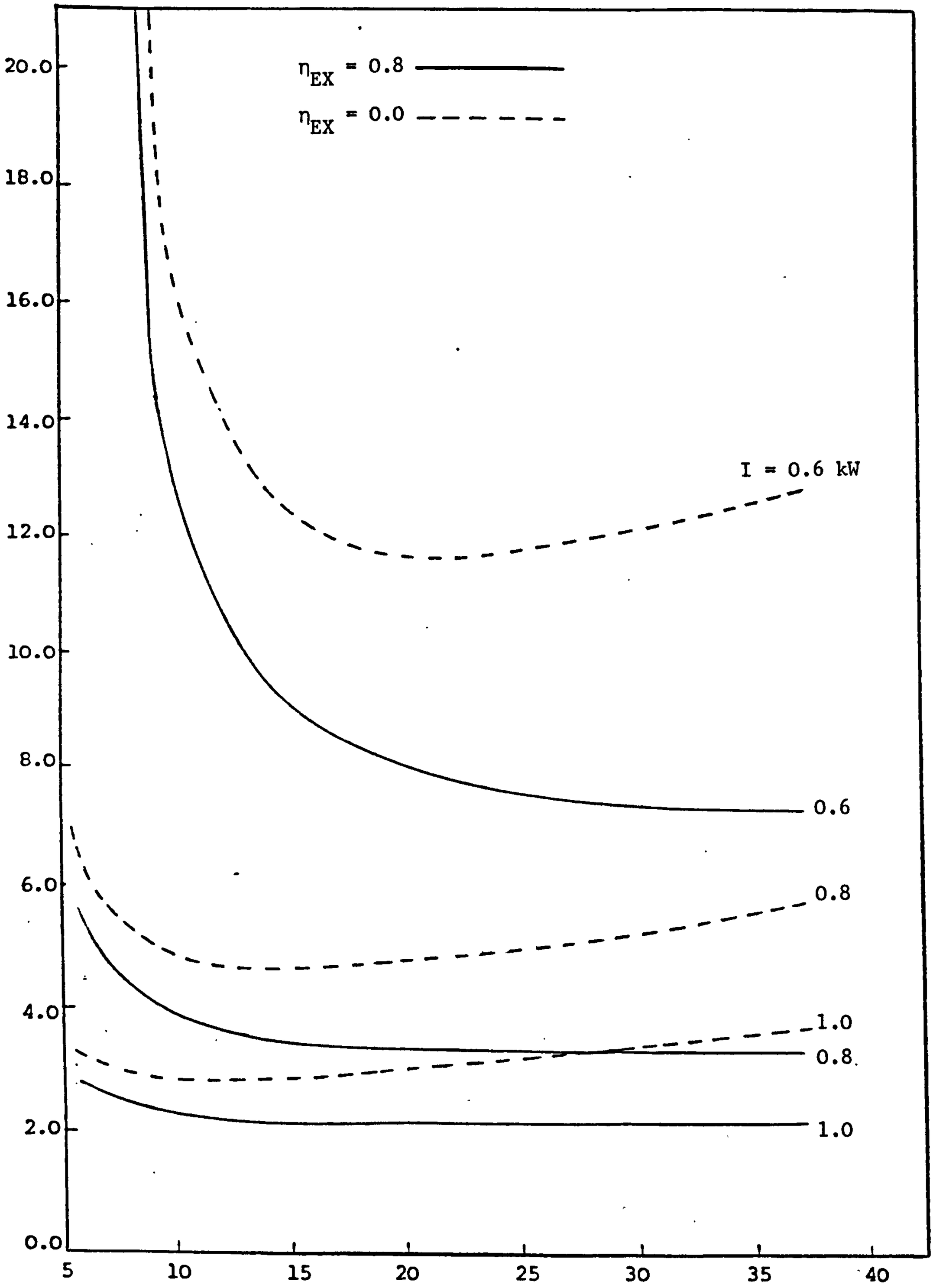

FIGURE 4.12 FLAT PLATE SOLAR COLLECTOR AREA AGAINST FLOW RATIO WITH ECONOMISER HEAT EXCHANGER EFFECTIVENESS AND SOLAR INSOLATION AS PARAMETERS FOR CLOSED CYCLE ABSORPTION COOLING SYSTEM USING WATER-LITHIUM BROMIDE

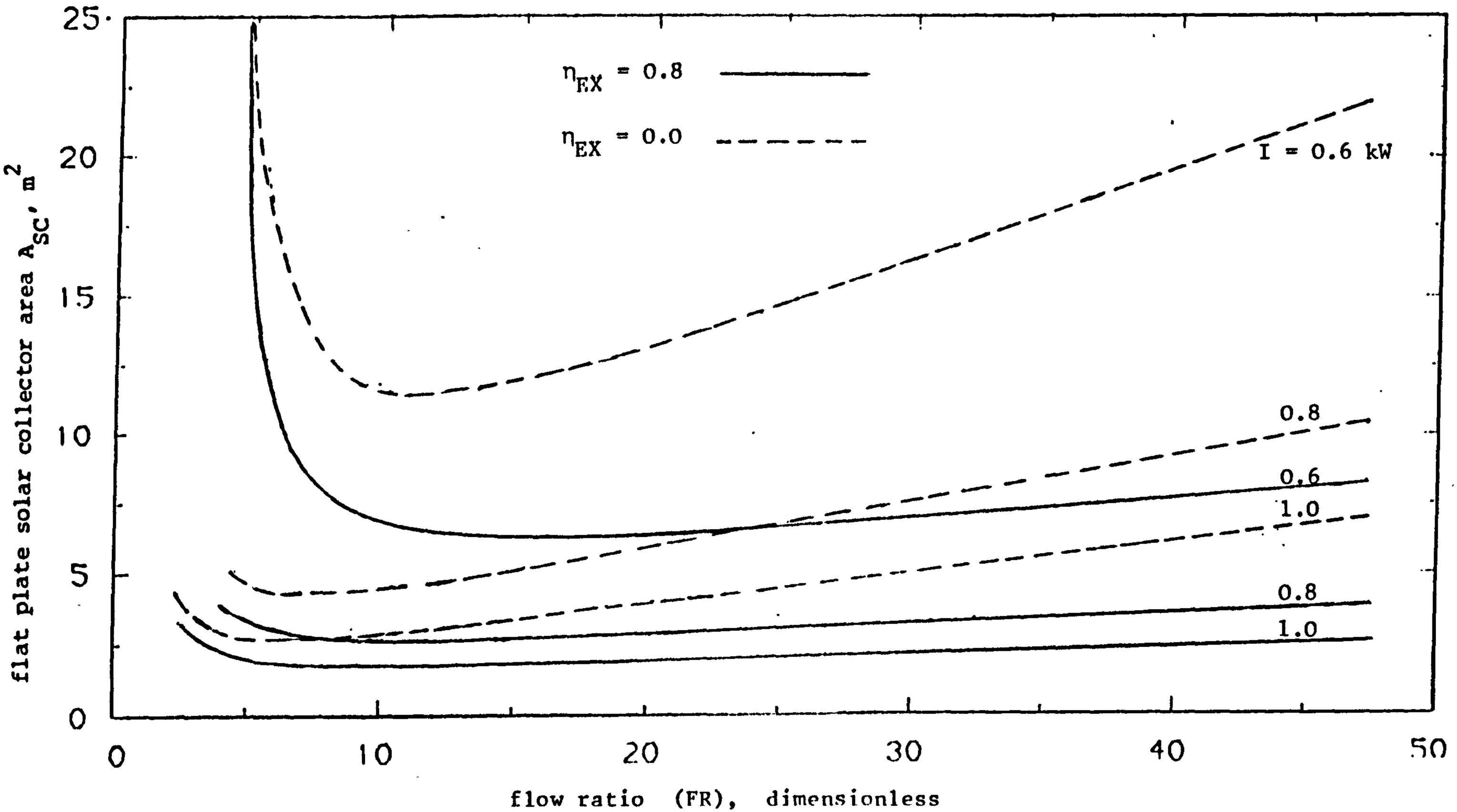

FIGURE 4.13 FLAT PLATE SOLAR COLLECTOR AREA AGAINST FLOW RATIO WITH ECONOMISER HEAT EXCHANGER EFFECTIVENESS AND SOLAR INSOLATION AS PARAMETERS FOR CLOSED CYCLE ABSORPTION COOLING SYSTEM USING AMMONIA-WATER

CHAPTER 5

PERFORMANCE STUDY OF AN EXPERIMENTAL CLOSED CYCLE ABSORPTION COOLING SYSTEM

PERFORMANCE STUDY OF AN EXPERIMENTAL CLOSED CYCLE ABSORPTION COOLING SYSTEM

5.1 INTRODUCTION

Water-lithium bromide is generally regarded as superior to other working fluid combinations for the production of chilled water using absorption cooling cycle. This is because water, apart from its availability, cheapness and lack of toxicity, has a higher latent heat of vaporisation than alternative working fluids such as ammonia. Such systems operate at pressures below atmosphere as compared to about 20 bar required to operate ammonia-water systems. A schematic diagram of the absorption cooling system used for experiments for this chapter is shown in Figure 5.1.

5.2 EQUIPMENT DETAILS

The unit was designed with glass as the material of construction. 1 kW bayonet type heaters in a horizontal alignment were used as the heat source in the generator and in the evaporator. These are not shown in Figure 5.1, but were enclosed in quartz tubes over which the circulating liquids were sprayed from sparge pipes.

The generator, which is shown in Figure 5.1 contained a sparge pipe extending longitudinally over the heater (not shown) and a sump which provided a constant level of solution in the generator. The overflow from the sump passed to the economiser on its way to the absorber. The absorber spray unit was in the form of a standard shower head, made from 0.1 m diameter 316 stainless steel drilled with 2 mm holes, which absorbed the water vapour leaving the evaporator by

direct contact with the solution recirculated by the absorber pump through the external cooler. A separate stream was circulated by a transfer pump through the economiser to the generator. Solution from the generator returned through the economiser to the liquid hold up in the absorber. The system was charged through a stopcock at the top of the absorber and air could be removed by the vacuum pump through another stopcock.

The solution returned to the generator by the transfer pump through the economiser was only a fraction of the volume circulated by the generator pump. The mixture was circulated through the sparge pipe. Water vapour evaporated in the generator passed through a nylon sparge spray eliminator located in a large dome at the top of the generator. This vapour passed through the condenser which was constructed from two standard glass units to form the shape indicated. The top of the condenser was connected to the vacuum pump by a stopcock to allow air to be removed from the condenser and generator during the start-up. The condensate passed to an accumulator which acted as a surge vessel and then through the adjustable expansion valve to the evaporator. The evaporator contained a sparge pipe extending over the heater (not shown) and a level indicator. In operation the energy inputs were adjusted so as to maintain this level constant, as this implied constant concentration of other solutions in the system and steady state operation. Liquid water was recirculated to the sparge pipe by the evaporator pump. The generator, absorber and evaporator pumps were 0.3 kW centrifugal pumps and the transfer pump was a 0.15 kW gear pump. All these pumps were supplied by Michael Smith Engineers Ltd., Surrey, U.K. The circulation rates were measured by a rotameter and were adjusted by speed controllers on the pump drives. The transfer rate from the absorber to the

external absorber cooler was indicated by a rotameter. The cooling water flow rates to the condenser and to the absorber cooler were controlled by needle valves and monitored by rotameters. The cooling water supply was circulated through a constant temperature bath.

Solution samples could be obtained through stopcocks from the generator and absorber. The stopcock in the evaporator had a variety of uses. It enabled the evaporator to be changed or discharged independently of the rest of the system.

The condenser was made from two multicoil condensers type C23/77/3 supplied, as was all glassware used, by Fisons, U.K. and had a total heat transfer area of 0.6 m^2. This was considerably in excess of requirement but the choice was made because the wider cone size reduced the pressure drop through the condenser to an acceptable level. The condenser had thermocouple pockets added which were filled with silicone oil to measure the temperatures of the cooling water stream and of the condensate. The surge vessel was a modified 500 ml separating funnel type D32/2/500. The economiser was a standard multicoil condenser type C4/12 with a heat transfer area of 0.06 m^2, modified by adding thermocouple pockets. Thermocouples measured the inlet and outlet temperatures of the strong and weak solutions.

The external cooler of the absorber was a multicoil condenser type C/23/77/3 with a heat transfer area of 0.3 m^2, modified by adding thermocouple pockets. Strong solution passed outside the coils in parallel with cooling water inside the coils. Thermocouples measured the inlet and outlet temperatures of the liquid streams. The absorber was constructed from a 2L spherical flask with a wide neck type FR 2LF, connected by flanges to a 0.8 mx 0.1 m glass tube, with 9 thermocouple

pockets spaced at 0.07 m intervals from the bottom. All thermocouples conformed to BS 4937 type K and were connected to a 30 point digital indicator type 206 CRL of ± 0.5 K accuracy. The temperature of the liquid phases in the generator, evaporator and absorber were monitored by a three point recorder (Chessell Ltd., UK, model 303). Steadiness of the temperature traces for more than 30 minutes was used as the criterion that steady state had been reached.

Electrical power to the heaters in the generator and the evaporator was controlled by a variac whose output power was measured by ammeter and voltmeter readings precalibrated against a standardising wattmeter.

The equipment worked under reduced pressure produced by a vacuum pump. Edwards model CG3 dial vacuum manometers were used to measure the absolute pressure against the generator and absorber with ranges of 0 to 125 mbar and 0 to 25 mbar respectively. These manometers had an accuracy of ± 5 per cent of full scale deflection.

5.3 EXPERIMENTAL TECHNIQUE

The variables measured and controlled in the experimental work were temperature, pressure, electrical power input and salt concentration. Twenty seven temperatures, two pressures, two concentrations, two flow rates and two power inputs were measured. Measurement points have been shown in Figure 5.2. The salt solutions were made from anhydrous lithium bromide of 99.7 per cent purity. It was considered that extra purification of the LiBr was not worthwhile beyond a double filtration of the solution to remove any insoluble matter. Analysis of such solutions based on the refractive index and on density measurements

showed excellent conformity with published data. For this re..., refrective index measurements, made with an Abbe 60/ED refractometer supplied by Bellingham and Stanley Ltd., U.K., were only used for a quick assessment of conditions when setting up an experiment.

The main difficulty in the experimental work with so many joints in the equipment was to maintain leak tightness. This was effectively achieved by the use of high vacuum grease in the cone and socket joints which were additionally coated with plastic sealant. Individual units were protected from vibration by smoothing out boiling and minimising pump fluctuations. The remaining danger, increased by the high salt concentrations, was crystallization. A safe temperature margin for a given concentration was decided by the crystallization characteristics. A specially designed temperature alarm was set to give an audible and visual warning of different kinds if the temperature of the strong solution at the outlet of the economiser or of the weak solution at the outlet of the absorber cooler fell below these values. This enabled rapid attention to be given if sudden changes occurred.

By adding about 500 ml of water to the system prior to shut down, no crystallisation occurred in the apparatus during experimentation. This represents about 10 per cent of the liquid holdup in the apparatus. Initially, the maximum possible vacuum was established over a period of about 2 hours. A solution containing about 55 per cent Li Br was then charged into the absorber and circulated by the transfer pump to the generator. Solution would already be present for subsequent runs. The vacuum pump was operated throughout an experiment to remove any air which might enter the system. It was necessary to provide a cold trap using dry ice to prevent any water

reaching the oil in the vacuum pump. The pump was started, the generator heater was operated at about 150 V and the condenser was supplied with cooling water at a temperature appropriate to the particular experimental run. The flow rate from the absorber to the generator was adjusted by controlling the speed of the transfer pump. As vapour passed to the condenser, the variac controller was gradually adjusted to a higher value of voltage to the heater. In about twenty minutes the volume of liquid in the accumulator reached a preset mark and the required concentration difference. The evaporator and the evaporator heater were switched on and the expansion valve adjusted to maintain the preset level in the accumulator. The variac controlling the evaporator heater was adjusted until the liquid level in the evaporator was constant, which was a clear indication that steady state conditions had been achieved. During this adjustment it was also necessary to adjust the flow rates of the cooling water to the condenser and to the absorber. Steady state conditions were considered to have been established when liquid temperature in the generator, evaporator and absorber, as shown by temperature recorder, were constant for at least 30 minutes.

5.4 PLAN OF THE EXPERIMENTS

There is a lack of published comprehensive experimental performance data for absorption cooling systems. Preliminary results have been presented elsewhere (Landauro-Paredes et al 1983). The authors studied the feasibility of air cooling the absorber and condenser in absorption cooler. The objective of the present work was to study the possibility of lower generator temperatures for a given cooling requirement. This would facilitate the use of low temperature heat energy sources such as waste heat from industrial processes,

5.4.1 Analysis of the reported data

The coefficient of performance of a cooling system is defined as the ratio of the energy extracted in the evaporator Q_{EV} to produce the desired cooling to the energy supplied to the generator Q_{GE}.

$$(COP) = \frac{Q_{EV}}{Q_{GE}} \tag{5.1}$$

The flow ratio (FR) which is defined as the ratio of the mass flow rate of solution from the generator to the absorber to that of the mass flow rate of vapour from the evaporator to the absorber, is used in this analysis. The flow ratio can be defined in terms of concentration as follows

$$(FR) = \frac{X_{AB}}{X_{GE} - X_{AB}} \tag{5.2}$$

From the experimental results reported by Landauro Paredes et al (Landauro-Paredes 1982) some data points were selected for which the concentration of lithium bromide in the generator was constant. Figure 5.3 illustrates the behaviour of the typical parameters as a function of the flow ratio for a fixed concentration in the generator $x_{GE} \simeq 0.65$. It can be seen that $(COP)_{ACL}$ remains nearly constant over the range of these experiments. It is also interesting to note that all the four temperatures T_{GE}, T_{CO}, T_{AB} and T_{EV} show similar trends with flow ratio and the temperatures differences $(T_{CO} - T_{EV})$, $(T_{AB} - T_{EV})$ and $(T_{GE} - T_{CO})$ remain almost constant. These constant values of $(T_{CO} - T_{EV})$ and $(T_{AB} - T_{EV})$ imply that, if higher condenser and absorber temperatures are required the system can only operate with correspondingly higher evaporator temperatures. Figure 5.4 shows the variation of heat loads with flow ratio. The trends of these heat loads are more or less the same so that $(COP)_{ACL}$ is

substantially independent of flow ratio. The performance of the economiser heat exchanger was found to vary with changes in flow ratio. The heat losses from the original experimental system were also seen to be high so that the lagging was improved.

5.4.2 Present experiments

Theoretical considerations indicate that for a required evaporator temperature, the generator temperatures can be decreased by operating at relatively high flow ratios (Chapter 4). Therefore, further experiments were carried out with the flow ratio as the main variable. The heat flux in the economiser varies with changes in flow ratio and this can complicate the interpretation of the results. Therefore, some of the experiments were carried out without it. For a particular condition the effect of the economiser heat exchanger on the performance is straightforward and the results obtained can be suitably modified. This was verified by conducting some experiments with economiser heat exchanger.

5.5 RESULTS AND DISCUSSION

5.5.1 Effect of flow ratio on the absorption cooling system

All the experiments for this section were carried out without the economiser heat exchanger. Figure 5.5 shows the variation of different parameters with varying flow ratio for an absorber solution concentration X_{AB} of about 59.5 per cent. The $(COP)_{ACL}$ values and the T_{GE} values have been plotted for different condenser temperatures. It can be seen that with increasing flow ratio, the T_{GE} values decrease and the curves tend to become flat for (FR) values beyond 30.0. It can also be seen that for a given flow ratio, T_{GE} decreases

and $(COP)_{ACL}$ increased with decrease in T_{CO}, but this limit is fixed by the temperature of the cooling medium. As the flow ratio is increased, the absorber temperature T_{AB} increases because of the enhanced thermal carry over by the hot solution from the generator. If the temperature T_{AB} could be kept constant by increasing the flow rate of the cooling medium to the absorber, the system could be operated without affecting the evaporator. However, because of the limitations in a practical system T_{AB} could not be maintained constant although the variation of T_{EV} is not significant. This is due to the fact that the heat loads Q_{GE} and Q_{EV} had to be manipulated to obtain this condition. This can be seen from Figure 5.6 which shows the variation of the heat loads for the corresponding range of flow ratios. Figure 5.6 shows that as the flow ratio is increased, Q_{AB} increases and Q_{CO} decreases. Both these heat loads are complimentary to each other. Therefore the total cooling load of the absorber and the condenser can be met by nearly the same amount of cooling medium. Therefore if the generator is to be operated at a higher flow ratio (FR), i.e., at a lower heat source temperature, the penalty is slight reduction in the cooling capacity.

It has been demonstrated experimentally that by using high flow ratios in an absorption cooling system it is possible for a given evaporator temperature to reduce the generator temperature. This broadens the scope for relatively low temperature heat source, like solar energy, to be used in these systems.

Although the economiser was not used in these experiments, $(COP)_{ACL}$ values are higher than the previous set of values presented in Figure 5.3. This can be attributed to the improved lagging on the unit.

The actual coefficient of performance $(COP)_{ACL}$ values were correlated by an equation of the following form with a root mean square residual (RMSR) of 0.0328 :

$$(COP)_{ACL} = B_1 + B_2 (FR) + B_3 (COP)_{CCL} \qquad (5.3)$$

where, $B_1 = -0.1704$

$B_2 = -9.95 \times 10^{-4}$

$B_3 = 0.3934$

where, $(COP)_{CCL}$ is the Carnot coefficient of performance defined by

$$(COP)_{CCL} = \left(\frac{T_{EV}}{T_{CO} - T_{EV}}\right)\left(\frac{T_{GE} - T_{AB}}{T_{GE}}\right) \qquad (5.4)$$

The ranges of experimental conditions were as follows

$X_{AB} = 0.575$ to 0.625

$T_{GE} = 72.0$ to $107.0^{o}C$

$T_{CO} = 34.5$ to $49.0^{o}C$

$T_{AB} = 24.0$ to $42.5^{o}C$

$T_{EV} = 5.5$ to $15.0^{o}C$

5.5.2 Interaction of economiser heat exchanger in absorption cooling systems

Economiser heat exchangers are normally incorporated in absorption cooling systems. They are used to transfer heat between the two solution streams as shown in Figure 5.1.

For an absorption cooling system without economiser heat exchanger, the coefficient of performance $(COP)'_{CL}$ can be defined as

$$(COP)'_{CL} = \frac{Q'_{EV}}{Q'_{GE}} \tag{5.5}$$

The incorporation of an economiser heat exchanger can interact with the system in two ways.

1) First consider the same cooling load Q'_{EV}.

   a) The heat transferred in the economiser heat exchanger Q_{EX} will increase the capacity of the absorber so that a smaller absorber can be used.

   b) The amount of heat required in the generator Q'_{GE} will be reduced by Q_{EX}.

   For this case the coefficient of performance can be written as

$$(COP)'_{CL} = \frac{Q'_{EX}}{Q'_{GE} - Q_{EX}} = \frac{Q'_{EV}}{Q_{GE}} \tag{5.6}$$

2) Secondly consider the same generator heat load Q'_{GE}.

a) The amount of vapour produced in the generator will be increased. Therefore the capacity of the condenser needs to be increased.

b) The capacity of the absorber will be increased.

c) For a steady evaporator temperature T_{EV}, the capacity of the evaporator needs to be increased.

For this case the coefficient of performance can be written as

$$(COP)_{CL}' = \frac{Q_{EV}' + Q_{EX}}{Q_{GE}'} = \frac{Q_{EV}}{Q_{GE}'} \qquad (5.7)$$

Results have already been presented without an economiser heat exchanger in Section 5.5.1. Further experiments have been carried out with an economiser heat exchanger. Typical performance data are presented in Figures 5.7 and 5.8. Figure 5.7 shows the variation of the different parameters with flow ratio for an absorber solution concentration of about 59.5 per cent. Curves for the actual coefficient of performance $(COP)_{ACL}$ and generator gemperature T_{GE} have been plotted for two different condensing temperatures. The trends are similar to the results presented in Section 5.5.1. For a typical flow ratio of 30.0, $(COP)_{ACL}$ is almost the same but the evaporator temperature T_{EV} is lower by about 2.0 to 3.0^{o}C. The generator and absorber heat loads have been decreased whilst the condenser and evaporator heat loads remain substantially the same.

Since the experimental conditions with and without the economiser heat exchanger were not identical, the data were analysed using an empirical correlation. Fifteen experimental data points were fitted to the correlation

$$(COP)'_{ACL} = \frac{Q_{EV} - B_2\, Q_{EX}}{Q_{GE} + B_1\, Q_{EX}} \qquad (5.8)$$

where Q_{EV}, Q_{GE} and Q_{EX} are experimental values. $(COP)'_{ACL}$ is the actual coefficient of performance for the unit without the economiser heat exchanger for identical conditions of temperature and concentration. $(COP)'_{ACL}$ was calculated from Equation (5.3) using actual experimental values of temperature (T_{GE}, T_{CO}, T_{AB} and T_{EV}) and concentrations (X_{GE} and X_{AB}).

The model given by Equation (5.8) was fitted using a nonlinear regression technique with a root mean square residual of 0.042.

The final correlation can be written as

$$(COP)'_{ACL} = \frac{Q_{EV} - 0.12\, Q_{EX}}{Q_{GE} + Q_{EX}} \qquad (5.9)$$

This implies that the evaporator capacity is limited whereas the generator heat load could be reduced by an amount equivalent to the heat transferred in the economiser.

If experimental data were to be obtained for comparative evaporating temperatures, the $(COP)_{ACL}$ values with the economiser would be relatively high. In the present work evaporating temperatures T_{EV} averaged about $7^{o}C$ compared to $10^{o}C$ in Section 5.5.1. The value of $(COP)_{ACL}$ is bound to decrease as the evaporating temperature is decreased (Lazzarin 1980).

5.6 DESIGN SEQUENCE FOR AN ABSORPTION COOLING SYSTEM

Figure 5.9 illustrates a design sequence for absorption cooling systems. As a starting point, four variables can be fixed independently. These are generator heat source temperature T_{GS}, condenser/absorber cooling medium temperature T_{CS}, evaporator heat source temperature T_{ES} and evaporator heat load Q_{EV} or generator heat load Q_{GE}. Specifications of these four variables fix the rest of the conditions with eleven design variables to be fixed by the designer. The first four design variables are the temperature approaches in the generator ΔT_{GE}, in the condenser ΔT_{CO}, in the absorber ΔT_{AB} and in the evaporator ΔT_{EV}. These temperature approaches fix the generator temperature T_{GE}, the condenser temperature T_{CO}, the absorber temperature T_{AB} and the evaporator temperature T_{EV}, as shown in Figure 5.9. Now because of condensation and evaporation of pure refrigerant vapour in the condenser and evaporator respectively, the condenser pressure P_{CO} and the evaporator pressure P_{EV} can be fixed to the corresponding saturation pressures. An allowance for the pressure drop between the absorber and evaporator $(\Delta P)_{AB}$ decides the absorber pressure P_{AB}. Minimum possible concentration of the absorbent in the absorber X_{AB} at steady state can be the equilibrium concentration corresponding to the temperature T_{AB} and pressure P_{AB}. The actual concentration of absorbent should be decided at this point depending on the design of the absorber. Similarly, the absorbent concentration in the generator X_{GE} could be decided. The flow ratio (FR) can now be calculated by Equation (5.2) and the Carnot coefficient of performance by Equation (5.4). At this stage a realistic value of thermodynamic effectiveness of the system based on experimental and theoretical analysis could lead to a reasonable value of $(COP)_{CL}$. This $(COP)_{CL}$ value could be used to find out the generator heat load Q_{GE} if the cooling load Q_{EV} is specified or vice versa. Finally, the energy balance

could be used to determine the absorber heat load Q_{AB} and the condenser heat load Q_{CO}.

All the experimental performance data of this Chapter are given in Appendix B.

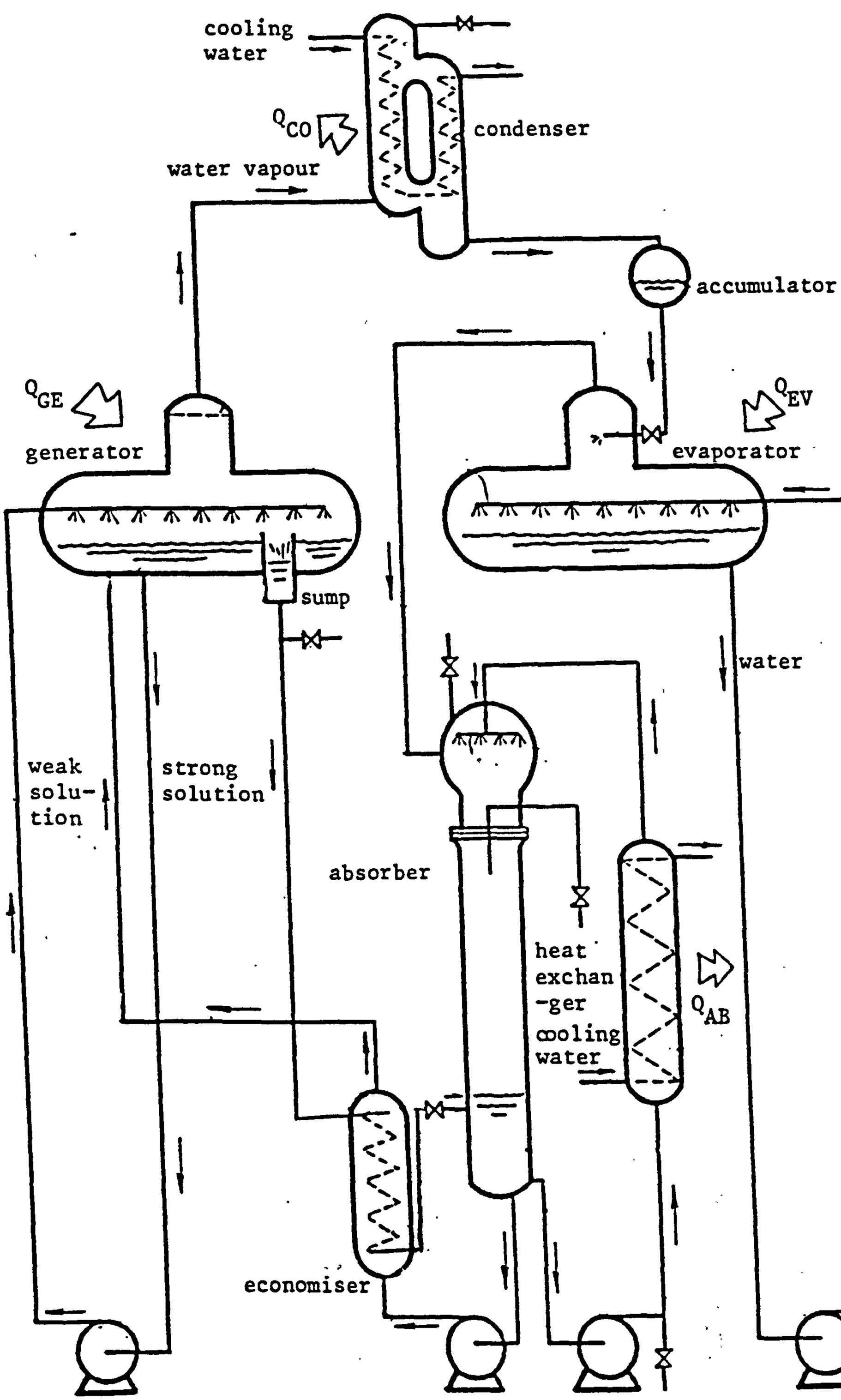

FIGURE 5.1 SCHEMATIC DIAGRAM OF THE EXPERIMENTAL ABSORPTION COOLING SYSTEM

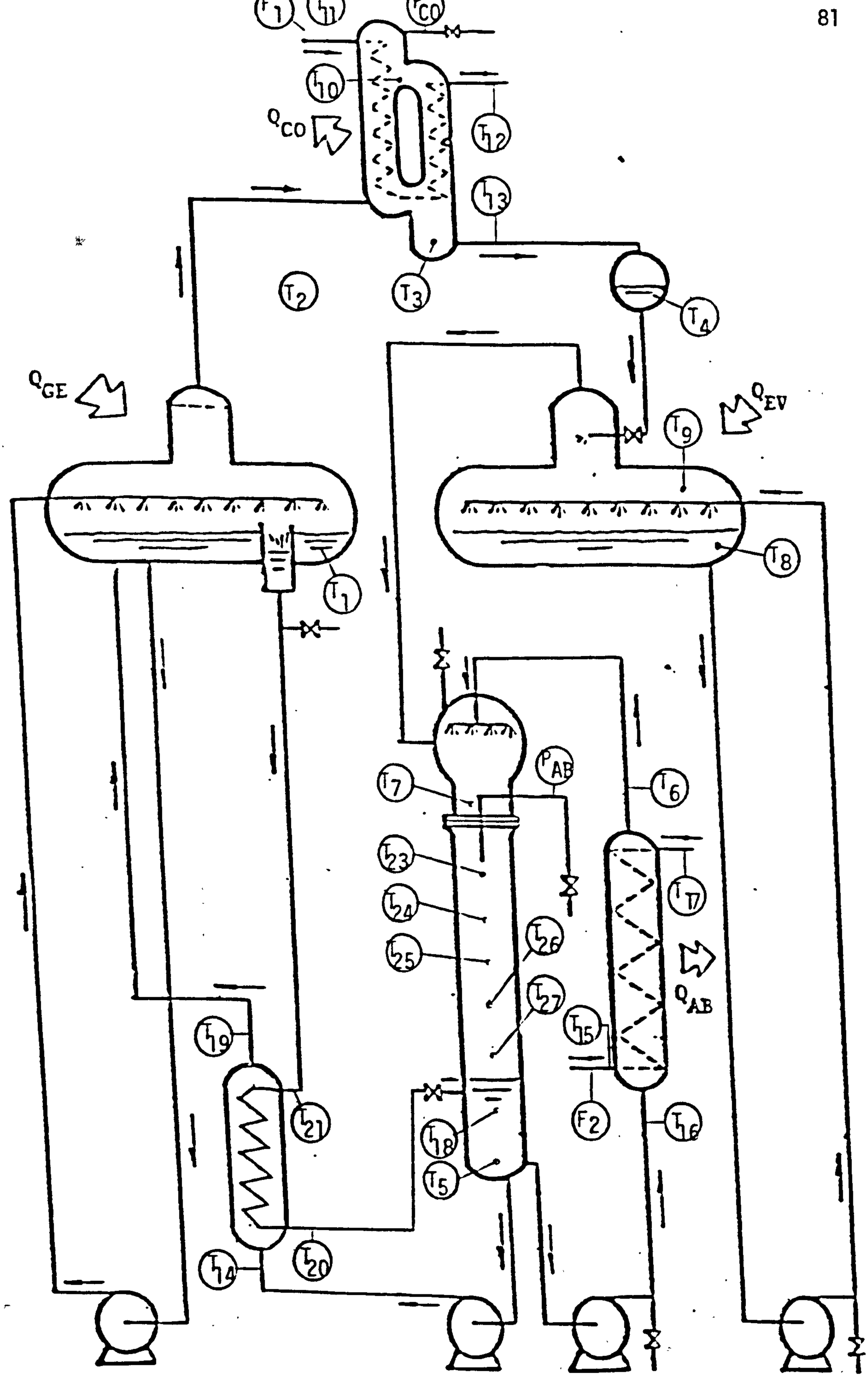

FIGURE 5.2 INSTRUMENTATION DIAGRAM OF ABSORPTION COOLING SYSTEM

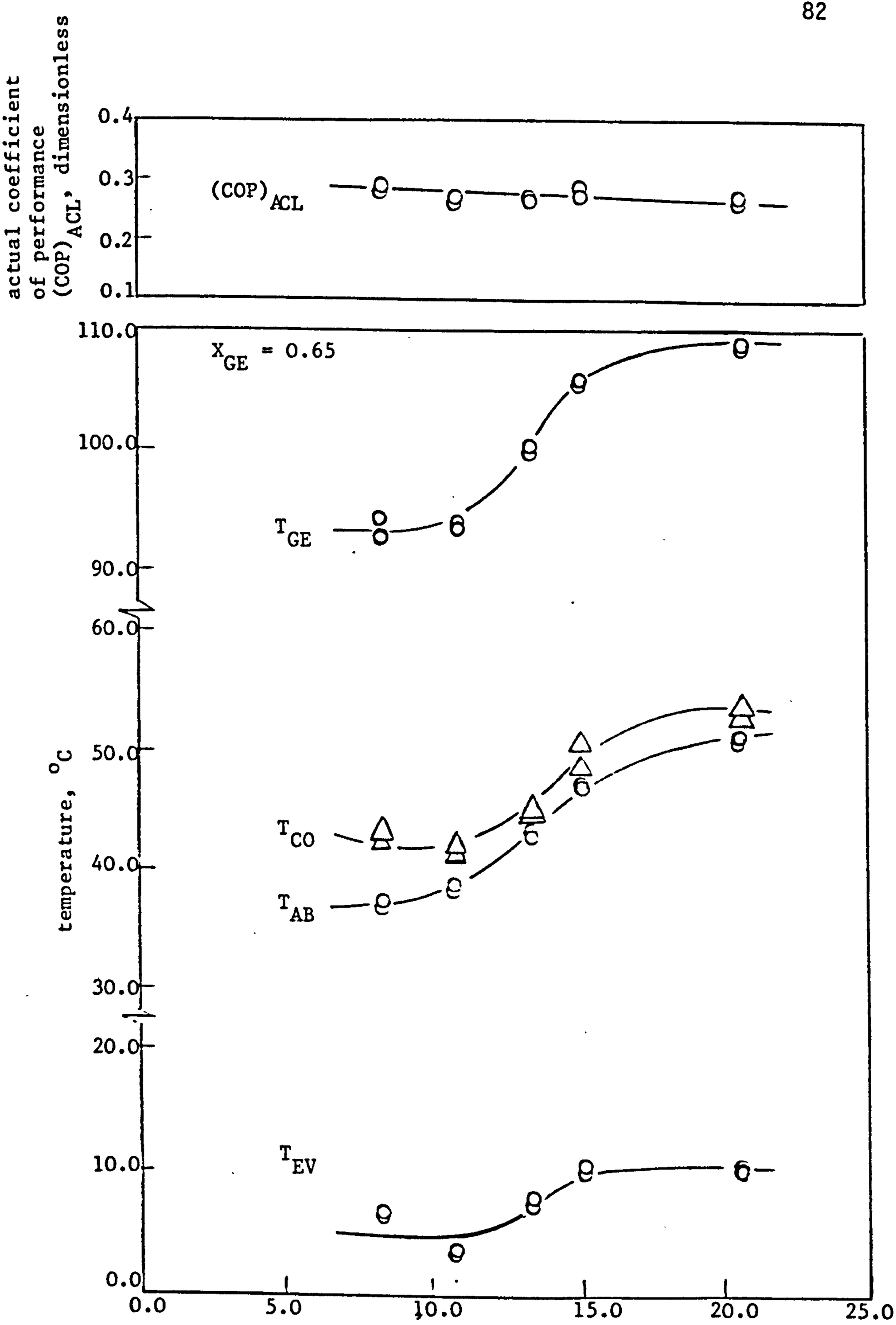

FIGURE 5.3 PERFORMANCE CHARACTERISTICS OF THE EXPERIMENTAL ABSORPTION COOLING SYSTEM AS A FUNCTION OF FLOW RATIO USING WATER-LITHIUM BROMIDE FOR X_{GE} = 0.65

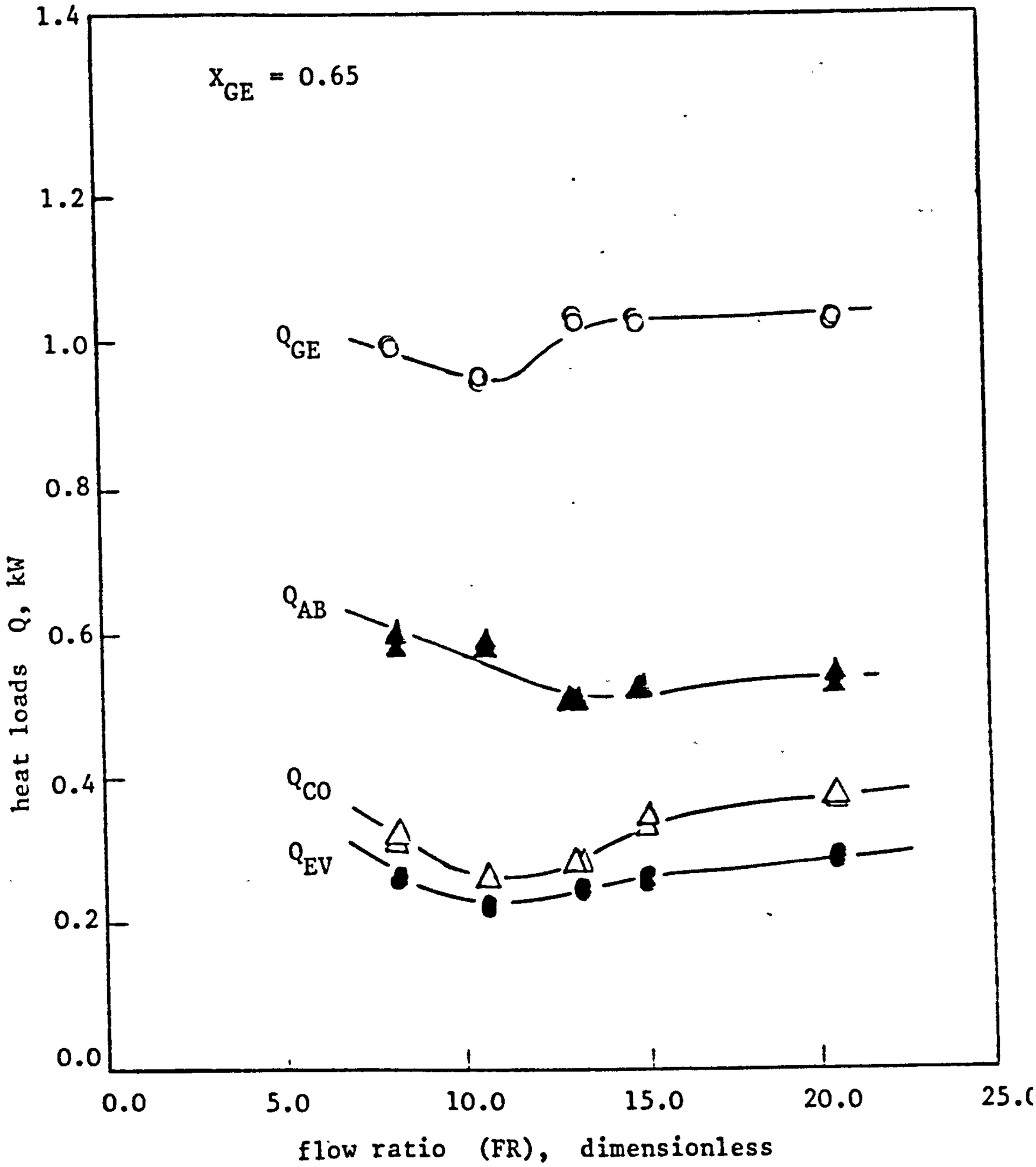

FIGURE 5.4 HEAT LOADS IN THE EXPERIMENTAL ABSORPTION COOLING SYSTEM AS A FUNCTION OF FLOW RATIO USING WATER-LITHIUM BROMIDE FOR X_{GE} = 0.65

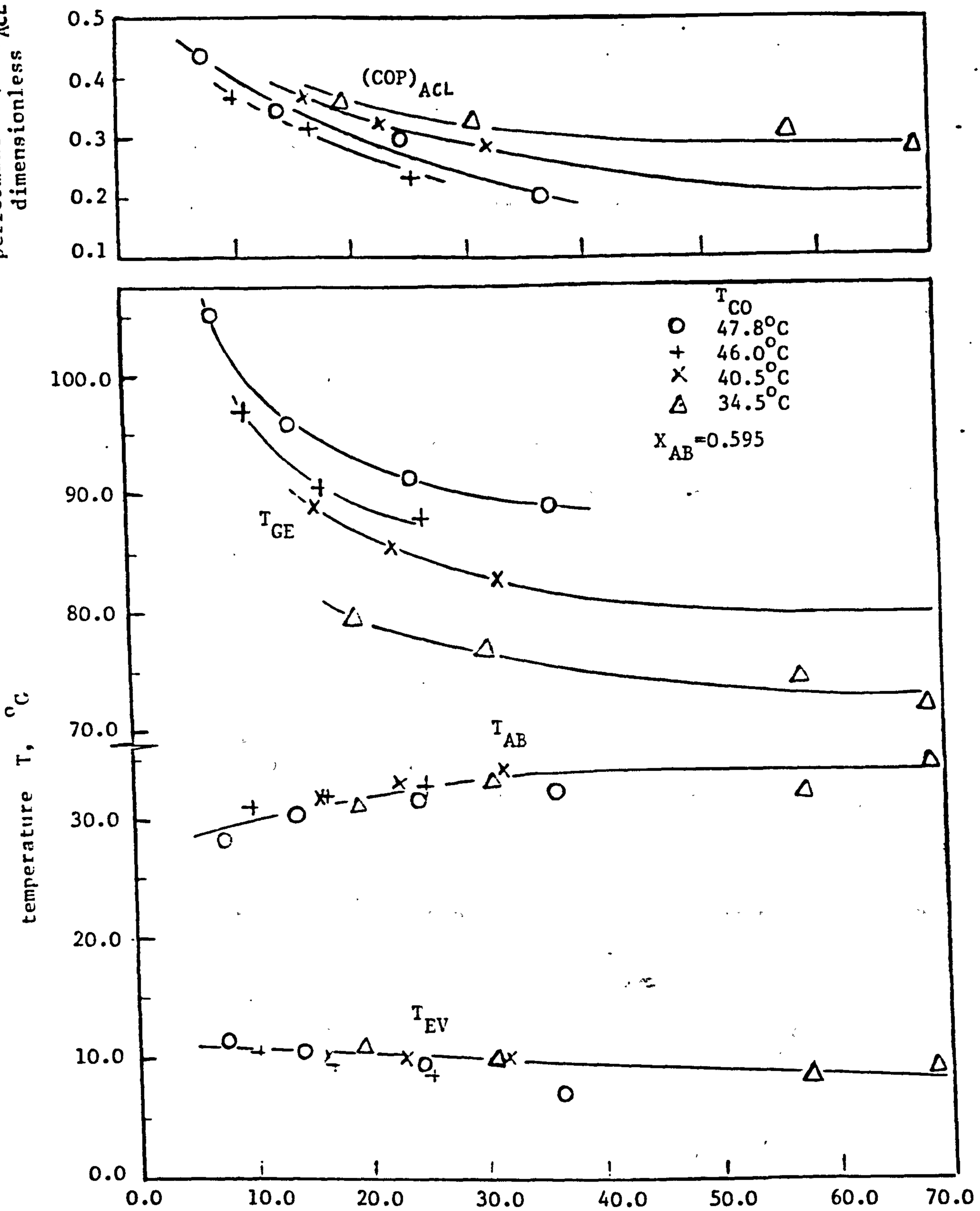

FIGURE 5.5 PERFORMANCE CHARACTERISTICS OF THE EXPERIMENTAL ABSORPTION COOLING SYSTEM AS A FUNCTION OF FLOW RATIO USING WATER-LITHIUM BROMIDE

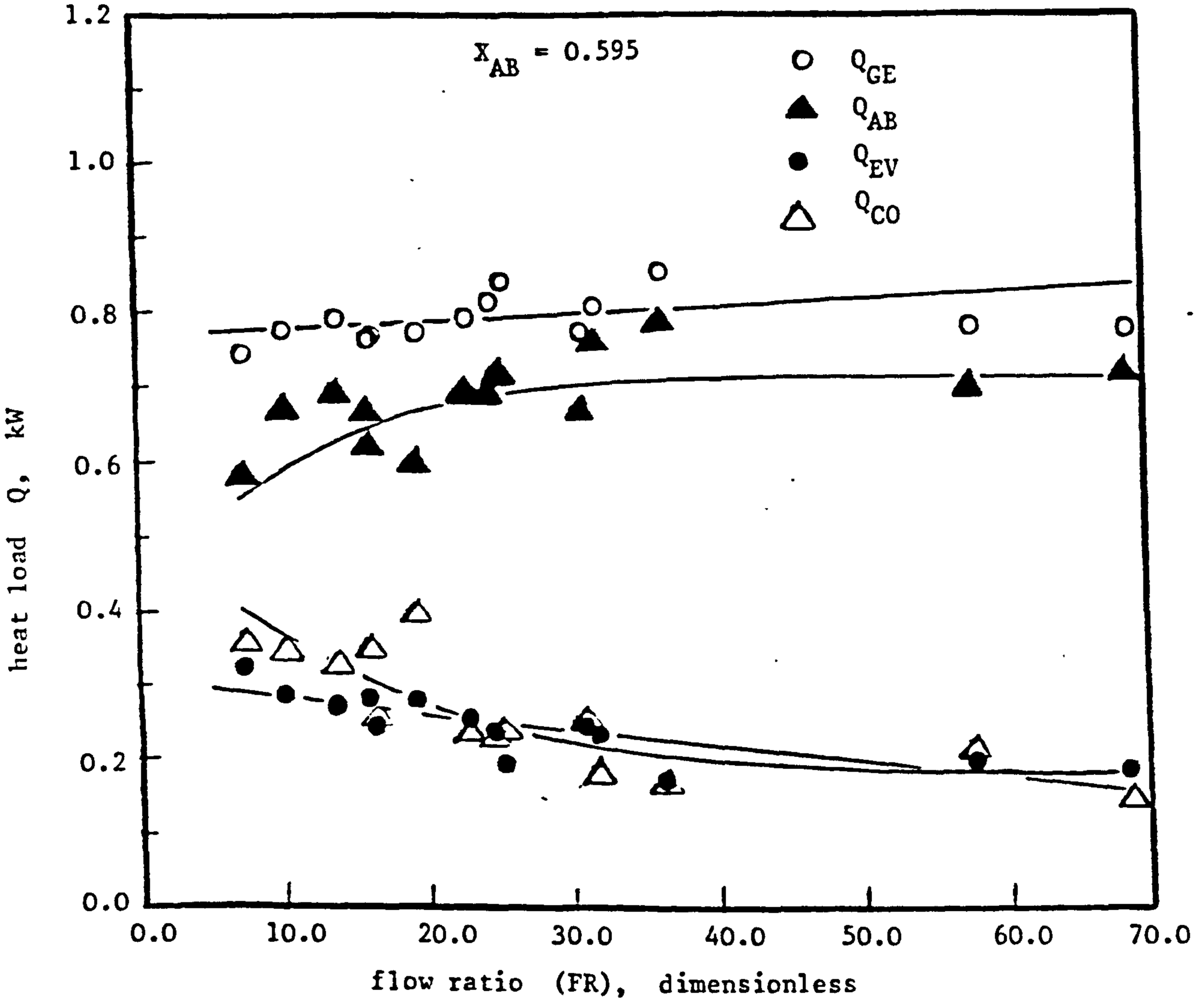

FIGURE 5.6 HEAT LOADS IN THE EXPERIMENTAL ABSORPTION COOLING SYSTEM AS A FUNCTION OF FLOW RATIO USING WATER-LITHIUM BROMIDE

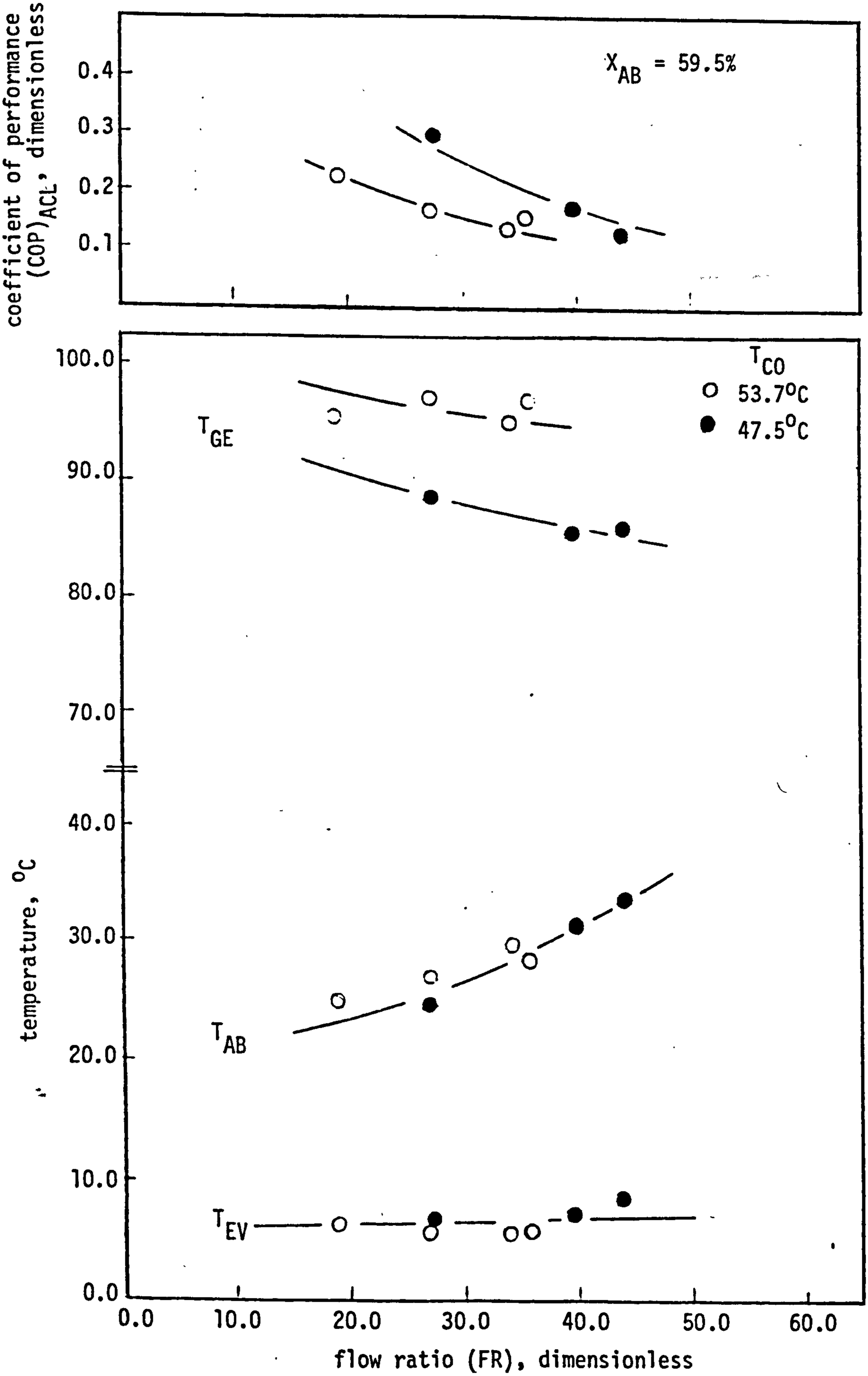

FIGURE 5.7 PERFORMANCE CHARACTERISTICS AS A FUNCTION OF FLOW RATIO

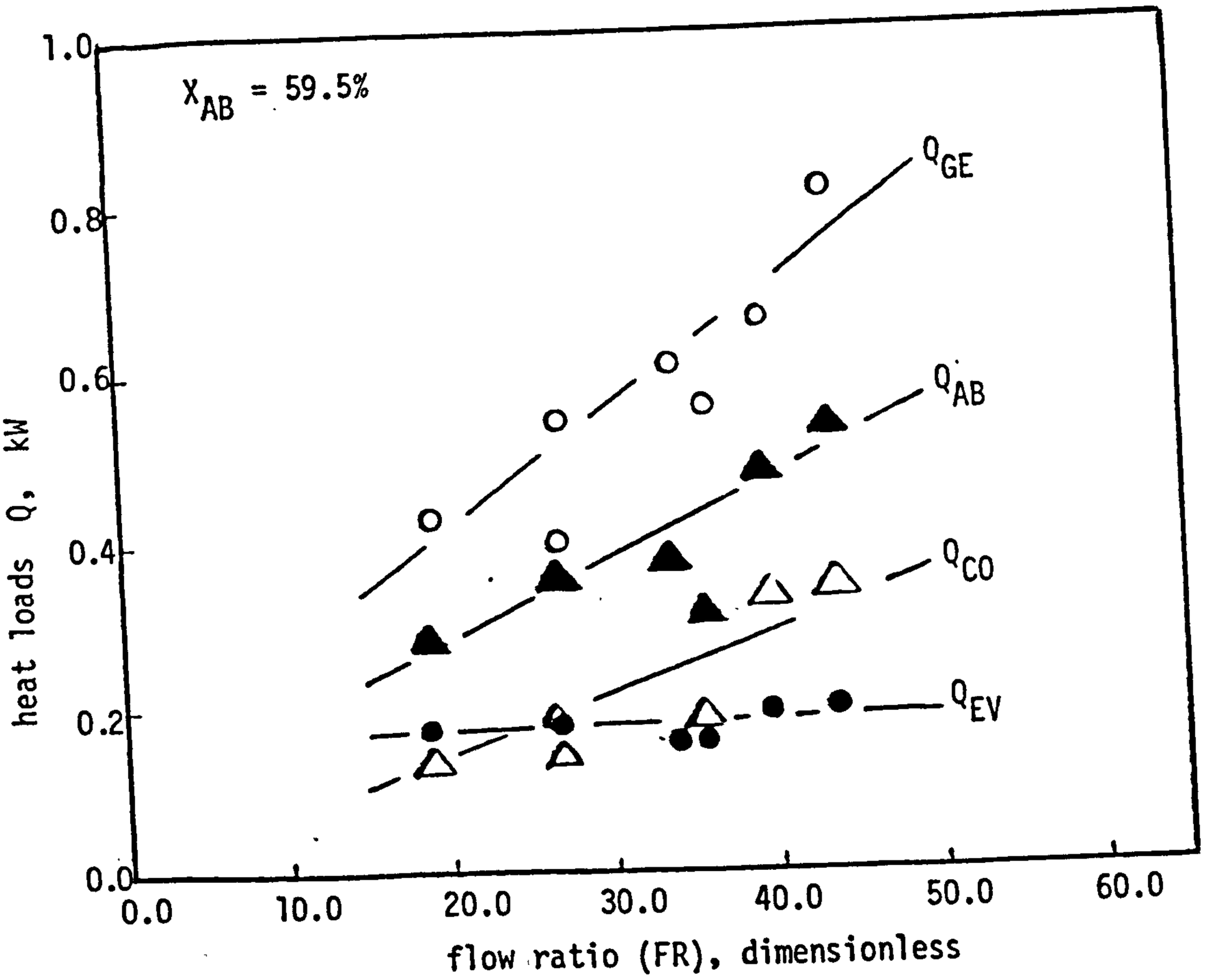

FIGURE 5.8 HEAT LOADS AS A FUNCTION OF FLOW RATIO

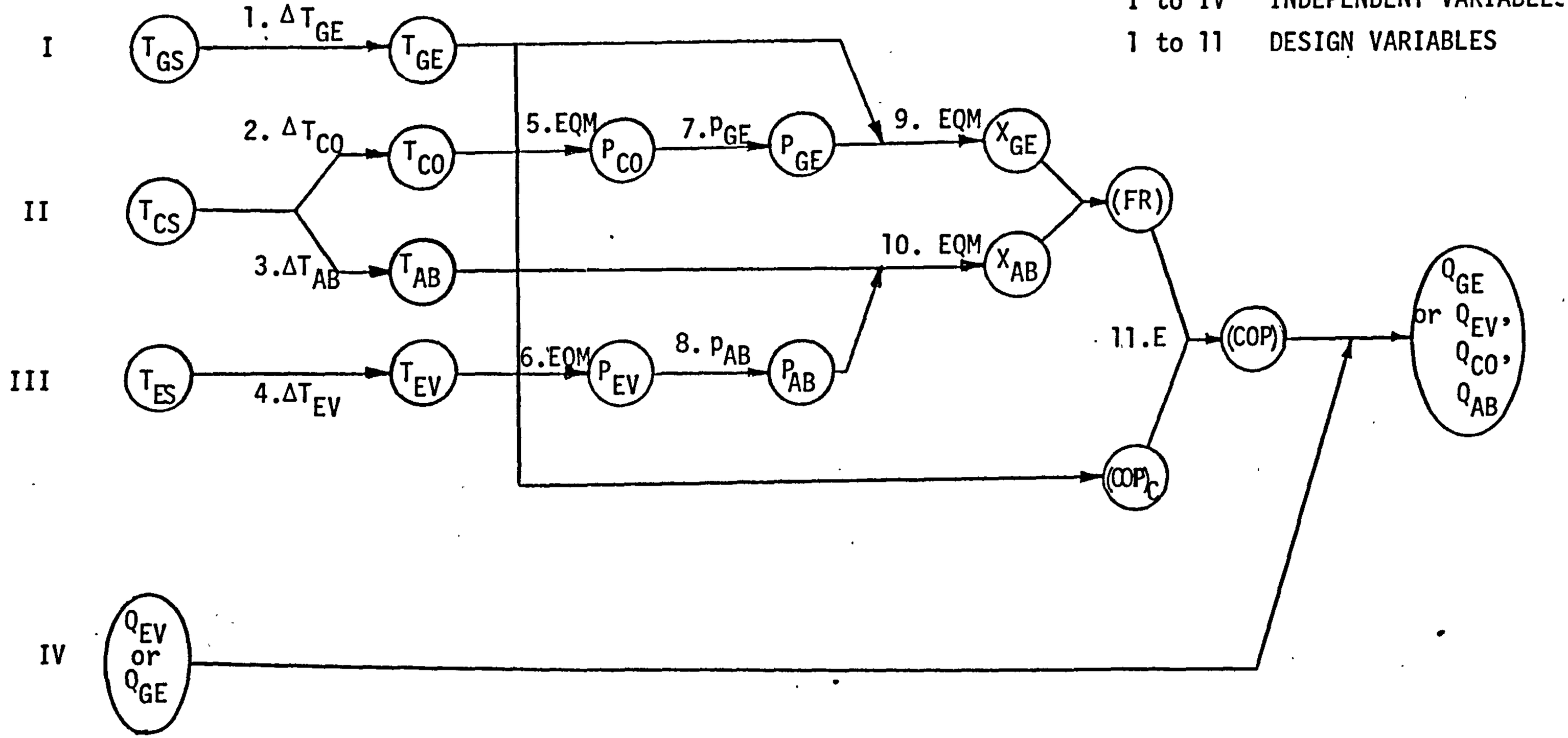

FIGURE 5.9 DESIGN SEQUENCE FOR AN ABSORPTION COOLING SYSTEM

CHAPTER 6

ANALYSIS OF A CLOSED CYCLE ABSORPTION SYSTEM FOR SIMULTANEOUS COOLING AND HEATING

ANALYSIS OF A CLOSED CYCLE ABSORPTION SYSTEM FOR SIMULTANEOUS COOLING AND HEATING

6.1 INTRODUCTION

Many industrial processes require both cooling and heating at different stages in their operation. An absorption system, capable of providing simultaneous cooling and heating, could save both energy and money in such processes.

If the main purpose is to remove heat at the evaporator, usually at a temperature below ambient, the system is an absorption cooling unit. On the other hand if the main purpose is to deliver heat at the absorber and condenser, usually at a temperature well above ambient, the system is an absorption heating unit.

Simultaneous cooling and heating would require a large gross temperature lift $(T_{CO} - T_{EV})$, and correspondingly a high compression ratio P_{CO}/P_{EV} (Holland et al 1982). This may not be feasible or economic with a mechanical vapour compression system. However, in an absorption system, the increase in pressure is accomplished in the liquid phase with an insignificant amount of mechanical energy.

6.2 PRACTICAL CONSIDERATIONS

Temperature lifts can be increased in absorption systems either by increasing the condenser temperature T_{CO} or by decreasing the evaporator temperature T_{EV}.

The increase in the condenser pressure P_{CO}, which accompanies an increase in T_{CO}, leads to a higher solution temperature in the generator which is almost at a pressure P_{CO}. This is undesirable since it leads to higher absorber temperatures T_{AB}. However, the condenser pressure P_{CO} could be increased without an increase in T_{AB} if the hot solution leaving the generator was cooled prior to entry into the absorber.

The evaporator temperature T_{EV} can be decreased by reducing the vapour pressure of the refrigerant in the absorber. This requires an increase in the mass transfer potential in order to increase the rate of absorption. The mass transfer potential is the difference between the vapour pressure of refrigerant in the absorber and the vapour pressure of the refrigerant corresponding to the temperature and solution concentration in the absorber.

The mass transfer potential can be increased either by decreasing the refrigerant concentration in the solution or by reducing the temperature of the solution.

The minimum concentration of refrigerant in the solution is fixed by the acceptable lower limit for the generator efficiency. This drops rapidly with a decrease in refrigerant concentration. In the water-lithium bromide system, where water is the refrigerant, the water concentration is limited by the crystallisation point. In the ammonia-water system, where ammonia is the refrigerant, the limitation is the size of the rectification column required to separate the ammonia.

In a conventional absorption system, the temperature of the solution from the generator is decreased by the economiser heat exchanger before entry into the absorber. The temperature of this solution can be further reduced by incorporating a second heat exchanger prior to the absorber. This would enable the condenser temperature T_{CO} to be increased and lead to a reduction in the evaporator temperature T_{EV} so that the gross temperature lift $(T_{CO} - T_{EV})$ would be increased.

In a water cooled system, the cooling water should first go to the absorber, then to the solution heat exchanger and finally to the condenser. In the following analysis, the heat exchanger load has not been considered separately but has been accounted for as part of the absorber heat load Q_{AB}.

6.3 THEORETICAL CONSIDERATIONS

A representation of the absorption system analysed is shown schematically in Figure 6.1 . The working fluid pair used for the analysis is water-lithium bromide. The heat losses and unintentional pressure drops in the pipeline and the equipment are assumed to be negligible. The water vapour, at state point 1, is assumed to be saturated vapour at T_{EV}. The water at state point 9 is also assumed to be saturated at T_{CO}. The aqueous solution of lithium bromide at state point 6 is assumed to be in equilibrium with water vapour at state point 8. Solution concentration and temperature at state point 3 are assumed to be 0.56 and $35^{o}C$ respectively. This corresponds to water vapour pressure of 8 mbar at equilibrium. These conditions are so chosen that the solution at the bottom of the absorber (state point 3)

attains equilibrium, when the evaporator temperatures is $5^{o}C$.

The coefficient of performance of an absorption system when it is operated as a heat pump and cooling system, can be defined by Equation (6.1) and Equation (6.2) respectively.

$$(COP)_H = (Q_{CO} + Q_{AB})/Q_{GE} \tag{6.1}$$

$$(COP)_{CL} = Q_{EV}/Q_{GE} \tag{6.2}$$

The overall energy blance of an absorption system assuming no heat losses to the environment, can be written as follows

$$Q_{EV} + Q_{GE} + W_P = Q_{CO} + Q_{AB} \tag{6.3}$$

The energy W_P added to the system through the solution pump is very small and can be neglected when compared to the other terms in Equation (6.3). Therefore, Equation (6.3) can be written as follows

$$Q_{EV} + Q_{GE} = Q_{CO} + Q_{AB} \tag{6.4}$$

Now from Equations (6.1), (6.2) and (6.4), it follows that

$$(COP)_H = 1 + (COP)_{CL} \tag{6.5}$$

Assuming that the utility value of the heating produced in the condenser and absorber, and the utility value of cooling produced in the evaporator are the same, an overall coefficient of performance can be written as

$$(COP)_{OV} = \frac{Q_{EV} + (Q_{CO} + Q_{AB})}{Q_{GE}}$$

$$= 1 + 2(COP)_{CL} \qquad (6.6)$$

An entropy balance for an ideal absorption system can be written as

$$\frac{Q_{EV}}{T_{EV}} + \frac{Q_{GE}}{T_{GE}} = \frac{Q_{CO}}{T_{CO}} + \frac{Q_{AB}}{T_{AB}} \qquad (6.7)$$

Equation (6.7) can be rearranged to define a Carnot coefficient for cooling as

$$(COP)_{CCL} = \frac{Q_{EV}}{Q_{GE}}$$

$$= \left[\frac{T_{EV}}{T_{CO} - T_{EV}(Q_{CO}/Q_{EV})}\right]\left[\frac{T_{GE}\,(Q_{AB}/Q_{GE}) - T_{AB}}{T_{GE}}\right]\left[\frac{T_{CO}}{T_{AB}}\right] \qquad (6.8)$$

At steady state, the rate of evaporation of the refrigerant vapour in the generator must be the same as in the evaporator. The latent heat of vaporization decreases with increasing pressure. The superheat of the vapour in the condenser is very small compared to the latent heat of condensation. Therefore, the (Q_{CO}/Q_{EV}) in Equation (6.8) is marginally greater than unity. It follows from Equation (6.4) that the ratio (Q_{AB}/Q_{GE}) is marginally less than unity.

It can be seen from Equation (6.8) that the effects of these two ratios tend to cancel out so that Equation (6.8) can be written to a first approximation as

$$(COP)_{CCL} = \left(\frac{T_{EV}}{T_{CO} - T_{EV}}\right)\left(\frac{T_{GE} - T_{AB}}{T_{GE}}\right)\left(\frac{T_{CO}}{T_{AB}}\right) \qquad (6.9)$$

For the simplified case of the absorption temperature T_{AB} being equal to the condensation temperature T_{CO}, Equation (6.9) reduces to the conventional expression

$$(COP)_{CCL} = \left(\frac{T_{EV}}{T_{CO} - T_{EV}}\right)\left(1 - \frac{T_{AB}}{T_{GE}}\right) \qquad (6.10)$$

Therefore, the expressions for the Carnot coefficient of performance of a heating system $(COP)_{CH}$ and the overall Carnot coefficient of performance $(COP)_{COV}$ could be obtained by the equations (6.5) and (6.6).

The mass balance for the absorber is given by Equation (6.11)

$$\left.\begin{aligned} m_1 + m_2 &= m_3 \\ m_1X_1 + m_2X_2 &= m_3X_3 \end{aligned}\right\} \qquad (6.11)$$

This can be used to define flow ratio (FR), which is the ratio of the mass flow rate of the strong absorbent solution to the mass flow rate of the refrigerant vapour entering the absorber

$$(FR) = \frac{m_2}{m_1} = \frac{(X_1 - X_3)}{(X_3 - X_2)} \qquad (6.12)$$

A heat balance over the absorber gives the amount of heat removed Q_{AB} by water in the absorber

$$Q_{AB} = m_1H_1 + m_2H_2 - m_3H_3 \qquad (6.13)$$

The heat exchanger effectiveness for a countercurrent flow exchanger has been defined by

$$\eta_{EX} = (T_6 - T_7)/(T_6 - T_4) \tag{6.14}$$

Therefore, the heat exchanged in the liquid-liquid heat exchanger is

$$Q_{EX} = \eta_{EX}\, m_6 (C_p)_6 (T_6 - T_7) \tag{6.15}$$

The condenser heat load is given by

$$Q_{CO} = m_8 H_8 - m_9 H_9 \tag{6.16}$$

The function of the expansion valves in the absorption cycle is merely to dissipate the pressure head through an isenthalpic process. Therefore, the following equations can be written for the two expansion valves in the cycle.

$$H_9 = H_{10} \tag{6.17}$$

$$H_7 = H_2 \tag{6.18}$$

The enthalpies per unit mass of solution at state points 4, 5 and 7 can be written as follows

$$H_4 = H_3 + W_P/m_3 \tag{6.20}$$

$$H_5 = H_4 + Q_{EX}/m_4 \tag{6.21}$$

$$H_7 = H_6 - Q_{EX}/m_6 \tag{6.22}$$

The heat removed in the evaporator is given by the evaporator heat balance

$$Q_{EV} = m_1 H_1 - m_{10} H_{10} \qquad (6.23)$$

Similarly, the generator heat balance gives the heat to be supplied to the generator.

$$Q_{GE} = m_8 H_8 + m_6 H_6 - m_5 H_5 \qquad (6.24)$$

In the present absorption system the following mass balance equations could be used to simplify the above equations.

$$\left.\begin{aligned} m_1 &= m_8 = m_9 = m_{10} \\ m_2 &= m_6 = m_7 \\ m_3 &= m_4 = m_5 \end{aligned}\right\} \qquad (6.25)$$

The vapour pressure-temperature-concentration data for the solution under consideration are taken from published literature (Ref.5).

For the purpose of illustration, a flow ratio of 14 (i.e. $X_3 = 0.56$, $X_6 = 0.60$), a rate of water evaporation of 1 kg h^{-1} and an economiser heat exchanger effectiveness of 0.8 were chosen as typical parameters.

6.4 RESULTS AND DISCUSSION

Figure 6.2 shows the variation of coefficient of performance as given by the heat and mass balance and Carnot coefficient of

performance for cooling against gross temperature lift $(T_{CO} - T_{EV})$. Separate curves have been drawn for the two extreme temperatures considered in this analysis namely, $35^{o}C$ and $100^{o}C$. For these extreme condenser temperatures, under typical conditions considered, the generator temperature required would be $85.5^{o}C$ and $158^{o}C$ respectively.

It may be noted here that for a constant condenser temperature considered, the generator temperature will be a constant because of the fixed generator concentration ($X_{GE} = 0.60$), even when the gross temperature lift $(T_{CO} - T_{EV})$ changes. Since the water vaporization rate is 1 kg h^{-1} in the evaporator and the flow ratio value is 14.0, the solution concentration at the absorber outlet (state point 3) will be 0.56. All the parameters on the high pressure side of the system (i.e., condenser, generator and economiser heat exchanger) remain the same when the gross temperature lift $(T_{CO} - T_{EV})$ is varied. This is because the temperature lift changes only by virtue of the change in evaporator temperature T_{EV}. For all the temperature lift values, at a constant condenser temperature condition, Q_{EX} remains the same. This is by virtue of the assumptions for the state point 3 ($X_3 = 0.56$, $T_3 = 35^{o}C$) and constant economiser heat exchanger effectiveness ($\eta_{EX} = 0.8$).

Now consider a specific case of a condenser temperature of $35^{o}C$. For a temperature lift of $30^{o}C$ (i.e. $T_{EV} = 5^{o}C$), the coefficient of performance $(COP)_{CL}$ works out to be 0.762. For a temperature lift of $5^{o}C$ (i.e. $T_{EV} = 30^{o}C$) the $(COP)_{CL}$ is 0.777. Since the variation of the latent heat of vaporization with change in T_{EV}, is not significant in the range considered, the effect on $(COP)_{CL}$ is marginal, as shown in Figure 6.2 . The same argument applies to the curve shown for a condenser temperature of $100^{o}C$.

Figure 6.4 is a plot of heat load against gross temperature lift $(T_{CO} - T_{EV})$ when T_{CO} is fixed $(T_{CO} = 100^{o}C)$. It shows that Q_{GE}, Q_{CO} and Q_{EX} remain constant but Q_{EV} and Q_{AB} change marginally. The above discussion for $(COP)_{CL}$ is also applicable for $(COP)_{H}$. However, the Carnot coefficients of performance $(COP)_{CCL}$ and $(COP)_{CH}$ change significantly with T_{EV} as shown in Figure 6.2

The thermodynamic effectiveness of the system for cooling E_{CL} and the heating E_{H} are defined by Equations (6.25) and (6.26) respectively

$$E_{CL} = (COP)_{CL}/(COP)_{CCL} \tag{6.25}$$

$$E_{H} = (COP)_{H}/(COP)_{CH} \tag{6.26}$$

It can be seen from Figure 6.3 that for a fixed T_{CO}, E_{H} is always greater than E_{CL} and both E_{H} and E_{CL} increase with temperature lift.

Now consider variations in the gross temperature lift $(T_{CO} - T_{EV})$ by virtue of changing the condenser temperature only. In this case, the evaporator temperature T_{EV} is kept constant at $5^{o}C$. Figure 6.5 is a plot of the coefficient of performance for cooling $(COP)_{CCL}$ as predicted by heat and mass balance and the Carnot coefficient of performance for cooling $(COP)_{CCL}$ against gross temperature lift $(T_{CO} - T_{EV})$. It shows that both coefficients of performance change with similar trends but the change is marginal. This is because a decrease in T_{CO} leads to a decrease in T_{GE} for a marginal change in T_{AB}, thereby minimising the overall change in $(COP)_{CCL}$ as predicted

by Equation (6.9). Figure 6.5 shows that E_{CL} also changes marginally for the same reason. Figure 6.6 shows the heat loads for the case when $(T_{CO} - T_{EV})$ changes by virtue of a change in T_{CO}, and T_{EV} remains constant at $5^{o}C$. It shows that economiser heat exchanger load Q_{EX} increases as $(T_{CO} - T_{EV})$ increases. The economiser heat exchanger load Q_{EX} has a direct influence on Q_{GE} and Q_{AB} so that the variation in these heat loads with $(T_{CO} - T_{EV})$ are relatively low. This leads to a marginal effect on the coefficient of performance values.

Figure 6.7 is a plot of overall coefficients of performance and overall Carnot coefficient of performance against temperature lift. This figure has been plotted for three condensing temperatures of $35^{o}C$, $70^{o}C$ and $100^{o}C$. Figure 6.8 is a plot of overall thermodynamic effectiveness against temperature lift for the above cases. The conclusions drawn from Figures 6.2 and 6.3 also apply to Figures 6.7 and 6.8 respectively.

Figure 6.9 is a plot of energy required by an ideal pump against temperature lift for three condensing temperatures considered. For a given temperature lift, because of higher pressure differential at higher condensing temperatures, the energy required is more than that required at lower condensing temperatures. It is interesting to note that for $T_{CO} = 100^{o}C$, the energy required by an ideal pump increases by a factor of 5, as $(T_{CO} - T_{EV})$ is varied from $5^{o}C$ to $95^{o}C$. Even though the energy required is significantly more at a higher condensing temperature, it is still insignificant with respect to the capacity of the system.

6.5 CONCLUSION

The absorption system is attractive from the primary energy point of view both as cooling units and as heating units, but it offers a great advantage when used simultaneously for cooling and heating.

The present concept of additional cooling of the strong solution prior to its entry into the absorber provides the scope for simultaneous heating and cooling using absorption systems without significant decrease in (COP). Experimental verification of this concept is presented in Chapter 7.

An overall coefficient of performance in the range of about 2.0 to 2.5 can be obtained depending on the condensing temperature and the temperature lift. However, in a practical system the $(COP)_{OV}$ is likely to decrease slightly with an increase in temperature lift and condensing temperature because of practical limitations.

The computer program for the above analysis is given in Appendix C.

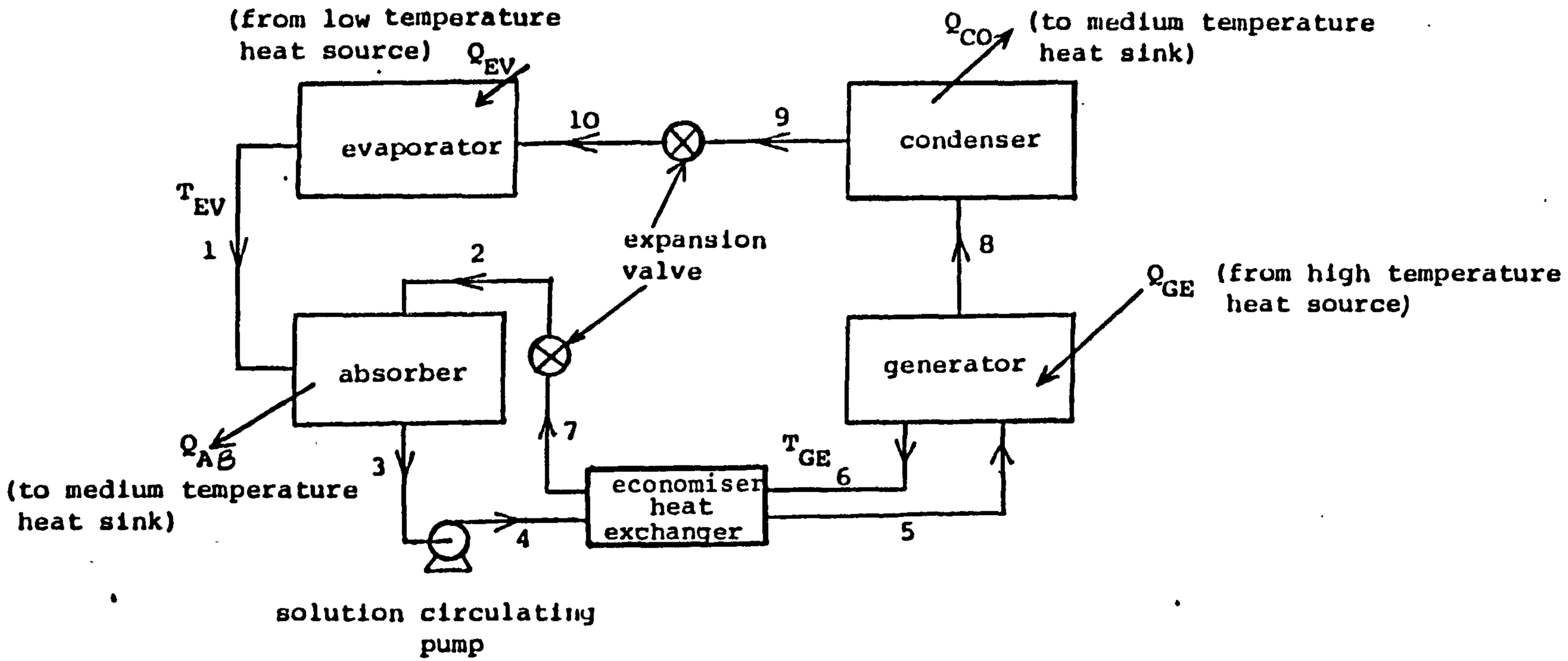

FIGURE 6.1 CLOSED CYCLE ABSORPTION COOLING SYSTEM USING WATER-LITHIUM BROMIDE

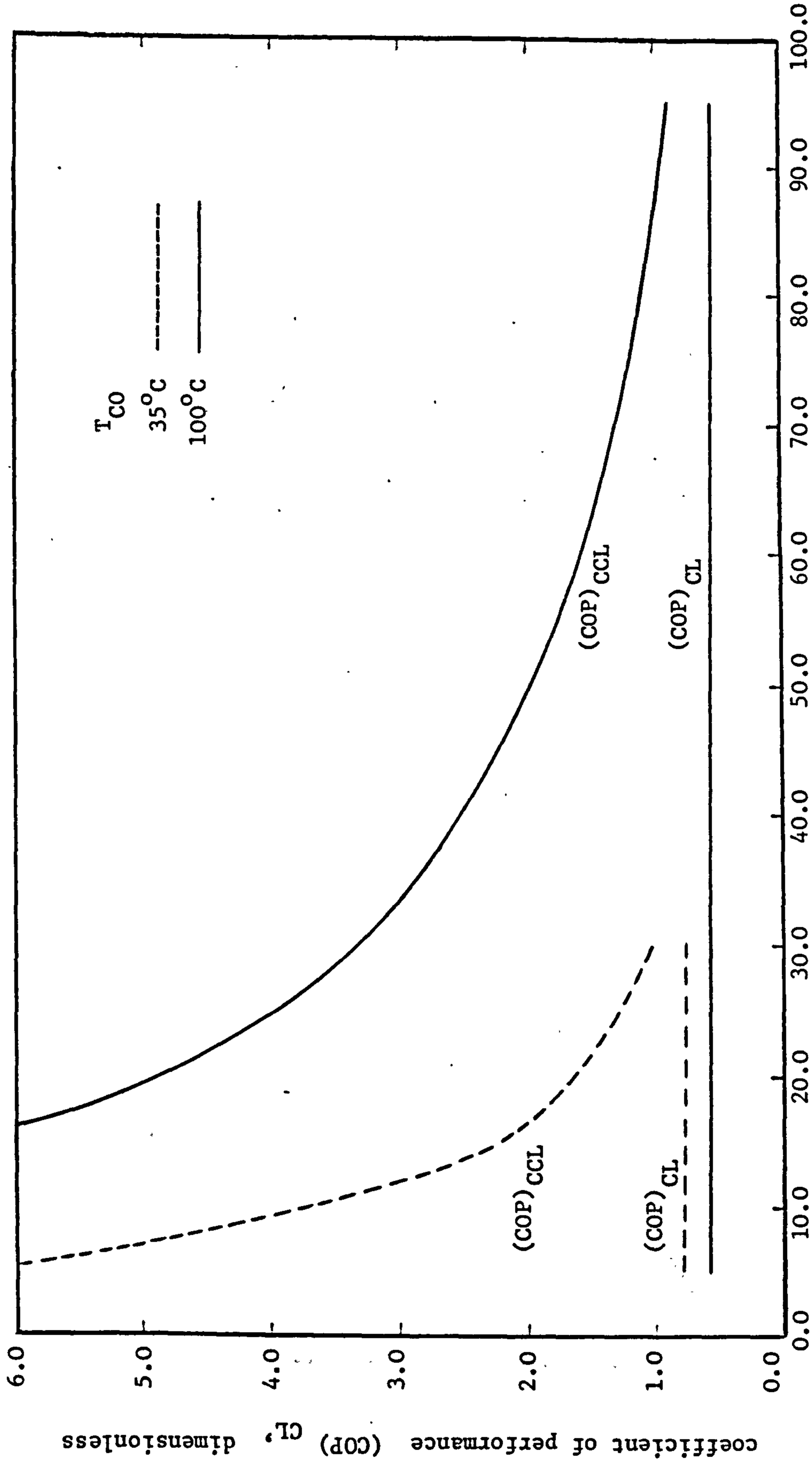

FIGURE (6.2) COEFFICIENT OF PERFORMANCE FOR COOLING AGAINST GROSS TEMPERATURE LIFT WITH CONDENSER TEMPERATURE AS PARAMETER

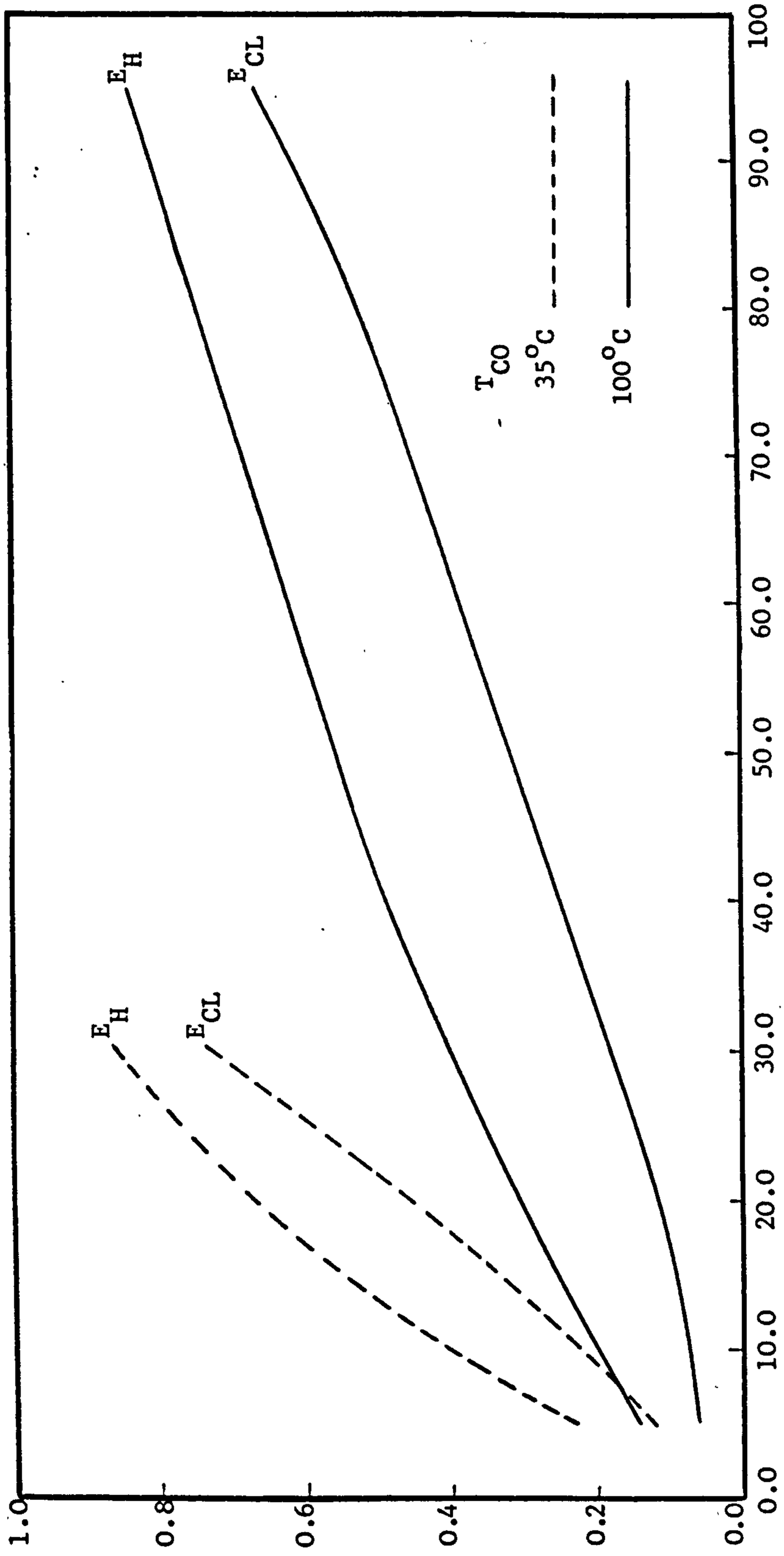

FIGURE (6.3) THERMODYNAMIC EFFECTIVENESS FOR COOLING AND HEATING AGAINST GROSS TEMPERATURE LIFT WITH CONDENSER TEMPERATURE AS PARAMETER

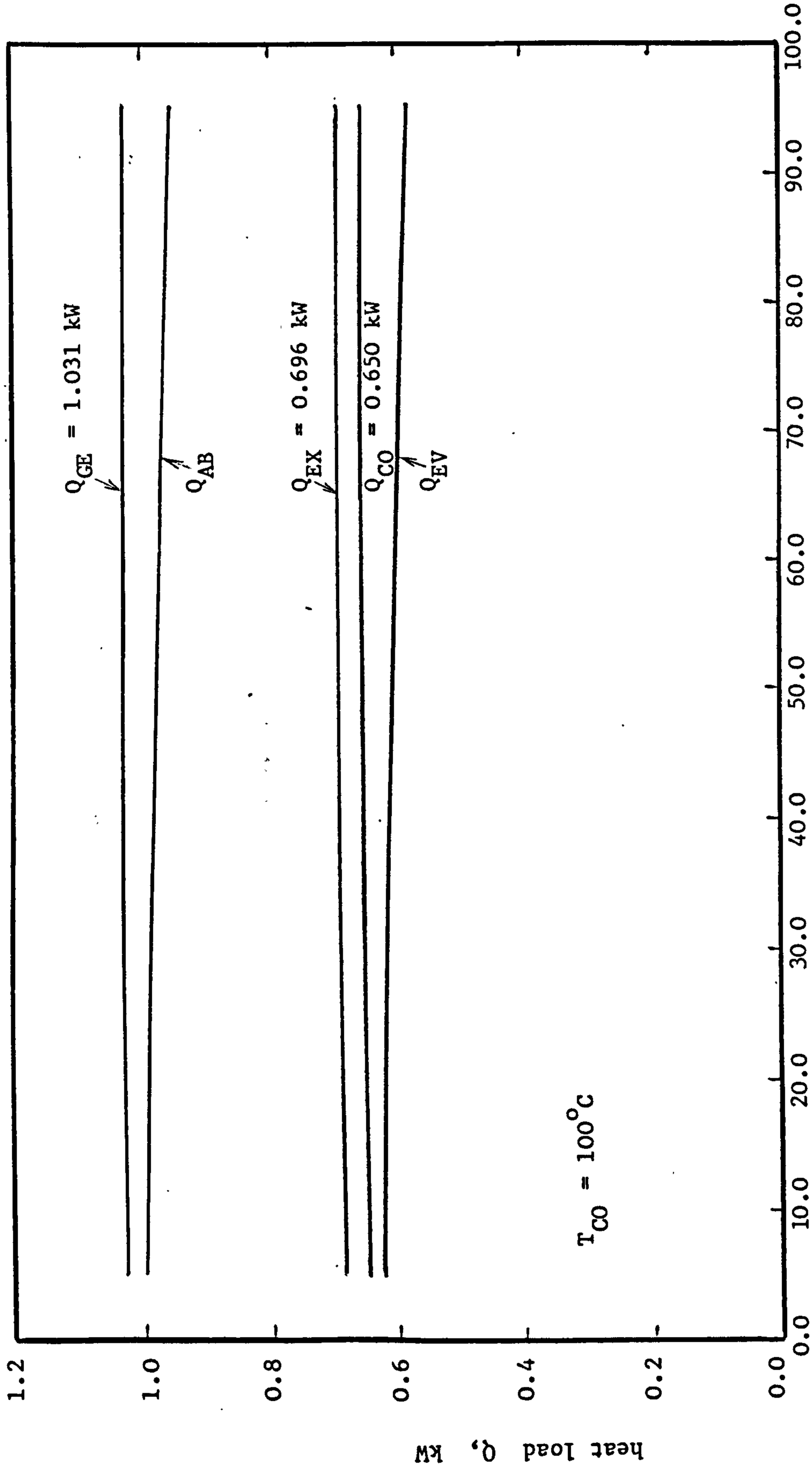

FIGURE (6.4) HEAT LOADS AGAINST GROSS TEMPERATURE LIFT FOR A CONSTANT CONDENSER

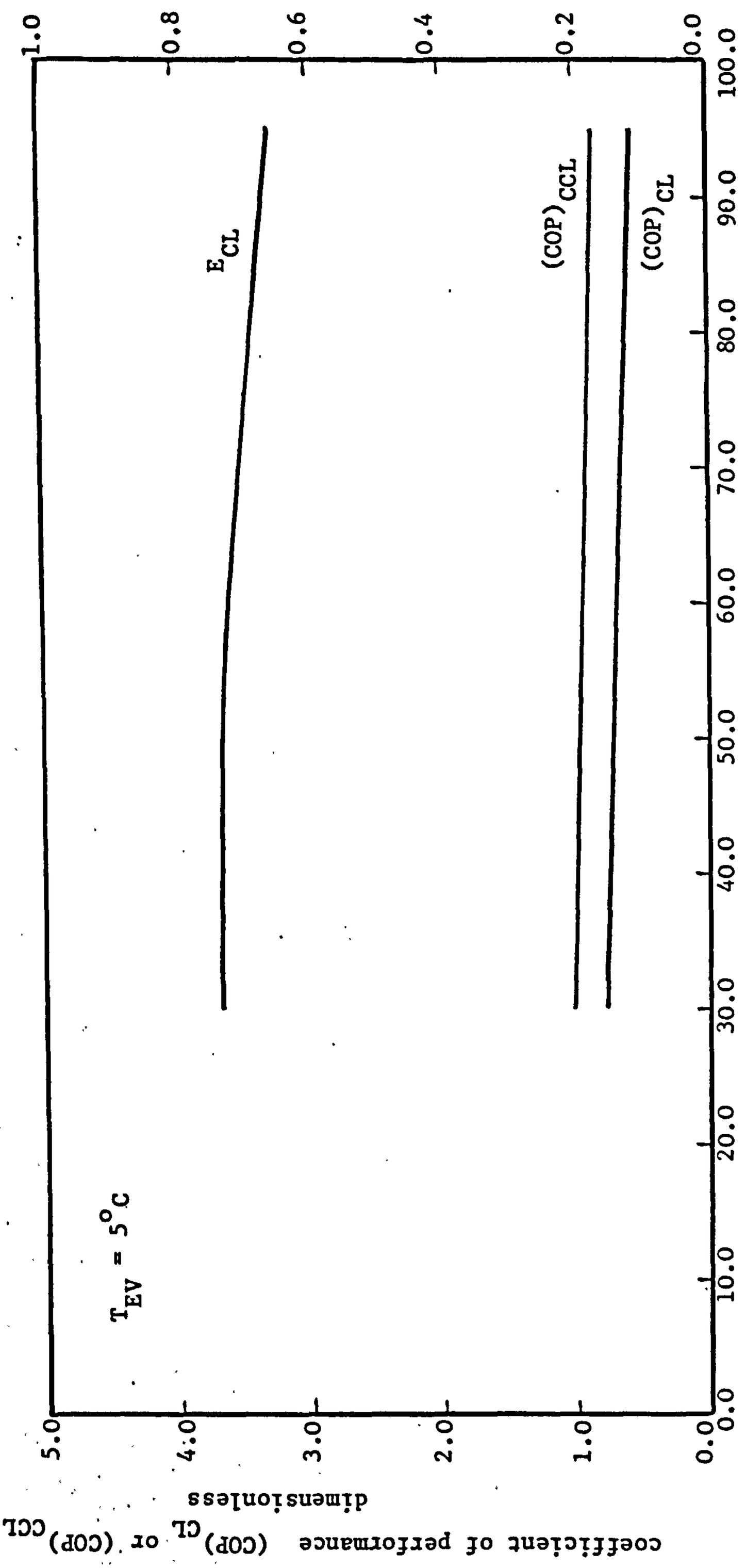

FIGURE (6.5) COEFFICIENT OF PERFORMANCE AND THERMODYNAMIC EFFECTIVENESS FOR COOLING AGAINST GROSS TEMPERATURE LIFT FOR A CONSTANT EVAPORATOR TEMPERATURE

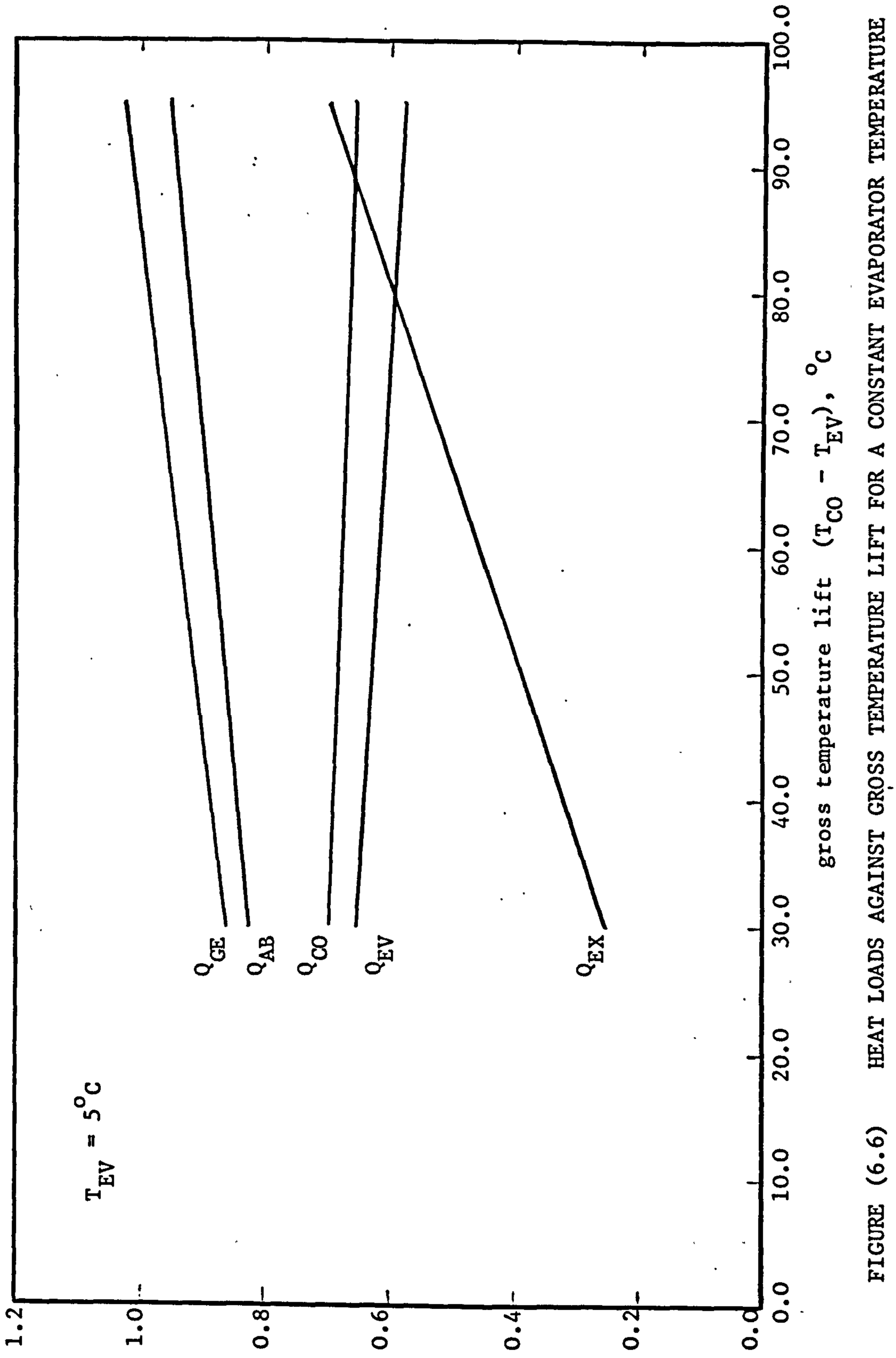
heat load Q, kW
1.2
1.0
0.8
0.6
0.4
0.2
0.0
T_{EV} = 5°C
Q_{GE}
Q_{AB}
Q_{CO}
Q_{EV}
Q_{EX}
20.0
30.0
40.0
50.0
60.0
70.0
80.0
90.0
100.0
gross temperature lift ($T_{CO} - T_{EV}$), °C
0.0
10.0
HEAT LOADS AGAINST GROSS TEMPERATURE LIFT FOR A CONSTANT EVAPORATOR TEMPERATURE

FIGURE (6.6)

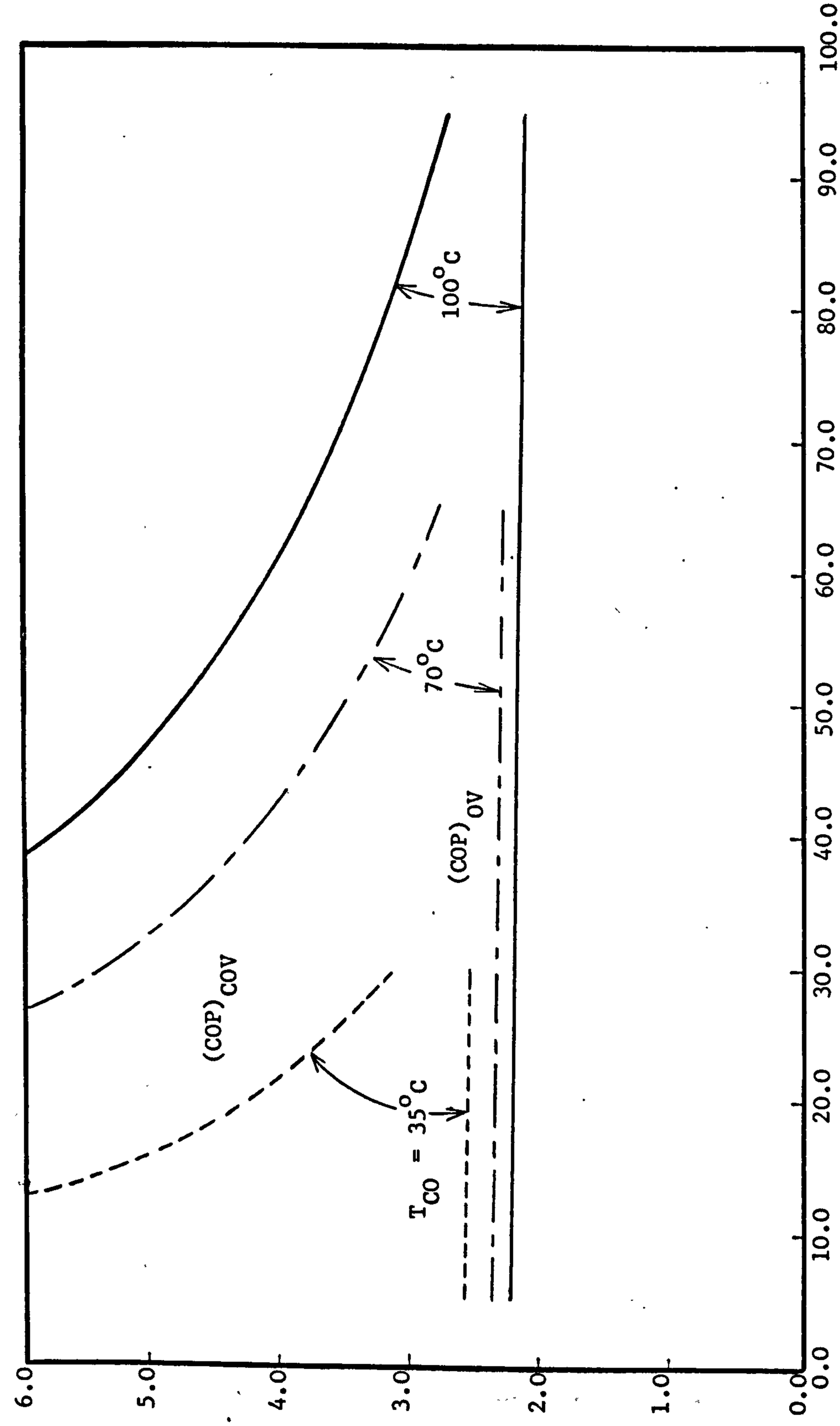

FIGURE (6.7) OVERALL COEFFICIENT OF PERFORMANCE AGAINST GROSS TEMPERATURE LIFT WITH CONDENSER TEMPERATURE AS PARAMETER

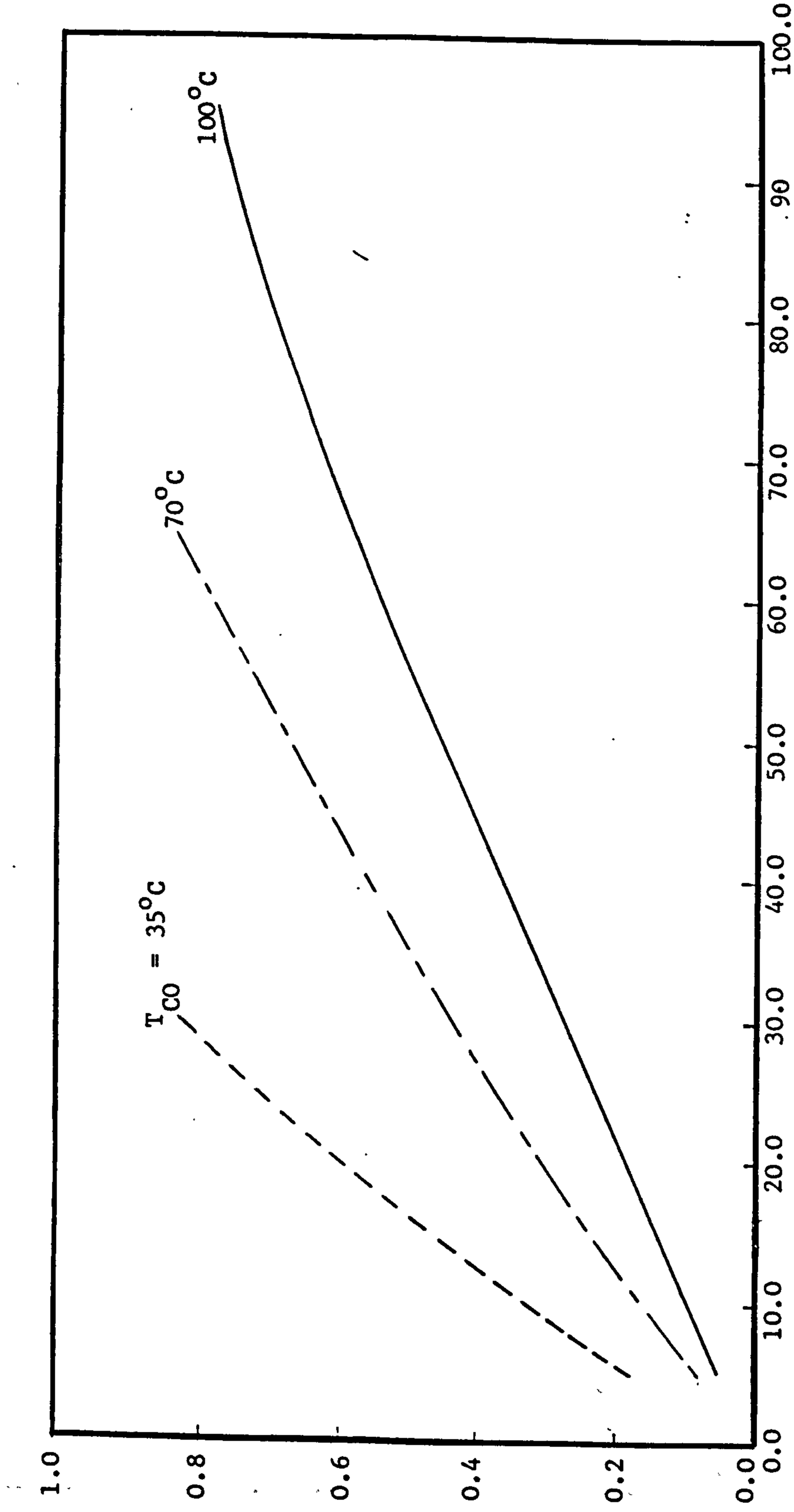

FIGURE (6.8)

OVERALL THERMODYNAMIC EFFECTIVENESS AGAINST GROSS TEMPERATURE LIFT
WITH CONDENSER TEMPERATURE AS PARAMETER

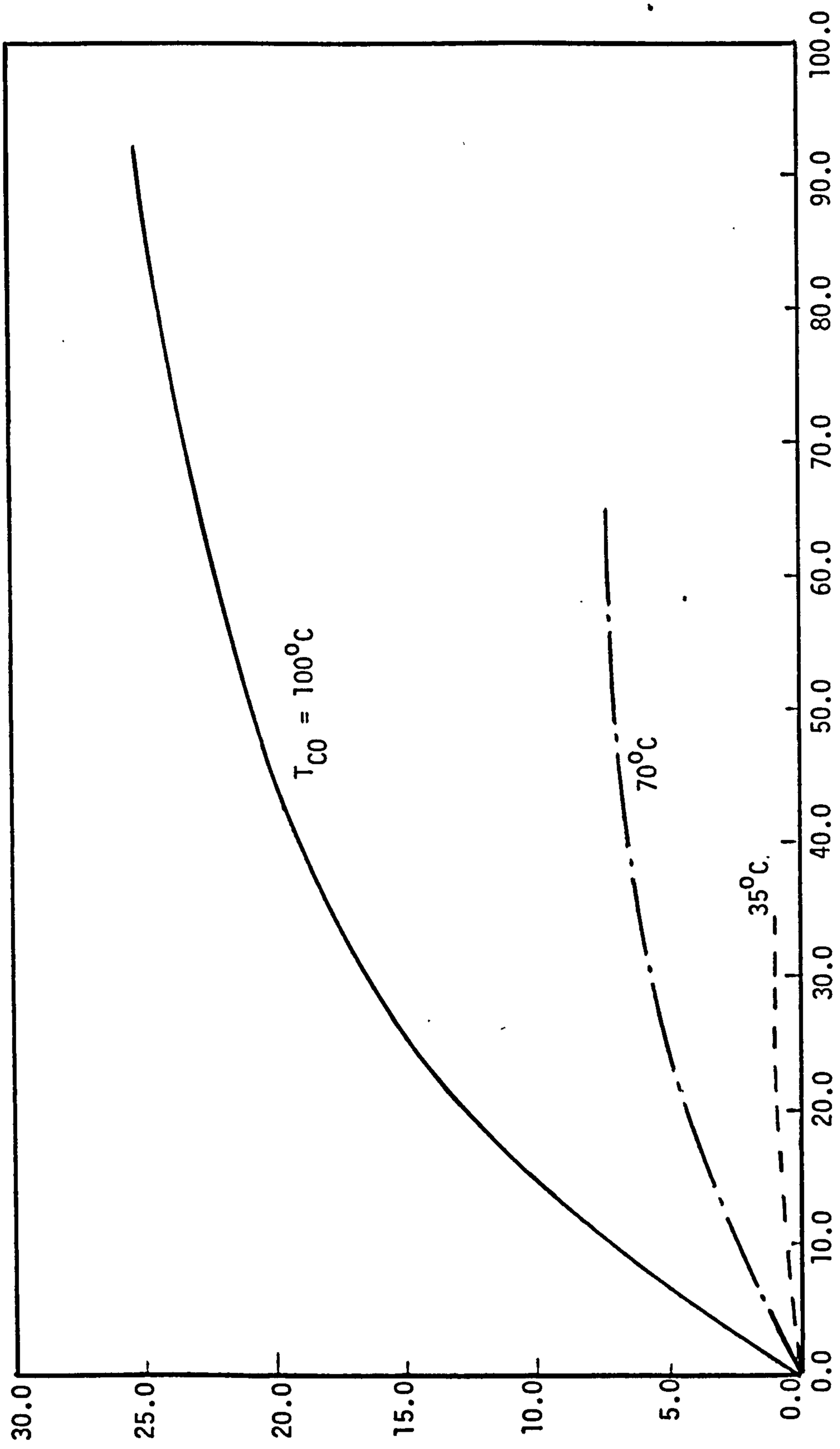

FIGURE 6.9 ENERGY REQUIRED BY AN IDEAL PUMP AGAINST TEMPERATURE LIFT

CHAPTER 7

PERFORMANCE STUDY OF AN EXPERIMENTAL ABSORPTION SYSTEM FOR SIMULTANEOUS COOLING AND HEATING

PERFORMANCE STUDY OF AN EXPERIMENTAL ABSORPTION SYSTEM FOR SIMULTANEOUS COOLING AND HEATING

7.1 EXPERIMENTAL

In order to operate the absorption system for simultaneous cooling and heating as pointed out earlier, a water cooled heat exchanger was introduced in the experimental system as shown in Figure 7.1. This heat exchanger was a standard multicoil glass condenser with a heat transfer area of 0.059 m^2, modified by adding thermocouple pockets. The strong absorbent solution was cooled down prior to its entry into the absorber by the cooling water flowing through the coil. The remainder of the experimental details are given in Chapter 5. Measurement points have been shown in Figure 7.2.

7.2 RESULTS AND DISCUSSION

Some typical experimental results are presented in Figures 7.3 to 7.7. Figure 7.3 shows the variation of T_{CO}, T_{AB}, T_{EV} and $(T_{CO} - T_{EV})$ with the generator temperature T_{GE}. T_{AB} and T_{EV} are almost independent of the generator temperatures, so that the increase in the temperature lift results from the increase in the condenser temperature T_{CO}.

The incorporation of the additional heat exchanger in the system makes the heat and mass transfer operations in the absorber and evaporator substantially independent of the condenser pressure P_{CO} and temperature T_{CO}.

Figure 7.4 is a plot of the actual experimentally determined coefficient of performance $(COP)_{ACL}$ and the Carnot coefficient of performance $(COP)_{CCL}$ against the gross temperature lift $(T_{CO} - T_{EV})$.

It is difficult to control heat losses in a small experimental system where the various components need to be readily accessible. Heat losses from the generator add to the generator heat load. Secondly, since the evaporator temperature T_{EV} is below ambient, the heat gain from the environment reduces the capacity of the evaporator.

Figure 7.5 shows the variations of heat loads with gross temperature lift $(T_{CO} - T_{EV})$. The overall energy balance can be written as

$$Q_{LOSS} = Q_{GE} + Q_{EV} - Q_{CO} - (Q_{AB} + Q_{EX}) \qquad (7.1)$$

where Q_{LOSS} represents the heat losses which increase with $(T_{CO} - T_{EV})$.

Figure 7.6 is a plot of the actual coefficient of performance for heating $(COP)_{AH}$ and the Carnot coefficient of performance for heating $(COP)_{CH}$ against the gross temperature lift $(T_{CO} - T_{EV})$. Figure 7.6 shows that $(COP)_{AH}$ is substantially independent of temperature lift. The experimental unit was designed as a cooler with air cooling of the absorber and condenser. Because of the relatively high heat losses from the unit, only modest $(COP)_{AH}$ values could be expected. The actual coefficients of performance have been modified for heat losses and plotted as $(COP)_{MH}$ in Figure 7.6. It should be possible to closely approach these values with a high level of insulation.

An overall coefficient of performance can be defined as

$$(COP)_{OV} = \frac{Q_{EV} + Q_{CO} + (Q_{AB} + Q_{EX})}{Q_{GE}} \qquad (7.2)$$

Figure 7.7 is a plot of the Carnot, modified and actual overall coefficients of performance against gross temperature lift $(T_{CO} - T_{EV})$. Figure 7.7 also shows the variation of the actual thermodynamic effectiveness factors for cooling E_{CL} and heating E_H with $(T_{CO} - T_{EV})$. Better design would result in higher values for both E_{CL} and E_H.

Figure 7.4 shows that for a gross temperature lift of 90^oC, a $(COP)_{CL}$ value of about 0.55 could be obtained in a unit with a thermodynamic effectiveness value $E_{CL} = 0.5$. It is interesting to note that for $T_{EV} = 10^oC$ and $T_{CO} = 100^oC$, the overall coefficient of performance would be 2.1.

7.3 CONCLUSION

It has been shown that the incorporation of an auxiliary heat exchanger, in addition to the economiser, enabled the unit to provide effective simultaneous cooling and heating. The size of this auxiliary heat exchanger, which is used to cool the hot solution from the generator prior to its entry into the absorber, is critical since it determines the extent of the temperature lift. In order to provide relatively high temperature lifts, an absorption system would require a relatively high temperature heat input to the generator.

All the experimental data for this chapter are given in Appendix D.

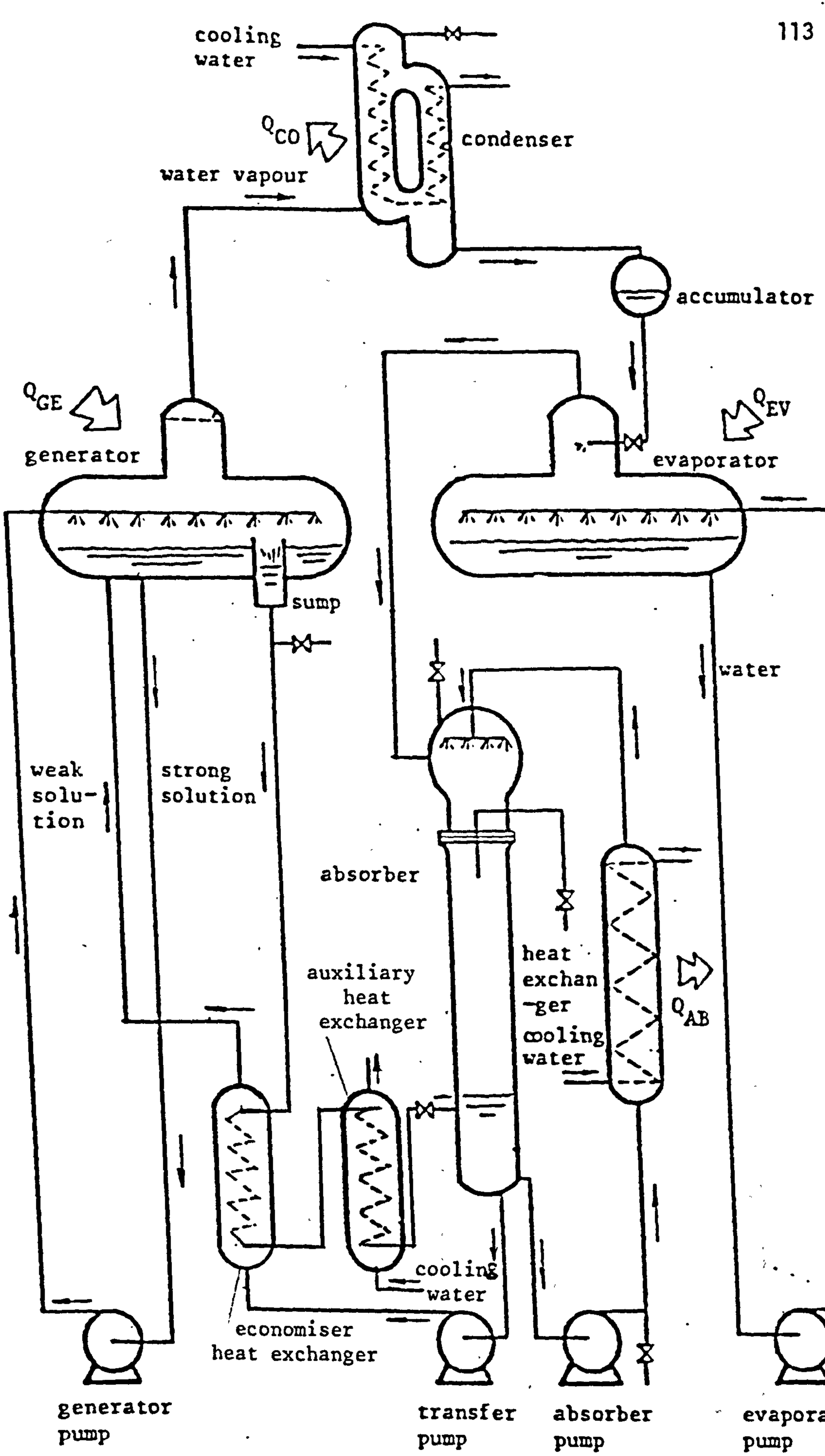

FIGURE 7.1 SCHEMATIC DIAGRAM OF THE EXPERIMENTAL ABSORPTION SYSTEM

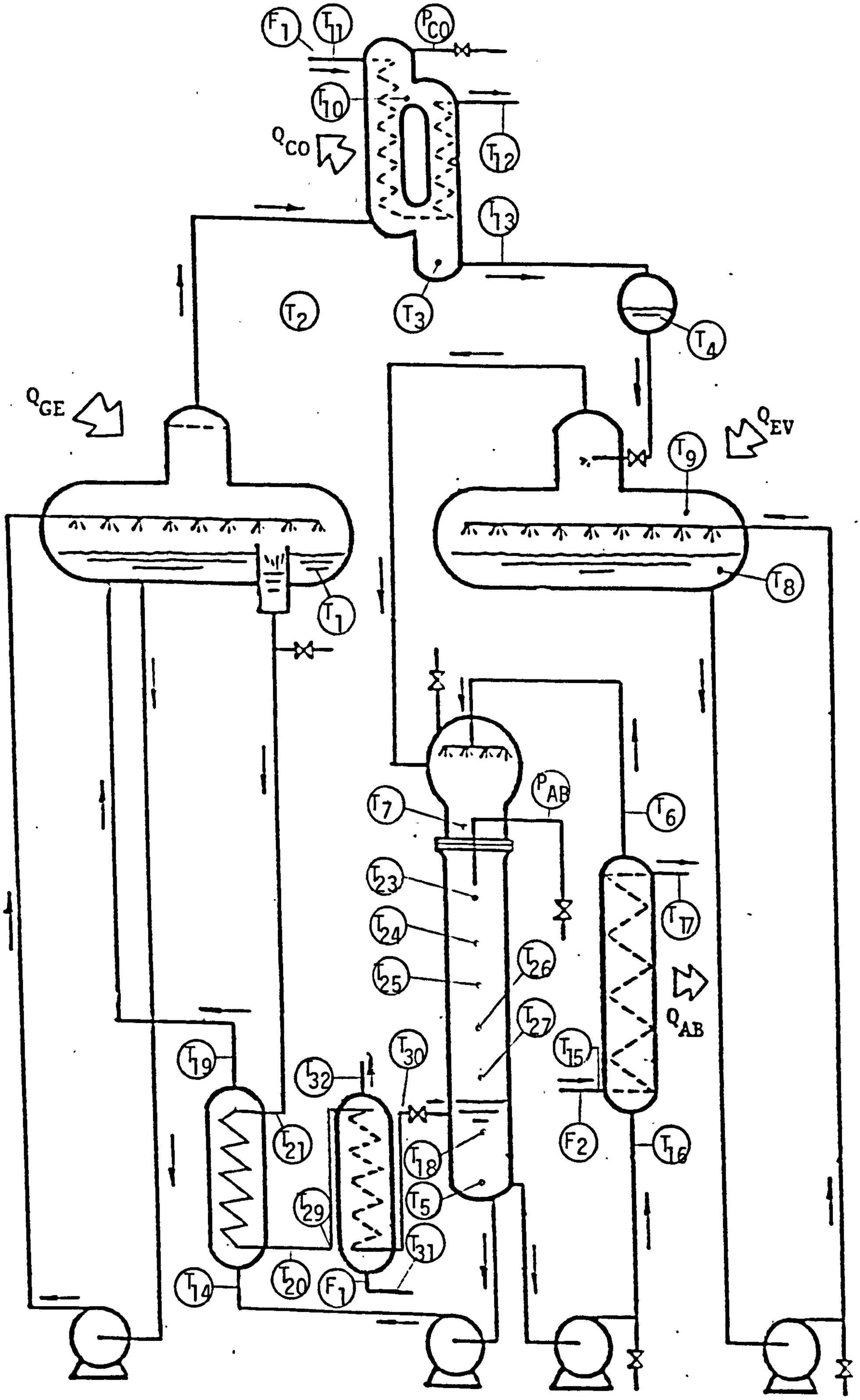

FIGURE 7.2 INSTRUMENTATION DIAGRAM OF ABSORPTION SYSTEM

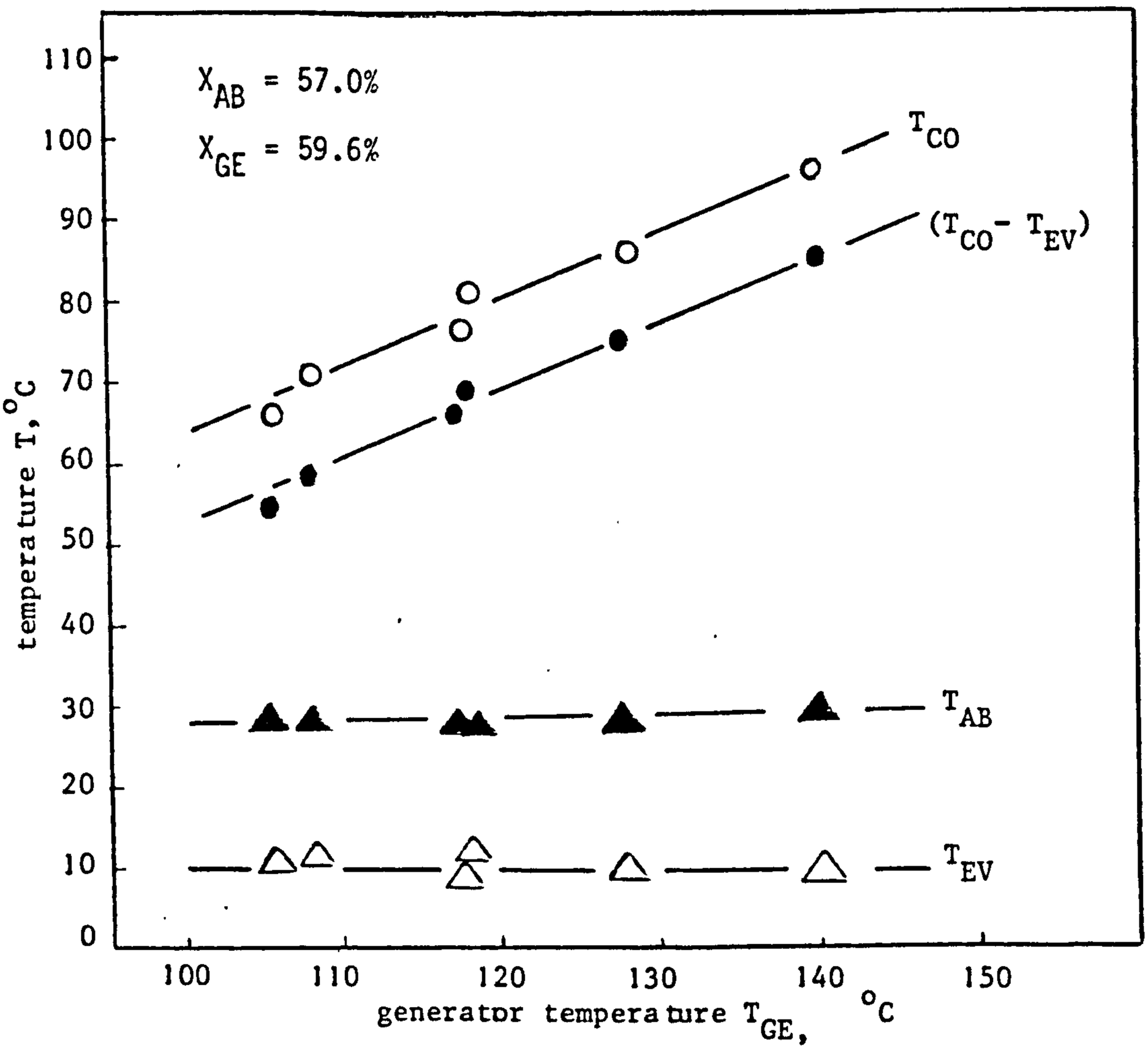

FIGURE 7.3 VARIATION OF CONDENSER, ABSORBER, EVAPORATOR TEMPERATURES AND GROSS TEMPERATURE LIFT AGAINST GENERATOR TEMPERATURE FOR SIMULTANEOUS COOLING AND HEATING.

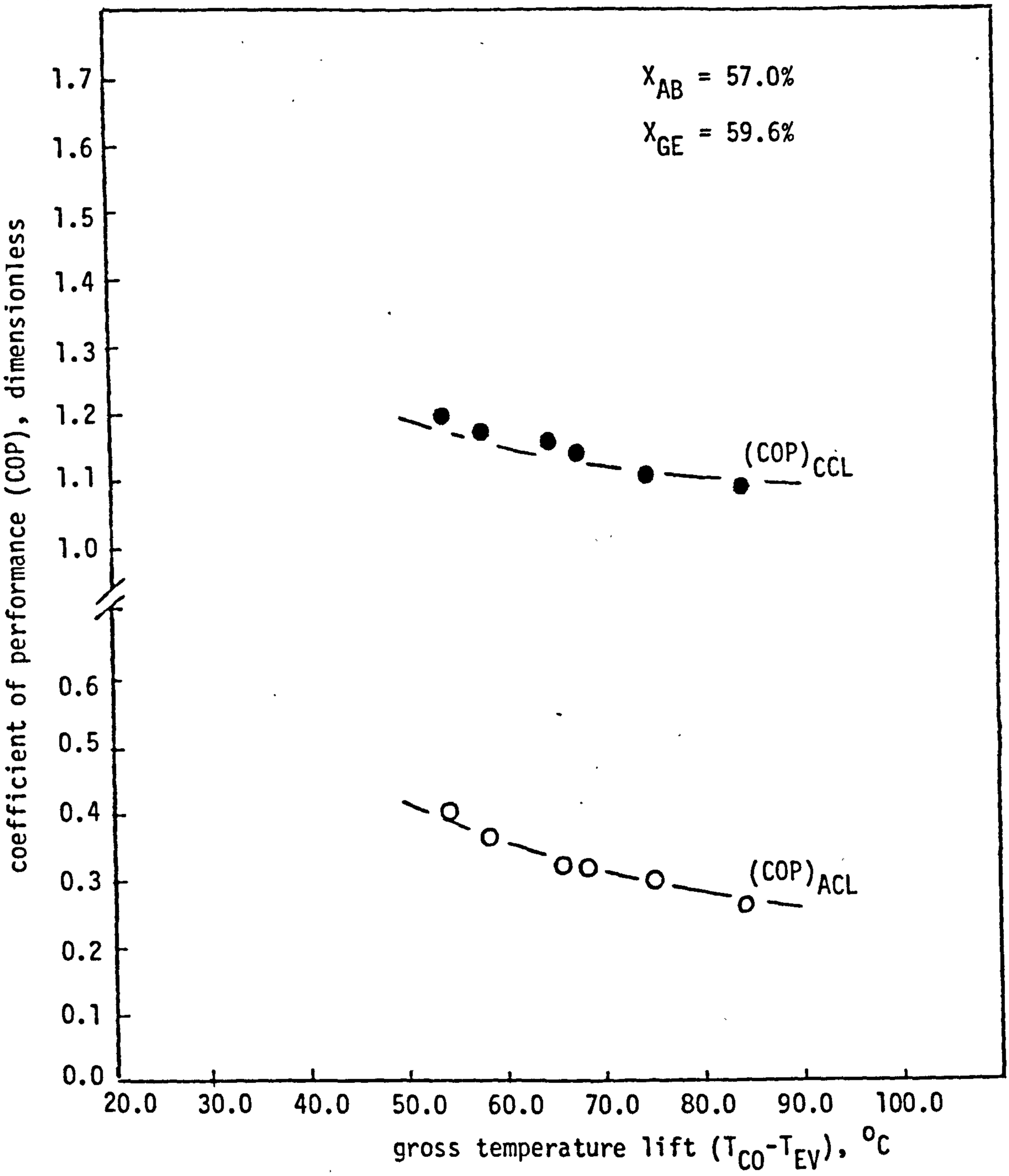

FIGURE 7.4 ACTUAL AND CARNOT COEFFICIENTS OF PERFORMANCE FOR COOLING AGAINST GROSS TEMPERATURE LIFT

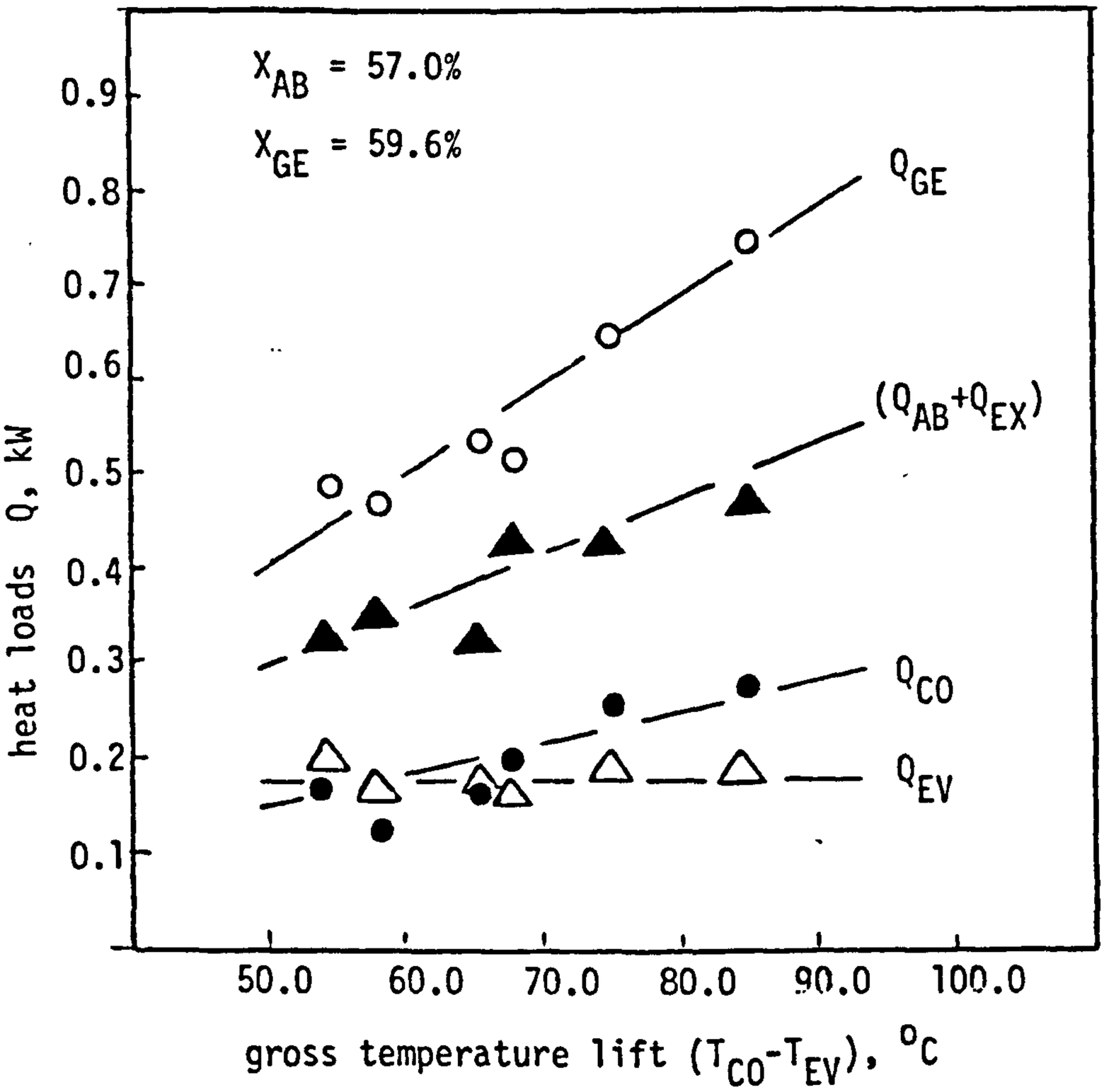

FIGURE 7.5 VARIATION OF HEAT LOADS AGAINST GROSS TEMPERATURE LIFT FOR SIMULTANEOUS COOLING AND HEATING

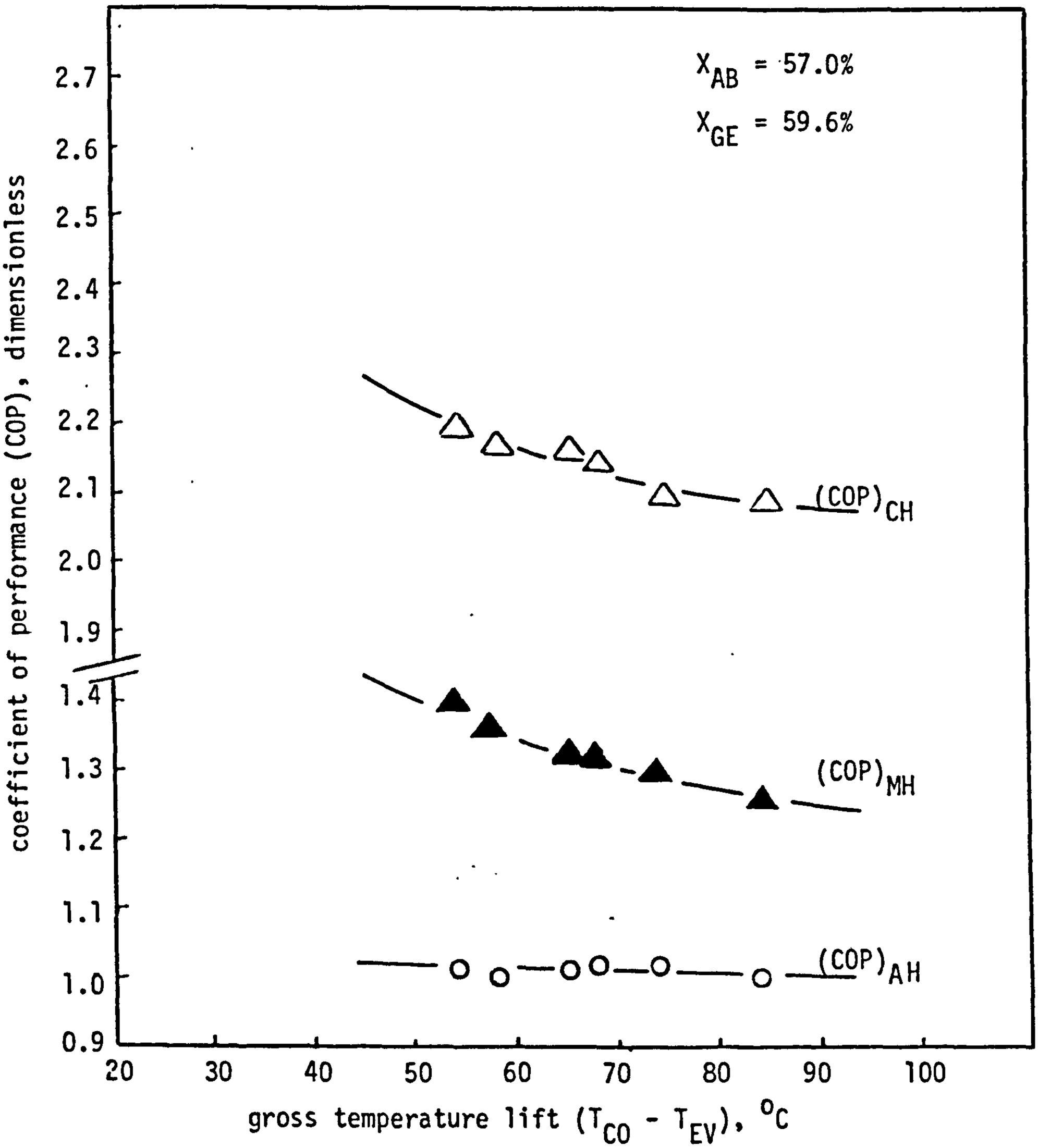

FIGURE 7.6 ACTUAL, MODIFIED AND CARNOT COEFFICIENTS OF PERFORMANCE FOR HEATING AGAINST GROSS TEMPERATURE LIFT

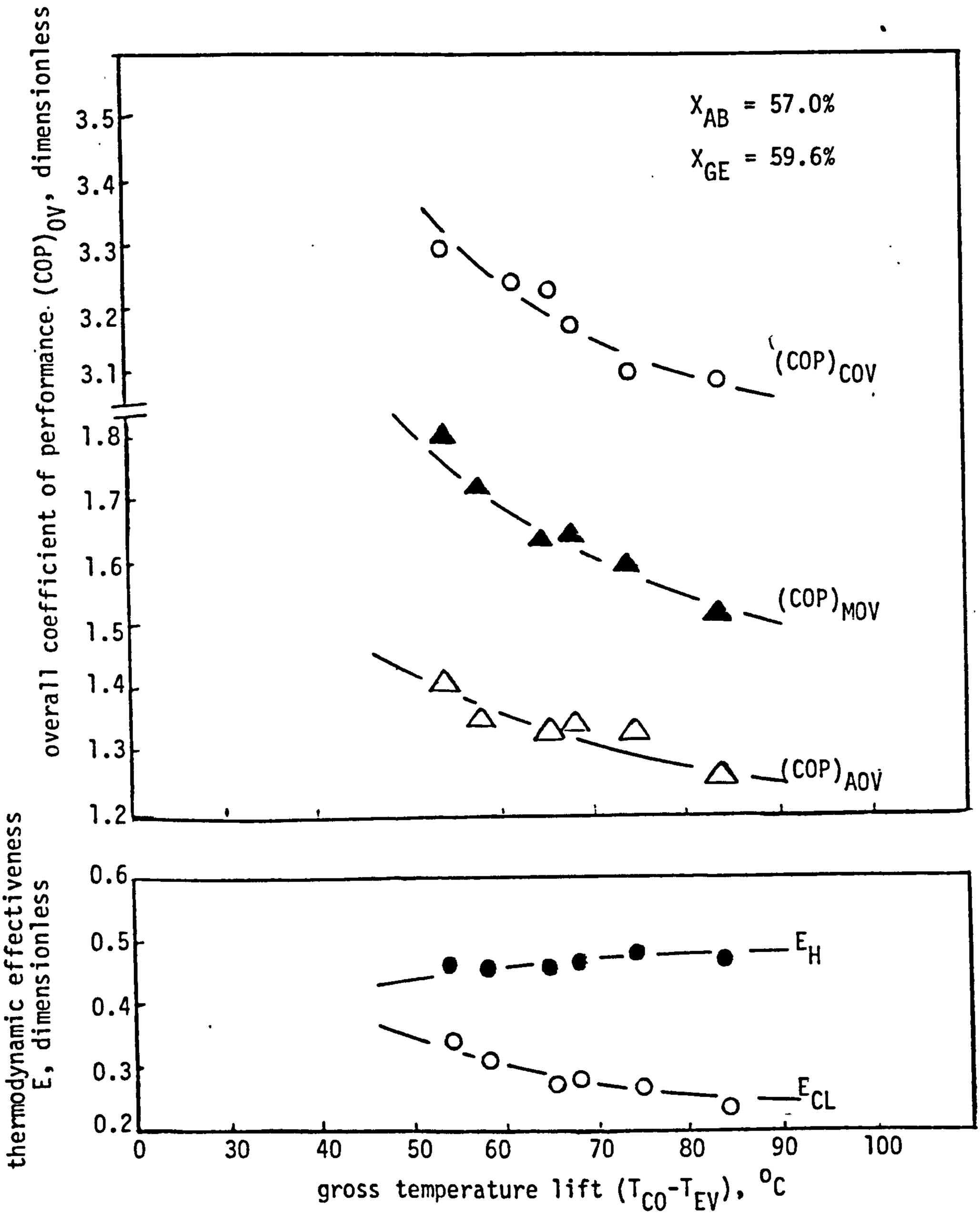

FIGURE 7.7 VARIATION OF ACTUAL, MODIFIED AND CARNOT OVERALL COEFFICIENTS OF PERFORMANCE AND THERMODYNAMIC EFFECTIVENESS AGAINST GROSS TEMPERATURE LIFT

CHAPTER 8

EXPERIMENTAL HEAT AND MASS TRANSFER STUDY ON SOLAR GENERATOR OF OPEN CYCLE ABSORPTION COOLING SYSTEM

EXPERIMENTAL HEAT AND MASS TRANSFER STUDY ON SOLAR GENERATOR OF OPEN CYCLE ABSORPTION COOLING SYSTEM

8.1 INTRODUCTION

Solar absorption cooling is especially attractive in tropical countries where solar insolation is high and electricity relatively scarce.

Theoretical and experimental investigations on open cycle solar absorption coolers have been reported by Kakabaev (Kakabaev et al 1969), (Kakabaev et al 1976). Collier (Collier 1979) and Prasad et al (Prasad et al 1981) have also analysed the generator performance of an open cycle system using generalised heat and mass transfer correlations. Kumar et al (Kumar et al 1984) compared open with closed cycle systems and demonstrated the advantages of the former. The heart of an open cycle system is the generator. The water evaporated in the generator is directly proportional to the cooling capacity of the system. Hitherto there has been insufficient heat and mass transfer data available to design a generator with confidence. The aim of the present study was to provide the required data.

It is not feasible to carry out systematic experiments using direct solar energy under repeatable and steady state conditions, since parameters such as air velocity, ambient humidity and solar insolation are not controllable. An experimental open cycle unit was therefore developed with simulated solar insolation in order to obtain the heat and mass transfer data required for the design of

a generator. The experiments were carried out using an aqueous lithium chloride solution rather than the more common aqueous lithium bromide solution to reduce both corrosion and instability in the presence of air (Kakabaev et al 1969), (Ref 53).

8.2 EXPERIMENTAL

8.2.1 Generator

Experiments were carried out on the system shown schematically in Figure 8.1. It has been shown that for a flat plate solar collector, for round the year operation, an optimum tilt angle to the horizontal lies in the range from about (latitude) to (latitude + 15^{o}). However, the variation of the collector performance for the whole range is marginal (Lof et al 1973). Therefore the generator was tilted at an angle of 16^{o} to suit tropical conditions. A thin film of aqueous lithium chloride solution flowed over the generator of dimensions 0.9m x 0.5m. The generator surface was black neoprene sheet covered with matt black cotton cloth to assist uniform flow distribution. The cloth was made of 0.3 mm diameter threads. Average space between adjacent threads was 0.25 mm.

Because of the absence of any device to measure the changing composition and temperature over the liquid film, it was assumed that the liquid film has a negligible resistance to heat and mass transfer. The assumption is supported by literature as discussed later in the calculation procedure.

The aqueous lithium chloride solution was pumped to a distributor at the top of the generator. The distributor was a sparge pipe of 0.09m diameter extending over the width of the generator. There were nineteen 3.0mm holes along the pipe spaced at 25mm intervals. The concentrated solution was fed to a trough at the bottom of the generator and collected in a tank.

8.2.2 Solar simulation

Two methods of solar simulation were used. In the first method four compact source mercury iodide (CSI) lamps provided the heat input. In the second method, this was provided by an electrical heater located beneath the generator surface. Both methods have limitations which are discussed as follows.

Solar simulation with lamps: There are continuous variations in the solar spectrum at ground level caused by changes in air density, turbidity and humidity. These variations cannot be simulated by any conventional lamp. The requirements of a lamp to be used for solar simulation depend on the particular objective. Gillettet al (Gillett et al 1980) gave the main requirements and these are summarised below.

1) The lamp should have an output spectrum which approximates to the solar spectrum.

2) It should have a high conversion efficiency to minimise cost, cooling load and the number of lamps required.

3) It should have a low thermal radiation emission of wavelengths greater than 2.5μm to minimise the corrections required when predicting outdoor collector performance characteristics from simulated test results.

4) It should be able to work at part load to permit variations in radiation without degrading beam uniformity.

5) Its output should be stable.

6) Its beam divergence should be narrow.

7) It should be able to work at any tilt angle.

8) Its stable life should be long.

The CSI lamp spectrum resembles the air mass 2 solar spectrum quite closely (Gillett et al 1980). However, a number of problems have been encountered related to the measurement of irradiance even outdoors (Gruter 1980), (Riches et al 1981). The measurement of simulated irradiance poses additional problems indoors (Gillett et al 1980).

Because of thermal radiation emission from CSI lamps a correction factor must be developed. Thermal radiation from the lamps and lamp housing may either be in the form of a focussed beam or a diffuse emission. If the lamps have open reflectors, the thermal radiation may form a part of the beam. It has been suggested that in this case the thermal radiation flux can be very high (Gillett et al 1980). If the lamp has a glass cover then this will absorb thermal radiation and re-emit diffusely from its front surface.

In a solar simulator, where the beam distribution is almost uniform, the irradiance is required to be measured quite infrequently and can be measured by means of a fixed cavity radiometer (Ley et al 1977). However, these simulators are likely to be very expensive. Since flat plate solar collectors act as integrators, beam non-uniformity could be tolerated up to a certain extent. If the beam uniformity is poor, the irradiance must be integrated over the aperture of the collector before each test. This requires a lightweight measurement device with rapid response. Further work is required in this direction. The peak intensities of the lamps, in the CSI lamp solar simulator installed at the University College, Cardiff, were found to change by

approximately ± 15 per cent. Therefore, the uniformity produced over a typical collector under test was no better than about ± 20 per cent (Gillett et al 1980).

The effect of diffuse irradiance on the collector performance is also one of the factors to be considered. The amount of diffuse irradiance depends upon the type of simulator.

Four 400W CSI mercury iodide lamps supplied by Thorn Lighting Ltd., London, U.K., were fitted in a 1.22m x 1.22m panel as shown in Figure 8.2. The panel was fitted with a shaft which moved at its own axis. The panel stand was provided with a number of holes to fix the shaft and the lamp panel at any desired angle. The lamps were kept cool by circulating air with a low power fan. The surface of the lamp panel was covered with aluminium foil to reflect scattered radiation towards the generator surface. The panel was also tilted at an angle of 16^{o} to the horizontal to make it parallel with the generator surface at a distance of 0.80m.

Solar simulation with an electrical heater: A disadvantage of using CSI lamps as a radiation source is that they are not recommended for use under part load conditions. This not only affects the life of the lamps but also changes the spectrum. Another way of using CSI lamps with variable irradiance could be by varying the distance between the lamps and the generator surface. However, this would lead to variation in the correction factors.

Preliminary measurements of the radiation from the lamp were done by using a radiometer/photometer model Q101, made by MACAM Photometrics Ltd., Livingston, Scotland. A simple heat and mass

balance showed that the total heat input to the solution was greater than that recorded by the photometer. This showed the significance of the correction factors discussed above. Even if the correction factors were evaluated quite accurately, the total heat input to the solution could not be estimated accurately due to the lack of precise data on absorptance of the surface-radiation combination.

There is little to be gained by attempting to accurately simulate a given spectral distribution, since the spectrum of solar radiation can vary widely during the course of a day. The most important parameter for the experiments described here, is the total heat input to the aqueous lithium chloride solution. This in turn depends on the combined absorptance of the solution and the generator surface. This absorptance is constant for a particular surface-radiation combination.

When the heat flux is provided by a well distributed electrical heater underneath the generator surface, the only factor missing in order to have a realistic solar simulation, is the combined absorptance of the solution and the generator surface. The simulated solar heat flux could therefore be obtained by dividing the electrically produced heat flux by this combined absorptance. Therefore, a new generator was constructed with a well distributed electrical heater underneath the generator surface. Further experiments were carried out using both types of simulators. The experiments with the electrical heater were conducted for a number of heat flux values. A comparison of these experiments with the experiments with CSI lamps provided a way to estimate the amount of radiation from CSI lamps absorbed by the generator surface. The simulation with an electrical heater underneath the generator surface not only eliminates the absorptance of the

surface-radiation combination but also avoids the estimation of correction factors in various situations. The correction factors, in any case, can only be approximate.

The electrical heater consisted of five separate 11.9 meter lengths of 0.45mm diameter nichrome wire. The wires of resistance 6.68 Ω/m were insulated with glass sleeves and uniformly laid over a 3.0mm thick asbestos-lux sheet. A 3.0mm thick aluminium sheet was placed over the wires to form a sandwich as shown in Figure 8.3. The top surface of the aluminium sheet was covered with a 1.5mm thick black neoprene sheet to protect it from corrosion. A silicon rubber compound was applied to both the aluminium and neoprene sheets before binding them together. The neoprene sheet was covered with a matt black cotton cloth. A 70mm thick block of fibre insulation was located below the asbestos-lux sheet to reduce any heat losses. The generator assembly was also insulated well from all the four sides. Some difficulty was faced in insulating the leading edge side of the generator. The leading edge had to be extended by 10mm in order to accommodate fibre insulation.

8.3 INSTRUMENTATION, CALIBRATION AND CONTROL

An air flow arrangement as shown in Figure 8.4 was constructed. The whole arrangement was also tilted at an angle of 16^{o} to the horizontal so that the generator surface was at zero incidence. A fan connected to a variac was used to provide a variable air flow rate over the generator. The incoming air was distributed over the generator surface through a 3mm wire mesh of 200mm diameter placed just before the honeycomb, as shown in Figure 8.4. It extended 200mm on either side of the generator. The details of the honeycomb are

shown in Figure 8.5. It was aligned with the generator surface so that an air column of about 180mm was flowing over the generator surface. An air velocity meter, model 1650, supplied by BIRAL Portishead Ltd., Bristol, U.K., was used to measure air flow over the generator. The air velocity was measured both in vertical and parallel planes to the generator. The measurements in the vertical plane were done from 40 mm to 120mm above the generator surface to ensure the measurement outside the boundary layer. It was found to be constant in the vertical plane. The measurements in the parallel plane were done at 25 points as shown in Figure 8.4. The variation of air velocity along the generator was marginal but variation across the generator was higher, especially at relatively high velocities. The velocity measurements near the leading edge are shown in Figure 8.6. Since variation of air velocity across the generator was significant and the profile was parabolic, Simpson's rule (Tuma 1979) was used to estimate an average air velocity across the generator. These average air velocity values along the generator for seven different readings of the variac have been plotted in Figure 8.7. Since these average velocity profiles are nearly linear, an arithmatic average air velocity was calculated for each of the variac readings. These average air velocity values were used to obtain the calibration curve shown in Figure 8.8. Local values of air velocity on the centre line of the generator have also been plotted in Figure 8.9. These values were used to draw a calibration curve for average centre line air velocities shown in Figure 8.10. This figure was used to calculate local Reynolds number.

Temperatures were read to the nearest $0.1^{o}C$ through a digital readout from chromel-alumel thermocouples. The 0.2mm diameter thermocouple wires were twin twisted with PTFE insulation. Calibrated thermocouples were distributed over the generator surface and were secured to the cotton cloth with a silicon rubber compound as shown in Figure 8.11.

The solution fed to the generator was first mixed in an agitated vessel and its temperature was controlled in a constant temperature bath, as shown in Figure 8.1.

Air temperatures and relative humidity values were also measured at 11 points, about 60mm above the generator surface, corresponding to each of the surface temperature measurements shown in Figure 8.11. Air temperature measurements were done with a thermocouple attached to a meter scale. The thermocouple was kept under the shadow of the scale while measuring air temperatures for the experiments (11 runs) carried out with CSI lamps. The relative humidity was measured using a relative humidity probe manufactured by Lee-Dickens Ltd., Kettering, Northants, U.K. It measured the relative humidity with an accuracy of $\pm$ 0.5 per cent and a response time of approximately 12 sec for a step change of 80 per cent in still air. These measurements were found to be constant on the plane vertical to the generator (from 40mm to 120mm). Both the relative humidity and the air temperature were found to be varying only marginally in the plane parallel to the generator. Typically, the relative humidity varied by about 2 per cent whereas the air temperature varied marginally ($0.6^{o}C$ at an air temperature of $22^{o}C$). Both the relative humidity and the air temperature increased along the length and on either side of the generator. The variation on the sides was symmetrical. Since the relative humidity decreases with temperature, the change in the relative humidity was minimised because of the simultaneous increase in relative humidity and air temperature. Even though the variation of both the relative humidity and the air temperature was marginal, all the local values were considered in the calculation of the results. The power supplied to the electrical heater, which produced the heat flux, was computed by

measuring the current and potential difference. The ammeter had a range 0-10 amps readable to 0.2A and the voltmeter a range 0-100 volts readable to 2.0V.

Tests were conducted under zero air flow conditions, to check the heat distribution in the generator and to measure the temperature distribution over the generator for three values of power inputs (22.5, 53.5, 113.5 $W\,m^{-2}$). The generator temperature was nearly uniform but for a change of about $0.7^{o}C$ increase along the length of the generator at the highest heat flux of 113.5 $W\,m^{-2}$.

The concentration of the aqueous lithium chloride solution was obtained indirectly by measuring its refractive index with an ABBE Refractometer, model 60/ED supplied by Bellingham and Stanley Ltd., Tunbridge Wells, Kent, U.K. The refractometer was calibrated with solutions of known concentration. Uniform inlet concentrations were assured by agitation in the tank and the constant temperature bath. The solution at the outlet was passed through a small mixing zone in the trough. This was considered adequate to provide samples to measure the average solution concentration at the outlet of the generator.

The flow rate of the solution was measured using a rotameter with a range 0.012 to 0.10 $m^3\,h^{-1}$. The rotameter was calibrated for various solution concentrations.

8.4 EXPERIMENTAL PROCEDURE

The experiments were carried out batchwise. The aqueous lithium chloride solution was prepared in the weak solution tank, shown in

Figure 8.1, which was provided with an electrical heater and an agitator. The tank was well insulated and was connected to a constant temperature bath.

After starting the agitator and heating of the weak solution to the desired temperature, valves 1, 2 and 4 were opened and the solution pump started. A uniform flow of solution over the generator surface was ensured by the distributor and the matt black cotton cloth sheet. A constant air flow rate was maintained over the generator surface. An extractor fan was used to remove moist air from the room. It was ensured that it did not disturb the air flow over the generator. The solar simulator was switched on and the concentrated solution was fed via the trough into the collection tank. Steady state was assumed to have been reached when the concentration at the trough and the temperature at the generator surface remained constant for about 20 minutes. It took up to 2½ hours to reach the steady state.

8.5 CALCULATION PROCEDURE

Final results were computed using the following steps :

1. The resistance in the liquid phase for mass transfer could be neglected as the equilibrium distribution curve is relatively flat, i.e., a large change in liquid phase concentration leads to a relatively small change in vapour phase concentration at equilibrium (Treybal 1980). This is true if the values of individual phase mass transfer coefficients are roughly equal. Chun et al (Chun et al 1972) have shown that for a falling film evaporator, with a salt solution film,

it is sufficiently accurate to consider the interphase concentration to be the same as the average concentration. It implies that, in such situations, the gas phase controls and the liquid phase concentration could be assumed to be of uniform composition across the liquid film at any vertical position.

In the present case, it can also be assumed that the liquid film has negligible thermal resistance so that the local generator surface temperature is equal to the liquid film temperature (Simpson et al 1974), (Collier et al 1964).

The local measurement of surface temperature T, air temperature TU, about 60 mm above the generator surface and relative humidity RH at TU were recorded. Subscripts from 1 to 14 refer to the positions shown in Figure 8.11.

Average values of T_{AV}, TU_{AV} and RH_{AV} were calculated using (T_{AV1}, T_{AV2}, T_{AV3}), (TU_{AV1}, TU_{AV2}, TU_{AV3}) and (RH_{AV1}, RH_{AV2}, RH_{AV3}) respectively. Subscripts AV1, AV2 and AV3 refer to the position of 0.05m, 0.45m and 0.85m away frcm the leading edge of the generator respectively. Each of these three values were calculated using three local values at each of the three positions. The average values were calculated using Simpson's rule (Tuma 1979) since the variation was nonlinear.

2. A log mean mass transfer potential Δp_M was calculated using the mass transfer potential at the trailing edge Δp_T and mass transfer potential at the leading edge Δp_L. The vapour pressure of solution at the trailing edge was calculated from

aqueous lithium chloride properties at initial solution concentration X_I and average solution temperature T_{AV3}. The partial pressure of water vapour in the air was calculated using RH_{AV3} and TU_{AV3}. Similarly, the vapour pressure at the leading edge was calculated using the final solution concentration X_F and T_{AV1}. The partial pressure of water vapour in the air at the leading edge was calculated using RH_{AV1} and TU_{AV1}.

3. A simple mass balance given by the following equation was used to estimate the rate of water evaporation m_W.

$$m_W = m_S (1 - X_I/X_F) \tag{8.1}$$

4. The mass transfer coefficient was calculated using the following relation

$$K_P = \frac{m_W}{\Delta p_M} \tag{8.2}$$

5. The latent heat of vaporisation was calculated at an arithmatic mean temperature value between the average solution temperature T_{AV} and the average air temperature TU_{AV} as suggested by Mullick et al (Mullick et al 1974). The rate of heat transfer by evaporation at steady state was calculated from

$$q_{EV} = m_W \lambda \tag{8.3}$$

6. The rate of heat transfer for the sensible heating of the solution was calculated from Equation (8.4).

$$q_{SEN} = m_S (Cp)_S (T_{AV} - T_I) \qquad (8.4)$$

The heat capacity of the solution was assumed to be constant with change in temperature. However, the variation with concentration was considered.

7. The heat transfer by radiation was calculated using the following relation

$$q_{RAD} = \sigma\varepsilon \left[(T_{AV} + 273.0)^4 - (T_{AM} + 273.0)^4\right] \qquad (8.5)$$

T_{AM} is the average room temperature. It was found to be less than TU_{AV}, typically by about $1^{o}C$.

The performance of the generator is affected by the thermal radiation environment in which it operates. Indoors, the wall and air temperature are nearly equal and the field of view temperature can be approximated by a black enclosure at the air temperature (Green et al 1979). Therefore, in the above relation T_{AM} has been used for the radiation heat transfer.

8. The rate of heat transfer by conduction through the insulation was calculated using heat losses by convection and radiation from the outer surface of the insulation.

Heat transfer by radiation was calculated using the following relation

$$(q_{RAD})_{INS} = \sigma\, \varepsilon_{INS} \left[(T_{12} + 273.0)^4 - (T_{AM} + 273.0)^4\right] \qquad (8.6)$$

Where T_{12} is the temperature of the insulation cover and ε_{INS} is the emisivity of the cover surface. T_{AM} was used because of the reasons already explained under point 7.

The rate of heat transfer by convection was calculated by Equation (8.7).

$$(q_{CONV})_{INS} = (h_C)_{INS} (T_{12} - T_{AM}) \quad (8.7)$$

The convective heat transfer coefficient $(h_C)_{INS}$ was calculated using Kutateladze's relation (Kutaleladze 1966) given by Equation (8.8).

$$(h_C)_{INS} = 0.0249\ k_{AIR}\ (N_{RE})^{0.8}/L \quad (8.8)$$

The average air velocity at the insulation surface was found to be approximately one fourth of the average air velocity over the generator surface. This air velocity was, therefore, used to calculate Reynold's number in the above equation. Since the generator is tilted at an angle and heat transfer is taking place from the surface facing downwards, the actual heat transfer coefficient is likely to be lower than calculated by the above relation. However, since the total heat loss calculated by the above procedure was found to be less than 2 per cent of the total heat flux, the above procedure was considered to be adequate for the purpose. The conductive losses from the sides of the heater were considered to be negligible.

9. Heat flux from the electrical heater was calculated using Equation (8.9).

$$q = \frac{C.V.\ 10^{-3}}{A_{GE}} \tag{8.9}$$

10. The rate of convective heat transfer q_{CONV} was calculated using the following expression.

$$q_{CONV} = q - q_{EV} - q_{SEN} - q_{RAD} - q_{COND} \tag{8.10}$$

11. The convective heat transfer coefficient h_C was calculated from Equation (8.11).

$$h_C = q_{CONV}/(T - TU)_{AV} \tag{8.11}$$

The average heat transfer driving potential $(T - TU)_{AV}$ was calculated from the average driving potential at three locations $\left[(T_{AV1} - TU_{AV1}), (T_{AV2} - TU_{AV2}), (T_{AV3} - TU_{AV3})\right]$ using Simpson's rule.

12. The convective heat transfer coefficient h_C for the experiments carried out with the electrical heater were correlated in the following form

$$h_C = f\left[(\rho v)^n\right] \tag{8.12}$$

13. The heat flux provided by the lamps was computed with the help of the correlation for the convective heat transfer coefficient developed from the experimental data with the electrical heater beneath the generator surface. The rates of heat transfer by conduction, radiation, evaporation and sensible heating were calculated as discussed earlier. Knowing the heat transfer driving potential $(T - TU)_{AV}$ and the convective heat

transfer coefficient frcm the correlation given by Equation (8.12), the heat transfer by convection q_{CONV} was calculated as follows

$$q_{CONV} = h_C (T - TU)_{AV} \qquad (8.13)$$

The addition of heat transferred by all the modes, i.e., conduction, convection, radiation, evaporation and sensible heating, gave the value of heat flux provided by the lamps. This value of heat flux was found to be approximately constant for all the experiments (11 runs) carried out with the lamps. This will be discussed further in Section 8.6.3.

14. Local values of the heat transfer coefficient on the centre line of the generator were calculated from Equation (8.14)

$$h_Y = (q - q_{COND})/(T_Y - TU_Y) \qquad (8.14)$$

These values were calculated at a distance of 0.05, 0.25, 0.45 0.65 and 0.85m away from the leading edge, on the centre line of the generator.

15. Local values of the Nusselt number $(N_{NU})_Y$ were also calculated using h_Y values. The local Reynolds number $(N_{RE})_Y$ was calculated using the air velocities from the calibration curve for centre line air velocities shown in Figure 8.10.

8.6 RESULTS AND DISCUSSION

8.6.1 Preliminary results and discussion

Preliminary experiments were carried out using the air flow arrangement as discussed earlier but for the following differences.

- The distance between the honeycomb and the leading edge of the generator was less than 0.5m. The cross-section of air flow after the honeycomb was reduced by adding another metallic part on the front face so that the vertical dimension of 250mm was reduced gradually to about 90mm. This reduced the variation of air velocity across the generator. Therefore, in the preliminary experiments, an arithmatic average of the series of air velocity measurements over the generator was used to calculate the Reynolds number. An extractor fan was also used to suck the moist air at the top end of the generator. This also appeared to affect the mechanism of heat and mass transfer over the generator surface. However, all the experimental data led to an empirical correlation shown in Figure 8.12. It was found that the heat and the mass transfer data were not analogous when compared using the Chilton-Colburn analogy. However, subsequently the air flow arrangement was changed to the one described in Section 8.3. The extractor fan at the trailing edge of the generator was also shifted and it was ensured that it did not affect the air flow over the generator.

8.6.2 Heat transfer from dry generator

In order to establish the suitability of the generator surface for experiments with the lithium chloride solution, experiments (13 runs) for forced convection were also conducted on the dry generator surface. These experiments were conducted in the same way and with the same generator surface, including the same cotton cloth and thermocouples, as the experiments with the wetted generator surface.

Centre line local heat transfer coefficients h_y were calculated. The measurements were taken at a distance of 0.05, 0.25, 0.45, 0.685 and 0.85m from the leading edge. In every case the h_y values decreased from a maximum value at 0.05m from the leading edge and thereafter dropped to almost a steady value as shown in Figure 8.13. This behaviour was probably caused by severe separation of air flow over the bluff leading edge. It appears that the separation of air flow inhibited the growth of the laminar boundary layer and the turbulent boundary layer was established quickly and grew with distance along the length of the generator. Similar shapes of heat transfer curves have been reported by Lewis (Lewis 1969). Later, Simpson et al (Simpson et al 1974) postulated and confirmed experimentally the existance of the separation region in a heat transfer study from a thick flat plate to air in turbulent flow. The growth of the separation region for flow over a bluff leading edge is shown in Figure 8.14.

The local heat transfer coefficients were reduced to local Nusselt numbers $(N_{NU})_Y$ and plotted against $(N_{RE})_Y$ in Figure 8.15. The trend is similar to the empirical equations proposed by Kutateladze et al (Kutateladze et al 1966) and Kays (Kays 1966) as shown in Figure 8.15. However, the Nusselt numbers in the present case are higher than those predicted by these empirical equations. This could be partly attributed to increased effective surface area because of the use of cotton cloth on the generator surface.

It has been suggested that main stream turbulence can increase the heat transfer coefficient from a surface to the fluid passing over it (Lewis 1969), (Petrie 1972). The honeycomb used in the present air flow arrangement did help in distributing the air across the generator to a certain extent. However, it appeared to increase the turbulence

in the incoming air over the generator. The increase in the heat transfer coefficient in the present experiments could also be due to the increased turbulence in the main air stream.

Bodies with sharp edges, such as a flat plate at zero incidence, are quite insensitive to surface roughness as the point of transition is determined by the edges. On the other hand, the drag of buff bodies is very sensitive to roughness. The value of the critical Reynolds number, for which the drag drops rapidly, depends significantly on the roughness of the surface. The critical Reynolds number decreases with increasing rcughness. The boundary layer appears to be disturbed by the roughness to such a degree that transition occurs at considerably lower Reynolds numbers than in the case of smooth surfaces. Another important factor which affects the value of the critical Reynolds number is free stream turbulence (Schlichting 1968).

In general, on a flat plate, the transition can occur at a Reynolds number in the range 8×10^4 to 5×10^5, depending upon various conditions. However, under special conditions turbulent layers have been observed for a Reynolds number of 8×10^4 (Chapman 1967). In the present case, because of the free stream turbulence, roughness of the surface and the bluff leading edge, there was probably a turbulent boundary layer over most of the length of the generator as suggested by Kutateladze et al (Katateĺadze et al 1966).

8.6.3 Heat transfer from wet generator

The ranges of parameters studied in the present experiments were as follows :

initial solution concentration X_I = 31 to 34 wt per cent

average air velocity $v = 1.0$ to 4.0 m s^{-1}

weak solution flow rate $m_S = 11.0$ to 16.0 kg h^{-1} m^{-2}

heat flux $q = 0.5$ to 1.0 kW m^{-2}

initial solution temperature $T_I = 25.5$ to 28.5 °C

ambient temperature $T_{AM} = 20$ to 25°C

relative humidity $RH_{AM} = 30$ to 50 per cent

In total 39 runs were carried out with lithium chloride solution; eleven runs were conducted with CSI lamps and the remainder with the electrical heater underneath the generator surface.

Figures 8.16 to 8.19 show the variation of the centre line local heat transfer coefficient h_y along the length of the generator for various air velocities. For a fixed distance from the leading edge the h_y values increased with air velocity. For a constant velocity, h_y values decreased to a minimum at a distance from the leading edge, and thereafter increased gradually as shown in these figures. This behaviour is probably because of the following reason.

When the dilute lithium chloride solution is distributed at the trailing edge of the generator, the cotton cloth ensures the wetting of the entire generator surface. The solution attains a particular temperature depending upon the value of the heat flux and starts evaporating. This appears to happen in the first few centimeters from the trailing edge of the generator. Because of the vaporisation, the concentration of the solution increases as it flows from the trailing edge to the leading edge of the generator. This leads to a gradual increase in the

solution temperature for most of the generator length. This increase in the solution temperature is reflected in all the figures for the local heat transfer coefficients. It may be noted here that Figure 8.19 is a plot for the data obtained from the experiments conducted with the CSI lamps. This plot is very similar to the plots for the experiments conducted with the electrical heater.

In general, the local heat transfer coefficients from these experiments were higher than the local heat transfer coefficients obtained with the dry generator surface. This is because of the contribution to heat transfer by evaporation. All these local heat transfer coefficients were reduced to local Nusselt numbers $(N_{NU})_Y$ using average bulk air properties. These $(N_{NU})_Y$ values have been plotted against $(N_{RE})_Y$ values in Figure 8.20. The trend of the data is similar to the data for dry generator experiments and other established empirical correlations. It appears that there is a break in the data trend at about $(N_{RE})_Y = 8 \times 10^4$. All the convective heat transfer data, for which N_{RE} values were greater than 8×10^4 (20 runs), were correlated as a function of air mass velocity ($v\ \rho_{AIR}$). The data fitted in Equation (8.15) with a root mean square residual (RMSR) value of 2.54×10^{-3}.

$$h_C = 0.00895\ (v\ \rho_{AIR})^{0.821} \qquad (8.15)$$

In order to have a direct comparison of available correlations with the present data, the experimental data were recorrelated with the air mass velocity ($v\ \rho_{AIR}$) exponent of 0.8. The data fitted to Equation (8.16) with a RMSR value of 2.48×10^{-3}.

$$h_C = 0.0092\ (v\ \rho_{AIR})^{0.8} \qquad (8.16)$$

Equation (8.16), along with the experimental data, has been plotted in Figure 8.21. This correlation was used to estimate the constant heat flux provided by the CSI lamps as discussed earlier. This constant value of the heat flux was found to be 0.715 $\pm$ 0.045 kW m^{-2} for all the experiments (11 runs) carried out with the lamps.

The convective heat transfer coefficients, calculated in the case of heat transfer from the dry generator surface, are also shown in the same figure. These values are similar to the values represented by Equation (8.16) as can be seen in Figure 8.21. This shows consistency of the experimental data. All the mass transfer coefficients K_p, for which N_{RE} was greater than 8.0×10^4 (31 runs), were correlated by Equation (8.17) with a RMSR value of 1.85×10^{-2}.

$$K_p = 0.0438 \, (v \, \rho_{AIR})^{0.515} \qquad (8.17)$$

However, when the exponent on the air mass velocity $(v \, \rho_{AIR})$ was kept constant at 0.8, the equation changed to

$$K_p = 0.0302 \, (v \, \rho_{AIR})^{0.8} \qquad (8.18)$$

The mass transfer data fitted to this equation with a RMSR value of 1.93×10^{-2}. Equation (8.18), along with all the mass transfer data, has been plotted in Figure 8.22. The mass transfer data, for the experiments with CSI lamps, have also been shown in the same figure.

The feasibility of solar simulation with the electrical heater underneath the generator surface is shown by;

1) the evidence of a constant heat flux from the CSI lamps (0.715 $\pm$ 0.045 kW m^{-2}),

2) the similarity of variation of local heat transfer coefficients along the length of the generator (Figures 8.16 to 8.19), and

3) the similarity of the variation of the mass transfer coefficients in Figure 8.22.

All the convective heat transfer coefficients, for which N_{RE} was greater than 8.0×10^4 (31 runs), were reduced to N_{NU} and j_H using the following definitions

$$N_{RE} = \frac{v \rho_{AIR} L}{\mu_{AIR}} \tag{8.20}$$

$$N_{NU} = \frac{h_C L}{k_{AIR}} \tag{8.21}$$

$$N_{PR} = \frac{Cp_{AIR} \mu_{AIR}}{k_{AIR}} \tag{8.22}$$

$$(N_{ST})_H = \left[\frac{N_{NU}}{N_{RE} \cdot N_{PR}}\right] \tag{8.23}$$

$$j_H = (N_{ST})_H (N_{PR})^{2/3} \tag{8.24}$$

The heat transfer data fitted to Equation (8.25) with a RMSR value of 6.19×10^{-4}.

$$j_H = 0.0695 (N_{RE})^{-0.206} \tag{8.25}$$

Equation (8.25) can also be written as

$$N_{NU} = 0.0695 \, (N_{RE})^{0.794} \, (N_{PR})^{0.333} \qquad (8.26)$$

In order to compare the data directly with typical existing correlations, the data were recorrelated keeping the exponent of N_{RE} as -0.2.

The heat transfer data fitted Equation (8.27), with a RMSR value of 6.09×10^{-4}.

$$j_H = 0.0645 \, (N_{RE})^{-0.2} \qquad (8.27)$$

or
$$N_{NU} = 0.0645 \, (N_{RE})^{0.8} \, (N_{PR})^{0.333} \qquad (8.28)$$

Nusselt numbers N_{NU} have been plotted against N_{RE}, along with Equation (8.28), in Figure 8.23. These data have been compared with existing correlations for turbulent and laminar flow over a flat plate. The heat transfer coefficients in the present case are higher because of the reasons explained earlier. All the mass transfer coefficients, for which N_{RE} was greater than 8.0×10^4, were reduced to N_{SH} and j_D using the following definitions.

$$N_{SH} = \frac{K_P \, L \, \left[P_{AM} - (p_{AM})_W\right]}{D \cdot \rho_{AIR}} \qquad (8.29)$$

$$N_{SC} = \frac{\mu_{AIR}}{D \cdot \rho_{AIR}} \qquad (8.30)$$

$$(N_{ST})_D = \frac{N_{SH}}{N_{RE} \cdot N_{SC}} \tag{8.31}$$

$$j_D = (N_{ST})_D \, (N_{SC})^{2/3} \tag{8.32}$$

The mass transfer data were fitted in Equation (8.33) with a RMSR value of 1.26×10^{-3}.

$$j_D = 1.876 \, (N_{RE})^{-0.492} \tag{8.33}$$

Equation (8.33) can also be written as

$$N_{SH} = 1.876 \, (N_{RE})^{0.508} \, (N_{SC})^{0.33} \tag{8.34}$$

In order to compare the data directly with typical existing correlations, the data were recorrelated keeping the exponent of N_{RE} as -0.2.

The mass transfer data fitted to Equation (8.35), with a RMSR value of 1.36×10^{-3}.

$$j_D = 0.058 \, (N_{RE})^{-0.2} \tag{8.35}$$

$$\text{or} \qquad N_{SH} = 0.058 \, (N_{RE})^{0.8} \, (N_{SC})^{0.333} \tag{8.36}$$

Sherwood numbers N_{SH} have been plotted against N_{RE}, along with Equation (8.36), in Figure 8.24. These data have been compared with existing correlations for turbulent and laminar flow over a flat plate. The data in this case are also higher for the reasons explained earlier.

The proposed correlations for the heat and mass transfer data were considered to be adequate because N_{PR} and N_{SC} were almost constant at 0.700 and 0.646 respectively. It can be found in the literature that N_{PR} and N_{SC} have been conventionally correlated with an exponent of 1/3 for a number of heat and mass transfer situations.

A non-linear regression technique was used to correlate the data in all the cases discussed above.

8.6.4 Heat and mass transfer analogy

Osborne Reynolds (Reynolds 1874) was probably the first to observe a remarkable relationship between heat transfer and skin friction given by Equation (8.37).

$$N_{ST} = f/2 \tag{8.37}$$

This relationship is valid only if the sum of the thermal diffusivities is equal to the sum of the momentum diffusivities, and for common gases where the Prandtl number is close to unity, the eddy diffusivities are of the same order and the temperature potential is moderate.

For flow past bluff bodies, the momentum analogies are no longer valid as the resistance to flow includes form drag as well as skin friction. The separation occurs for flow past a sphere or a cylinder at right angles or any bluff object. In such situations the friction factor based on total drag includes not only the skin friction but also the form drag due to flow separation. It is therefore expected to follow a function different from that of the mass transfer and heat transfer

groups. However, Chilton-Colburn represented heat and mass transfer data in the following form (Treybal 1980)

$$j_H = (N_{ST})_H (N_{PR})^{2/3} = \phi (N_{RE}) \quad (8.38)$$

$$j_D = (N_{ST})_D (N_{SC})^{2/3} = \phi (N_{RE}) \quad (8.39)$$

These equations were found to be quite useful especially when comparing heat and mass transfer data for bluff objects. For identical surface geometries j_H has been found to be equal to j_D. A number of analogies have been proposed by different workers. However, the Chilton-Colburn analogy for heat and mass transfer was considered to be adequate for the present work.

Finally, the heat transfer data as j_H and the mass transfer data as j_D were plotted in Figure 8.25. This figure shows that the variation and magnitude of the heat transfer data are adequately analogous to the mass transfer data.

All the experimental data for this chapter are given in Appendix E and computer program for the calculation is given in Appendix F.

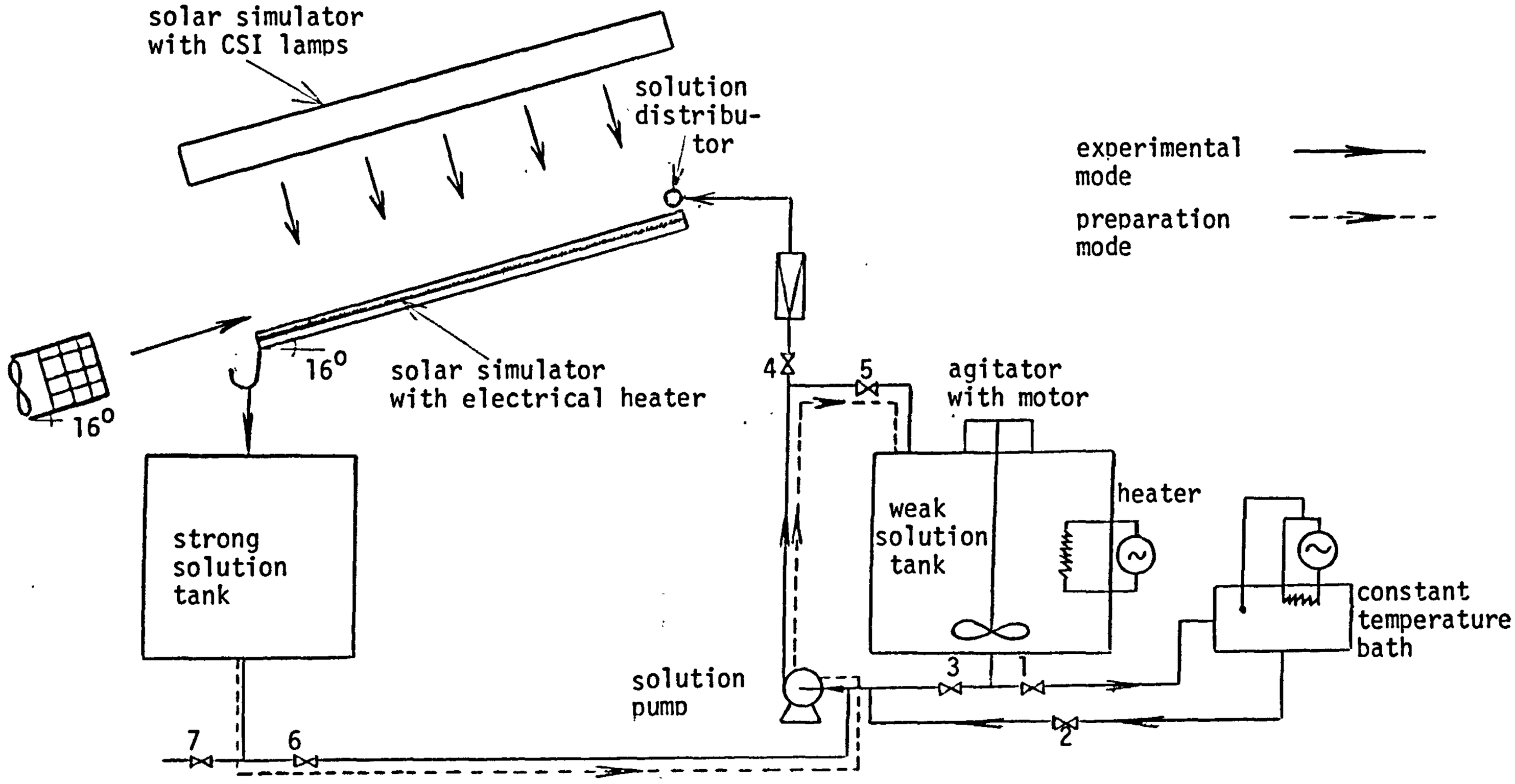

FIGURE 8.1 EXPERIMENTAL SYSTEM FOR HEAT AND MASS TRANSFER STUDIES ON THE SOLAR GENERATION OF OPEN CYCLE ABSORPTION COOLING SYSTEM

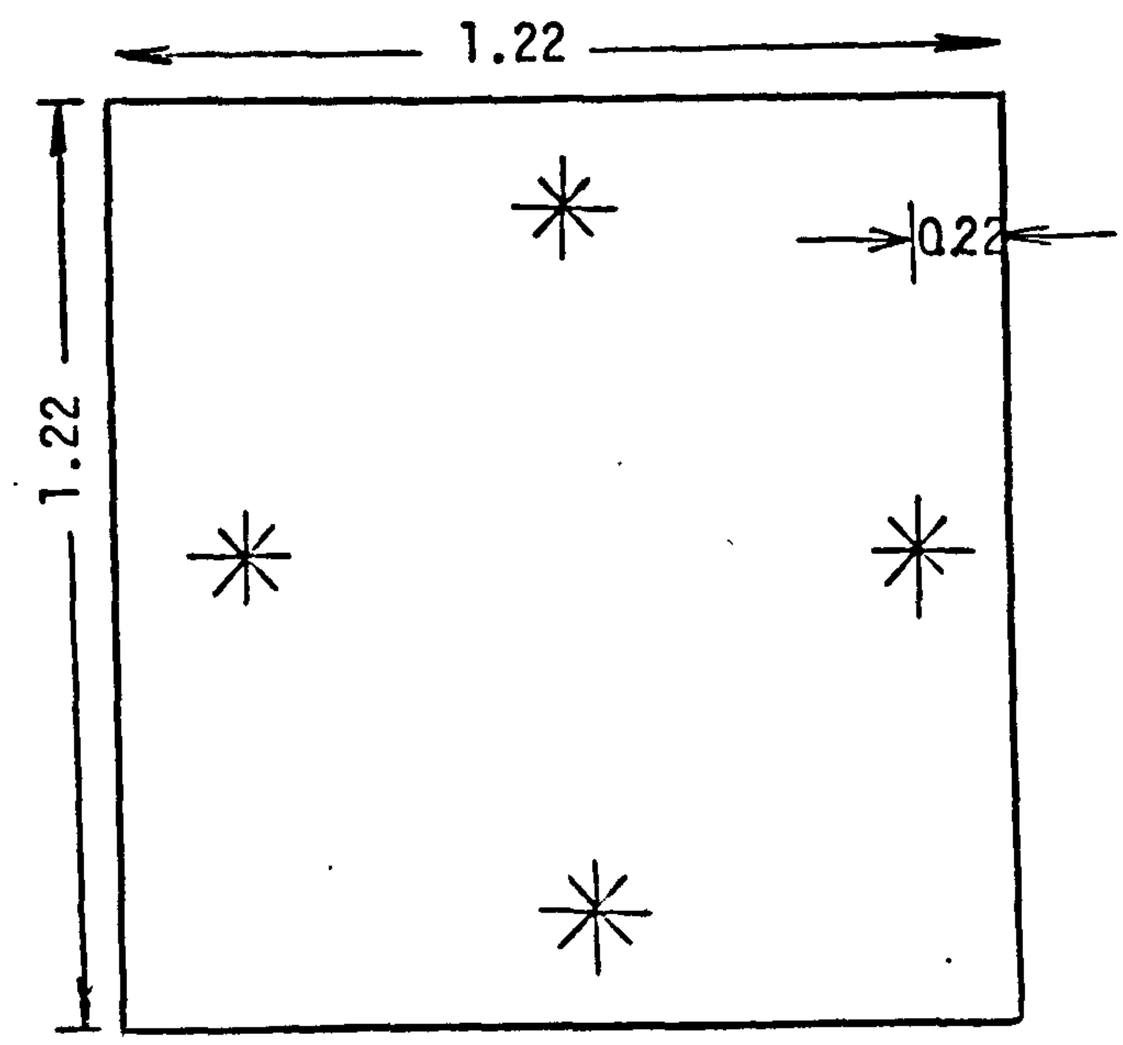

✳ CSI lamp (0.400 kW)
all dimensions are in meter

FIGURE 8.2 POSITIONS OF CSI LAMPS IN SOLAR SIMULATOR

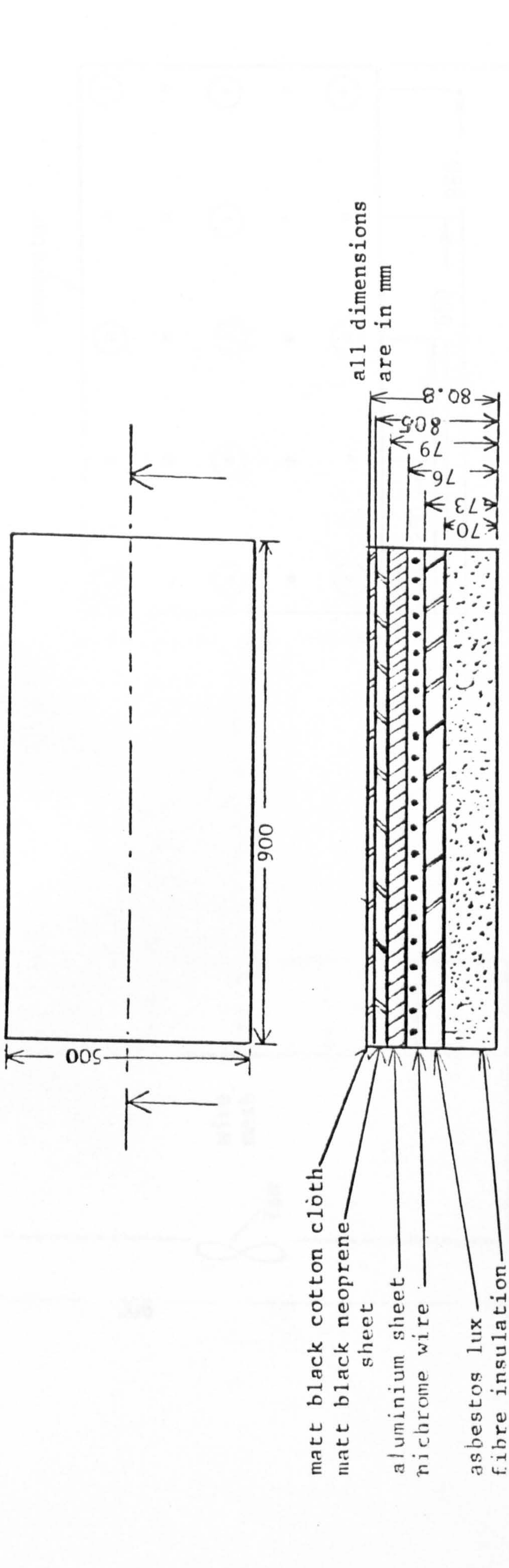

FIGURE 8.3 CROSS-SECTIONAL VIEW OF SOLAR GENERATOR

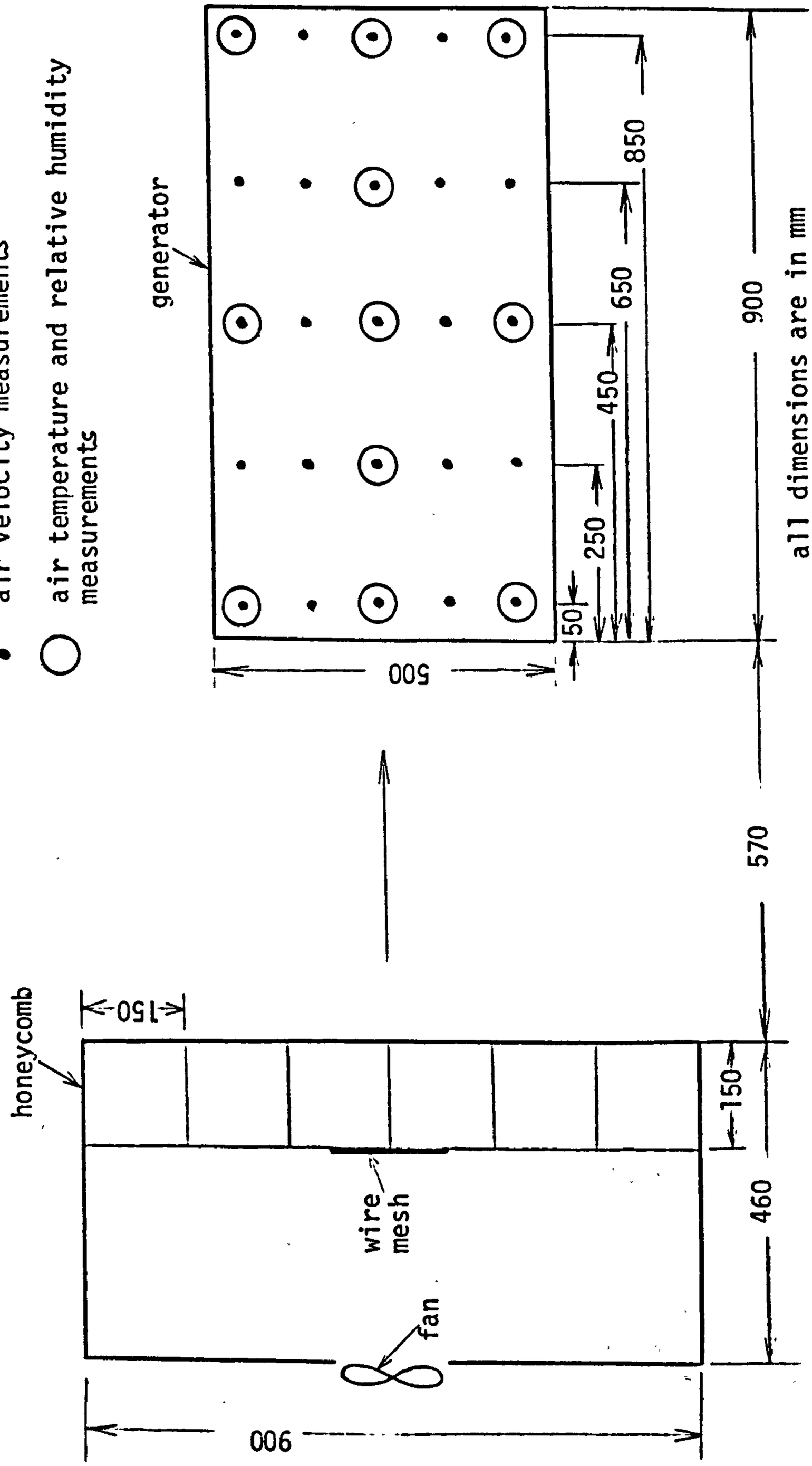

FIGURE 8.4 AIR FLOW ARRANGEMENT

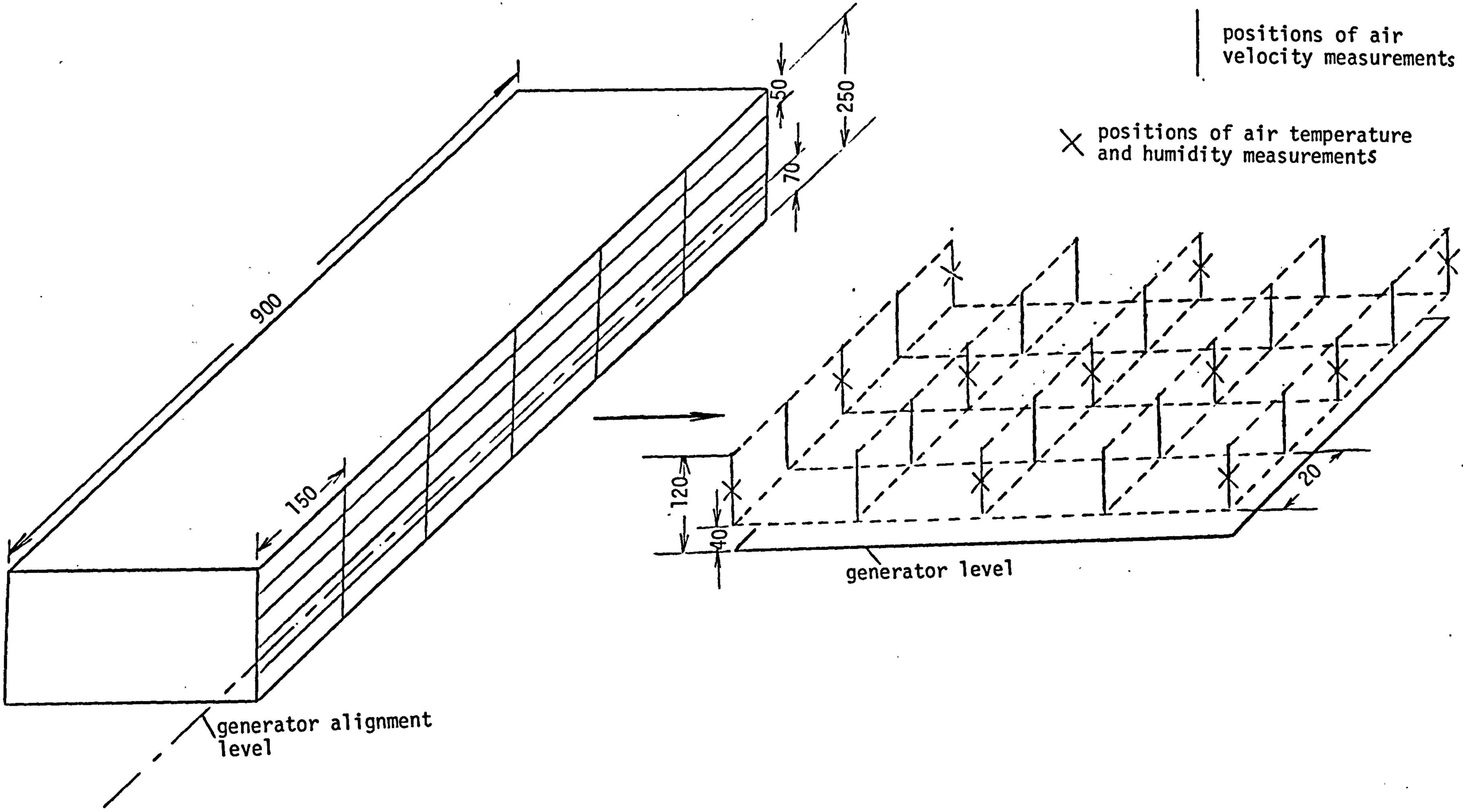

FIGURE 8.5 : DETAILS OF HONEYCOMB AND MEASUREMENT POSITIONS

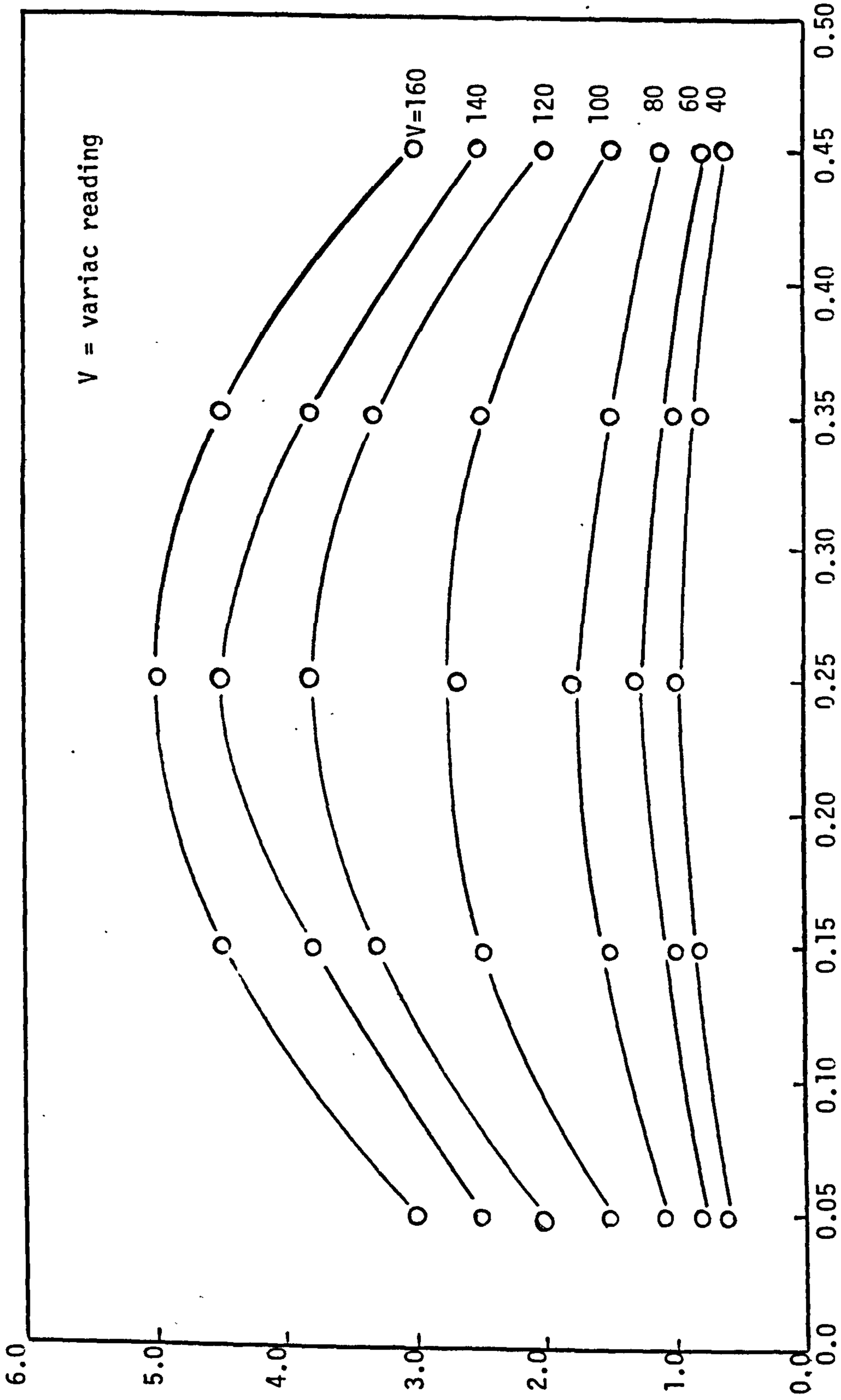

FIGURE 8.6 AIR VELOCITY DISTRIBUTION ACROSS THE GENERATOR AT THE LEADING EDGE

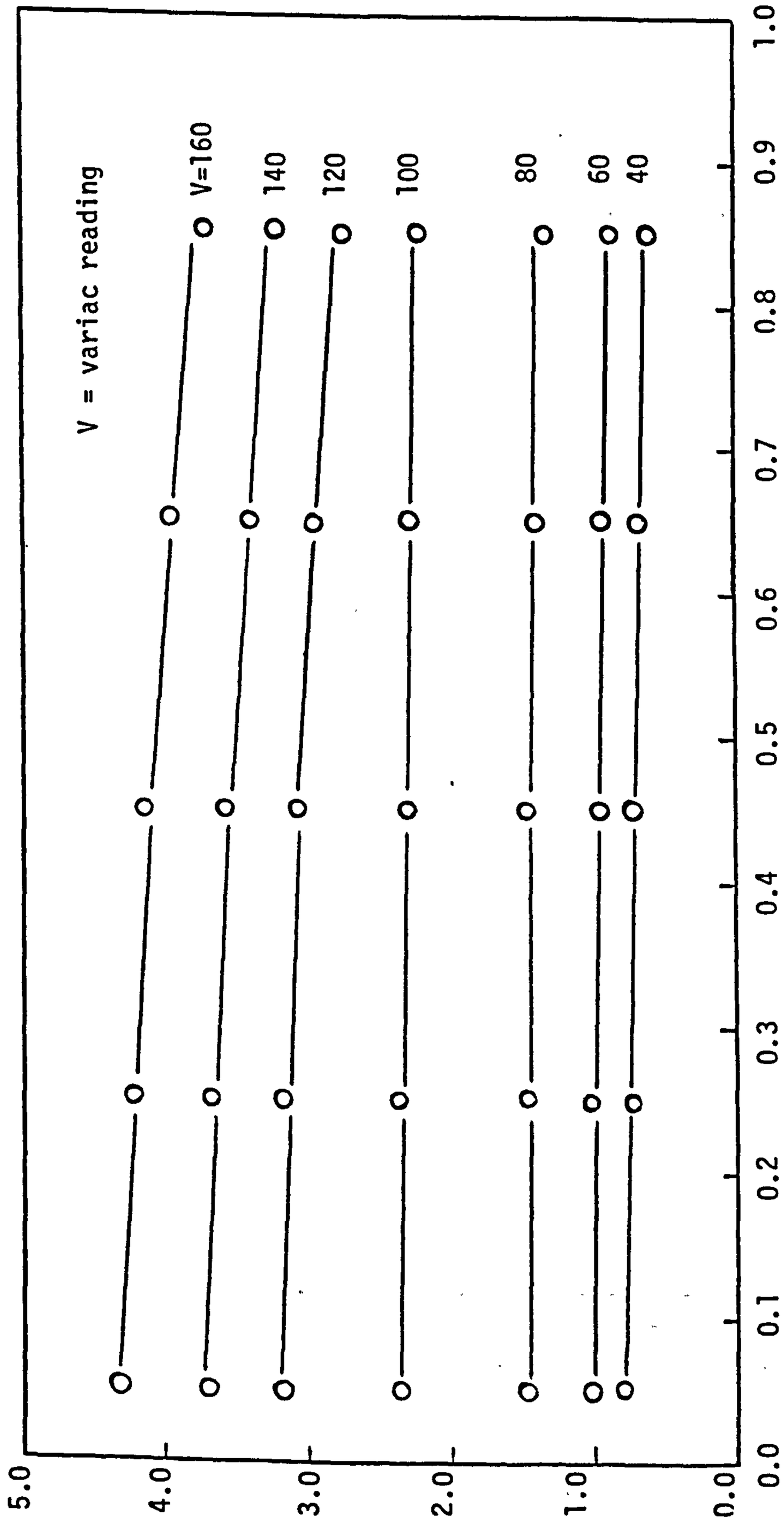

FIGURE 8.7 AVERAGE AIR VELOCITY ALONG THE LENGTH OF THE GENERATOR

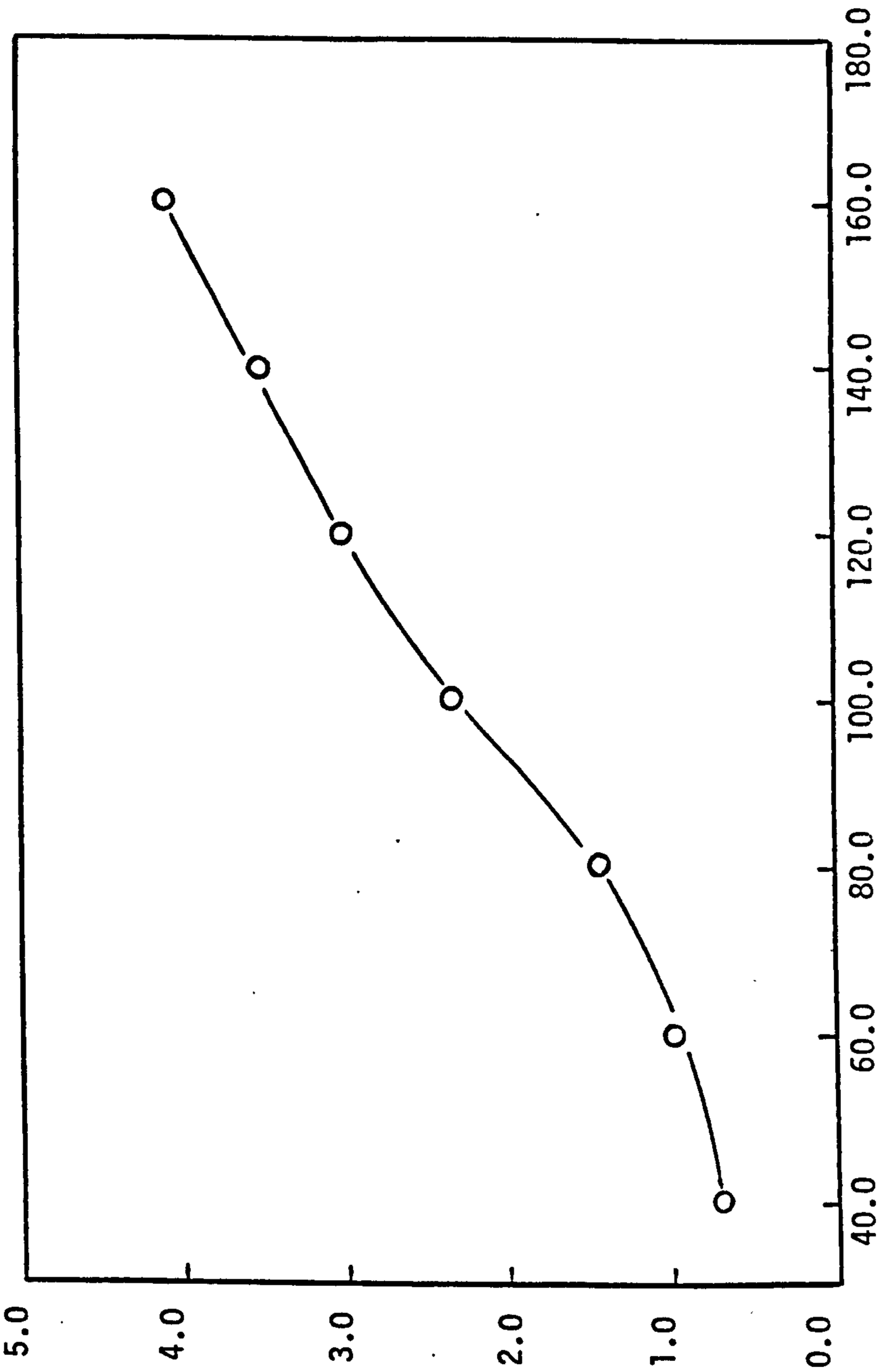

FIGURE 8.8 CALIBRATION CURVE FOR AVERAGE AIR VELOCITY

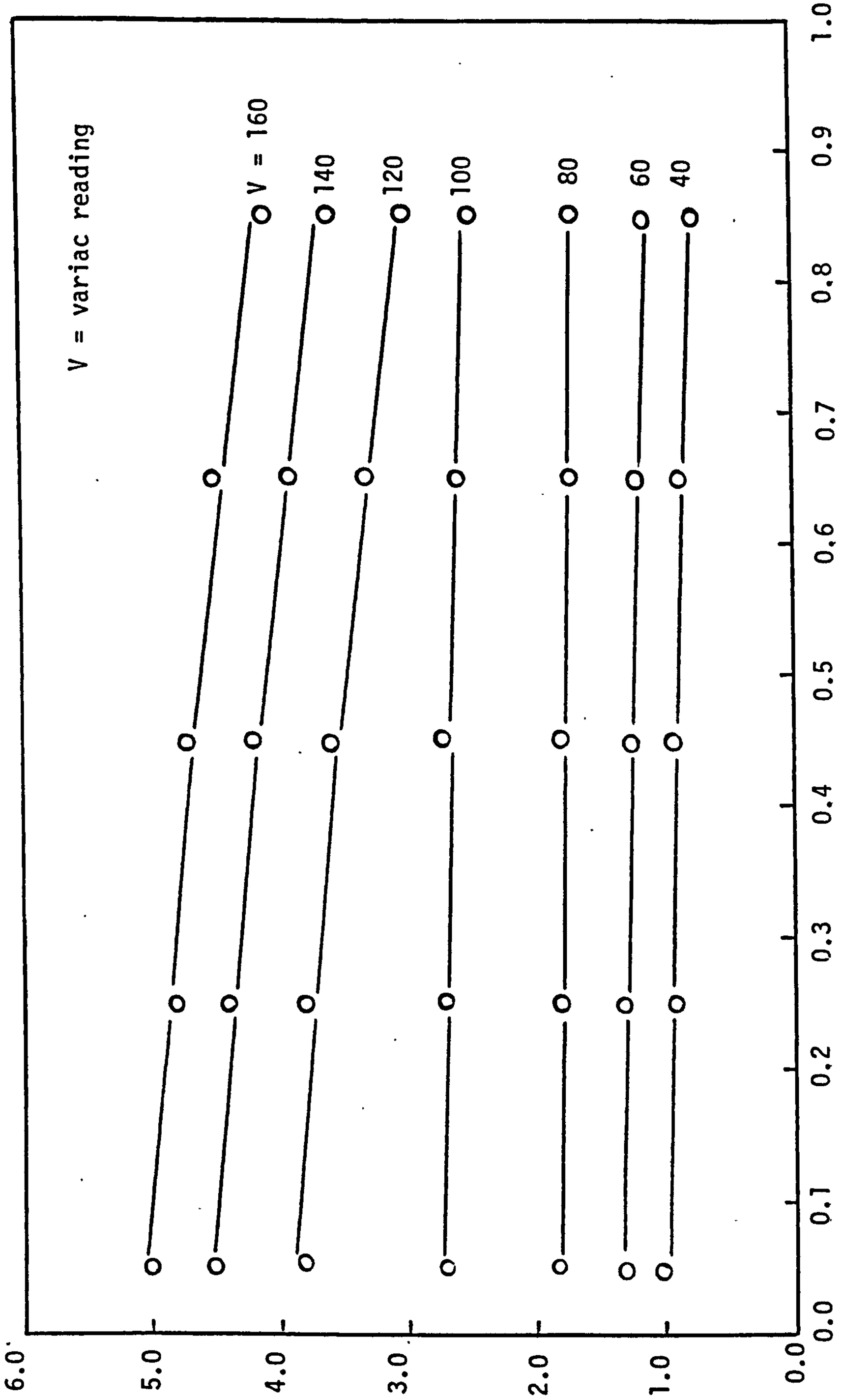

FIGURE 8.9 CENTRELINE LOCAL AIR VELOCITY

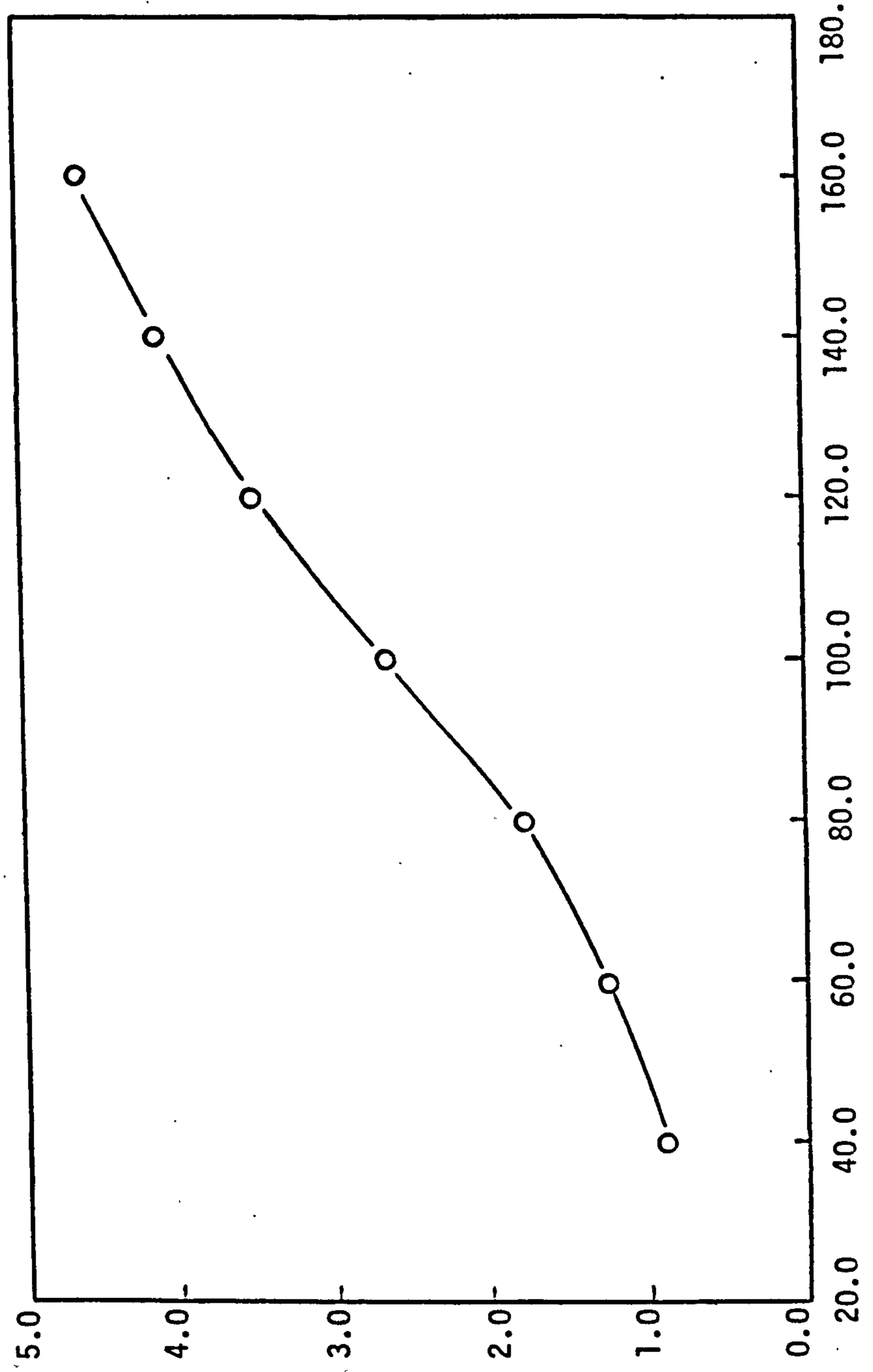

FIGURE 8.10 CALIBRATION CURVE FOR CENTRELINE AVERAGE AIR VELOCITY

10 solution temperature at the outlet
11 solution temperature at the inlet
12 insulation temperature below the generator

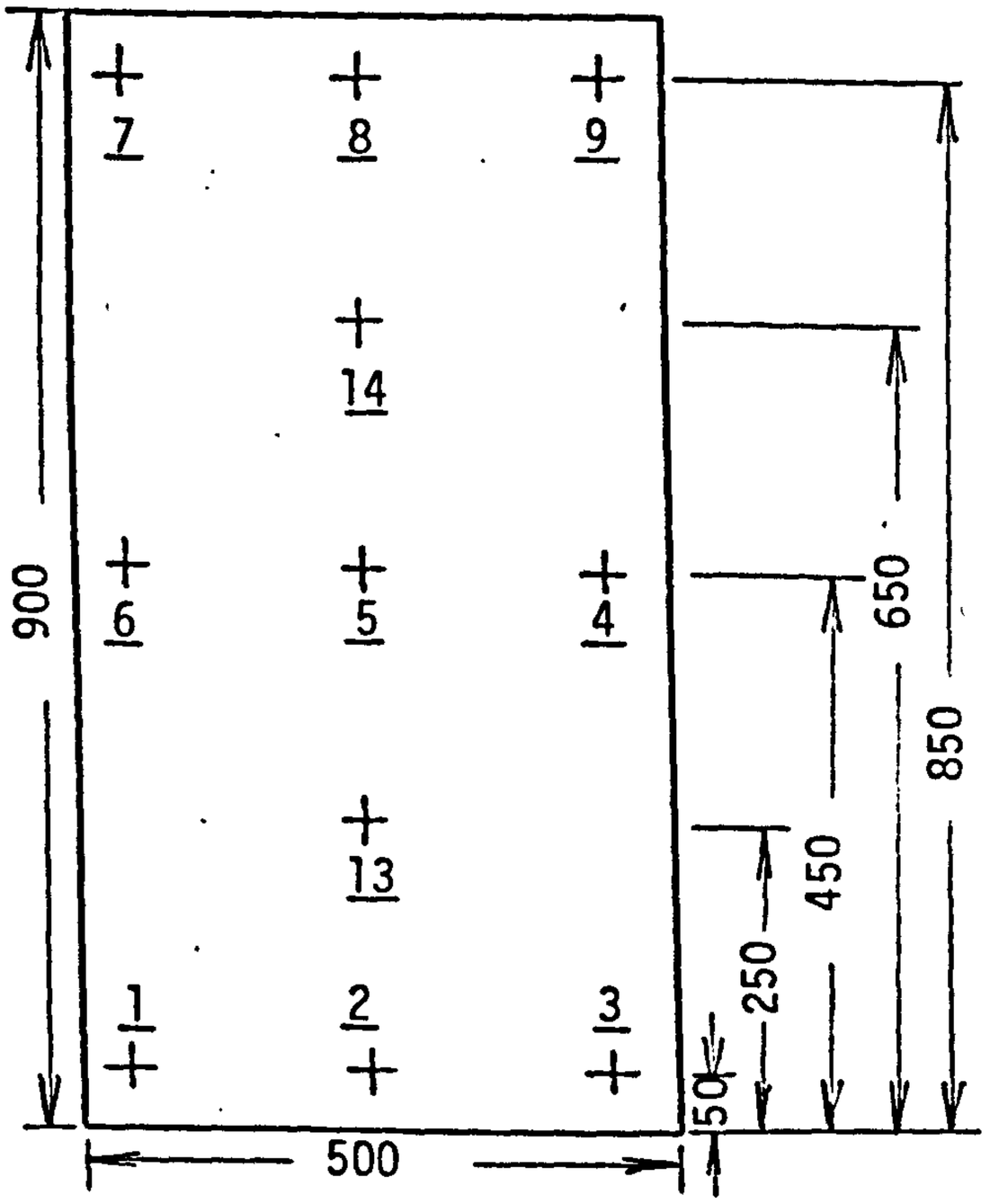

1 to 14 are thermocouple positions

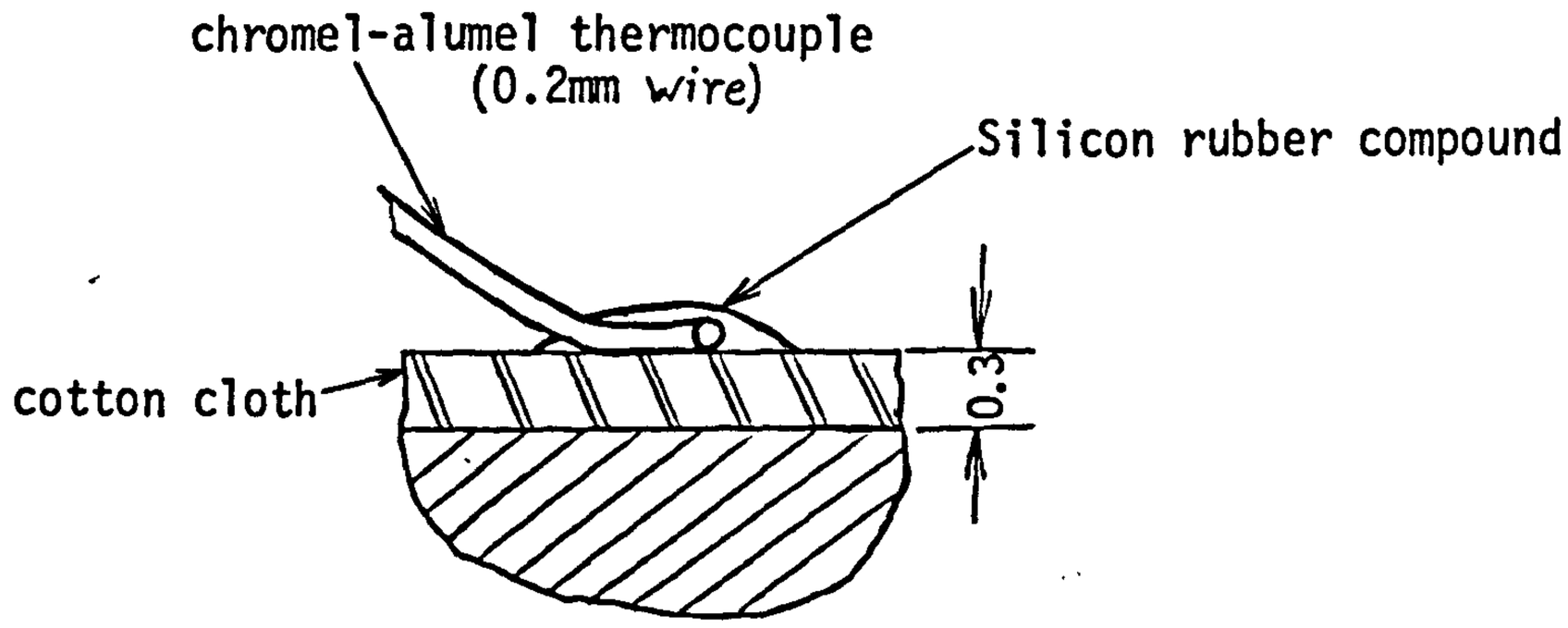

all dimensions are in mm

FIGURE 8.11 POSITIONS OF THERMOCOUPLES

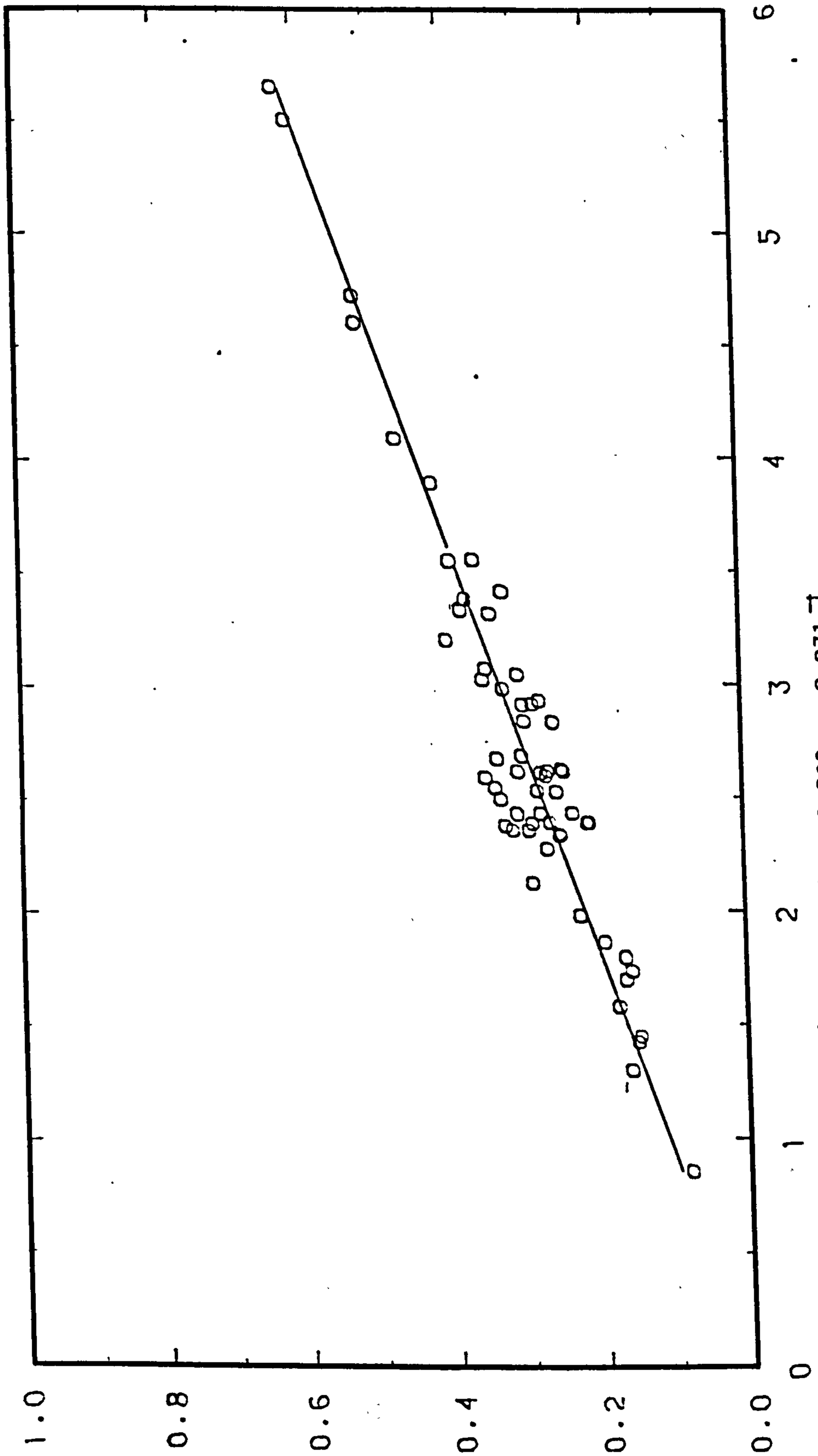

FIGURE 8.12 CORRELATION FOR THE RATE OF WATER EVAPORATION

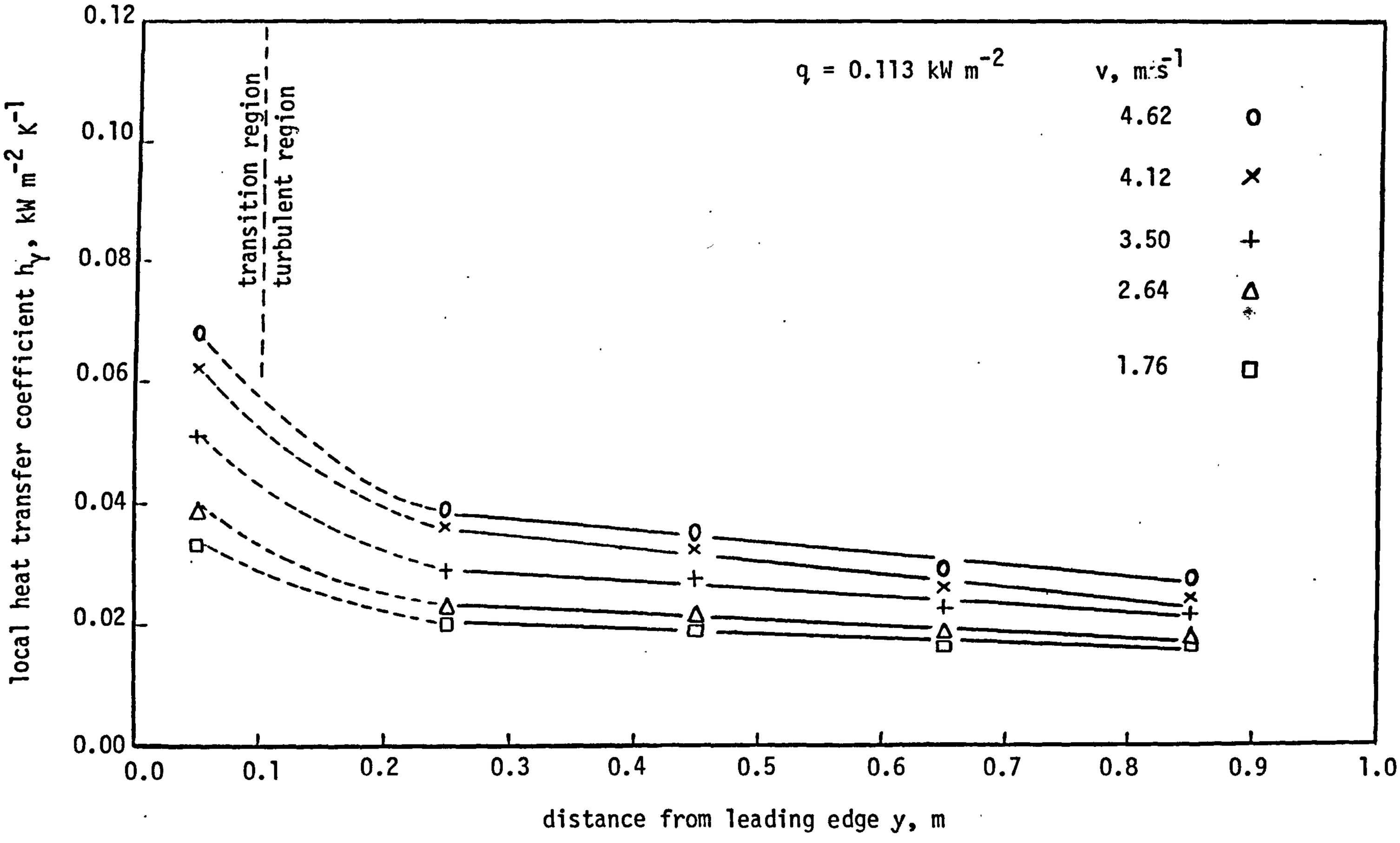

FIGURE 8.13 VARIATION OF LOCAL HEAT TRANSFER COEFFICIENT WITH DISTANCE FOR DRY GENERATOR SURFACE

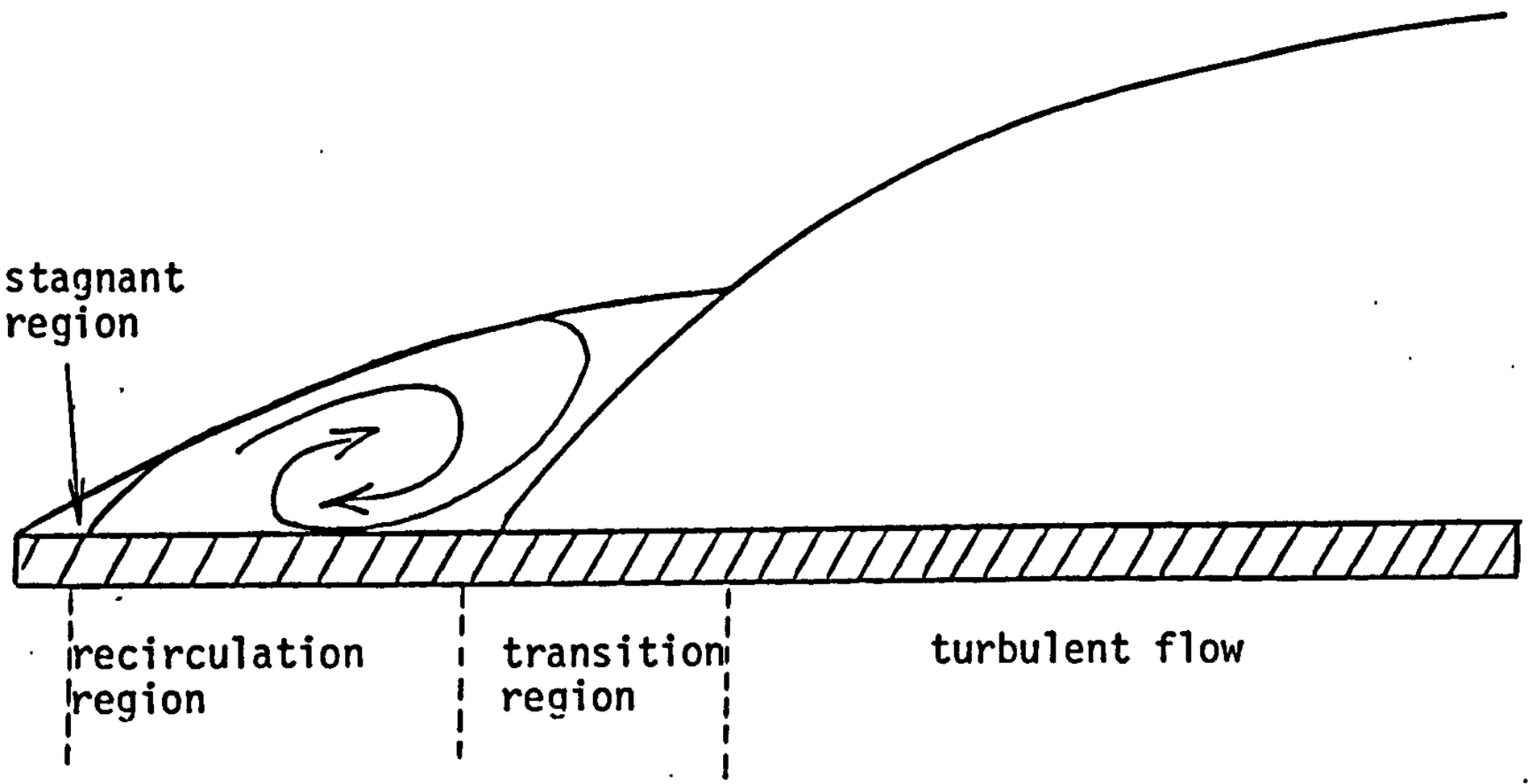

FIGURE 8.14 GROWTH OF SEPARATION REGION FOR FLOW OVER A BLUFF LEADING EDGE

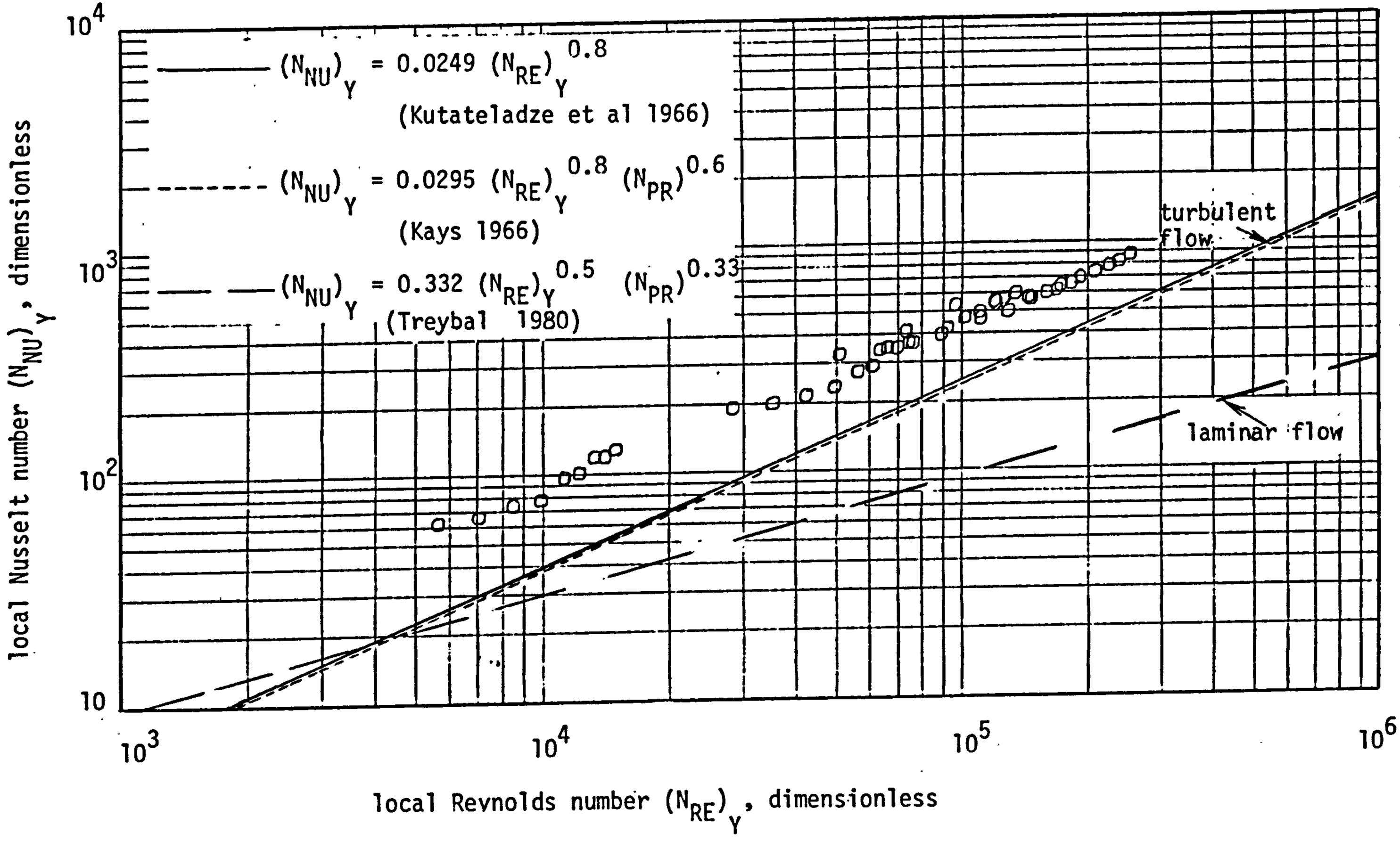

FIGURE 8.15 LOCAL NUSSELT NUMBER AGAINST LOCAL REYNOLDS NUMBER FOR HEAT TRANSFER FROM DRY GENERATOR SURFACE

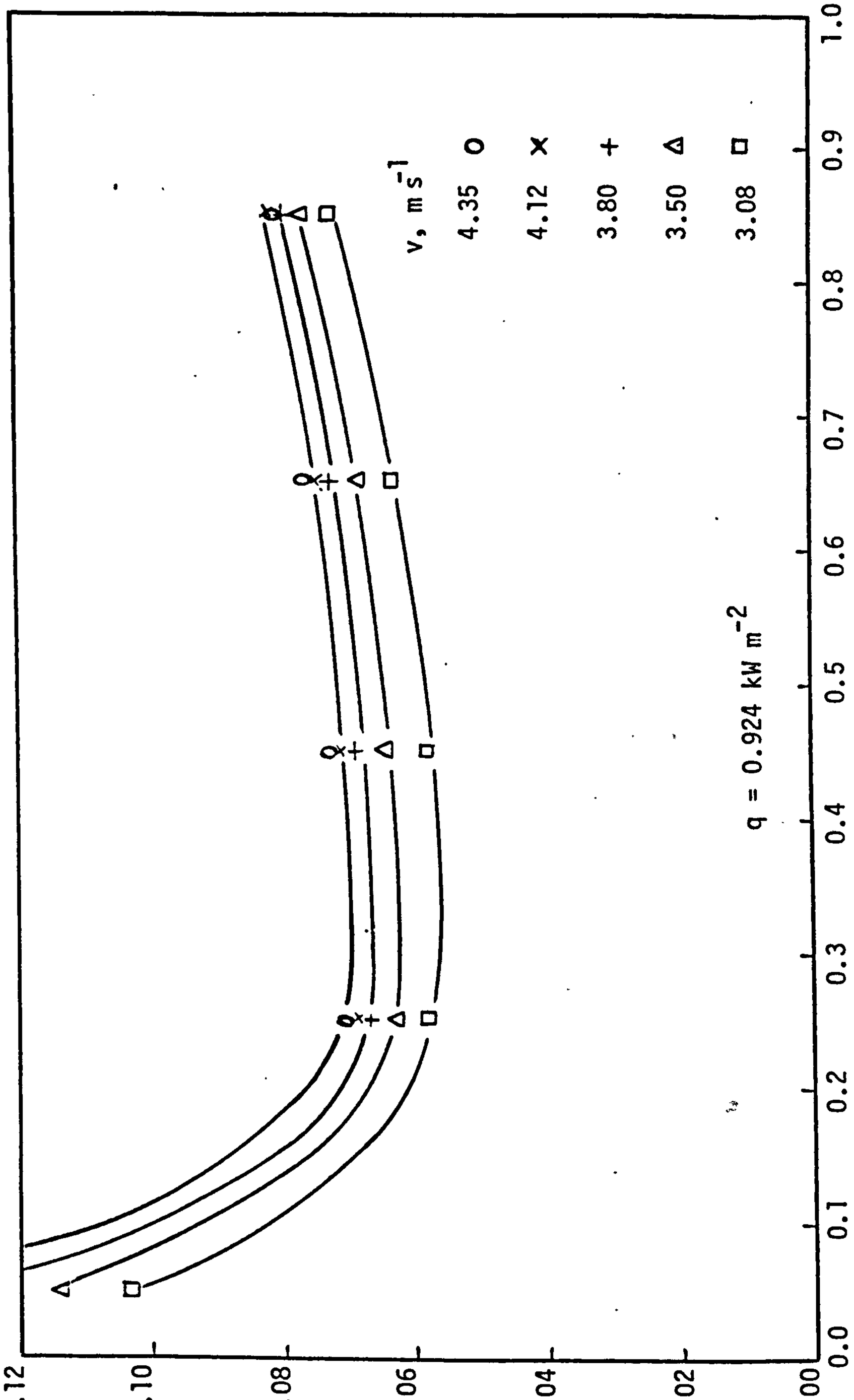

FIGURE 8.16 VARIATION OF LOCAL HEAT TRANSFER COEFFICIENT WITH DISTANCE ON WET GENERATOR SURFACE

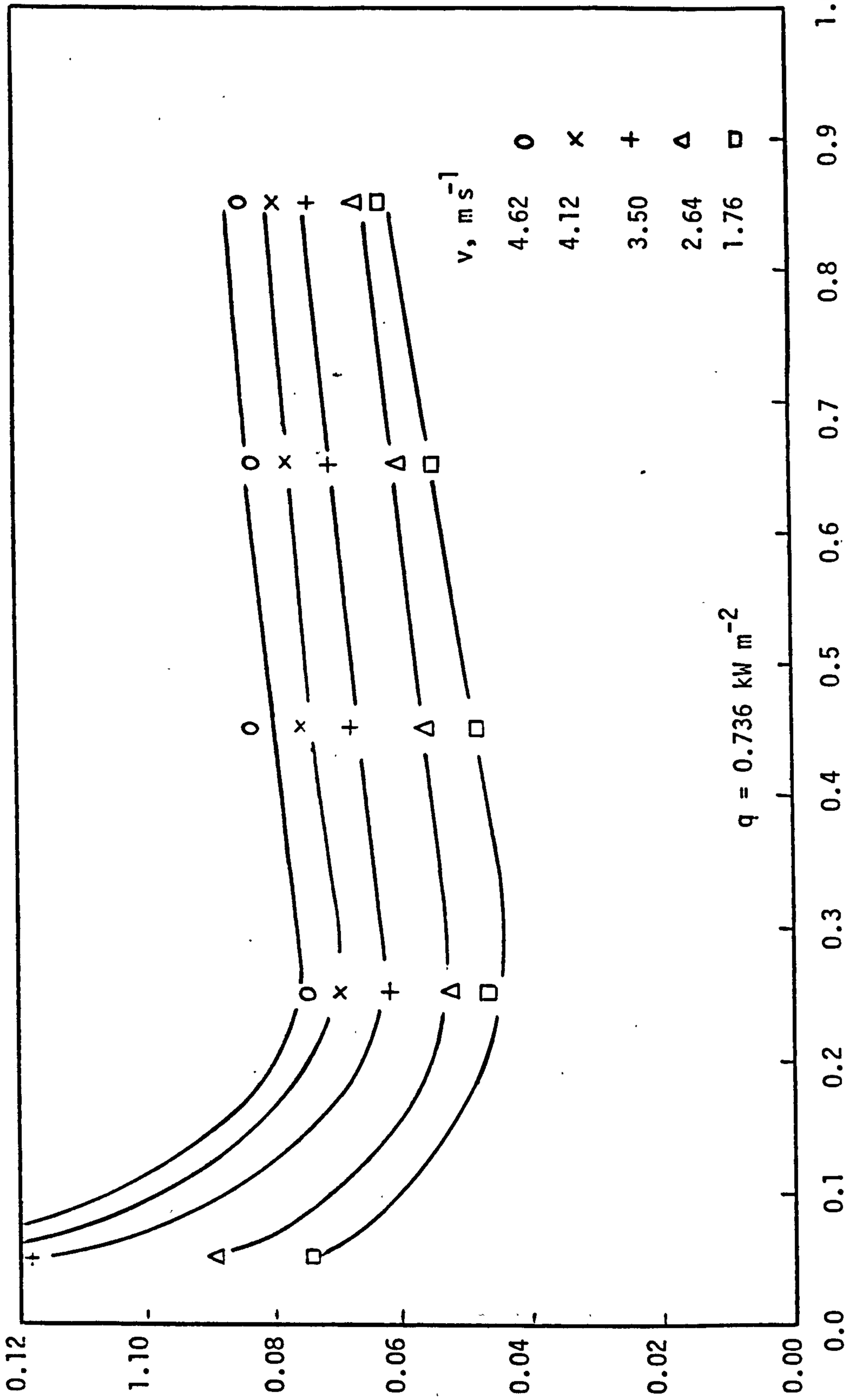

FIGURE 8.17 VARIATION OF LOCAL HEAT TRANSFER COEFFICIENT WITH DISTANCE ON WET GENERATOR SURFACE

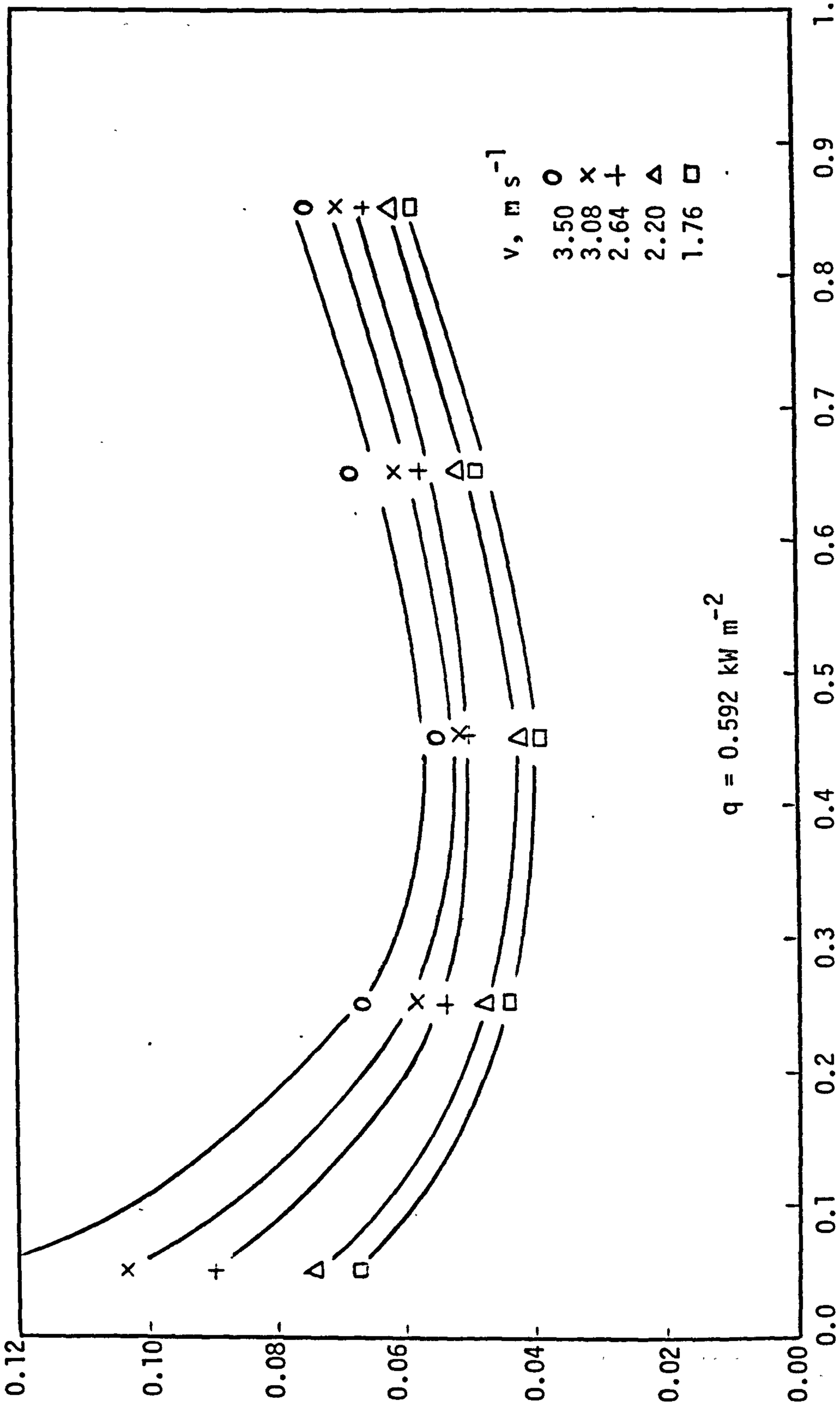

FIGURE 8.18 VARIATION OF LOCAL HEAT TRANSFER COEFFICIENT WITH DISTANCE ON WET GENERATOR SURFACE

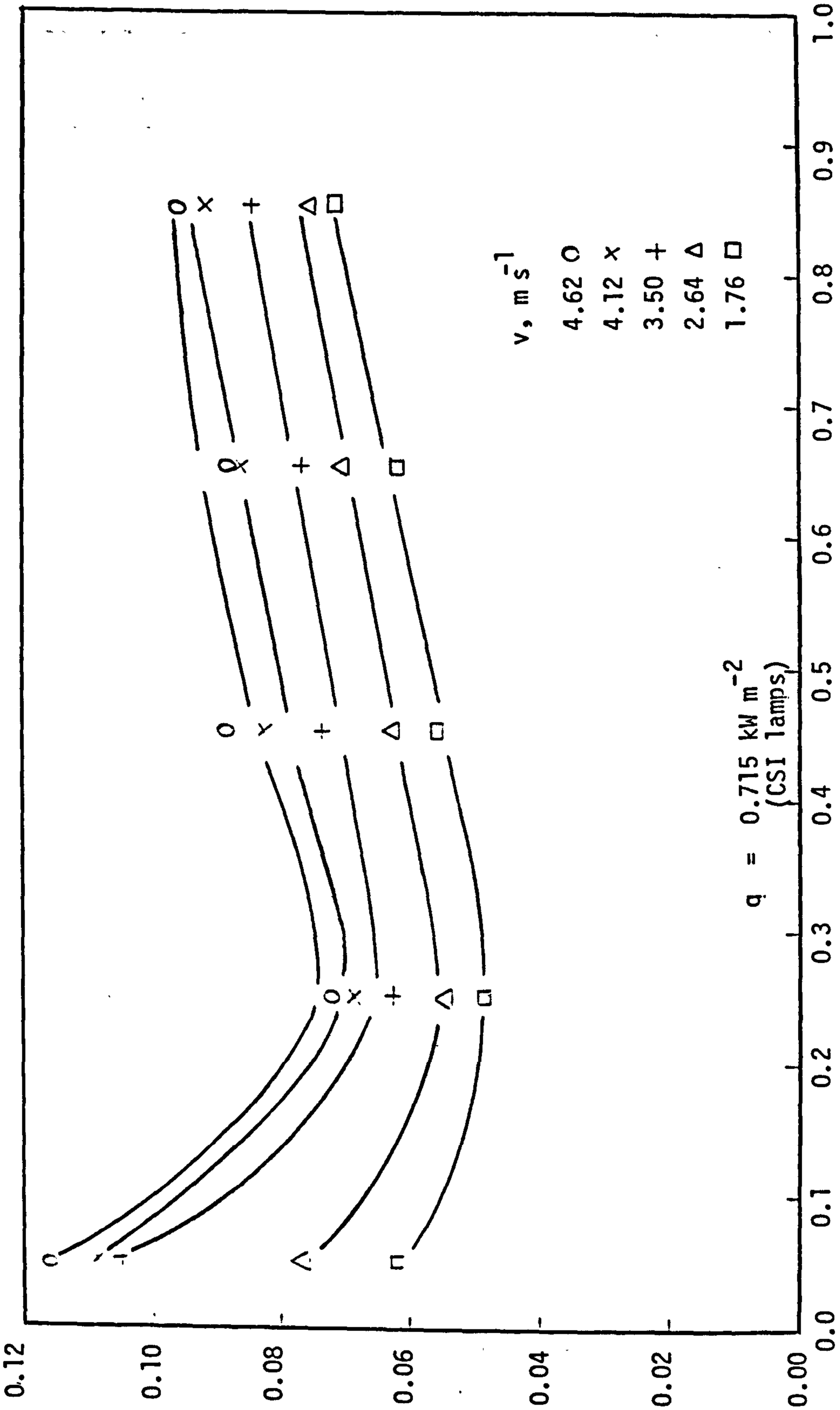

FIGURE 8.19 VARIATION OF LOCAL HEAT TRANSFER COEFFICIENT WITH DISTANCE ON WET GENERATOR SURFACE

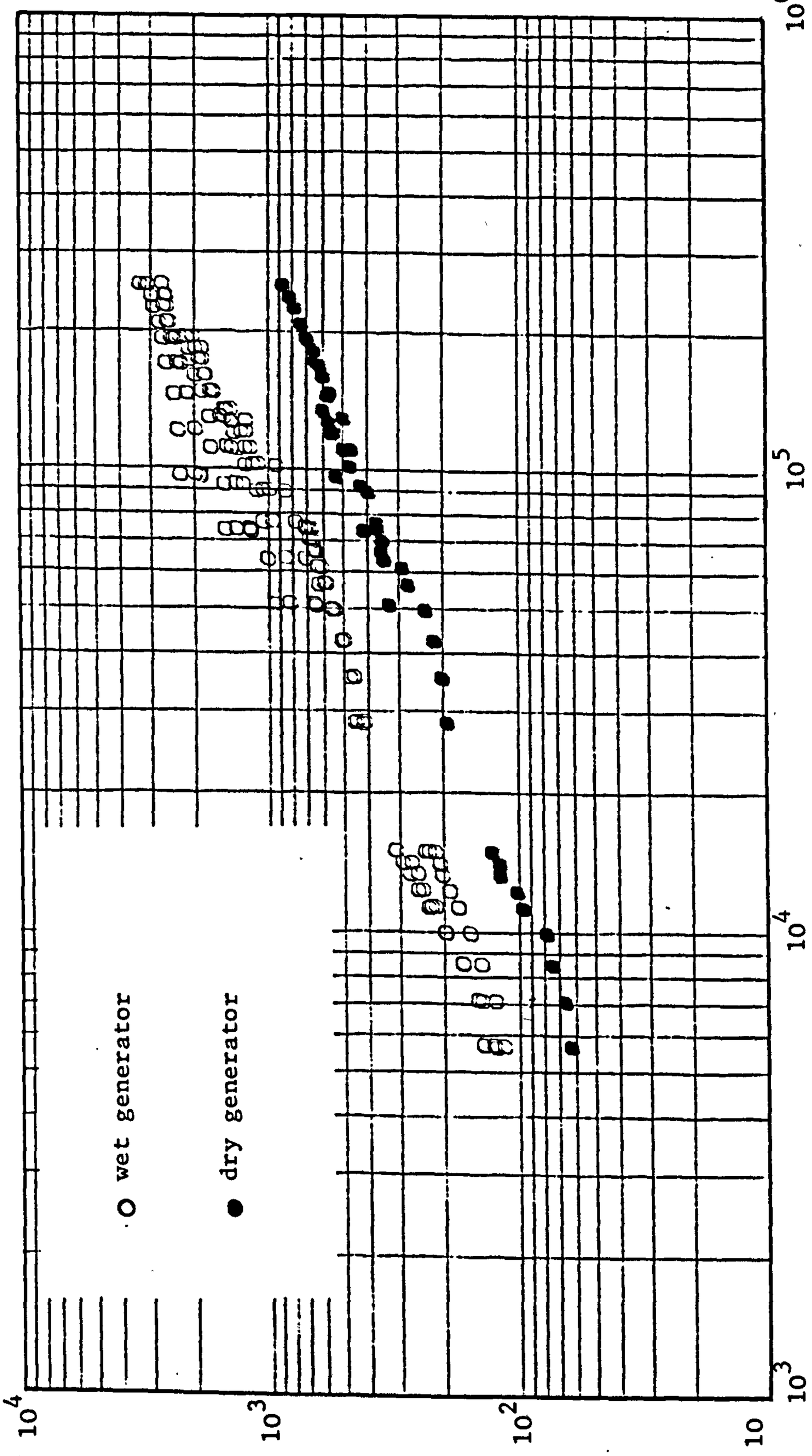

FIGURE 8.20 LOCAL NUSSELT NUMBER AGAINST REYNOLDS NUMBER FOR HEAT TRANSFER FROM WET AND DRY GENERATOR SURFACE

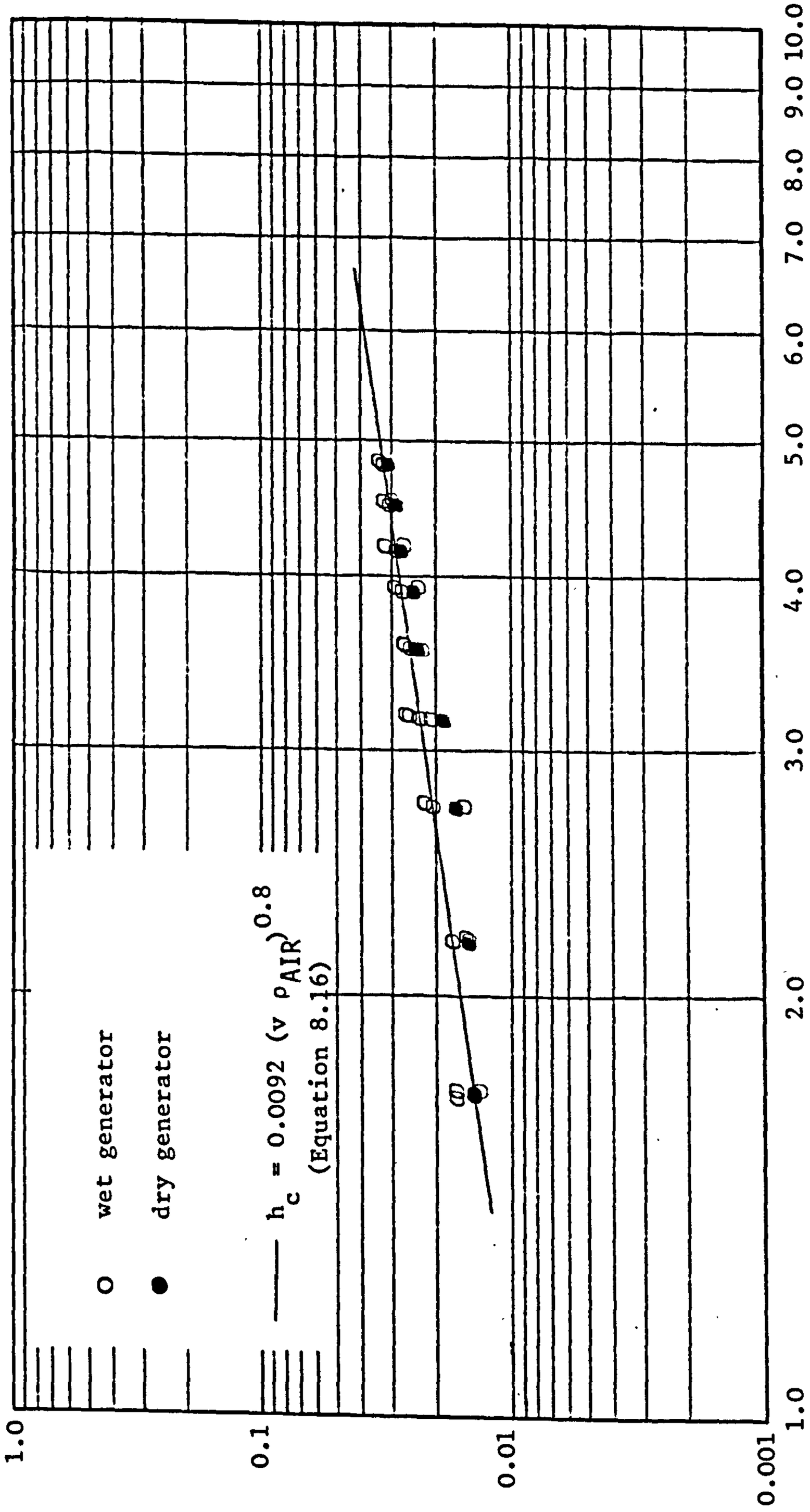

FIGURE 8.21 VARIATION OF CONVECTIVE HEAT TRANSFER COEFFICIENT AGAINST AIR MASS VELOCITY

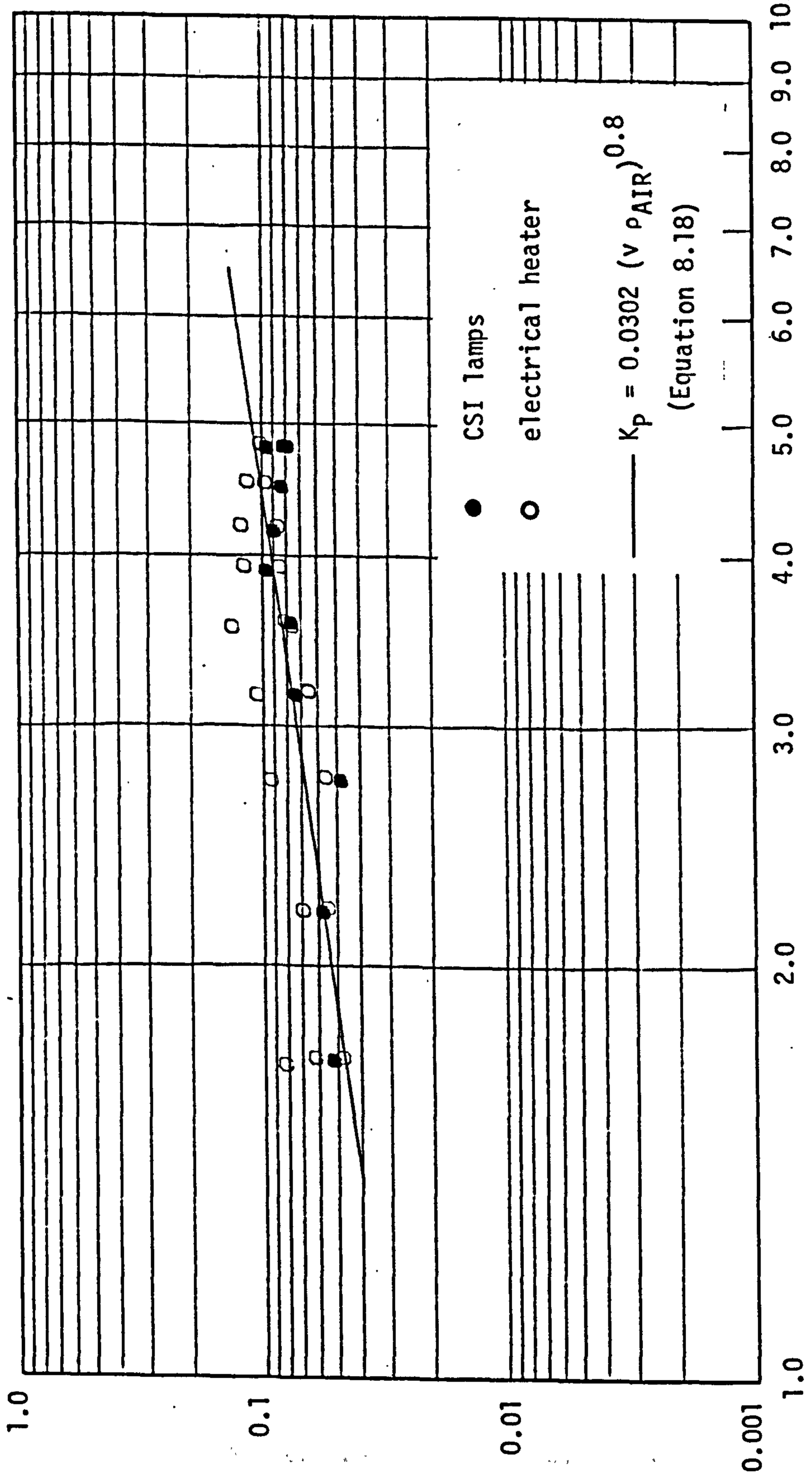

FIGURE 8.22 VARIATION OF MASS TRANSFER COEFFICIENT AGAINST AIR MASS VELOCITY

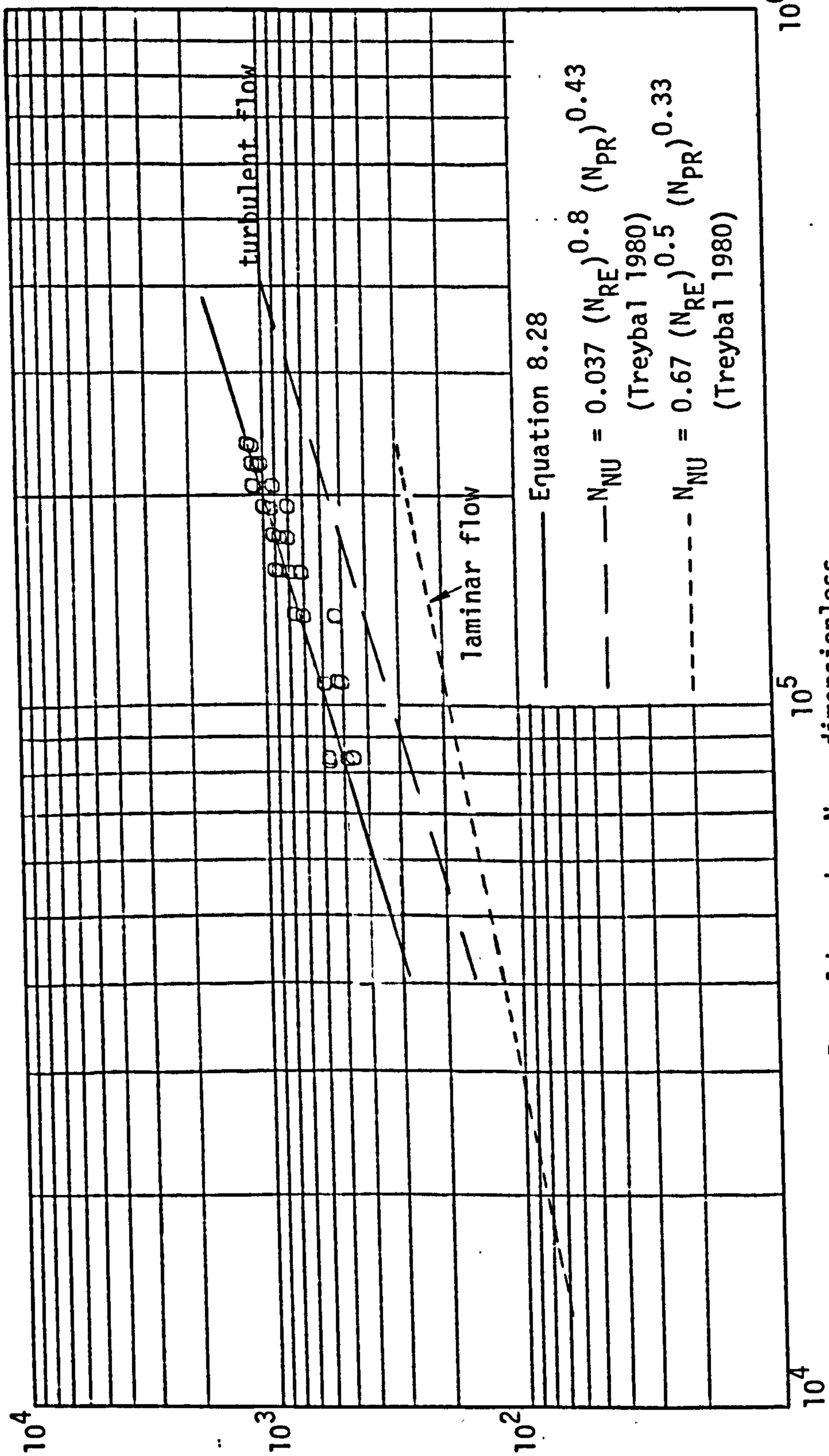

FIGURE 8.23 VARIATION OF NUSSELT NUMBER AGAINST REYNOLDS NUMBER AND ITS COMPARISON WITH EXISTING CORRELATIONS

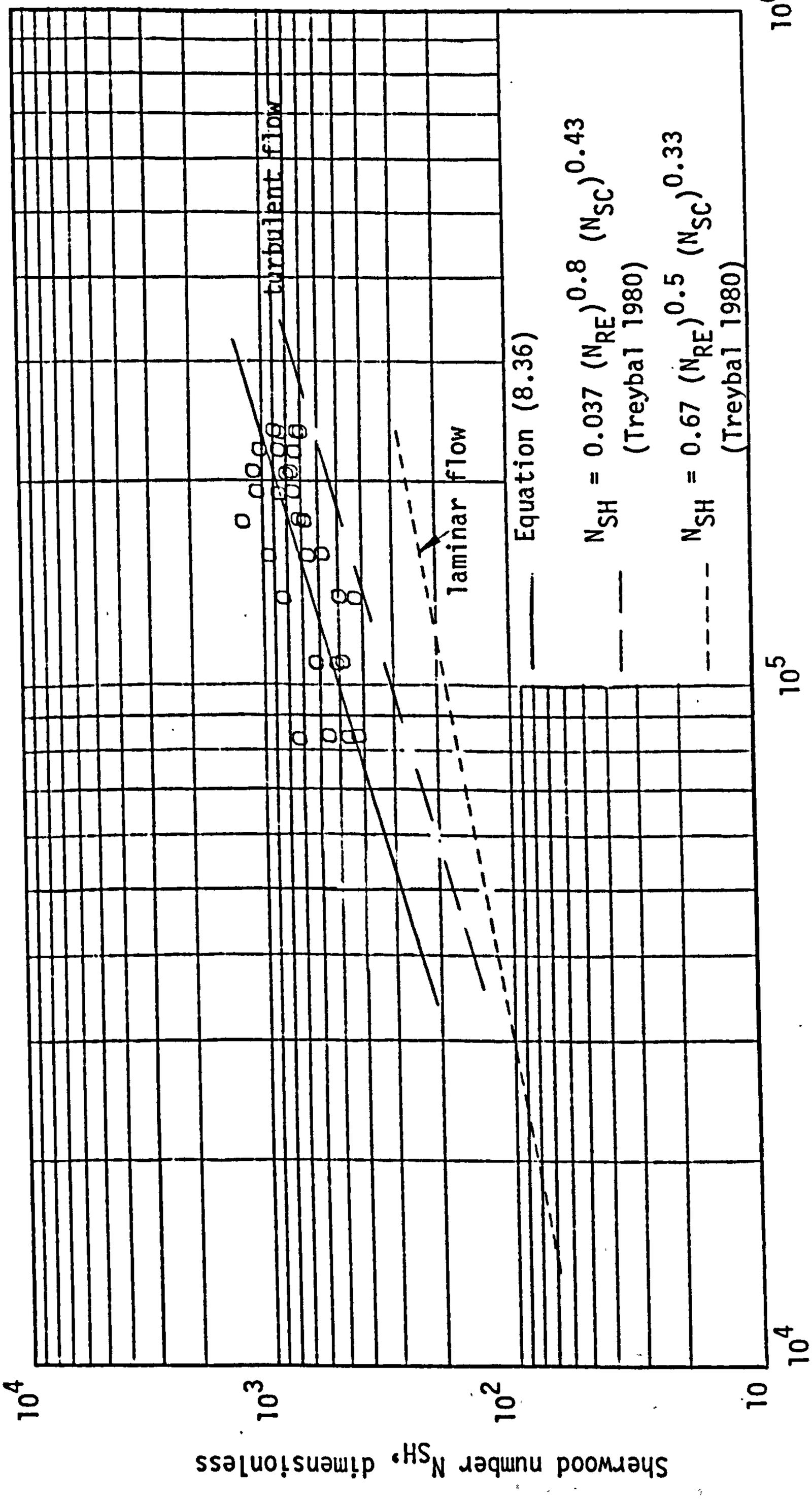

FIGURE 8.24 VARIATION OF SHERWOOD NUMBER AGAINST REYNOLDS NUMBER AND ITS COMPARISON WITH EXISTING CORRELATIONS

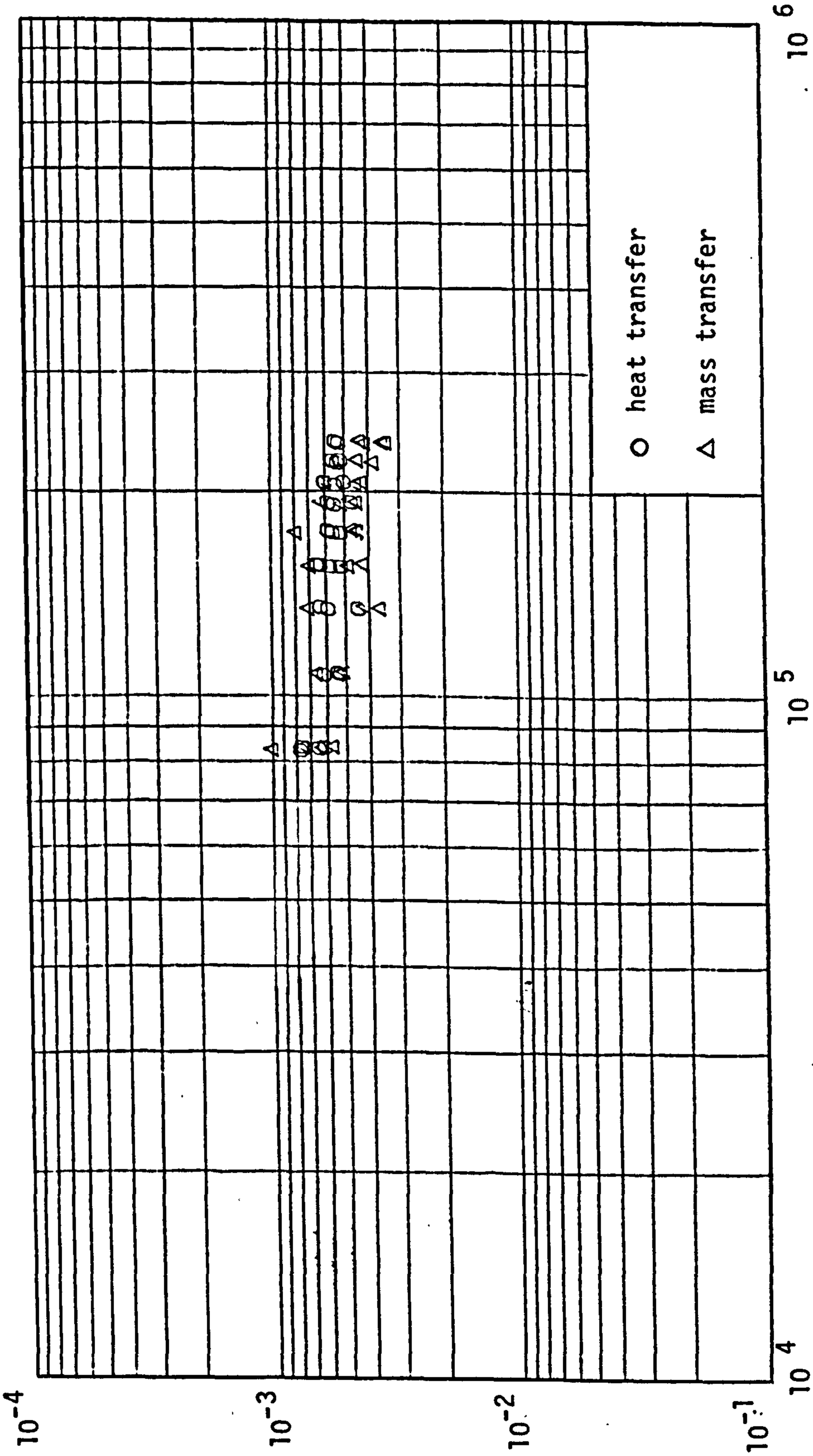

FIGURE 8.25 ANALOGY FOR THE HEAT AND THE MASS TRANSFER DATA

CHAPTER 9

MODELLING OF A SOLAR GENERATOR

MODELLING OF A SOLAR GENERATOR

9.1 THE MODEL

A solar generator is the heart of an open cycle absorption cooling system. A mathematical model of a generator has been developed. This incorporates the correlations presented in Chapter 8. Details of a computer program developed for this mathematical model for a variety of conditions are also given.

The generator concentrates the weak solution from the absorber. This concentrated strong solution can be reused in an absorption cooling system. A thin film of solution flows over a flat black surface. Interception of the solar radiation is improved by tilting the surface to a suitable angle. The solar radiation falling on the generator is partially absorbed by the solution which is heated up and the water vapour from the solution starts to evaporate. The solution is more concentrated by the time it reaches the bottom end of the generator. For a differential element of the generator surface with flow length dy and unit width, as shown in Figure 9.1, an energy balance for steady state condition can be written as

$$I\alpha\, dy - U(T - T_{AM})\, dy - M_S\, (C_P)\, dT - \lambda\, dM_W = 0 \qquad (9.1)$$

Mass balance over the same element can be written as

$$dM_W = K_P\, (p - p_{AM})\, dy \qquad (9.2)$$

$$X = \frac{M_A}{M_S - M_W} \qquad (9.3)$$

A relationship between temperature, pressure and concentration for water-lithium chloride solution can be expressed in the following form.

$$p = a\,T + b/X + C \tag{9.4}$$

The values of a, b and c are 0.87, 20.60 and -77.00 respectively (Kakabaev et al 1972).

It has been assumed in this analysis that the values of mass transfer coefficient K_p, heat transfer coefficient U and latent heat of vaporisation λ are constant within the range of temperatures and concentrations considered. M_W has been considered very small compared to M_S. Substituting Equations (9.2), (9.3) and (9.4) in Equation (9.1).

$$\frac{d^2 M_W}{dy^2} + \left[A_1/M_S\right] \frac{d M_W}{dy} + \left[A_2/M_S^2\right] M_W - A_3/M_S = 0 \tag{9.5}$$

where $$A_1 = K_p b/X_I + K_p\, a\lambda/C_p + U/C_p \tag{9.6}$$

$$A_2 = K_p U b/X_I\, C_p \tag{9.7}$$

$$A_3 = (K_p/C_p)\left[a(I\alpha + U\,T_{AM}) + U(b/X_I + c - p_{AM})\right] \tag{9.8}$$

$$X_I = \frac{M_A}{M_S} \tag{9.9}$$

The general solution of Equation (9.5) is

$$M_W = Z_1\left[\exp\, k_1 y/M_S\right] + Z_2\, \exp\left[k_2 y/M_S\right] + (A_3/A_2)\, M_S \tag{9.10}$$

where

$$k_1 = \frac{-A_1 + \sqrt{A_1^2 - 4A_2}}{2} \tag{9.11}$$

$$k_2 = \frac{-A_1 - \sqrt{A_1^2 - 4A_2}}{2} \tag{9.12}$$

The constants Z_1 and Z_2 are determined by the following boundary conditions $y = 0$, $M_W = 0$;

$$y = 0, \quad \frac{d\,M_W}{dy} = K_P\,(p_I - p_{AM}) \tag{9.13}$$

Solving Equation (9.10) for Z_1 and Z_2

$$Z_1 = \frac{M_S\left[(A_3/A_2)k_2 + K_P(p_I - p_{AM})\right]}{(k_1 - k_2)} \tag{9.14}$$

$$Z_2 = \frac{-M_S\left[(A_3/A_2)k_1 + K_P(p_I - p_{AM})\right]}{(k_1 - k_2)} \tag{9.15}$$

Substituting Equation (9.14) and Equation (9.15) in Equation (9.10)

$$M_W = \frac{M_S\left[(A_3/A_2)k_2 + K_P(p_I - p_{AM})\right]}{(k_1 - k_2)}$$

$$\exp\left[k_1 y/M_S\right]$$

$$- \frac{M_S \left[(A_3/A_2)k_1 + K_p(p_I - p_{AM})\right]}{(k_1 - k_2)}$$

$$\exp\left[k_2 y/M_S\right] + (A_3/A_1)\, M_S \qquad (9.16)$$

It can be noted from Equation (9.16) that if both sides of this equation are divided by y, the resulting equation relates the rate of water evaporation of the generator (M_W/y) to the initial mass flow rate of solution per unit area of the generator (M_S/y) and meteorological conditions. There chould be an optimum value of (M_S/y) i.e., (M_W/y) is maximum for some given values of meteorological conditions, heat and mass transfer coefficients and initial solution parameters. This value can be found by solving the following equation for (M_S/y)

$$d(M_W/y)/d(M_S/y) = 0 \qquad (9.17)$$

These equations are essentially identical to those presented by Kakabaev (Kakabaev et al 1969) and later used by Collier (Collier 1979).

The overall heat transfer coefficient for heat loss to the environment from the generator can be expressed by Equation (9.18)

$$U = h_C + h_R + h_{COND} \qquad (9.18)$$

The convective heat transfer coefficient h_C is calculated from the following correlation (Chapter 8).

$$N_{NU} = 0.0695(N_{RE})^{0.794}\ (N_{PR})^{0.333} \qquad (9.19)$$

The radiation heat transfer coefficient h_R is calculated by

$$h_R = \sigma\varepsilon(T^4 - T_{SKY}^4)/(T - T_{AM}) \qquad (9.20)$$

The effective sky temperature T_{SKY} is calculated from Brunt's relation (Duffie et al 1974) expressed as

$$T_{SKY} = 0.0552\ (T_{AM})^{1.5} \qquad (9.21)$$

T_{SKY} and T_{AM} in Equation (9.21) are in K. However, T_{AM} was used in place of T_{SKY} for the present analysis. The conductive heat transfer coefficient h_{COND} could be calculated from Equation (9.22). However, conductive losses were considered negligible for this analysis.

$$h_{COND} = k_{INS}/w_{INS} \qquad (9.22)$$

The mass transfer coefficient is calculated by the following correlation (Chapter 8)

$$N_{SH} = 1.876(N_{RE})^{0.508}\ (N_{SC})^{0.333} \qquad (9.23)$$

9.2 COMPUTATION PROCEDURE

A block diagram of a computer program developed to solve the mathematical model is shown in Figures 9.3 and 9.4. The computer program is given in Appendix G. Solution mass flow rate at the generator inlet M_S, solution temperature at the generator inlet T_I, ambient temperature T_{AM}, total solar insolation I, ambient air velocity v, water vapour partial pressure in ambient air p_W and solution concentration at the generator inlet X_I were varied one by

one with the rest of the parameters fixed. The average solution concentration over the generator X_{AV} was calculated by taking the arithmetic mean of the solution concentrations at the inlet and the outlet conditions. Iteration was done for the final solution concentration X_F until X_{AV} was matched with its previous value within $\pm 10^{-5}$. The Newton-Raphson convergence technique was used to determine the optimum solution flow rate value.

The subroutine of the generator model was modified and added to the general computer program used for the processing of the experimental data presented in Chapter 8. It was then used to compare the experimental values with the values predicted by the model.

9.3 RESULTS AND DISCUSSION

The experimental values of the rate of water evaporation have been compared with the values predicted by the mathematical model as shown in Figure 9.2. It can be seen that the model predicts the values of the rate of water evaporation with an average error of ± 9.3 per cent. This shows that the model predicts the generator performance quite adequately. Therefore, the model should be useful in analysing the effect of individual parameters on the performance of the generator.

The model has been solved for some typical conditions. These are

$$T_I = 40^{o}C, \quad T_{AM} = 35^{o}C, \quad I = 0.9\ kW\ m^{-2},$$

$$v = 2.0\ m\,s^{-1}, \quad p_W = 0.010\ bar, \quad X_I = 0.36.$$

The results of the computation have been plotted in Figures 9.5 to 9.7. The mass flow rate of the solution at the generator inlet m_S and the rate of water evaporation from the generator m_W have been chosen as independent and dependent variables respectively in all the three figures.

Figure 9.5 is a plot showing the effect of solution temperature at the generator inlet T_I and the ambient air temperature T_{AM} as parameters with reference to the typical conditions. The effect of T_I increases with solution mass flow rate. The optimum value of m_S shifts from about 11.0 kg h^{-1} m^{-2} to 20 kg h^{-1} m^{-2} as T_I is changed from 35^oC to 40^oC. However, the optimum shifts to a considerably higher value for T_I of 45^oC. This appears to be because of higher thermal carry-over as m_S is increased. It can also be seen that maxima of curves, representing variation of T_{AM}, are reached at m_S values of more than 15.0 kg h^{-1} m^{-2} in all the three cases considered. The rate of water evaporation m_W increases proportionally as T_{AM} is increased from 30^oC to 40^oC.

The parameters chosen for Figure 9.6 are air velocity v and total solar insolation I. The rate of water evaporation increases as the air velocity is increased. However, the effect of air velocity is more at a higher value of m_S and the rate of increase of m_W, for a given value of m_S, decreases with air velocity. It can also be noted that the optimum value of m_S increases with air velocity. The rate of water evaporation m_W increases almost proportionally as the total solar insolation I is increased. It can be also seen from this figure that the optimum value of m_S shifts from a lower value to a higher value as I is changed from 1.1 kW m^{-2} to 0.7 kW m^{-2}.

Partial pressure of water in ambient air p_W and solution concentration at the generator inlet X_I have been chosen as parameters in Figure 9.7. The effects of both these parameters are similar as they affect the mass transfer driving force directly. The rate of water evaporation increases as p_W and X_I are decreased. The optimum solution mass flow rate also increases as both these parameters are decreased.

9.4 CONCLUSION

A computer model, incorporating the correlations obtained in the experimental study, has been developed. This mathematical model could be used to predict performance of a solar generator. This could also be used to determine the optimum initial solution flow rate for a particular set of conditions.

The computer program for the mathematical model of this chapter is given in Appendix G.

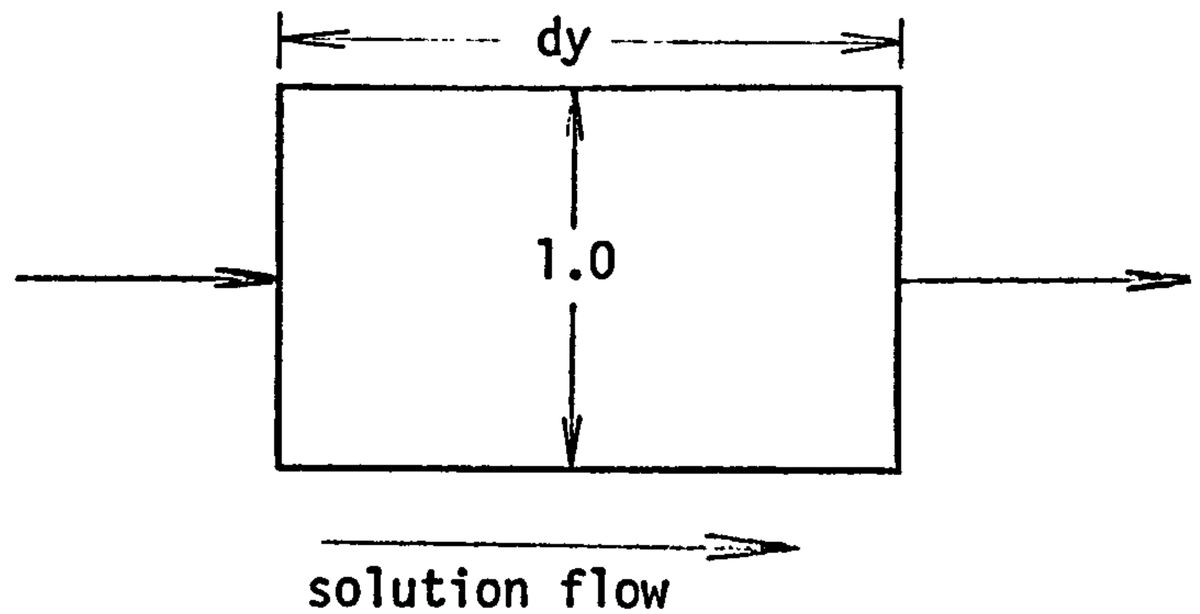

input

absorbed solar energy $I \propto dy$

output

heat losses $U(T - T_{AM})\ dy$

sensible heating $(M_S - M_W)\ C_P\ dT$

energy used in evaporation $\lambda\ dM_W$

at steady state

energy input - energy output = 0

FIGURE 9.1 ENERGY BALANCE FOR DIFFERENTIAL ELEMENT ON THE GENERATOR

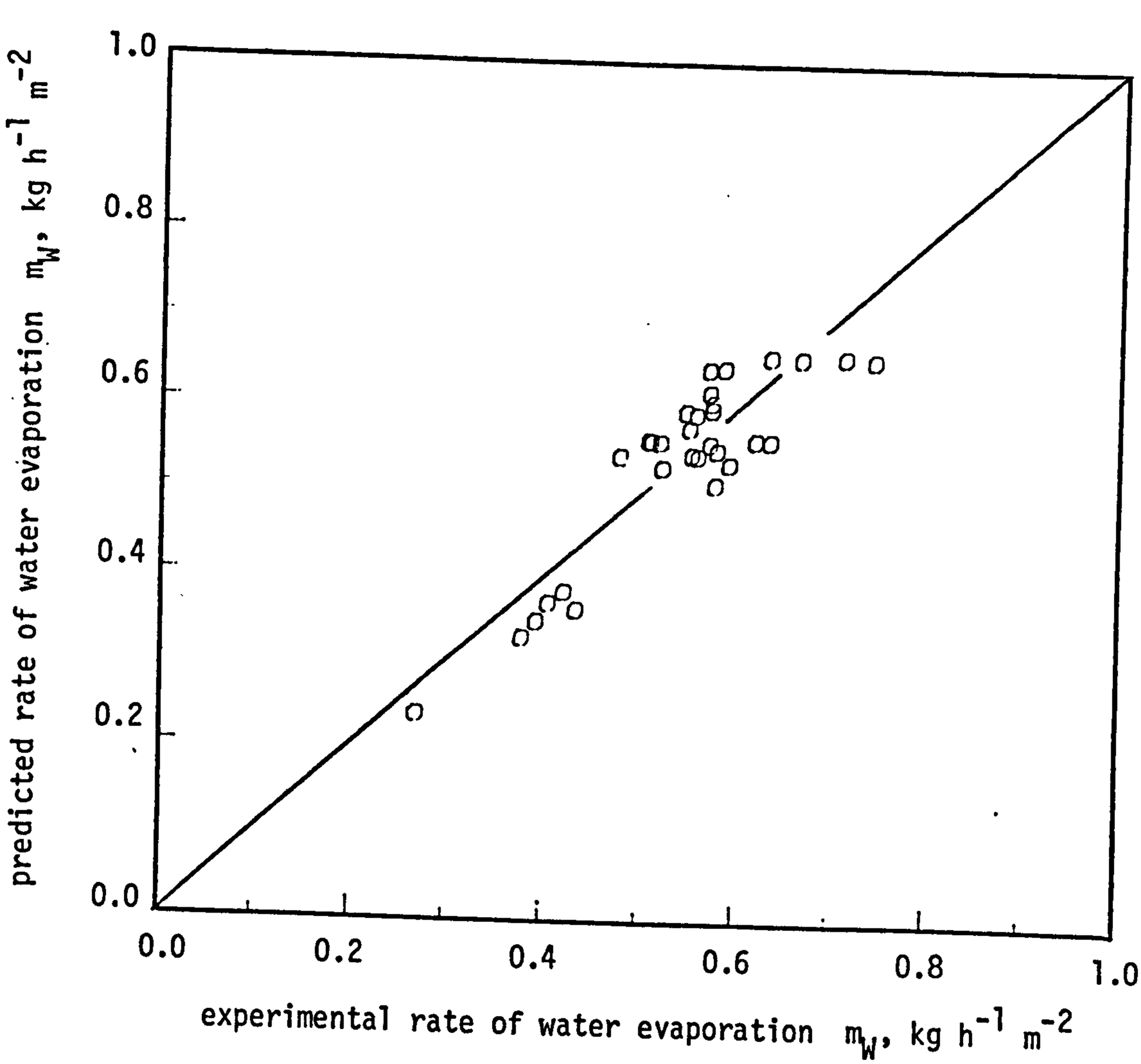

FIGURE 9.2 PREDICTED RATE OF WATER EVAPORATION AGAINST EXPERIMENTAL RATE OF WATER EVAPORATION.

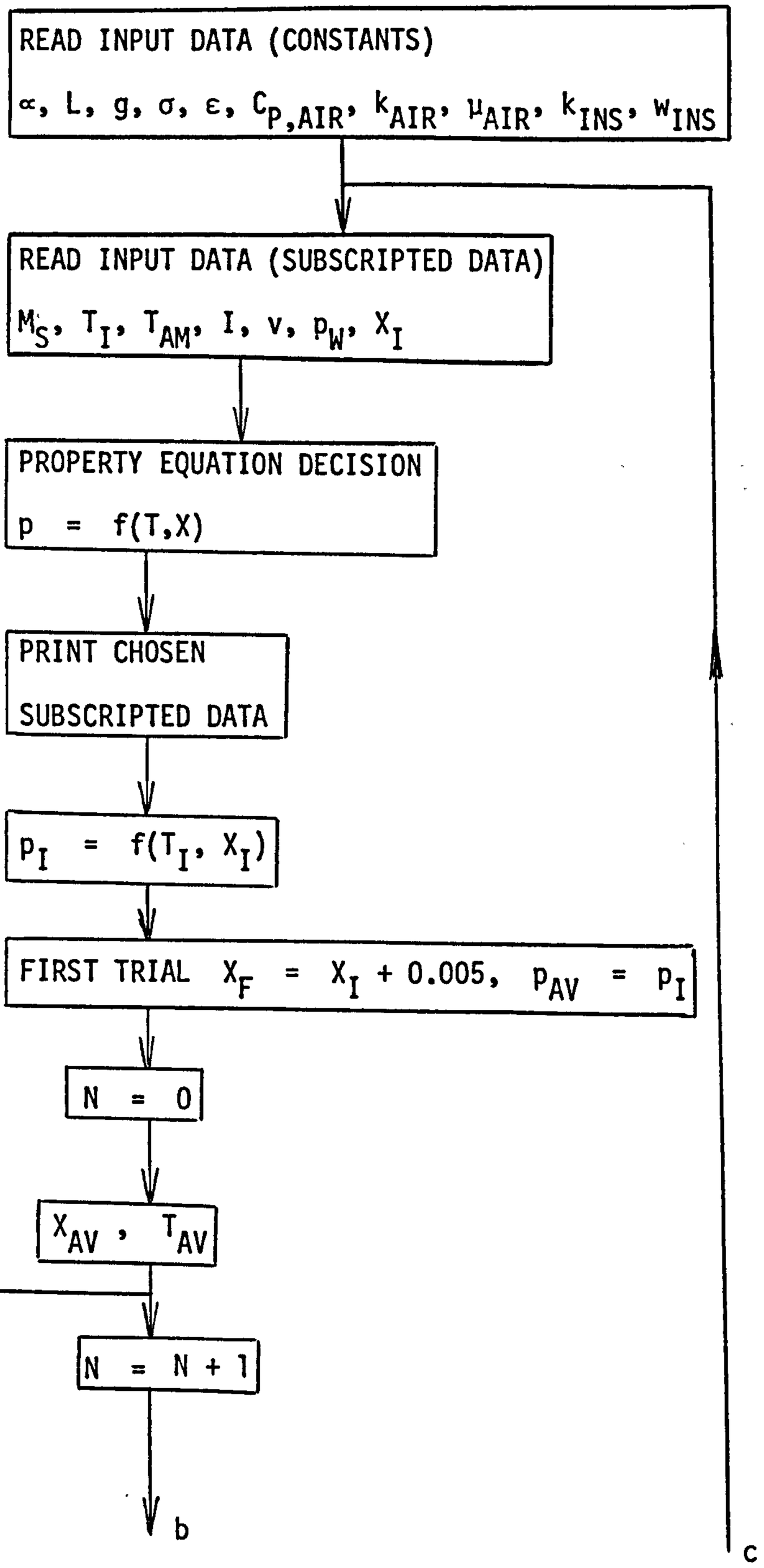
READ INPUT DATA (CONSTANTS)
α, L, g, σ, ε, $C_{P,AIR}$, k_{AIR}, μ_{AIR}, k_{INS}, w_{INS}
READ INPUT DATA (SUBSCRIPTED DATA)
M_S, T_I, T_{AM}, I, v, p_W, X_I
PROPERTY EQUATION DECISION
p = f(T,X)
PRINT CHOSEN
SUBSCRIPTED DATA
p_I = $f(T_I, X_I)$
FIRST TRIAL X_F = X_I + 0.005, p_{AV} = p_I
N = 0
X_{AV} , T_{AV}
N = N + 1
a
b
c

(continued)

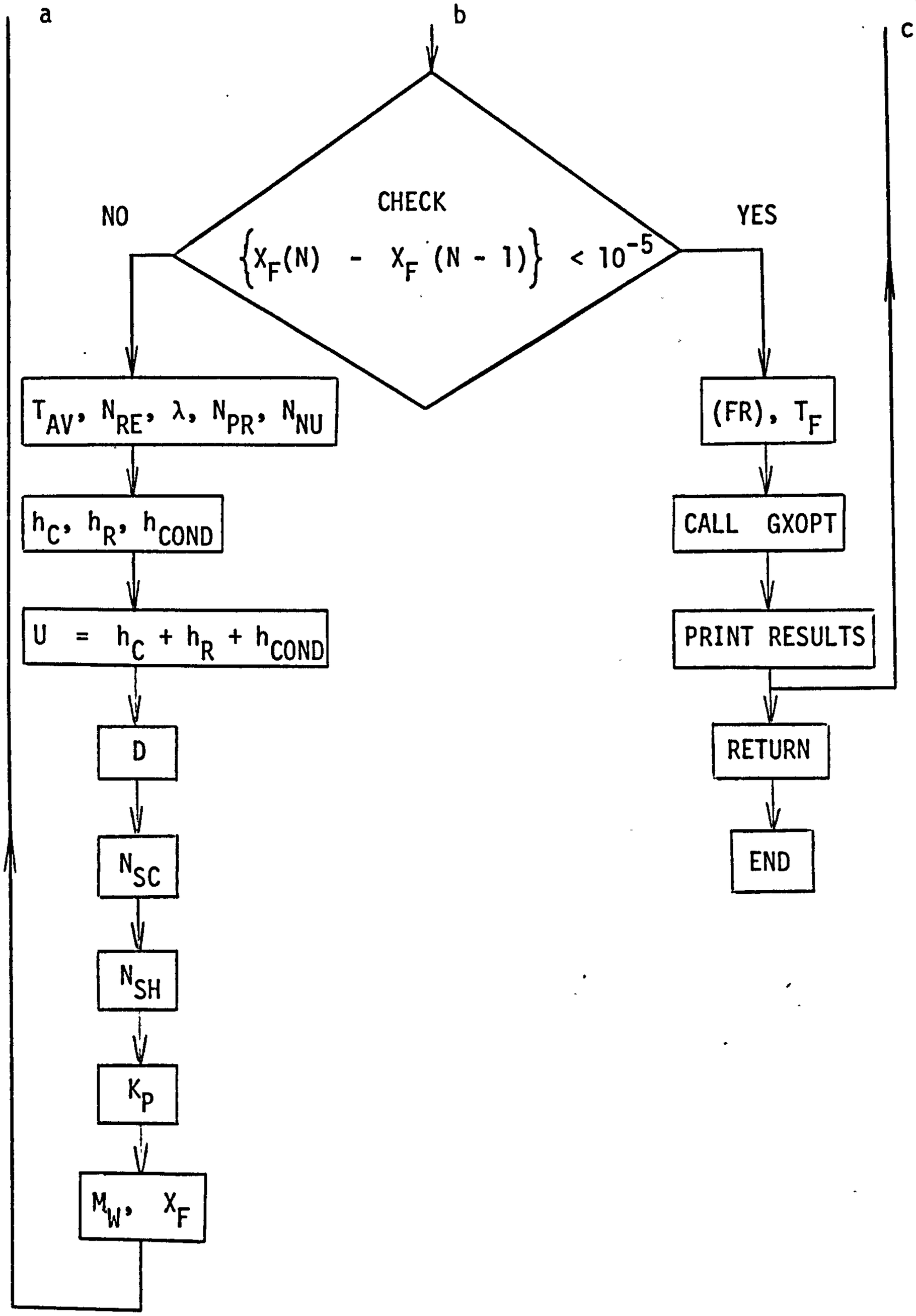

FIGURE 9.3 FLOW DIAGRAM FOR THE COMPUTER PROGRAM OF THE MODEL (SUBROUTINE XFETC)

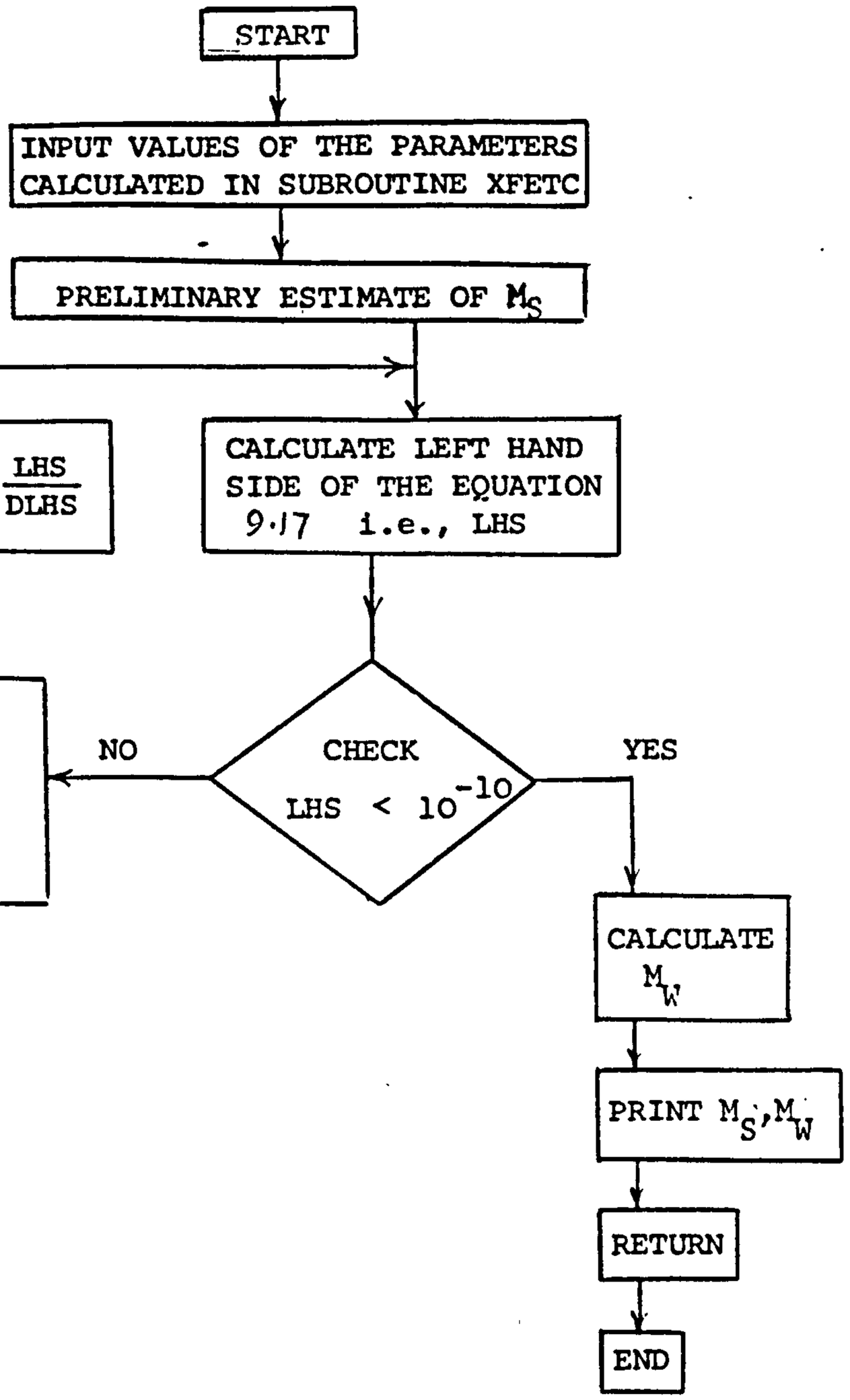

FIGURE 9.4 FLOW DIAGRAM FOR DETERMINING THE OPTIMUM VALUE OF INITIAL SOLUTION FLOWRATE BY NEWTON-RAPHSON METHOD (SUBROUTINE GXOPT)

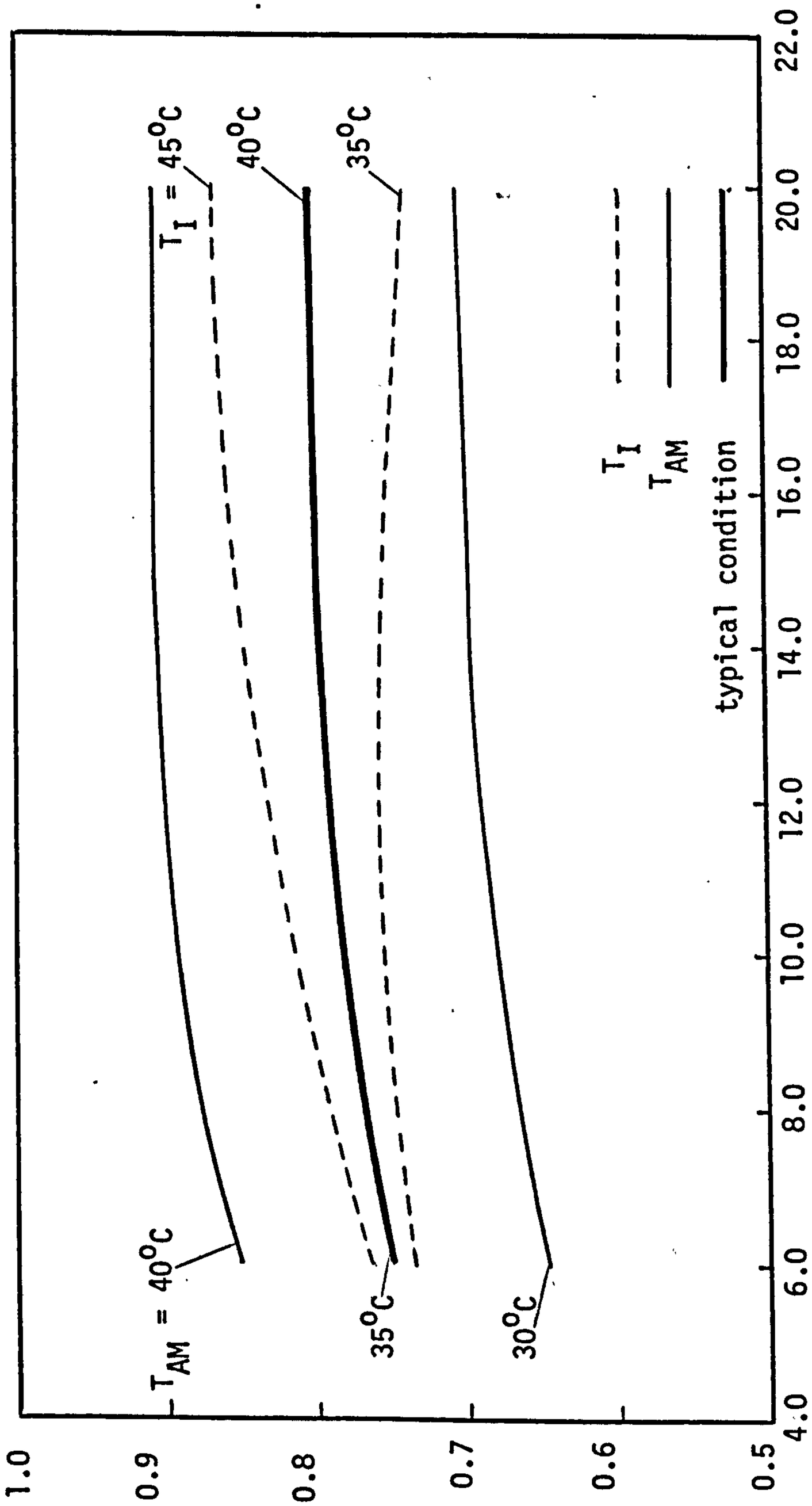

FIGURE 9.5 RATE OF WATER EVAPORATION AGAINST INITIAL SOLUTION FLOW RATE WITH AMBIENT TEMPERATURE AND INITIAL SOLUTION TEMPERATURE AS PARAMETER.

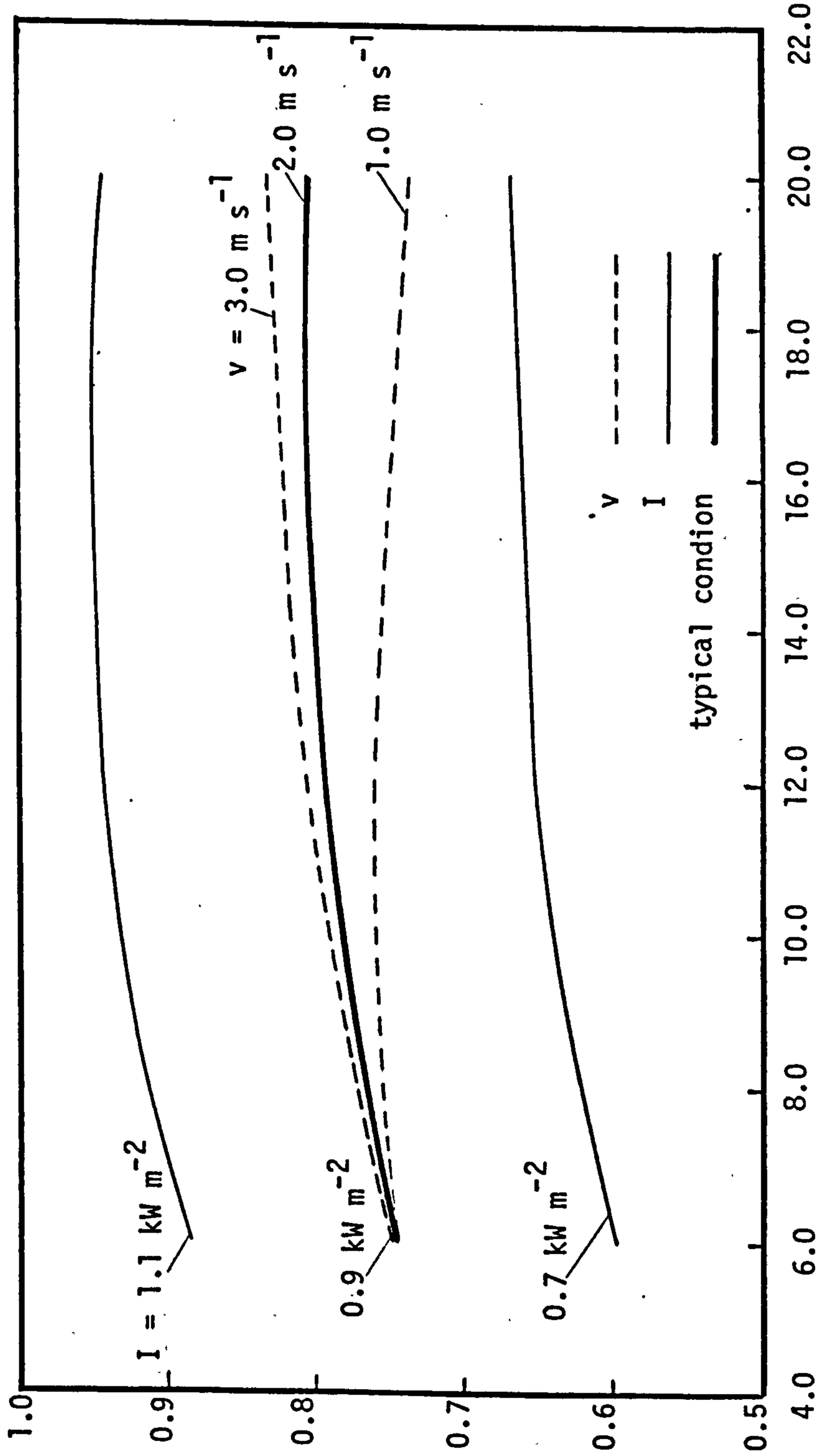

FIGURE 9.6 RATE OF WATER EVAPORATION AGAINST INITIAL SOLUTION FLOW RATE WITH SOLAR INSOLATION AND AIR VELOCITY AS PARAMETERS.

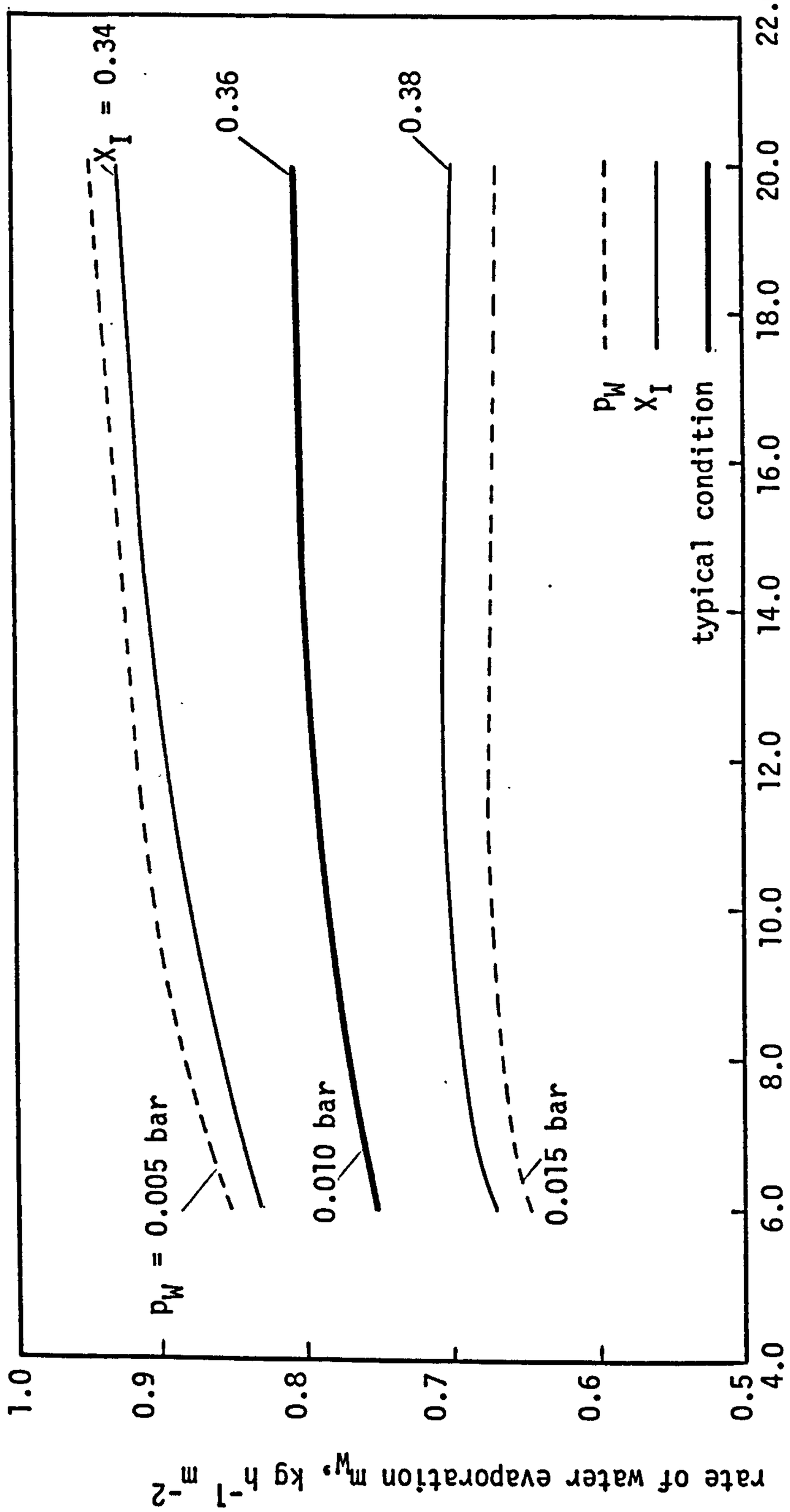

FIGURE 9.7 RATE OF WATER EVAPORATION AGAINST INITIAL SOLUTION FLOW RATE WITH WATER VAPOUR PARTIAL PRESSURE AND INITIAL SOLUTION CONCENTRATION AS PARAMETERS.

CHAPTER 10

CONCLUSIONS AND RECOMMENDATIONS

CONCLUSIONS AND RECOMMENDATIONS

10.1 CONCLUSIONS

(1) Closed cycle absorption cooling systems using water-lithium bromide and ammonia-water as working fluid pairs have been analysed. Open cycle system using water-lithium bromide has also been analysed. Flat plate collector has been considered for heat supply to the generator of the closed cycle systems. The effect of high flow ratios on the overall solar collector area required is studied. It has been shown that daily operating time of a cooling system can be increased by employing relatively high flow ratios. The open cycle system has been analysed for four different ambient conditions and is compared with the closed system.

(2) An experimental closed cycle absorption cooling system using water-lithium bromide has been used to verify the conclusions drawn from the above theoretical analysis.

(3) The interaction of an economiser heat exchanger on the performance of an absorption cooling system has been studied experimentally. It was found that the generator heat load could be reduced equivalent to the heat transferred in the economiser. However, due to the limited capacity of the evaporator the cooling capacity of the system could not be improved significantly.

(4) A design sequence for absorption cycle system has been proposed and discussed.

(5) A concept for achieving relatively high temperature lifts in a single stage absorption system has been proposed. This concept has been used for a mathematical model of an absorption system for simulataneous cooling and heating.

(6) An expression for coefficient of performance of an ideal absorption cycle, when the condensing temperature is not equal to the absorber temperature, has been derived.

(7) A mathematical model for simultaneous cooling and heating incorporating the above expression has been solved for some typical conditions. It has been shown that a temperature lift as high as $95^{o}C$ with an evaporator temperature of $5^{o}C$ could be obtained without significant decrease in the values of coefficient of performance.

(8) The theoretical concept for simultaneous cooling and heating has been verified on the experimental closed cycle absorption cooling system using water-lithium bromide. It has been established that the temperature lift can be manipulated by adjusting the size of an auxiliary heat exchanger to cool the solution prior to its entry into the absorber. However, for relatively high temperature lifts, the system would require relatively high temperature heat input to the generator.

(9) Heat and mass transfer experiments have been carried out on the Solar Generator of an open cycle cooler with solar simulation. The latter was done first using a radiation source consisting of CSI lamps and then by an electric heater. The working fluid pair was water-lithium chloride. Experimental data on heat and mass transfer were obtained for a range of

parameters. Correlations have also been presented.

(10) A computer model, incorporating the correlations obtained in the above experimental investigation, has been developed. This mathematical model has been used to predict performance of a solar generator. Optimum conditions in various situations have been discussed. Experimental values of the rate of water evaporation from the generator have been compared with the values predicted by the above model.

10.2 RECOMMENDATIONS

(1) Operation of an absorption cooling system, using liquid-solid working fluids with air cooling of absorber and condenser, becomes critical because of high solid concentrations involved. Some work has been reported with limited success to find out a third component so as to avoid crystallization. Some more work is required in this direction.

(2) Multi-staging of the absorption cooling system is at a very elementary stage. The system becomes relatively more expensive because of the increase in equipment used in the system, but it might be inevitable because of the particular application, i.e. when a particular set of conditions cannot be achieved without multi-staging. This aspect should be studied with different absorbent-refrigerant pairs.

(3) A very interesting possibility is the use of a mechanical vapour compression pump between the condenser and the generator so that the heat released in the condenser is transferred

by the heat pump to the generator of an absorption cycle.

(4) Another desirable area of research is the investigation of the thermal stability of working fluids. Organic compounds, whether in vapour compression systems or in absorbent systems are especially to be studied for reliability under prolonged use. Stability of working fluids in contact with the materials of construction is also an important field which needs extensive experimental investigation. Suitable corrosion inhibitors may need to be developed.

(5) Systems using liquid-solid refrigerant-absorbent pair appears to be superior to the systems using liquid-liquid or gas-liquid pairs. Comparatively less work has been done on systems using the latter two pairs of refrigerant-absorbent. Water has proved to be a very useful refrigerant because of high latent heat of vaporisation, but it has the limitation for temperatures below $0^{o}C$. Alcohol is one of the alternatives which can overcome this limitation. The drawbacks of using alcohol are lower latent heat of vaporisation and higher corrosivity. New refrigerant-absorbent pairs are to be investigated taking into consideration the particular application of the absorption cycle and factors such as crystallization, relative volatility, operating pressures, latent heat of vaporisation, viscosity, corrosivity, chemical and thermal stability, toxicity, and inflammability.

(6) One of the disadvantages in solar energy operated systems is non-availability of sun for 24 hours. This can be overcome in an open cycle absorption cooling system by having weak and strong solution storage tanks. The strong solution

may be generated in excess during sunshine hours. This way solar energy can be stored in the form of strong solution which could be used in the night. The use of storage tanks is advisable even in sunshine hours as this helps in stratification. The effect of continuous variation of concentration and temperature at the generator outlet, because of continuously changing environmental conditions, is minimised. Some work is required to optimise an open cycle system incorporating the above suggestions.

(7) The use of plastics as materials of construction is an attractive idea. This should eventually lead to cheaper and more durable absorption systems. There seems to be very little current work in this area except for the use of rubberoid for the solar generator of the open cycle absorption cooling system in the experiments conducted by Russian investigators. Plastics as material of construction look very promising in the case of open cycle solar absorption cooling systems because of low generator temperatures which are compatible with the thermal and chemical stability of plastics.

BIBLIOGRAPHY

1. Aker, J.E., Squires, R.G. and Albright, L.F., "An evaluation of alcohol-salt mixtures as absorption refrigeration solution", ASHRAE Journal, 7, 90-92, (1965).

2. Alefeld, G., "Energy flux and energy storage in heat transformation devices", I.Chem.E. Symposium Series No. 78, P6/1-P6/13, (1982).

3. Alizadeh, S., Bahar, F. and Geoola, F., "Design and optimisation of an absorption refrigeration system operated by solar energy", Solar Energy, 22, 149-154, (1979).

4. Allen, R.W. and Anand, D.K., "Parameteric study of a dynamic solar powered absorption cycle" in "Sharing the sun-solar technology in the seventies", Boer, K.W. (Ed.), Volume 3: Solar heating and cooling of buildings, Pergamon Press, New York, 27-33, (1976).

5. ASHRAE Handbook, Fundamentals, Chapter 8: Physiological principles, comfort and health", Published by American Society of Heating Ventilating and Air-Conditioning Engineers, Inc., New York, (1977).

6. Baum, V. and Kakabaev, A., "The use of solar radiation for creating comfortable temperature conditions in Turkmanà, SSR. Proceedings of the International Solar Energy Congress, New Delhi, India, 1556, (January 1978).

7. Baum, V.A., Kakabaev, A. and Khandurdyev, "Efficiency of a solar cooler with an open flat solution refrigerator", Applied Solar Energy, 8(1), 26-30, (1972).

8. Beckmann, W.A., Kleen, S.A. and Duffie, J.A., "Solar heating design: by F-Chart method", John Wiley and Sons Inc., New York, 18, (1977).

9. Beeson, E.J.G., "The CSI lamp as a source of radiation for solar simulators", Lighting Research and Technology, 10(3), 164-166, (1978).

10. Bessler, W. and Shen, C.N.,
"Study of parameter variations for solar-powered lithium bromide absorption cooling",
Proceedings of a forum on solar heating and cooling convened by ERDA at the School of Continuing Studies, University of Miami, Florida, U.S.A. (December 1976).

11. Best, G. and Geoffrey, E.,
"Refrigeration from solar and residual energy",
Bull. Inst. Int. Froid, Annexe (1), 1633-40, (1976).

12. Biermann, W.J.,
"An absorption machine for solar cooling",
ASHRAE Trans., 85(2), 406-412, (1979).

13. Blytas, G.C. and Daniels, F.,
"Concentrated solutions of sodium thiocynate in liquid ammonia: solubility, density, vapour pressure, viscosity, thermal conductance, heat of solution and heat capacity",
Journal of American Chemical Society, 84(7), 1075-83 (1962).

14. Borde, I., Yaron, I. and Jelinek, M.,
"Performance of an absorption cycle operating with low thermal potential energy source for direct contact cooling applications",
The 12th Intersoc. Energy Conversion Engineering Conference (1977).

15. Briley, G.C.,
"Conserve energy: Refrigerate with waste heat",
ASHRAE Journal, 21-25, (December 1976).

16. Butz, L.W., Beckman, W.A. and Duffie, J.A.,
"Simulation of a solar heating and cooling system",
Solar Energy, 16, 129 (1974).

17. Chapman, A.J.,
"Heat Transfer", II Edition,
The MacMillan Company, London, (1967).

18. Chun, K.R. and Seban, R.A.,
"Performance prediction of falling film evaporators",
Journal of heat transfer:
Trans. ASME, Series C, 94, 432-436 (1972).

19. Chung, R., Duffie, J.A. and Lof, G.O.G.,
"A study of solar air conditioner",
Mechanical Engineer, 25, 31, (1963).

20. Collier, J.G. and Pulling, D.J.,
"Heat Transfer to two-phase gas-liquid systems, Part 2, Further data on steam/water mixtures in the liquid dispersed region in an annulus",
Transactions of the Institute of Chemical Engineers, 42, 127, (1964).

21. Collier, R.K.,
"The analysis and simulation of an open cycle absorption refrigeration system",
Solar Energy, 23, 357-366 (1979).

22. Collier, R.K.,
"The analysis of an improved solar powered cooling system utilizing open cycle absorption refrigeration",
Proceedings of the American Section of the International Solar Energy Society, 2(1), 449-454, (August 1978).

23. Dao, K., Simmons, M., Wolgast, R. and Wahlig, M.,
"Performance of air cooled ammonia-water absorption air conditioner at low generator temperatures", in "Sharing the sun-solar technology in the seventies",
Editor: K.W. Boer, Volume 3: Solar heating and cooling of buildings, Pergamon Press, New York, 49-52, (1976).

24. "Demand, supply and fuel prices forecast to the year 2000",
Energy World, Bulletin of the Institute of Energy,
N 111, 9 (Feb 1984).

25. Eiseman, B.J., "Why refrigerant-22 should be favoured for absorption refrigeration", ASHRAE Journal, 45-50 (December 1959).

26. "Energy conservation of new measures and long term strategy",
Energy Paper No. 33, Department of Energy, H.M.S.O. London, 34-35, (February 1979).

27. Farnham, R.S.,
"Peat resonances-classification, properties and geographical distribution",
Symposium on management and assessment of peats as an energy resonance, Arlington, (22-24 July 1979), (7-8 June 1980).

28. Fells, I.,
"World Energy: a study in inequality"
Energy World, Bulletin of the Institute of Energy, N 110, 20 (Jan 1984).

29. Gandhidasan, P. and Gupta, M.C.,
"A new method of sun powered airconditioning",
Conference of International Institute of Refrigeration,
Melbourne, Australia, 665-672, (September 1976).

30. Gandhidasan, P., Sriramulu, V. and Gupta, M.C.,
"Heat and mass transfer in a solar regenerator",
The Chemical Engineering Journal, 21, 59-63 (1981)

31. Gillett, W.B., Rawcliffe, R.W. and Green, A.A.,
"Collector testing using solar simulators",
UK-ISES Conference (C22), Solar Energy Codes of
Practice and Testing Procedures, London (April 1980).

32. Gosling, C.T.,
"Applied air conditioning and refrigeration",
II Edition, Applied Science Publishers Limited, London,
124, (1980).

33. Grassie, S.L. and Sheridan, N.R.,
"Modelling of a solar operated absorption air conditioner
system with refrigerant storage", in "Sharing the sun-
solar technology in the seventies", Editor: Boer, K.W.,
Volume 3: Solar heating and cooling of buildings, Pergamon
Press, New York, 53-67, (1976).

34. Grosman, E.R. and Zhuravelenko, V. Ya.,
"Absorption refrigeration machine operating with a solution
of methanol and lithium bromide",
Kholodilnaya Technika, 45(1), 4-5 (1968).

35. Grosman, E.R.,
"Properties of a solution of methanol and lithium
bromide studied as working substances of absorption
refrigeration machines",
Kholadilnaya Tekh. Teknol., 11, 24-26 (1971).

36. Green, A.A. and Gillet, W.B.,
"The significance of longwave radiation in flat plate solar
collector testing",
Proceedings of IEE Conference-Future Energy Concepts,
London, (1979).

37. Gruter, J.W. (Ed.),
"Proceedings of workshop on the accuracy of pyranometers",
Commission of the European Communities, DG12, Brussesls
(Sept 1980).

38. Holland, F.A.,
"Potential for heat pumps in India",
Indian Chemical Engineer, XXI, No. 2, 1-8 (April-June 1979).

39. Holland, F.A., Watson, F.A. and Devotta, S.,
"Thermodynamic design data for heat pump systems",
Pergamon Press, Oxford (1982).

40. Hollands, K.G.T.,
"The regeneration of lithium chloride brine in a solar still",
Solar Energy, 7(2), (1962).

41. Holldorff, G.,
"Revisions of absorption refrigeration efficiency,
Hydrocarbon Processing, 149-155 (July 1979).

42. Ingra, O.,
"Compact shrouds for wind turbines",
Energy Conservation, 16, 149-157, (1977).

43. Ishida, J.,
"Recent application of large absorption units in Japan",
ASHRAE Trans., 85(1), 395-405, (1979).

44. Jacob, X, Albright, L.F. and Tucker, W.H.,
"Factors affecting the coefficient of performance for absorption air conditioning systems",
ASHRAE Trans., 75(1), 103-109 (1969).

45. Jain, P.C. and Gable, G.K.,
"Equilibrium property data equations for aqua-ammonia mixtures",
ASHRAE Trans., 77(1), 149-151, (1971).

46. Johan, C.C. and Bouvin, J.,
"Transferring heat from relatively cold to relatively hot locations",
Exxon Research and Engineering Company, U.S., 4, 138, 855 (Feb 13 1979).

47. Johnston, A.M.,
"Ammonia/water absorption cycles with relatively high generator temperatures",
Solar Energy, 25, 243-254 (1980).

48. Kakabaev, A. and Khandurdyev, A.,
"Absorption solar refrigeration unit with open regeneration of solution",
Applied Solar Energy, 5(4), 69-72 (1969).

49. Kakabaev, A., Khandurdyev, A., Klyshchaev, O. and Kurbenov, N.,
"A large-scale solar air-conditioning pilot plant and its test results",
International Chemical Engineering, 16(1), (January 1976).

50. Kakabaev, A., Klyshchaeva, O. and Khandurdyev, A., "Refrigeration capacity of an absorption solar refrigeration plant with flat glazed solution regenerator", Applied Solar Energy, 8(2), 90-95, (1972).

51. Kakabaev, A. and Rakhmanov, A., "An absorption solar cooling system with spray chamber: Description and test results", Applied Solar Energy, 7(4), 77-79 (1971).

52. Kays, W.M., "Convective heat and mass transfer", McGraw-Hill Book Company, New York, (1966).

53. Kirk-Othemer Encyclopædia of Chemical Technology, II Edition, John Wiley and Sons, Inc., New York, 7, 393, (1975).

54. Kreider, J.F. and Kreith, F., "Solar Energy Handbook", McGraw-Hill Book Company, New York, (1981)

55. Krueger, R.H., "Corrosion inhibitors for absorption refrigeration systems", U.S., 4, 019, 99 (Cl 252/68)(April 1977).

56. Kumar, P., Devotta, S. and Holland, F.A., "The effect of flow ratio on the performance of an experimental absorption system", Chemical Engineering Research and Design, Transactions of Institute of Chemical Engineers, 62(3), 194-196 (1984).

57. Kumar, P. and Devotta, S., "Study of solar absorption cooling systems with low generator temperatures", International Journal of Refrigeration (communicated).

58. Kumar, P., Watson, F.A. and Holland, F.A., "The effect of high circulation ratios on the performance of absorption cooling systems", Technical Memorandum No. 48, Department of Chemical Engineering, University of Salford, Salford, (Feb. 1982).

59. Kumar, P., Devotta, S. and Holland, F.A., "Experimental heat and mass transfer study on solar generator of open cycle absorption cooling system", Tech. Memo. No. 69, Department of Chemical Engineering, University of Salford, (1984).

60. Kumar, P., Sane, M.G., Devotta, S. and Holland, F.A., "Experimental studies with an absorption system used for cooling and simultaneous cooling and heating", Chemical Engineering Research and Design, Transactions of the Institute of Chemical Engineers, (in press).

61. Kutateladze, S.S. and Borishanski, V.M., "A concise encyclopeadia of heat transfer", Pergamon Press, Oxford (1966).

62. Landauro-Paredes, J.M., "The design and development of a glass absorption cooler", Ph.D. Thesis, Department of Chemical Engineering, University of Salford, Salford, UK. (1982).

63. Landauro-Paredes, J.M., Watson, F.A. and Holland, F.A., "Experimental study of the operating characteristics of a water-lithium bromide absorption cooler", Chemical Engineering Research and Design, Transactions of the Institute of Chemical Engineers, 61(6), 362-370 (1983).

64. Lazzarin, R., "Study and transient behaviour of lithium bromide chillers of low capacity", International Journal of Refrigeration, 3(5), 213-218, (1980).

65. Lewis, J.S., "A heat and mass transfer analogy and its application to finned surfaces", Ph.D. Thesis, University of Strathclyde, Glasgow, (1969).

66. Ley, W. and Rehmann, K.V., "Investigation of selective surfaces and honeycomb structures with the use of a molar simulator", DFVLR report No. 1B, 353, 77-15 (Dec 1977).

67. Lof, G.O.G. and Tybout, R.A., "Cost of house heating with solar energy", Solar Energy, 14, 253, (1973).

68. Lof, G.O.G. and Tybont, R.A., "The design and cost of optimised systems for cooling dwellings by solar energy", Solar Energy, 16, 9 (1974).

69. Macriss, R.A., Weil, S.A. and Rush, W.F., "Absorption refrigeration systems containing solutions of monomethylamine"., U.S. 3, 458, 455 (1969).

70. Mansoori, G.A. and Patel, V.,
"Thermodynamic basis for the choice of working fluids for solar absorption cooling systems",
Solar Energy, 22(6), 483-91, (1979).

71. Meinel, A.B. and Meinel, M.P.,
"Applied solar energy",
Addison-Wesley Publishing Company, Reading (1977).

72. Mosteza, V.E.,
"Difluorochloromethane-perchloroethylene mixture for absorption refrigeration plants".,
Germ. Offen. 1, 930, 007 (Cl. C09K) (Dec 17 1970).

73. Mullick, S.C., and Gupta, M.C.,
"Solar desorption of absorbent solutions",
Solar Energy, 16, 19-24, (1974).

74. Namkoong, D.,
"Performance of a lithium bromide water chiller in a laboratory scale experimental solar system test loop",
Proceedings of International Solar Energy Society Conference, Winnipeg, Vol. 3, (1976).

75. Odell, P.R.,
"Oil and World Power", 6th Edition,
Pelican Books, (1981).

76. Orekhov, I.I., Tinofaevskii, L.S. and Gerchikova, M.N.,
"Binary mixtures for an absorption refrigerating machine",
USSR 627 100, (25 Sep 1973).

77. Oonk, R.L., Beckman, W.A. and Duffie, J.A.,
"Modelling of the CSU heating/cooling systems",
Solar Energy, 17, 21 (1975).

78. Pechatnikov, M.Z. and K'Yachenko, Yu.I.,
"Selection of thermodynamic optimum pair for hydrocarbon absorption refrigeration machines",
Tr. Vsesoyuznoki Nauchuo-Tekhnicheskoi Knof, Thermodin Spornik Dokladov, Sektsii Novye Tepl., 379-326, (1968).

79. Parker, S.P.,
"McGraw-Hill encyclopaedia of energy",
McGraw-Hill Book Company, New York, 8, 494 (1981).

80. Petrie, A.M. and Simpson, H.C.,
"An experimental study of the sensitivity to free stream turbulence of heat transfer in makes of cylinders in crossflow",
International Journal of Heat and Mass Transfer, 15, 1497-1513, (1972).

81. Praires, P.D.,
"World Petroleum supply limits"
World Energy Resources, 1985-2020,
World Energy Conference, 1978,
IPC Science and Technology Press, 2-14 (1978).

82. Prasad, M. and Kumar, P.,
"Open solar regeneration of lithium chloride brine",
Mechanical Engineering Bulletin, Central Mechanical Engineering Research Institute, Durgapur, W. Bengal, India, 12(2) (June 1981).

83. Prasad, M., Kumar, P. and Raychaudhuri, B.C.,
"Solar still generators for brine",
Mechanical Engineering Bulletin, Central Mechanical Engineering Research Institute, Durgapur, W. Bengal, India, 12(4), (December 1981).

84. Raldow, W. (Editor),
"New working pairs for absorption processes",
Proceedings of a workshop in Berlin, April 14-16,
Spangbergs Tryckerier AB, (1982).

85. Reay, D.A.,
"Industrial energy conservation",
Pergamon Press Ltd., Oxford, 296 (1977).

86. Reynolds, O.,
"On the extent and action of the heating surface for steam boilers",
Proceedings of Manchester Lit.Phil.Soc., 14, 7-12, (1874).

87. Riches, M.R., and Stoffel, T.L.,
"International Energy Agency Conference on pyranometer measurements",
Boulder, Colorado (March 1981).

88. The Royal Society,
Coal Age, 85(15), 45, 52, (May 1980).

89. Salter, S.H.,
"Wave power",
Nature, 249, (June 1974).

90. Schlichting, H.,
"Boundary layer theory",
McGraw-Hill Book Company, New York, (1968).

91. Sheridan, N.R.,
"Lithium bromide-water refrigerator cycle analysis with applications for solar operations",
Thermofluids Conference, Inst.Eng., Aust: Sydney, 66-70 (1974).

92. Sheridan, N.R.,
"Performance of the Brisbane solar house",
Solar Energy, 12, 395, (1962).

93. Simmons, M. and Wahlig, M.,
"Ammonia-water absorption air conditioner",
Proceedings of 2nd workshop on the use of solar energy for the cooling of buildings, Los Angeles, California (1975).

94. Simpson, H.C., Brolls, E.K.,
"Multiphase flow systems",
I.Chem.E. Symposium Series No. 8, 2, 112, (1974).

95. Stingel, D.E.,
"A new energy emphasis for the United States: transferring energy-intensive industry from the United States to developing countries",
Natural Resources Forum,
The Division of Natural Resources and Energy of the United Nations, United Nations, New York, 4(3), 260 (July 1980).

96. Stoecker, W.F. and Reed, L.D.,
"Effect of operating temperatures on the coefficient of performance of aqua ammonia refrigerant systems",
ASHRAE Trans., 77(1), 163-170 (1971).

97. Treybal, R.E.,
"Mass transfer operations",
3rd edition, McGraw-Hill, New York, (1980).

98. Tuma, J.J.,
Engineering Mathematics Handbook,
II Edition,
McGraw-Hill Book Company, New York, (1979).

99. Usyukin, I.P. and Koloskov, Yu.D.,
"Operation of an absorption refrigeration plant based on a methylamine-water solution for heating and cooling",
Kholodilnaya Tekhnika, 48(10), 20-26, (1971).

100. Usyukin, I.P. and Chumachenko, A.D.,
"Testing of the performance of an absorption refrigeration plant based on a solution of Freon-22 and the dimethyl ether of tetraethylene glycol",
Kholodilnaya Tekhnika, 48(5), 7-10, (1971).

101. Usukin, I.P., Kiloskov, Yu.D., Taubaer, A.I. and Romanzanov, Yu.P.,
"Use of a solution of methylamine in tetraethylene glycol dimethyl ether for absorption refrigerating machines",
Khim. Mashinok (Mosk.Inst.Khim.Mashinostr.), 1, 49-51, (1977).

102. Vemura, T.,
"Methanol-lithium iodide-zinc bromide absorption refrigerating machine",
Reito, 50(568), 95-101, (1975).

103. Vermura, T.,
"Studies on the methanol-zinc bromide refrigerating machine",
Reito, 51, 1027-1036, (1976).

104. Vemura, T.,
"Physical properties of refrigerant-absorbent systems for absorption refrigeration",
Reito, 53(600), 224-40, (1977).

105. Vielroge, R.,
"West African crude suddenly is crucial",
Oil and Gas Journal,
47 (Jan 1981).

106. Ward, D.S.,
"Performance of the CSU solar house I cooling systems",
Proceedings of 2nd workshop on use of solar energy for the cooling of buildings, Los Angeles, California, 42, (1975).

107. Ward, D.S.,
"Solar absorption cooling feasibility",
Solar Energy, 22, 259-268, (1979).

108. Ward, D.S., Duff, W.S., Ward, J.C. and Lof, G.O.G., "Integration of evacuated tubular solar collectors with lithium bromide absorption cooling systems", Solar Energy, 22, 335-341, (1979).

109. Ward, D.S. and Lof, G.O.G., "Design and construction of a residential solar heating and cooling system", Solar Energy, 17, 13, (1975).

110. Ward, D.S., Smith, C.C. and Ward, J.C., "Operational modes of solar heating and cooling systems", Solar Energy, 19, 55, (1977).

111. Ward, D.S., Weiss, T.A. and Lof, G.O.G., "Preliminary performance of CSU solar house I heating and cooling systems", Proceedings of International Solar Energy Society Congress, Los Angeles, California, (1975).

112. Whitlow, E.P., "Use of an absorber heat exchanger in the absorption refrigerating machine", ASHRAE Trans., 77, Part II, 166-173, (1971).

113. Whitlow, E.P., "Relationship between heat source temperature, heat sink temperature and coefficient of performance for solar-powered absorption air conditioners", ASHRAE Trans., 82(1), 950-958, (1976).

114. Write, J.K., "Large scale electrical power generation and storage", in "Aspect of energy conservation", Blair, I.M., Jones, B.D. and Van Horn, A.J., (Editor), Pergamon Press, Oxford, 462, (1976).

AUTHOR'S PUBLICATIONS

1. "The effect of flow ratio on the performance of an experimental absorption system",
Chemical Engineering Research and Design,
Transactions of Institute of Chemical Engineers,
62(3), p 194-196, (May 1984).

2. "Study of solar absorption cooling systems with low generator temperatures",
International Journal of Refrigeration (communicated)

3. "Experimental studies with an absorption system used for cooling and simultaneous cooling and heating",
Chemical Engineering Research and Design,
Transactions of the Institute of Chemical Engineers (in press)

4. "Analysis of an absorption system for simultaneous cooling and heating",
(being communicated)

5. "Derived thermodynamic design data for Rankine power cycle systems operating on R216",
Journal of Heat Recovery Systems,
3(4), p 321-325, (1983)

```
C       THIS PROG CALCULATES THE PERFORMANCE OF A CLOSED CYCLE
C       ABSORPTION COOLING SYSTEM USING WATER-LITHIUM BROMIDE
C       ALL THE CALCULATION IN THIS PROG ARE DONE FOR
C       1 KG OF H2O EVAPORATED IN THE EVAPORATOR
C       NOMENCLATURE
C       A -AREA OF SOLAR COLLECTOR
C       B -EFFECTIVENESS OF THE ECONOMISER HEAT EXCHANGER
C       CP -SPECIFIC HEAT
C       COP -COEF OF PERFORMANCE
C       COPCNT -CARNOT COEF OF PERFORMANCE
C       COT -COEF OF TRANSFORMATION
C       E -SYSTEM EFFICIENCY
C       F -FLOW RATIO
C       H -ENTHALPY
C       P -PRESSURE
C       Q -HEAT LOAD
C       SIT -TOTAL SOLAR INSOLATION
C       T -TEMPERATURE
C       X -CONCENTRATION OF SOLUTION,FRACTION
C       SUBSCRIPTS
C       C -TEMP IN C
C       CO -CONDENSER
C       E -EVAPORATOR
C       G -GENERATOR
C       O -AMBIENT
C       S -SOLUTION
C       SC -SOLAR COLLECTOR
C       SI -VALUE IN SI UNITS
C       1 TO 10 SUBSCRIPTS DENOTE THE STATE POINTS IN THE
C       ABSORPTION CYCLE SYSTEM, SEE FIG4.1 OF CHAPTER 4
        DIMENSIONX2(10),B(7),SIT(5)
        READ 1,X1,X3,TE,T3,TO,TCO,PCO
1       FORMAT(7F10.3)
C       THE EQUILIBRIUM PROP HAVE BEEN TAKEN FROM
C       BESSELER W P AND SHEN C M , STUDY ON PARAMETER VARIATION
C       FOR A SOLAR POWERED LIBR ABSORPTION COOLING SYSTEM,PROC OF A FORUM
C       ON SOLAR HEATING AND COOLING CONVENED BY ERDA AT THE SCHOOL OF
C       CONT STUDIES,UNIV OF MIAMI,FLORIDA,USA(DEC 1976)
C       THE REFRENCE TEMP FOR ALL THE ENTHLPY RELATIONS IS 77F
        H1=0.43*TE+1017.0
        H10=TCO-77.0
        QE=H1-H10
        CPS3=.48*X3**2-1.23*X3+1.01
        H3=750.0*X3**2-822.0*X3+122.5+CPS3*(T3-77.0)
        READ 2,(SIT(K),K=1,5)
2       FORMAT(5F10.3)
        READ 3,(B(J),J=1,7)
3       FORMAT(7F7.3)
        READ 4,(X2(I),I=1,10)
4       FORMAT(10F7.3)
        DO 9 J=1,7
        DO 8 I=1,10
        PRINT *,X2(I),B(J)
        F=(X1-X3)/(X3-X2(I))
        CPS6=.48*X2(I)**2-1.23*X2(I)+1.01
        T20=(10.0*X2(I))**3/2.92+72.0
        T600=(10.0*X2(I))**3/2.03+202.0
        CM=3.3905/(T600-T20)
        CB=2.996-T20*CM
        TG=(LOG(PCO)-CB)/CM
C       ALL THE CALCULATIONS HAVE BEEN DONE IN BTU
C       THE RESULTS HAVE BEEN PRINTED IN SI UNITS
```

```
C       APPROPRIATE CONVERTION FACTORS HAVE BEEN USED
C       AT DIFFERENT PLACES
        TGC=(TG-32.0)/1.8
        HEX=F*CPS6*B(J)*(TG-T3)
        HEXSI=HEX*0.6461E-3
        H6=750.0*X2(I)**2-822.0*X2(I)+122.5+CPS6*(TG-77.0)
        H7=H6-HEX/F
        T2=TG-(TG-T3)*B(J)
        T2C=(T2-32.0)/1.8
        QA=H1+F*H7-H3*(F+1.0)
        QASI=QA*0.6461E-3
        H5=H3+HEX/(F+1.0)
        COPCNT=9.09*(TG-TO)/(TG+460.0)
        H8=0.46*TG-0.03*TCO+1017.0
        QCO=H8-H10
        QG=(H8-H5)+F*(H6-H5)
        QCOSI=QCO*0.6461E-3
        QGSI=QG*0.6461E-3
        COP=QE/QG
        COT=(QA+QCO)/QG
        E=COP/COPCNT
        QESI=QE*0.6461E-3
        QCSI=QCO*0.6461E-3
        PRINT 5,B(J),X2(I),F,QESI,QGSI,TGC,QCSI,COP
    5   FORMAT(8F10.3,/)
        DO 7 K=1,5
        TI=TG+9.0
        ESC=0.77-1.233*(TI-TO)/SIT(K)
        A=QG/(ESC*SIT(K))
        ASI=A*.2048
        SITSI=SIT(K)*3.1546E-3
        PRINT 6,SITSI,ASI,ESC
    6   FORMAT(10X,3F10.3,/)
    7   CONTINUE
    8   CONTINUE
    9   CONTINUE
        STOP
        END
```

```
C THIS PROGRAM CALCULATES THE PERFORMANCE OF THE CLOSED CYCLE
C ABSORPTION COOLING SYSTEM USING AMMONIA-WATER
C NOMENCLATURE IS SIMILAR TO THE PREVIOUS PROGRAMS
      DIMENSIONX2(10),B(7),SIT(5),FF(10),QASI(10),QGSI(10),HEXI(10)
      READ 1,X1,X3,PC,TC,T3,TE,TO,V3,X10,PE
1     FORMAT(10F8.4)
      H101=(((561.86*X10-1929.6)*X10+2343.3)*X10-828.41)*X10
      H10=(H101-103.48)*X10-76.824+1.12703*TC
      R1=((((108.485*X10-229.009)*X10+155.247)*X10-41.0442)*X10)*X10
      R=R1+11.2925-0.031256*PE+0.0213337*PE*X10**2
      XV=1.0-(1.0-X10)**R
      H11=530.976+(((4.05554E-05*TE-0.0290022)*TE+6.79126)*TE)*(1.-XV)
      H1=((-4.948E-06*TE+1.49518E-03)*TE+.415871)*TE+H11
      QE=H1-H10
      CPS3=0.16986*X3+1.0
      H31=(((-656.458*X3+1358.93)*X3-498.318)*X3-182.534)*X3
      H3=H31-57.1775+1.09174*T3
      READ 2,(B(J),J=1,7)
2     FORMAT(10F8.3)
      READ 2,(X2(I),I=1,10)
      READ 2,(SIT(K),K=1,5)
      DO 9 J=1,7
      DO 8 I=1,10
C     PRINT*,B(J),X2(I)
      F=(X1-X3)/(X3-X2(I))
      FF(I)=F
      HP=(PC-PE)*V3*.18509*(F+1.0)
      PKW=HP*0.6461E-3
      T4=T3+HP/CPS3
      TGO=((-240.11*X2(I)+346.31)*X2(I)-27.12)*X2(I)
      TG1=((TGO+166.94)*X2(I)-535.76)*X2(I)
      TG2=(0.038839-0.18053E-03*PC)*X2(I)*PC+305.04
      TG=TG1+TG2+(.44631-.24284E-03*PC)*PC
      TGSI=(TG-32.0)/1.8
      CPS6=0.16986*X2(I)+1.0
      HEX=F*CPS6*B(J)*(TG-T4)
      HEXSI=HEX*0.6461E-3
      H61=(((561.86*X2(I)-1929.6)*X2(I)+2343.3)*X2(I)-828.41)*X2(I)
      H6=(H61-103.48)*X2(I)-76.824+1.12703*TG
      H7=H6-HEX/F
      T2=TG-(TG-T4)*B(J)
      QA=H1+F*H7-H3*(F+1.)
      QASI(I)=QA*0.6461E-3
      H5=H3+HEX/(F+1.)
      COPCNT=9.09*(TG-TO)/(TG+460.)
      RR1=((10.749*X10-17.869)*X10+4.0279)*X10-1.3086)*X10
      RR=(RR1+2.5622E-03*PC*X10)*X10-4.256E-03*PC+7.1588
      XVR=1.0-(1.0-X10)**RR
      XVT=LOG(1.0-XVR)
      H81=(((0.068765*XVT+2.0794)*XVT+24.839)*XVT+144.63)*XVT
      H82=(((-3.7752E-05*TC+.027252)*TC-5.9429)*TC)*(1.-XVR)
      H8=H81+911.73+8.37E-09*TC**4+H82+.54663*TC*(1.-XVR)**2-3.1313
      QC=(H8-H10)*1.2
      QCSI=QC*0.6461E-3
      QG=(H8-H5)+F*(H6-H5)+.2*(H8-H10)
      QGSI(I)=QG*0.6461E-3
      COP=QE/QG
      COT=(QA+QC)/QG
      REF=COP/COPCNT

      QESI=QE*0.6461E-3
3     FORMAT(2F15.5)
```

```
      PRINT 4,X2(I),F,B(J),QCSI,QGSI(I),TGSI,QESI,COP
4     FORMAT(8F10.3,/)
5     FORMAT(5F15.10)
      DO 7 K=1,5
      TI=TG+9.0
      ESC=.77-1.233*(TI-TO)/SIT(K)
      SITSI=SIT(K)*3.1546
C SITSI ISIN WATTS
      A=QG/(ESC*SIT(K))
      ASI=A*0.2048
      PRINT 6,SITSI,ASI,ESC
6     FORMAT(3F15.5)
7     CONTINUE
8     CONTINUE
9     CONTINUE
      STOP
      END
```

```
C       THIS PROG CALCULATES THE PERFORMANCE OF AN OPEN CYCLE
C       ABSORPTION COOLING SYSTEM USING H2O-LIBR
C       NOMENCLATURE IS SIMILAR TO THE LAST PROGRAM
C       IT SHOULD BE ENSURED THAT (VP),SOL,T2<PE,EVAP
        DIMENSIONX2(10),B(7),P(4)
        READ 1,X1,X3,TE,T3,TO,H10
1       FORMAT(6F10.3)
        H1=0.43*TE+1017.0
        QE=H1-H10
        CPS3=.48*X3**2-1.23*X3+1.01
        H3=750.0*X3**2-822.0*X3+122.5+CPS3*(T3-77.0)
        READ 2,(P(K),K=1,4)
2       FORMAT(4F10.3)
        READ 3,(B(J),J=1,7)
3       FORMAT(7F7.3)
        READ 4,(X2(I),I=1,10)
4       FORMAT(10F7.3)
        DO 8 K=1,4
        PRINT *,P(K)
        DO 7 J=1,7
        DO 6 I=1,10
        F=(X1-X3)/(X3-X2(I))
        CPS6=.48*X2(I)**2-1.23*X2(I)+1.01
        T20=(10.0*X2(I))**3/2.92+72.0
        T600=(10.0*X2(I))**3/2.03+202.0
        CM=3.3905/(T600-T20)
        CB=2.996-T20*CM
        TG=(LOG(P(K))-CB)/CM
        TGC=(TG-32.0)/1.8
        HEX=F*CPS6*B(J)*(TG-T3)
        HEXSI=HEX*0.6461E-3
        H6=750.0*X2(I)**2-822.0*X2(I)+122.5+CPS6*(TG-77.0)
        H7=H6-HEX/F
        T2=TG-(TG-T3)*B(J)
        QA=H1+F*H7-H3*(F+1.0)
        QASI=QA*0.6461E-3
        H5=H3+HEX/(F+1.0)
        COPCNT=9.09*(TG-TO)/(TG+460.0)
        H8=0.43*(TG+TO)/2.0+1017.0
        QG=(H8-H5)+F*(H6-H5)
        QGSI=QG*0.6461E-3
        COP=QE/QG
        COT=QA/QG
        E=COP/COPCNT
        PR=P(K)/750.0
        PRINT 5,X2(I),F,B(J),QASI,QGSI,TGC,HEXSI,COP
5       FORMAT(8F10.3,/)
6       CONTINUE
7       CONTINUE
8       CONTINUE
        STOP
        END
```

APPENDIX B (Chapter 5)

S.No.	1	2	3	4	5	6	7
T_1	88.4	95.5	87.3	94.2	96.4	91.2	87.7°C
T_2	24.2	26.6	26.7	26.7	26.7	26.6	27.1°C
T_3	49.0	47.5	40.6	45.9	45.9	45.7	46.2°C
T_4	39.7	40.6	34.3	40.3	40.2	37.0	36.2°C
T_5	34.9	42.5	42.3	31.2	31.6	34.7	35.9°C
T_6	27.8	35.9	35.5	24.6	24.7	10.5	28.1°C
T_7	33.1	41.9	41.7	30.2	30.9	32.6	33.1°C
T_8	10.5	15.0	13.8	9.5	11.0	15.4	9.5°C
T_9	13.4	15.6	12.9	54.8	65.6	49.8	43.1°C
T_{10}	23.8	28.1	32.9	23.7	24.0	24.5	24.6°C
T_{11}	22.1	28.2	28.4	19.7	19.8	20.6	20.9°C
T_{12}	24.6	36.0	37.5	26.0	26.6	24.9	23.5°C
T_{13}	25.4	32.5	34.2	24.7	25.0	23.5	23.0°C
T_{15}	22.0	28.2	28.3	19.2	19.3	20.1	20.3°C
T_{16}	34.9	42.7	42.4	31.4	32.0	35.1	36.0°C
T_{17}	26.2	34.9	35.7	22.0	22.2	23.5	23.8°C
T_{18}	58.7	46.6	48.5	31.3	31.8	34.7	36.0°C
T_{22}	41.2	46.9	46.8	33.1	33.9	36.0	37.6°C
T_{23}	32.9	41.7	41.5	30.3	31.3	32.7	33.3°C
T_{24}	33.4	42.1	41.8	30.3	31.1	32.6	33.7°C
T_{25}	33.6	42.4	42.4	30.3	31.3	32.9	34.6°C
T_{26}	34.0	42.4	42.1	30.3	31.4	31.1	35.1°C
T_{27}	34.4	42.5	42.1	30.3	31.6	33.8	35.5°C
$m_{W,AB}$	118.5	72.0	56.0	197.8	197.8	197.8	197.8 kg h^{-1}
$m_{W,CO}$	61.7	36.8	30.6	42.3	39.7	38.6	37.7 kg h^{-1}
X_{AB}	0.594	0.614	0.624	0.585	0.586	0.578	0.575
X_{GE}	0.608	0.637	0.643	0.607	0.616	0.591	0.585
P_{AB}	12.5	16.7	14.5	12.0	12.9	12.5	11.8 m bar
P_{CO}	110.0	100.0	67.0	100.0	100.0	100.0	100.0 m bar

TABLE B.1 RAW EXPERIMENTAL PERFORMANCE DATA FOR CLOSED CYCLE ABSORPTION COOLING SYSTEM WITHOUT ECONOMISER HEAT EXCHANGER

S.No.	8	9	10	11	12	13	14
T_1	77.1	72.2	74.5	89.2	85.8	83.1	79.7°C
T_2	25.9	26.0	26.1	25.7	27.5	26.3	26.3°C
T_3	34.6	34.3	35.0	40.8	40.2	40.6	40.8°C
T_4	30.7	29.0	30.3	35.4	34.8	33.3	32.7°C
T_5	33.3	34.7	32.4	31.8	33.2	34.3	35.1°C
T_6	26.5	27.1	25.4	25.2	26.7	27.0	27.2°C
T_7	32.4	33.1	31.8	31.3	32.5	33.0	33.1°C
T_8	10.0	9.0	8.5	10.0	10.0	10.0	9.0°C
T_9	15.2	72.2	71.8	72.8	57.9	60.1	55.3°C
T_{10}	24.3	24.4	24.4	23.1	24.0	24.5	24.5°C
T_{11}	21.2	21.0	21.3	21.0	21.0	21.1	21.2°C
T_{12}	25.4	23.2	24.6	28.1	24.8	24.0	22.7°C
T_{13}	24.8	23.5	24.3	25.3	24.6	24.0	24.0°C
T_{15}	21.0	20.9	20.5	20.6	20.8	20.8	20.8°C
T_{16}	33.4	35.0	32.7	32.1	33.8	34.9	35.7°C
T_{17}	23.9	24.0	23.5	23.3	23.8	24.1	24.3°C
T_{18}	33.4	33.5	31.7	32.1	32.4	34.6	35.1°C
T_{22}	39.8	42.8	41.4	39.6	42.6	43.4	42.1°C
T_{23}	32.2	33.3	29.1	31.6	32.5	33.4	33.3°C
T_{24}	32.1	32.9	28.9	31.6	32.4	33.2	33.4°C
T_{25}	32.2	33.1	29.3	31.7	32.8	33.8	34.2°C
T_{26}	32.5	34.5	29.3	31.9	33.2	34.4	34.8°C
T_{27}	33.3	35.3	29.7	32.1	33.7	34.8	35.3°C
$m_{W'AB}$	197.8	197.8	197.8	197.8	197.8	197.8	197.8 kg h^{-1}
$m_{W'CO}$	52.0	55.3	56.0	42.8	54.0	54.6	56.0 kg h^{-1}
X_{AB}	0.598	0.591	0.592	0.600	0.601	0.598	0.591
X_{GE}	0.617	0.600	0.608	0.637	0.627	0.617	0.598
P_{AB}	12.2	11.5	11.2	12.3	12.2	12.2	11.5 m bar
P_{CO}	55.5	55.0	55.0	75.0	75.0	75.0	75.0 m bar

TABLE B.1 (continued) RAW EXPERIMENTAL PERFORMANCE DATA FOR CLOSED CYCLE-ABSORPTION COOLING SYSTEM WITHOUT ECONOMISER HEAT EXCHANGER

S.No	15	16	17	18	19	20	21
T_1	92.4	81.2	105.3	96.1	91.6	89.2	97.0°C
T_2	24.2	25.7	26.3	26.0	24.3	25.4	24.9°C
T_3	45.9	40.9	47.8	47.8	47.8	47.6	46.1°C
T_4	39.3	33.1	42.5	41.4	39.3	36.9	39.4°C
T_5	28.1	23.8	28.3	30.4	31.7	32.5	31.0°C
T_6	22.2	18.7	22.6	23.5	24.5	24.7	23.9°C
T_7	28.0	23.4	28.4	29.8	30.6	30.5	30.2°C
T_8	9.5	5.5	11.5	10.5	9.5	7.0	10.5°C
T_9	89.1	63.3	12.8	11.3	9.6	7.5	24.4°C
T_{10}	21.9	21.2	23.4	23.2	22.6	22.6	22.5°C
T_{11}	18.8	16.3	18.1	18.4	18.5	18.6	20.0°C
T_{12}	22.8	17.9	24.0	23.8	22.3	21.6	26.1°C
T_{13}	22.2	18.3	24.1	23.1	23.1	21.0	24.9°C
T_{15}	18.4	15.8	17.7	17.9	18.2	18.2	19.5°C
T_{16}	28.4	23.8	28.5	30.5	31.9	33.0	31.1°C
T_{17}	20.7	17.5	20.2	20.9	21.2	21.6	22.4°C
T_{18}	28.2	23.7	28.6	32.6	34.4	33.3	31.1°C
T_{22}	35.1	31.2	36.8	39.1	41.5	41.6	40.0°C
T_{23}	28.1	23.2	28.8	30.0	30.6	30.7	30.5°C
T_{24}	27.9	23.1	28.6	29.8	30.5	30.9	30.4°C
T_{25}	27.9	23.0	28.7	30.0	31.0	31.6	30.6°C
T_{26}	28.1	23.4	28.8	30.3	31.4	32.3	31.0°C
T_{27}	28.8	24.1	29.2	30.7	31.7	32.6	31.3°C
$m_{W'AB}$	197.8	197.8	197.8	197.8	197.8	197.8	197.8kg h^{-1}
$m_{W'CO}$	52.9	60.8	52.0	52.5	52.3	48.7	48.2kg h^{-1}
X_{AB}	0.585	0.577	0.589	0.597	0.599	0.596	0.588
X_{GE}	0.625	0.607	0.667	0.640	0.623	0.612	0.646
P_{AB}	11.9	8.9	13.7	12.5	11.7	9.8	12.6m bar
P_{CO}	100.0	75.0	110.0	110.0	110.0	110.0	100.0m bar

TABLE B.1 (continued) RAW EXPERIMENTAL PERFORMANCE DATA FOR CLOSED CYCLE ABSORPTION COOLING SYSTEM WITHOUT ECONOMISER HEAT EXCHANGER

S.No	22	23	24	25	26	27
T_1	90.7	88.1	103.1	80.1	92.5	91.8°C
T_2	25.4	25.8	25.3	23.9	25.0	25.8°C
T_3	46.0	46.0	47.4	46.5	45.9	46.1°C
T_4	39.2	38.2	37.0	33.9	40.0	39.1°C
T_5	32.1	32.9	40.5	36.6	35.2	33.9°C
T_6	25.6	25.9	33.8	29.9	26.0	25.6°C
T_7	31.2	31.5	39.2	34.3	33.5	32.8°C
T_8	9.5	8.5	13.0	10.8	13.0	13.0°C
T_9	22.1	18.1	13.9	14.1	23.6	45.8°C
T_{10}	23.6	24.0	24.4	24.5	22.5	22.1°C
T_{11}	20.6	20.4	21.8	23.5	19.7	19.5°C
T_{12}	25.7	25.5	24.6	24.6	27.4	25.7°C
T_{13}	24.1	24.2	23.6	24.6	25.2	24.3°C
T_{15}	19.8	19.9	21.6	23.4	19.2	19.0°C
T_{16}	32.6	33.5	40.9	37.0	35.2	34.4°C
T_{17}	22.7	23.0	34.1	28.0	22.7	22.5°C
T_{18}	32.7	33.6	57.8	36.6	34.7	34.0°C
T_{22}	41.1	41.2	52.8	41.5	45.7	44.4°C
T_{23}	31.3	31.6	39.7	34.2	33.8	33.1°C
T_{24}	31.3	31.6	40.0	35.1	33.8	33.2°C
T_{25}	31.7	32.2	40.8	35.8	34.5	33.8°C
T_{26}	32.2	32.8	41.2	36.2	35.6	35.0°C
T_{27}	32.5	33.2	41.7	36.5	36.4	35.8°C
$m_{W'AB}$	197.8	197.8	36.7	119.5	197.8	197.8 kg h^{-1}
$m_{W'CO}$	42.6	40.2	45.0	59.0	32.0	36.7
X_{AB}	0.591	0.592	0.606	0.575	0.597	0.593
X_{GE}	0.627	0.615	0.663	0.579	0.614	0.611
P_{AB}	12.0	11.0	14.6	13.2	14.7	14.7 m bar
P_{CO}	100.0	100.0	110.0	100.0	100.0	100.0 m bar

TABLE B.1 (continued) RAW EXPERIMENTAL PERFORMANCE DATA FOR CLOSED CYCLE ABSORPTION COOLING SYSTEM WITHOUT ECONOMISER HEAT EXCHANGER

S.No	1	2	3	4	5	6	7
T_{AB}	34.9	42.5	42.3	31.2	31.6	34.7	35.9°C
T_{CO}	49.0	47.5	40.6	45.9	45.9	45.7	46.2°C
T_{GE}	88.4	95.5	87.3	94.2	96.4	91.2	87.8°C
T_{EV}	10.5	15.0	12.5	9.5	11.0	10.5	9.5°C
Q_{AB}	485.9	562.5	481.9	644.0	667.0	782.0	805.0W
Q_{CO}	179.4	333.8	323.8	309.9	313.9	193.0	113.7W
Q_{GE}	860.5	843.6	843.6	832.0	814.2	837.9	843.6W
Q_{EV}	175.0	296.9	209.9	269.0	336.0	227.1	189.0W
$(COP)_{ACL}$	0.203	0.352	0.249	0.323	0.413	0.271	0.224
(FR)	41.0	26.5	32.5	26.6	19.5	45.2	58.7

TABLE B.2 EXPERIMENTAL PERFORMANCE DATA OF CLOSED CYCLE ABSORPTION COOLING SYSTEM WITHOUT ECONOMISER HEAT EXCHANGER

S.No.	8	9	10	11	12	13	14
T_{AB}	33.3	34.7	32.4	31.8	33.2	34.3	35.1°C
T_{CO}	34.6	34.3	35.0	40.8	40.2	40.6	40.8°C
T_{GE}	77.1	72.2	74.5	89.2	85.8	83.1	79.7°C
T_{EV}	10.0	9.0	8.5	10.0	10.0	10.0	9.0°C
Q_{AB}	667.0	713.0	690.0	621.0	690.0	759.0	805.0W
Q_{CO}	253.9	141.5	214.9	343.4	238.6	184.1	97.7W
Q_{GE}	771.7	777.5	777.5	761.7	795.6	808.4	817.6W
Q_{EV}	249.0	189.0	197.1	281.6	257.42	234.0	170.0W
$(COP)_{ACL}$	0.323	0.243	0.254	0.370	0.324	0.290	0.208
(FR)	31.0	68.7	57.7	16.2	22.9	32.0	79.9

TABLE B.2 (continued) EXPERIMENTAL PERFORMANCE DATA OF CLOSED CYCLE ABSORPTION COOLING SYSTEM WITHOUT ECONOMISER HEAT EXCHANGER

S.No.	15	16	17	18	19	20	21
T_{AB}	28.1	23.8	28.3	30.4	31.7	32.5	31.0°C
T_{CO}	45.9	40.9	47.8	47.8	47.8	47.6	46.1°C
T_{GE}	92.4	81.2	105.3	96.1	91.6	89.2	97.0°C
T_{EV}	9.5	5.5	11.5	10.5	9.5	7.0	10.5°C
Q_{AB}	529.0	391.0	575.0	690.0	690.0	782.0	667.0W
Q_{CO}	246.1	112.9	356.7	329.7	230.9	169.9	341.9W
Q_{GE}	601.7	422.4	740.2	792.0	801.4	855.6	775.3W
Q_{EV}	249.0	138.13	323.2	271.9	239.0	171.0	282.9W
$(COP)_{ACL}$	0.414	0.327	0.437	0.343	0.298	0.200	0.365
(FR)	15.4	19.31	7.5	14.0	24.5	36.6	10.2

TABLE B.2 (continued) EXPERIMENTAL PERFORMANCE DATA OF CLOSED CYCLE ABSORPTION COOLING SYSTEM WITHOUT ECONOMISER HEAT EXCHANGER

S.No.	22	23	24	25	26	27
T_{AB}	32.1	32.9	40.5	36.6	35.2	33.9°C
T_{CO}	46.0	46.0	47.4	46.5	45.9	46.1°C
T_{GE}	90.7	88.1	103.1	80.1	92.5	91.8°C
T_{EV}	9.5	8.5	13.0	10.8	13.0	13.0°C
Q_{AB}	667.0	713.0	533.4	636.5	805.0	805.0W
Q_{CO}	252.6	238.2	146.5	75.5	286.5	264.6W
Q_{GE}	769.5	845.5	674.0	837.9	916.3	854.5W
Q_{EV}	244.0	195.3	200.0	70.0	340.6	333.6
$(COP)_{ACL}$	0.317	0.231	0.297	0.084	0.372	0.390
(FR)	16.5	25.4	10.8	127.7	35.1	33.7

TABLE B.2 (continued) EXPERIMENTAL PERFORMANCE DATA OF CLOSED CYCLE ABSORPTION COOLING SYSTEM WITHOUT ECONOMISER HEAT EXCHANGER

S.No.	1	2	3	4	5	6	7	8
T_1	83.5	78.4	78.0	90.2	88.0	81.0	86.8	88.6°C
T_2	22.3	20.3	19.7	20.9	21.1	25.9	20.9	22.8°C
T_3	40.9	41.1	41.1	47.4	47.8	47.0	47.9	47.5°C
T_4	31.9	29.7	30.1	35.4	34.8	34.7	36.2	34.4°C
T_5	25.6	29.7	29.1	30.5	31.1	27.8	31.8	24.8°C
T_6	23.0	26.1	25.9	26.1	27.0	26.9	27.8	22.7°C
T_7	26.2	29.4	28.4	31.0	31.7	27.7	32.5	25.1°C
T_8	6.3	7.5	7.0	8.8	8.8	9.0	9.0	6.3°C
T_9	32.8	35.8	27.0	25.8	25.6	25.8	25.6	24.1°C
T_{10}	21.6	23.6	23.5	23.4	23.6	23.8	23.9	22.7°C
T_{11}	20.0	23.5	23.3	23.2	23.7	22.8	24.0	19.9°C
T_{12}	23.5	26.9	26.6	27.1	26.4	25.5	27.9	22.3°C
T_{13}	22.0	25.4	25.1	26.0	25.8	24.5	26.4	21.5°C
T_{14}	25.3	27.5	27.5	28.7	29.4	27.7	30.6	25.3°C
T_{15}	19.9	23.8	23.5	23.2	23.6	22.5	24.1	19.6°C
T_{16}	25.8	29.3	29.1	30.5	31.3	28.1	32.6	25.2°C
T_{17}	22.2	26.0	25.7	26.3	26.9	24.9	27.7	21.8°C
T_{18}	25.8	30.0	29.2	30.8	31.1	27.9	32.1	25.1°C
T_{19}	66.2	61.7	61.8	73.4	69.4	53.6	66.7	71.0°C
T_{20}	34.6	40.6	42.0	44.9	46.1	44.3	49.1	38.5°C
T_{21}	78.5	73.5	74.1	89.4	84.6	73.6	82.5	83.8°C
T_{22}	25.6	29.0	28.5	29.7	30.4	28.0	32.6	24.9°C
T_{23}	26.3	29.8	29.0	31.0	31.5	27.9	32.4	25.4°C
T_{24}	26.3	30.0	29.2	31.7	32.2	27.9	33.1	25.5°C
T_{25}	26.6	30.3	29.8	32.2	32.8	27.9	33.9	25.6°C
T_{26}	26.1	29.5	28.8	30.9	31.5	27.7	32.3	25.3°C
T_{27}	26.2	29.4	28.9	30.8	31.4	27.9	32.3	25.5°C
$M_{W,AB}$	107.5	105.0	105.0	98.0	98.0	106.5	100.5	107.5kg h^{-1}
$M_{W,CO}$	49.5	37.0	53.0	48.5	53.0	51.0	52.5	49.5kg h^{-1}
P_{AB}	12.0	12.5	10.0	11.2	11.2	11.5	11.5	9.5 m bar
P_{CO}	75.0	75.0	75.0	100.0	100.0	100.0	100.0	100.0 m bar

TABLE B.3 RAW EXPERIMENTAL PERFORMANCE DATA FOR CLOSED CYCLE ABSORPTION COOLING SYSTEM WITH ECONOMISER HEAT EXCHANGER

S.No.	9	10	11	12	13	14	15
T_1	95.6	97.1	94.8	95.9	94.5	95.5	94.6°C
T_2	22.5	20.8	21.8	21.8	24.2	28.8	27.8°C
T_3	53.6	53.8	53.6	53.8	47.3	47.4	46.6°C
T_4	39.1	39.1	39.2	37.5	37.5	41.3	42.1°C
T_5	25.0	27.2	30.0	28.5	31.5	34.4	31.4°C
T_6	22.7	24.4	26.1	25.2	26.3	47.5	26.5°C
T_7	25.1	27.4	29.7	28.6	30.6	33.2	31.7°C
T_8	6.3	5.5	5.5	5.5	7.0	8.8	12.5°C
T_9	25.0	28.0	27.4	26.9	23.1	13.8	38.2°C
T_{10}	22.7	22.4	23.3	22.8	23.1	27.3	25.8°C
T_{11}	19.8	22.0	22.9	22.3	21.1	23.1	22.5°C
T_{12}	22.2	25.6	25.6	25.9	26.1	31.3	27.2°C
T_{13}	21.8	24.7	24.8	24.8	25.4	28.4	26.2°C
T_{14}	25.3	26.6	29.4	28.0	64.4	65.7	60.3°C
T_{15}	19.5	21.9	22.7	22.3	21.4	22.5	21.8°C
T_{16}	25.2	27.5	30.3	28.9	31.6	34.1	31.6°C
T_{17}	21.8	24.2	25.8	24.9	25.7	26.4	25.4°C
T_{18}	25.1	27.5	29.9	28.6	40.7	36.9	31.4°C
T_{19}	73.6	76.1	72.2	75.2	61.1	65.2	50.1°C
T_{20}	40.2	42.8	49.0	49.3	41.9	37.5	42.4°C
T_{21}	84.4	92.1	92.0	91.9	58.2	51.5	55.4°C
T_{22}	24.7	26.9	31.5	28.1	39.1	38.7	31.0°C
T_{23}	25.2	27.5	29.7	28.6	30.7	33.3	31.8°C
T_{24}	25.2	27.9	30.0	28.9	30.9	33.3	31.8°C
T_{25}	25.3	28.3	30.6	29.4	31.5	33.4	31.9°C
T_{26}	25.1	27.4	29.7	28.5	30.8	33.3	31.7°C
T_{27}	25.1	27.4	29.9	28.5	31.4	33.8	42.0°C
$M_{W,AB}$	107.5	105.5	102.5	105.0	102.5	115.5	105.5 kg h^{-1}
$M_{W,CO}$	48.0	47.0	47.5	45.0	58.4	36.5	64.0 kg h^{-1}
P_{AB}	9.5	9.1	9.1	9.1	10.0	11.2	14.5 mbar
P_{CO}	110.0	110.0	110.0	110.0	100.0	100.0	100.0 mbar

TABLE B.3 (continued) RAW EXPERIMENTAL PERFORMANCE DATA FOR CLOSED CYCLE ABSORPTION COOLING SYSTEM WITH ECONOMISER HEAT EXCHANGER

S. No	(FR)	X_{GE}	X_{AB}	T_{GE} °C	T_{CO} °C	T_{AB} °C	T_{EV} °C	Q_{GE} W	Q_{EV} W	Q_{AB} W	Q_{CO} W	$(COP)_{ACL}$	$(COP)_{CCL}$	E_{CL}	Q_{EX} W
1	21.6	0.621	0.594	83.50	40.90	25.60	6.30	404.82	210.90	287.50	201.45	0.5209	1.5146	0.3439	151.9
2	40.33	0.605	0.590	78.40	41.10	29.70	7.50	413.40	203.50	268.60	146.27	0.4922	1.1569	0.4254	205.0
3	45.38	0.603	0.590	78.00	41.10	29.10	7.00	440.80	146.70	268.60	203.37	0.3329	1.1439	0.2910	165.9
4	27.36	0.624	0.602	90.20	47.40	30.50	8.80	481.16	252.89	353.25	214.94	0.5255	1.2000	0.4379	233.8
5	30.05	0.620	0.601	88.00	47.80	31.10	8.80	519.0	252.89	376.04	166.39	0.4870	1.1388	0.4276	222.2
6	34.00	0.577	0.561	81.00	47.00	27.80	9.00	367.50	116.25	297.20	160.12	0.3163	1.1150	0.2836	87.9
7	39.73	0.611	0.596	86.80	47.90	31.80	9.00	552.00	252.89	420.08	238.08	0.4580	1.1081	0.4133	254.8
8	27.44	0.611	0.590	88.60	47.50	24.80	6.30	395.25	150.75	275.00	138.14	0.3814	1.1960	0.3188	140.7
9	19.01	0.610	0.580	95.60	53.60	25.00	6.30	420.00	136.00	287.50	133.95	0.3238	1.3238	0.2860	144.6
10	27.15	0.619	0.597	79.10	53.80	27.20	5.50	531.00	142.18	282.15	146.74	0.2677	1.0890	0.2458	86.8
11	34.25	0.617	0.599	94.80	53.60	30.00	5.50	604.80	142.18	369.47	149.13	0.2350	1.0200	0.2300	159.0
12	35.72	0.617	0.600	96.90	53.80	28.50	5.50	555.00	142.18	317.44	188.37	0.2560	1.0530	0.2431	166.9
13	39.80	0.633	0.617	44.50	47.30	31.50	7.00	666.60	185.40	476.00	339.00	0.2780	1.1910	0.2334	160.4
14	43.81	0.631	0.617	95.50	47.40	34.40	8.80	814.00	180.00	523.77	348.02	0.2200	1.2104	0.1817	198.5
15	12.10	0.638	0.589	94.60	46.60	31.40	12.50	710.60	284.80	441.62	349.76	0.4000	1.4394	0.2778	65.4

TABLE B.4 : EXPERIMENTAL PERFORMANCE DATA OF CLOSED CYCLE ABSORPTION COOLING SYSTEM WITH ECONOMISER HEAT EXCHANGER

```
C THIS PROGRAM CALCULATES THE PERFORMANCE OF ABSORPTION SYSTEM
C USING WATER-LITHIUMBROMIDE FOR SIMULTANEOUS COOLING AND HEATING
C NOMENCLATURE IS SIMILAR TO OTHER PROGRAMS
      DIMENSIONX2(10),PC(5),TC(5),TE(11),SIT(5),PE(11),V3(5),B(7),T3(5)
      DIMENSIONIT(18),CNTCC(20),CNTHH(20),CNTOO(20),COPACC(20),PKWW(20),
     CCOPAHH(20),COPAOO(20),TLFT(20),HPECC(20),HPEHH(20),HPEOO(20)
C     DATA IT /20,20H COOLING AND HEATING,6,6H TLIFT,4,4H HPE /
      READ 2,X1,X3,TO
      READ 1,(B(J),J=1,7)
1     FORMAT(7F10.3)
2     FORMAT(3F10.3)
      CPS3=.48*X3**2-1.23*X3+1.01
      READ 4,(SIT(K),K=1,5)
      READ 3,(X2(I),I=1,10)
3     FORMAT(10F7.3)
      READ 4,(PC(K1),K1=1,5)
4     FORMAT(5F10.3)
      READ 4,(TC(K2),K2=1,5)
      READ 5,(TE(L1),L1=1,11)
5     FORMAT(11F7.3)
      READ 4,(T3(L2),L2=1,5)
      READ 5,(PE(L11),L11=1,11)
      READ 6,(V3(L12),L12=1,5)
6     FORMAT(10F10.6)
      DO 11 J=1,1
      DO 10 I=1,1
      PRINT *,B(J),X2(I)
      DO 9 K1=1,5
      K2=K1
      DO 8 L1=1,10
      L11=L1
      L2=1
      L12=1
      IF((K1.EQ.2).AND.(L1.GT.9))GOTO 9
      IF((K1.EQ.3).AND.(L1.GT.9))GOTO 9
      IF((K1.EQ.4).AND.(L1.GT.9))GOTO 9
      IF((K1.EQ.5).AND.(L1.GT.5))GOTO 9
      F=(X1-X3)/(X3-X2(I))
      CPS6=.48*X2(I)**2-1.23*X2(I)+1.01
      TLIFT=TC(K2)-TE(L1)
      H10=TC(K2)-32.0
      H1=0.43*TE(L1)+1062.0
      QE=H1-H10
      QESI=QE*0.6461E-3
      CALL SOHAL(H3,X3,T3(L2))
      HP=(PC(K1)-PE(L11))*V3(L12)*0.18509*(1.333/68.95)*(45.36/2.832)
     1*(F+1.0)
      PKW=HP*0.6461E-3
      XS=X2(I)*100.0
      A=-2.00755+0.16976*XS-(3.133362E-3)*(XS**2)+(1.97668E-5)*(XS**3)
      BS=321.128-19.322*XS+0.374382*(XS**2)-(2.0637E-3)*(XS**3)
      TG=A*TC(K2)+BS
      TGC=(TG-32.0)/1.8
      HEX=F*CPS6*B(J)*(TG-T3(L2))
      HEXSI=HEX*0.6461E-3
      CALL SOHAL(H6,X2(I),TG)
      H7=H6-HEX/F
      T2=TG-(TG-T3(L2))*B(J)
      QA=H1+F*H7-H3*(F+1.0)
      QASI=QA*0.6461E-3
      H5=H3+HEX/(F+1.0)
      TA=(T3(L2)+T2)/2.0
```

```
      COPCNT=((TE(L1)+460.0)/(TC(K2)-TE(L1)))*((TG-TA)/(TG+460.0))
     C*((TC(K2)+460.0)/(TA+460.0))
      CNTH=1+COPCNT
      CNTO=COPCNT+CNTH
      H8=.46*TG-0.03*TC(K2)+1062.0
      QC=H8-H10
      QCSI=QC*0.6461E-3
      QG=(H8-H5)+F*(H6-H5)
      QGSI=QG*0.6461E-3
      COPAC=QE/QG
      COPAH=(QA+QC)/QG
      COPAO=1.0+2.0*COPAC
      HPEC=COPAC/COPCNT
      HPEH=COPAH/CNTH
      HPEO=COPAO/CNTO
      TCC=(TC(K2)-32.0)/1.8
      TEC=(TE(L1)-32.0)/1.8
      T3C=(T3(L2)-32.0)/1.8
      T2C=(T2-32.0)/1.8
      TLIFTC=(TLIFT)/1.8
      PW=PKW*1000.0
      PRINT *,K1,L1
      PRINT 7,TLIFTC,COPCNT,CNTH,CNTO,COPAC,COPAH,COPAO,PW
      PRINT 7,F,HPEC,HPEH,HPEO,PC(K1)/PE(L11),TCC,TEC,PW,TCC,TGC
      PRINT *,QESI,QGSI,QCSI,QASI,HEXSI
7     FORMAT(10F8.3,/)
      TLFT(L1)=TLIFTC
      CNTCC(L1)=COPCNT
      CNTHH(L1)=CNTH
      CNTOO(L1)=CNTO
      COPACC(L1)=COPAC
      COPAHH(L1)=COPAH
      COPAOO(L1)=COPAO
      PKWW(L1)=PKW
      HPECC(I)=HPEC
      HPEHH(I)=HPEH
      HPEOO(I)=HPEO
8     CONTINUE
C     CALL A4
C     CALL FGPLT(TLFT,HPEOO,9,1,3,1,0,IT)
C     CALL FGPLT(TLFT,COPAOO,9,1,7,1,1,IT)
9     CONTINUE
10    CONTINUE
11    CONTINUE
C     CALL DEVFIN
      STOP
      END
```

```
C SUBROUTINE FOR CALCULATION OF SOLUTION ENTHALPY
      SUBROUTINE SOHAL(H,X,T)
      XS=X*100.0
      A=-1015.07+79.5387*XS-2.358016*(XS**2)+0.03031583*(XS**3)
     C-(1.400261E-4)*(XS**4)
      B=4.68108-(3.037766E-1)*XS+(8.44845E-3)*(XS**2)-
     C(1.047721E-4)*(XS**3)+(4.80097E-7)*(XS**4)
      C=-(4.9107E-3)+(3.83184E-4)*XS-(1.078963E-5)*(XS**2)
     C+(1.3152E-7)*(XS**3)-(5.897E-10)*(XS**4)
      H=A+B*T+C*(T**2)
      RETURN
      END
```

S. No.	1	2	3	4	5	6	7	8	9
T_1	107.8	105.8	108.3	108.3	117.9	118.2	117.8	128.1	140.0 °C
T_2	24.5	21.3	22.3	24.3	20.6	22.5	24.3	23.7	24.2 °C
T_3	65.3	65.3	70.4	75.1	75.2	80.2	85.2	85.0	95.0 °C
T_4	44.4	45.7	43.1	46.5	47.9	50.0	53.0	51.4	75.1 °C
T_5	28.4	28.4	28.1	28.5	27.9	28.0	28.2	28.7	29.1 °C
T_6	26.1	26.0	26.3	26.1	25.8	26.2	26.3	26.7	27.0 °C
T_7	29.1	28.9	28.4	28.8	28.3	28.4	29.0	29.2	29.5 °C
T_8	11.2	11.0	12.1	11.2	9.8	12.4	11.2	10.3	10.6 °C
T_9	22.3	12.6	33.4	30.3	28.4	42.6	36.6	26.5	35.5 °C
T_{10}	26.8	25.0	26.4	27.3	25.3	27.0	27.5	27.3	40.6 °C
T_{11}	26.6	25.1	26.3	27.6	26.0	26.3	27.5	27.4	39.8 °C
T_{12}	30.2	28.3	29.0	31.1	29.2	31.0	32.6	32.5	63.8 °C
T_{13}	29.5	27.6	28.6	30.5	28.9	29.4	31.0	31.5	49.6 °C
T_{14}	27.8	27.1	27.3	27.9	26.8	27.4	28.0	27.7	28.6 °C
T_{15}	23.7	23.8	23.7	23.7	23.3	23.9	23.7	24.1	24.2 °C
T_{16}	28.7	28.5	27.9	28.6	27.9	28.1	28.6	28.7	29.3 °C
T_{17}	25.7	25.8	25.6	25.6	25.3	25.7	25.6	25.9	26.2 °C
T_{18}	29.0	28.7	28.3	29.1	27.9	28.2	28.8	28.8	29.3 °C
T_{19}	86.2	80.2	81.2	93.1	92.2	82.8	102.1	104.2	106.8 °C
T_{20}	50.0	45.9	45.1	35.1	34.5	37.6	34.0	34.7	35.2 °C
T_{21}	103.9	99.6	101.0	106.9	109.1	107.7	113.3	119.6	131.2 °C
T_{22}	29.0	28.9	28.6	29.0	28.2	28.3	28.9	28.9	29.4 °C
T_{23}	29.1	28.7	28.6	29.0	28.2	28.3	28.8	29.1	29.6 °C
T_{24}	29.5	29.5	28.9	29.3	28.8	28.7	29.3	29.5	29.9 °C
T_{25}	29.2	29.0	28.6	29.0	28.4	28.4	29.0	29.2	29.7 °C
T_{26}	29.2	29.0	28.5	29.0	28.3	28.2	28.9	29.1	29.6 °C
T_{27}	29.0	28.9	28.5	28.9	28.3	28.1	28.7	29.1	29.5 °C
T_{29}	44.2	43.0	43.5	45.8	47.5	39.3	49.5	52.2	51.6 °C
T_{30}	26.0	25.3	25.7	24.9	27.3	25.3	26.3	26.7	29.2 °C
T_{31}	23.8	23.4	23.9	23.7	23.3	23.7	24.0	23.9	23.7 °C
T_{32}	26.5	25.0	26.0	25.3	25.6	25.1	27.6	26.7	36.7 °C
$M_{W,AB}$	107.5	107.5	111.0	114.0	107.5	109.5	110.0	110.0	108.0 kg h^{-1}
$M_{W,CO}$	31.5	44.0	38.0	32.5	43.0	36.0	32.0	44.5	10.0 kg h^{-1}
P_{AB}	12.0	12.5	12.0	10.0	11.8	10.0	10.0	12.2	12.5 m bar
P_{CO}	220.0	220.0	380.0	400.0	300.0	500.0	580.0	600.0	895.0 m bar

TABLE D.1 RAW EXPERIMENTAL PERFORMANCE DATA OF ABSORPTION SYSTEM FOR SIMULATANEOUS COOLING AND HEATING

S.No.	(FR)	X_{GE}	X_{AB}	T_{GE} ^oC	T_{AB} ^oC	T_{CO} ^oC	T_{EV} ^oC	$(T_{CO}-T_{EV})$ ^oC	Q_{GE} W	Q_{EV} W	Q_{AB} W	Q_{CO} W	Q_{EX} W
1	21.54	0.620	0.593	107.8	28.4	65.30	11.20	54.10	453.60	170.00	250.00	131.86	102.55
2	23.20	0.603	0.578	105.80	28.40	65.30	11.00	54.30	494.40	200.75	250.00	163.72	86.97
3	25.82	0.590	0.568	108.30	28.10	70.40	12.10	58.30	467.50	170.00	245.23	119.30	106.04
4	24.18	0.617	0.593	108.3	28.5	75.10	11.20	63.90	467.00	170.00	251.86	170.60	109.05
5	21.22	0.600	0.573	117.90	27.90	75.20	9.80	65.40	541.12	175.00	250.00	160.00	140.00
6	37.53	0.578	0.563	118.20	28.00	80.20	12.40	67.80	522.00	170.00	229.18	196.74	208.84
7	21.03	0.617	0.584	117.8	28.2	85.20	11.20	74.00	555.00	170.00	243.02	189.76	140.24
8	26.63	0.608	0.586	128.10	28.70	85.00	10.30	74.70	655.00	197.10	230.23	263.89	181.11
9	18.00	0.608	0.576	140.00	29.10	95.00	10.60	84.40	752.50	197.10	288.83	279.00	187.27

TABLE D.2 EXPERIMENTAL PERFORMANCE DATA OF ABSORPTION SYSTEM FOR SIMULTANEOUS COOLING AND HEATING

S.No	(FR)	X_{GE}	X_{AB}	$(COP)_{AC}$	$(COP)_{CC}$	E_{CL}	$(COP)_{AH}$	$(COP)_{CH}$	E_H	$(COP)_{AOV}$	$(COP)_{COV}$
1	21.54	0.620	0.593	0.3747	1.2290	0.2048	1.0670	2.2290	0.4786	1.4417	3.458
2	23.20	0.603	0.578	0.406	1.1987	0.3387	1.0120	2.1987	0.4600	1.4180	3.3974
3	25.82	0.590	0.568	0.3636	1.1724	0.3101	1.0060	2.1724	0.4630	1.3639	3.3448
4	24.18	0.617	0.593	0.3636	1.0737	0.3386	1.1369	2.0737	0.5482	1.4936	3.1474
5	21.22	0.600	0.573	0.3234	1.1676	0.2769	1.0166	2.1676	0.4686	1.3390	3.3352
6	37.53	0.578	0.563	0.3256	1.1388	0.2859	1.0240	2.1388	0.4787	1.3496	3.2776
7	21.03	0.617	0.589	0.3060	1.040	0.2942	1.0140	2.0400	0.4970	1.3200	3.0800
8	26.63	0.608	0.586	0.3009	1.1035	0.2726	1.0300	2.1035	0.4896	1.3309	3.2070
9	18.00	0.608	0.576	0.2619	1.0960	0.2388	1.0030	2.0960	0.4785	1.2649	3.1920

TABLE D.2 (continued) EXPERIMENTAL PERFORMANCE DATA OF ABSORPTION SYSTEM FOR SIMULTANEOUS COOLING AND HEATING

APPENDIX E (Chapter 8)

S.NO.	T 1	T 2	T 3	T 4	T 5	T 6	T 7	T 8	T 9	T 10	T 11	T 12	T 13	T 14
1	34.3	30.4	33.7	37.6	37.5	37.7	36.5	34.6	36.3	29.9	25.9	23.2	37.5	36.1
2	33.1	29.6	32.5	36.1	36.0	36.3	35.7	33.9	35.3	28.8	25.8	23.2	36.3	35.1
3	32.6	29.1	32.0	35.4	35.4	35.5	35.4	33.7	35.1	28.3	25.8	23.3	35.8	34.7
4	32.0	28.6	31.5	34.7	34.6	34.9	34.8	33.3	34.6	27.8	25.7	23.2	35.1	34.1
5	31.7	28.2	31.2	34.5	34.4	34.6	34.5	33.2	34.3	27.5	25.5	23.3	34.8	33.8
6	34.8	32.2	34.1	37.5	37.6	37.8	36.4	34.4	36.3	30.8	28.6	24.1	38.0	35.9
7	34.2	31.3	33.5	36.5	36.6	36.7	36.0	34.0	35.9	30.2	28.1	24.0	37.2	35.4
8	33.1	30.3	32.6	35.4	35.3	35.5	35.3	33.5	35.0	29.3	27.9	23.9	36.1	34.5
9	32.4	29.5	31.8	34.4	34.4	34.6	34.6	33.1	34.5	28.7	27.9	24.0	35.3	33.9
10	31.4	28.5	30.8	33.3	33.2	33.4	33.7	32.5	33.6	27.7	27.7	23.8	34.1	32.9
11	31.1	28.0	30.4	32.7	32.6	32.8	33.3	32.1	33.2	27.2	27.6	23.9	33.5	32.4
12	30.3	27.4	29.7	32.2	32.2	32.4	32.7	31.7	32.6	26.6	27.4	23.7	32.8	31.9
13	30.1	27.1	29.5	31.3	31.4	31.5	32.6	31.5	32.4	26.3	27.2	23.7	32.5	31.6
14	29.7	26.8	29.2	31.1	31.2	31.4	31.7	31.2	31.6	26.0	27.1	23.6	32.1	31.3
15	35.2	33.4	34.6	39.5	39.5	39.7	35.4	32.8	35.2	31.5	24.3	22.5	37.9	35.4
16	34.8	32.9	34.2	39.1	39.2	39.4	35.4	32.9	35.3	31.1	24.5	22.8	37.5	35.4
17	34.3	32.1	33.7	38.8	38.7	38.9	35.2	32.8	35.0	30.7	24.8	23.0	37.1	35.3
18	33.7	31.4	33.1	38.1	37.9	38.1	34.8	32.6	34.6	34.5	24.8	23.0	36.3	34.8
19	33.6	31.1	32.8	38.0	37.8	38.1	34.9	32.8	34.6	32.5	25.3	23.9	36.0	34.8
20	33.4	31.0	32.9	37.7	37.4	37.8	34.9	33.0	34.6	30.9	25.8	24.5	35.6	34.9

TABLE E1 EXPERIMENTAL PERFORMANCE DATA OF GENERATOR
(WET GENERATOR, SURFACE TEMPERATURE, °C)

S.NO.	T 1	T 2	T 3	T 4	T 5	T 6	T 7	T 8	T 9	T 10	T 11	T 12	T 13	T 14
21	32.5	30.3	32.1	36.6	36.6	36.7	34.2	32.9	34.1	30.1	26.4	24.8	34.7	34.2
22	31.7	29.6	31.4	35.5	35.7	35.8	33.7	32.5	33.6	30.0	26.8	25.0	33.9	33.6
23	31.5	29.2	30.9	35.2	35.1	35.3	33.3	32.4	33.2	29.5	27.2	25.2	33.2	33.2
24	35.7	34.0	35.3	39.4	39.3	39.5	35.7	33.9	35.6	32.7	27.2	25.0	37.9	36.3
25	35.6	33.8	35.1	39.3	39.2	39.4	35.9	33.9	35.7	32.4	27.3	25.3	37.8	36.3
26	35.3	33.3	34.6	39.1	39.0	39.2	35.8	33.9	35.7	31.8	27.5	25.5	37.3	36.2
27	34.9	33.0	34.4	38.9	38.7	39.0	35.8	34.0	35.6	31.5	27.6	25.8	37.0	36.2
28	35.1	33.1	34.6	38.8	38.8	39.0	36.2	34.3	35.9	32.1	28.2	26.5	36.9	36.2
29	35.9	34.8	35.3	37.3	37.1	37.4	35.3	34.8	35.1	31.8	27.2	23.2	38.6	36.1
30	35.6	34.3	35.1	36.6	36.6	36.7	35.0	34.6	34.9	31.7	27.5	23.6	38.4	36.0
31	34.3	32.7	33.7	35.7	35.5	35.7	33.6	33.6	33.4	30.3	27.3	23.9	36.9	34.2
32	33.6	31.8	33.1	34.8	34.7	34.9	33.2	33.1	33.1	29.8	27.6	24.3	36.1	34.1
33	33.2	31.3	32.7	34.0	33.8	33.9	32.8	32.8	32.7	29.2	27.7	24.3	35.5	33.6
34	32.8	31.0	32.3	33.8	33.6	33.8	32.7	32.8	32.5	29.2	27.8	24.6	35.1	33.3
35	32.6	30.7	31.9	33.3	33.2	33.4	32.5	32.5	32.3	28.8	27.9	24.7	34.7	33.0
36	32.3	30.4	31.7	33.0	32.8	33.0	32.0	32.2	32.0	28.5	27.8	24.7	34.3	32.8
37	31.9	30.1	31.3	32.5	32.3	32.4	31.9	31.9	31.8	28.3	27.7	24.5	34.0	32.5
38	31.4	29.6	30.9	32.2	32.2	32.4	31.5	31.6	31.3	27.6	27.7	24.4	33.6	32.0
39	31.1	29.2	30.5	32.0	31.9	32.1	30.9	31.0	30.8	27.3	27.5	24.3	33.1	31.0

TABLE E1(CONTD.)EXPERIMENTAL PERFORMANCE DATA OF GENERATOR
(WET GENERATOR,SUFACE TEMPERATURE, °C)

S.NO.	TU 1 /TU 3	TU 2	TU 4 /TU 6	TU 5	TU 7 /TU 9	TU 8	TU 13	TU 14
1	21.8	21.6	22.0	21.8	22.4	22.0	21.8	21.8
2	21.8	21.6	22.0	21.8	22.2	22.0	21.8	21.8
3	22.1	22.0	22.4	22.2	22.6	22.2	22.2	22.2
4	21.9	21.8	22.0	21.9	22.4	22.2	21.8	22.0
5	22.0	21.8	22.0	21.8	22.3	21.8	21.8	21.8
6	22.6	22.4	22.8	22.6	23.0	22.7	22.6	22.7
7	22.2	22.0	22.4	22.2	22.8	22.3	22.2	22.2
8	22.4	22.2	22.5	22.4	22.9	22.6	22.3	22.4
9	22.6	22.6	22.8	22.6	23.0	22.7	22.6	22.6
10	22.6	22.4	22.8	22.5	23.0	22.6	22.4	22.6
11	22.8	22.6	22.8	22.6	23.0	22.8	22.6	22.6
12	22.6	22.4	22.7	22.6	22.8	22.6	22.4	22.6
13	22.6	22.4	22.7	22.6	22.8	22.6	22.5	22.6
14	22.4	22.4	22.6	22.5	22.8	22.5	22.4	22.5
15	21.2	21.0	21.5	21.3	21.8	21.5	21.2	21.4
16	21.4	21.2	21.6	21.4	22.0	21.6	21.3	21.5
17	21.5	21.4	21.8	21.5	22.0	21.7	21.4	21.6
18	21.6	21.6	21.8	21.7	22.2	21.8	21.6	21.8
19	22.6	22.4	22.8	22.6	23.0	22.8	22.6	22.7
20	23.4	23.2	23.4	23.4	23.7	23.5	23.4	23.5

TABLE E2 EXPERIMENTAL PERFORMANCE DATA OF GENERATOR
(WET GENERATOR,AIR TEMPERATURE, °C)

S.NO.	TU /TU 1 3	TU 2	TU /TU 3 5	TU 4	TU /TU 7 9	TU 8	TU 13	TU 14
21	23.8	23.8	24.0	23.8	24.2	24.0	23.8	24.0
22	24.0	24.0	24.0	24.1	24.4	24.2	24.0	24.1
23	24.4	24.4	24.6	24.4	24.7	24.6	24.4	24.6
24	24.0	23.8	24.2	24.0	24.6	24.2	24.0	24.2
25	24.2	24.0	24.5	24.2	24.6	24.4	24.2	24.3
26	24.4	24.2	24.6	24.4	24.9	24.5	24.4	24.4
27	24.8	24.7	25.0	24.8	25.2	25.0	24.8	24.8
28	25.6	25.5	25.8	25.6	26.1	25.8	25.6	25.7
29	23.3	23.2	24.2	24.2	24.8	24.8	23.8	24.5
30	23.8	23.6	24.2	24.6	24.6	24.8	24.2	24.5
31	23.8	23.4	24.4	24.1	24.4	24.2	23.8	24.1
32	23.8	23.4	24.5	24.0	24.5	24.4	23.8	24.2
33	24.6	23.8	24.6	24.2	24.6	24.4	24.2	24.4
34	24.4	24.0	24.6	24.6	24.8	24.6	24.2	24.6
35	24.8	24.2	25.2	24.6	25.2	24.8	24.4	24.8
36	24.4	24.0	24.8	24.4	24.8	24.6	24.3	24.6
37	24.6	24.0	24.7	24.3	25.0	24.6	24.2	24.5
38	24.4	23.8	24.6	24.1	24.6	24.4	24.0	24.4
39	24.4	23.6	24.2	24.0	24.5	24.2	23.8	24.0

TABLE E2(CONTD.) EXPERIMENTAL PERFORMANCE DATA OF GENERATOR
(WET GENERATOR,AIR TEMPERATURE, °C)

S.NO.	RH 1 /RH 3	RH 2	RH 4 /RH 6	RH 5	RH 7 /RH 9	RH 8	RH 13	RH 14
1	45.8	45.6	45.8	45.6	46.3	45.9	45.4	45.6
2	44.3	44.1	44.4	44.3	44.5	44.4	44.2	44.4
3	44.5	44.4	44.6	44.3	45.0	44.5	44.4	44.4
4	44.7	44.5	45.0	44.7	45.3	45.0	44.5	44.6
5	44.5	44.3	44.6	44.1	45.0	44.5	44.1	44.5
6	40.4	40.4	40.7	40.3	40.7	40.2	40.2	40.4
7	39.8	39.6	39.6	39.2	40.0	39.6	38.4	39.6
8	41.4	41.3	41.6	41.3	42.1	41.7	41.3	41.5
9	42.6	42.4	42.7	42.4	42.6	42.5	42.5	42.5
10	40.5	40.3	40.6	40.3	40.8	40.3	40.3	40.3
11	40.0	39.9	40.0	39.8	40.2	39.8	39.8	39.8
12	39.1	39.0	39.3	39.0	39.4	39.1	39.0	39.1
13	38.8	38.6	38.9	38.7	39.1	38.8	38.7	38.8
14	38.2	38.2	38.3	38.2	38.6	38.3	38.2	38.3
15	39.9	39.7	40.3	39.7	40.7	40.0	39.7	40.0
16	41.5	41.2	41.6	41.1	42.0	41.6	41.1	41.3
17	42.2	41.7	42.3	41.8	42.5	41.9	41.7	41.8
18	40.0	39.5	40.2	39.6	40.4	39.7	39.5	39.7
19	40.1	39.8	40.1	39.8	40.3	39.8	39.8	39.8
20	39.2	39.1	39.3	39.1	39.7	39.2	39.1	39.1

TABLE E3 EXPERIMENTAL PERFORMANCE DATA OF GENERATOR
(WET GENERATOR,RELATIVE HUMIDITY,PER CENT)

S.NO.	RH 1	/RH 3	RH 2	RH 4	/RH 6	RH 5	RH 7	/RH 9	RH 8	RH 13	RH 14
21	38.4		38.3	38.8		38.3	38.9		38.4	38.3	38.4
22	38.1		38.1	38.3		38.1	38.3		38.2	38.1	38.1
23	37.7		37.5	37.7		37.5	37.8		37.5	37.5	37.5
24	40.2		40.8	40.4		40.9	41.7		41.0	40.8	40.9
25	41.3		40.9	41.5		41.0	41.8		41.1	40.9	41.1
26	41.1		40.8	41.3		40.8	41.5		41.0	40.8	40.9
27	42.6		42.4	42.8		42.4	43.0		42.5	42.4	42.5
28	44.5		44.3	44.7		44.3	44.7		44.3	44.3	44.3
29	34.7		34.7	34.8		34.7	34.9		35.0	34.6	34.8
30	35.6		35.6	35.5		35.5	35.6		35.7	35.6	35.7
31	35.4		35.4	35.5		35.4	35.4		35.4	35.4	35.5
32	34.7		34.7	34.8		34.7	34.9		34.7	34.7	34.7
33	35.8		35.7	35.7		35.7	35.8		35.7	35.7	35.7
34	36.9		36.7	36.8		36.7	36.9		36.7	36.7	36.7
35	37.5		37.3	37.4		37.3	37.5		37.3	37.3	37.3
36	37.4		37.3	37.4		37.4	37.6		37.4	37.3	37.5
37	37.0		36.9	37.0		36.9	37.1		37.0	36.9	36.9
38	32.7		32.6	32.6		32.5	32.7		32.6	32.6	32.5
39	30.3		30.3	30.3		30.2	30.3		30.2	30.3	30.2

TABLE E3(CONTD.) EXPERIMENTAL PERFORMANCE DATA OF GENERATOR
(WET GENERATOR,RELATIVE HUMIDITY,PER CENT)

S.NO.	v	q	m S	X I	X F	RH AM	T AM	P AM
	$m\ s^{-1}$	$kW\ m^{-2}$	$kg\ h^{-1}\ m^{-2}$	%	%	%	°C	mbar
1	2.67	0.9244	12.64	31.50	32.99	46.40	21.40	1017.25
2	3.00	0.9244	12.64	31.50	33.17	44.60	21.40	1017.25
3	3.30	0.9244	12.64	31.50	33.47	45.40	21.60	1017.25
4	3.53	0.9244	12.64	31.50	33.39	45.60	21.60	1017.25
5	3.80	0.9244	12.64	31.50	33.26	45.30	21.40	1017.25
6	1.44	0.7360	12.67	31.45	32.79	40.40	21.40	1017.25
7	1.85	0.7360	12.67	31.45	32.93	40.40	21.40	1017.25
8	2.31	0.7360	12.67	31.45	32.76	42.40	21.80	1017.25
9	2.67	0.7360	12.67	31.45	32.76	43.00	22.00	1017.25
10	3.00	0.7360	12.67	31.45	32.87	41.30	21.80	1017.25
11	3.30	0.7360	12.67	31.45	32.89	40.10	22.20	1017.25
12	3.53	0.7360	12.67	31.45	32.86	39.50	22.00	1017.25
13	3.80	0.7360	12.67	31.45	32.94	39.00	22.00	1017.25
14	4.06	0.7360	12.67	31.45	32.94	38.50	22.00	1017.25
15	0.70	0.5922	11.86	32.92	33.81	40.60	20.60	1026.58
16	0.80	0.5922	11.86	32.92	33.91	42.00	20.90	1026.58
17	0.96	0.5922	11.86	32.92	34.05	40.50	21.00	1026.58
18	1.15	0.5922	11.86	32.92	34.09	40.20	21.20	1026.58
19	1.44	0.5922	11.86	32.92	34.00	40.60	22.00	1026.58
20	1.85	0.5922	11.86	32.92	34.05	39.50	22.80	1026.58

TABLE E4 EXPERIMENTAL PERFORMANCE DATA OF GENERATOR
(WET GENERATOR)

S.NO.	v	q	m S	X I	X F	RH AM	T AM	P AM
	m s^{-1}	kW m^{-2}	kg h^{-1} m^{-2}	%	%	%	°C	mbar
21	2.31	0.5922	11.86	32.92	34.17	38.20	23.20	1026.58
22	2.67	0.5922	11.86	32.92	34.08	38.10	23.40	1026.58
23	3.00	0.5922	11.86	32.92	34.13	37.80	23.90	1026.58
24	0.70	0.5067	11.54	33.50	34.28	41.20	23.40	1025.92
25	0.80	0.5067	11.54	33.50	34.34	41.30	23.40	1025.92
26	0.96	0.5067	11.54	33.50	34.38	41.10	23.60	1025.92
27	1.15	0.5067	11.54	33.50	34.39	42.80	24.00	1025.92
28	1.44	0.5067	11.54	33.50	34.30	44.40	25.00	1025.92
29	1.44	0.7150	11.70	32.02	33.68	34.60	23.20	1024.58
30	1.85	0.7150	11.70	32.02	33.72	35.30	23.60	1024.58
31	2.31	0.7150	15.62	32.02	33.02	35.50	23.20	1024.58
32	2.67	0.7150	12.36	32.02	33.70	35.00	23.20	1024.58
33	3.00	0.7150	12.36	32.02	33.59	36.40	23.00	1024.58
34	3.30	0.7150	12.36	32.02	33.75	37.20	23.80	1024.58
35	3.53	0.7150	12.36	32.02	33.53	37.60	23.50	1024.58
36	3.80	0.7150	12.36	32.02	33.42	37.80	23.80	1024.58
37	4.06	0.7150	12.36	32.02	33.51	36.10	23.20	1024.58
38	4.06	0.7150	13.99	32.02	33.38	33.00	23.60	1024.58
39	4.06	0.7150	15.62	32.02	33.26	30.40	23.40	1024.58

TABLE E4(CONTD.) EXPERIMENTAL PERFORMANCE DATA OF GENERATOR
(WET GENERATOR)

S.NO.	T 1	T 2	T 3	T 4	T 5	T 6	T 7	T 8	T 9	T 10	T 11	T 12	T 13	T 14
40	30.1	29.3	29.6	31.9	31.7	31.9	32.5	32.5	32.3	24.7	25.8	25.3	31.8	32.4
41	30.1	29.3	29.5	31.8	31.7	31.9	32.4	32.4	32.3	25.2	26.2	25.7	31.3	32.4
42	30.0	28.9	29.4	31.4	31.3	31.5	32.3	32.2	32.1	25.3	26.1	25.7	31.0	32.1
43	29.2	28.2	28.6	30.9	30.7	30.9	31.7	31.5	31.5	25.0	25.5	25.4	30.3	31.4
44	29.3	28.2	28.7	30.6	30.5	30.7	31.6	31.4	31.4	25.2	25.8	25.6	30.2	31.3
45	28.7	27.8	28.4	30.1	30.0	30.2	31.2	31.0	31.0	25.2	25.7	25.5	29.7	30.9
46	28.4	27.5	28.2	29.9	29.7	29.9	30.7	30.7	30.6	25.3	25.7	25.5	29.4	30.4
47	28.3	27.3	27.9	29.4	29.3	29.5	30.5	30.3	30.4	25.4	25.7	25.4	29.0	30.0
48	27.7	26.8	27.6	28.8	28.6	28.8	29.9	29.7	29.8	25.3	25.5	25.3	28.4	29.4
49	27.3	26.5	27.1	28.4	28.2	28.4	29.3	29.2	29.2	25.0	25.2	25.1	28.0	28.9
50	27.1	26.3	26.9	28.1	27.9	28.0	29.0	29.0	28.9	25.0	25.1	25.1	27.5	28.7
51	26.8	26.0	26.7	27.6	27.5	27.6	28.5	28.5	28.5	24.8	24.9	24.9	27.2	28.3
52	26.4	25.8	26.3	27.5	27.3	27.5	28.4	28.2	28.3	24.5	24.7	24.8	27.0	28.0

TABLE E5 EXPERIMENTAL PERFORMANCE DATA OF GENERATOR
(DRY GENERATOR,SURFACE TEMPERATURE, °C)

S.NO.	v	q	RH AM	T AM	RH	TU	P AM
	m s^{-1}	kW m^{-2}	%	°C	%	°C	mbar
40	0.70	0.1133	42.90	23.80	43.50	24.80	1013.25
41	0.80	0.1133	43.90	24.20	43.60	25.10	1013.25
42	0.96	0.1133	43.20	24.00	42.70	25.00	1013.25
43	1.15	0.1133	41.30	23.60	41.30	24.70	1013.25
44	1.44	0.1133	41.00	24.20	40.70	25.00	1013.25
45	1.85	0.1133	40.80	24.00	40.90	24.80	1013.25
46	2.31	0.1133	41.10	24.20	41.50	24.80	1013.25
47	2.67	0.1133	41.90	24.40	41.50	24.70	1013.25
48	3.00	0.1133	41.60	24.40	41.10	24.70	1013.25
49	3.30	0.1133	40.00	24.20	40.00	24.50	1013.25
50	3.53	0.1133	39.60	24.20	39.60	24.60	1013.25
51	3.80	0.1133	37.70	24.00	38.10	24.30	1013.25
52	4.06	0.1133	37.20	24.10	36.90	24.20	1013.25

TABLE E6 EXPERIMENTAL PERFORMANCE DATA OF GENERATOR
(DRY GENERATOR)

```
C     THIS PROG EVALUATES THE PERFORMANCE OF SOLAR-GENERATOR
C       (EXPERIMENTS)
      DIMENSIONXI(150),FMSR(150),V(150),XF(150),
     CT2(150),T3(150),T4(150),T5(150),T6(150),T7(150),T8(150),T9(150),
     CTS1(150),T10(150),ZI(150),JRHCDE(150),JHTCDE(150),
     CT11(150),T12(150),T13(150),T14(150),C(150),E(150),PMM(150)
     C,DHJ(100),TU1(70),TU2(70),TU3(70),TU4(70),TU5(70),TU6(70),TU7(70),
     +TU8(70),TU9(70),TU13(70),TU14(70),TAM(70),RH1(70),RH2(70),DHJL(60)
     +,RH3(70),RH4(70),RH5(70),RH6(70),RH7(70),RH8(70),RH9(70),RH13(70),
     +RH14(70),RHAM(70),RH(100),T15(100),TU(100),HHCC(100),GG(100)
     +,CALSHL(60),CALSHR(60)
     +,CALHC(100),STHH(100),STDM(100),CALKP(60),CALNUL(60)
      DIMENSIONIT(16),DJD(150),HJH(150),RERE(150),G(100),
      CWMWM(150),ANUNU(100),SHSH(100),HCKP(100),VV(100),
      CXXI(100),DELPP(100),CALJ(100),HHC(100),CALJD(60)
      C,PPK(100),CALNU(100),CALSH(100),FFI(100),CALNUR(60)
      C,FCONV(60),FCOND(60),FRAD(60),FSEN(60),FEVAP(60)
      C,COP(100)
       DATA IT /17,17H CORLTN FOR MHETR,4,4H   G,3,3H KP /
C       READING THE DATA----------------------------------------
       DO 3 I=1,52
C    JRHCDE IS CODE FOR TYPE OF EXPERIMENTS;0 FOR WET & 5 FOR DRY GENERATOR
C    JHTCDE IS CODE FOR TYPE OF HEATING;1 FOR CSI LAMPS & 0 FOR ELECTRICAL
C    HEATER
       READ *,JRHCDE(I),JHTCDE(I)
       IF(JRHCDE(I).EQ.5)GOTO 2
       IF(JHTCDE(I).EQ.0)GOTO 1
       READ *,XI(I),FMSR(I),V(I),XF(I),TS1(I),T2(I),T3(I),T4(I),T5(I),T6(
      +I),T7(I),T8(I),T9(I),T10(I),T11(I),T12(I),T13(I),T14(I),ZI(I),PMM(
      +I),TU1(I),TU2(I),TU3(I),TU4(I),TU5(I),TU6(I),TU7(I),TU8(I),TU9(I),
     +TU13(I),TU14(I),TAM(I),RH1(I),RH2(I),RH3(I),RH4(I),RH5(I),RH6(I),R
     +H7(I),RH8(I),RH9(I),RH13(I),RH14(I),RHAM(I)
       GOTO 3
1      READ *,XI(I),FMSR(I),V(I),XF(I),TS1(I),T2(I),T3(I),T4(I),T5(I),T6(
     +I),T7(I),T8(I),T9(I),T10(I),T11(I),T12(I),T13(I),T14(I),C(I),E(I),
     +PMM(I),TU1(I),TU2(I),TU3(I),TU4(I),TU5(I),TU6(I),TU7(I),TU8(I),TU9
     +(I),TU13(I),TU14(I),TAM(I),RH1(I),RH2(I),RH3(I),RH4(I),RH5(I),RH6(
     +I),RH7(I),RH8(I),RH9(I),RH13(I),RH14(I),RHAM(I)
       GOTO 3
2      CONTINUE
       READ *,V(I),TS1(I),T2(I),T3(I),T4(I),T5(I),T6(I),T7(I),T8(I),T9(I)
     +,T10(I),T11(I),T12(I),T13(I),T14(I),T15(I),TAM(I),RHAM(I),TU(I),RH
     +(I),C(I),E(I)
3      CONTINUE
       NUM=0
C-----MASS BALANCE----------------------------------------------------
       GA=0.45
C      GA-GENERATOR SURFACE AREA,M2
       J=0
       DO 20 I=1,39
C      PRINT992,I,TS1(I),T2(I),T3(I),T4(I),T5(I),T6(I),T7(I),T8(I)
C     +,T9(I),T10(I),T11(I),T12(I),T13(I),T14(I)
       PRINT 4,I,RH1(I),RH2(I),RH4(I),RH5(I),RH7(I),RH8(I),RH13(I),RH14(I
      +)
4      FORMAT(I2,2X,8F8.1,/)
       IF(JRHCDE(I).EQ.5)GOTO 5
       CALL FMSKG(FMSR(I),XI(I),FMS)
       SM=FMS/GA
       WM=SM*(1-B(XI(I))/B(XF(I)))
       PBAR=PMM(I)*1013.25/760.0
       XAV=(B(XI(I))+B(XF(I)))/2.0
5      CONTINUE
```

```
      CALL MEAN(TS1(I),T2(I),T3(I),TAV1)
      CALL MEAN(T4(I),T5(I),T6(I),TAV2)
      CALL MEAN(T7(I),T8(I),T9(I),TAV3)
      CALL MEAN(TAV1,TAV2,TAV3,TAV)
      IF(JRHCDE(I).EQ.5)GOTO 6
      CALL MEAN(TU1(I),TU2(I),TU3(I),TUAV1)
      CALL MEAN(TU4(I),TU5(I),TU6(I),TUAV2)
      CALL MEAN(TU7(I),TU8(I),TU9(I),TUAV3)
      CALL MEAN(TUAV1,TUAV2,TUAV3,TUAV)
      CALL MEAN(RH1(I),RH2(I),RH3(I),RHAV1)
      CALL MEAN(RH4(I),RH5(I),RH6(I),RHAV2)
      CALL MEAN(RH7(I),RH8(I),RH9(I),RHAV3)
      CALL MEAN(RHAV1,RHAV2,RHAV3,RHAV)
      CALL SPR(PS1,TAV1,B(XF(I)))
      PAM1=RHAV1*PW(TUAV1)*0.01
      DELP1=PS1-PAM1
      CALL SPR(PS2,TAV2,XAV)
      PAM2=RHAV2*PW(TUAV2)*0.01
      DELP2=PS2-PAM2
      CALL SPR(PS3,TAV3,B(XI(I)))
      PAM3=RHAV3*PW(TUAV3)*0.01
      DELP3=PS3-PAM3
      CALL MEAN(PAM1,PAM2,PAM3,PAMAV)
      CALL LMEAN(DELP1,DELP3,DELPAV)
      AMCOEF=WM/DELPAV
C-----ENERGY BALANCE-----------------------------------------------
C-----ENERGY USED IN EVAPORATION-----------------------------------
      TAVEV=(TAV+TUAV)/2.0
      HEVAP=(1049.0-0.57*TAVEV)*6.46E-4
      ENEVAP=WM*HEVAP
C-----SENSIBLE HEATING---------------------------------------------
      CPS=(-3.14*.01*B(XI(I))+3.94)*2.74E-4
      ENSEN=SM*CPS*(TAV-T11(I))
      CALL DENSIT(PAMAV,TUAV,DENAIR)
C-----HEAT LOSSES TO THE ENVIRONMENT-------------------------------
      GOTO 7
C     DUMMY STATEMENTS FOR DRY GENERATOR CALCULATIONS
6     AMCOEF=0.0
      TUAV=TU(I)
      PMM(I)=760.0
      PAMAV=RH(I)*PW(TUAV)*0.01
7     CONTINUE
      CALL HTLOSS(QCOND,QRAD,TAV,T12(I),TAM(I),V(I),SH,STD,SC,AMCOEF,PMM
     +(I),JRHCDE(I),RE,PR,DJ,VISAIR,PAMAV,TUAV)
C-----HEAT USED----------------------------------------------------
      IF(JHTCDE(I).EQ.0)GOTO 8
      FI=ZI(I)
      GOTO 9
8     FI=.001*C(I)*E(I)/GA
9     ABCOEF=0.9
      IF(JRHCDE(I).EQ.5)GOTO 10
      QCONV=FI-QCOND-QRAD-ENEVAP-ENSEN
      DLTAV1=TAV1-TUAV1
      DLTAV2=TAV2-TUAV2
      DLTAV3=TAV3-TUAV3
      CALL MEAN(DLTAV1,DLTAV2,DLTAV3,DLTAV)
      GOTO 11
10    CONTINUE
      QCONV=FI-QCOND-QRAD
      DLTAV=TAV-TUAV
11    CONTINUE
      IF(JHTCDE(I).EQ.1)GOTO 14
```

```
      HC=QCONV/DLTAV
      IF(JRHCDE(I).EQ.5)GOTO 12
      GOTO 13
12    HHCC(I)=HC
      CALL DENSIT(PAMAV,TUAV,DENAIR)
      J=J+1
      GG(I)=V(I)*DENAIR
13    CONTINUE
      GOTO 15
14    HC=0.0092*((V(I)*DENAIR)**0.8)
      HHCC(I)=0.02
      GG(I)=1.0
      QCONV=HC*DLTAV
C     FOR EXPERIMENTS WITH CSI LAMPS
C     FI=QCONV+QCOND+QRAD+ENEVAP+ENSEN
      FI=0.715
15    CONTINUE
      AKAIR=2.63E-5
      AL=0.90
      ACPAIR=2.79E-4
      CALL DENSIT(PAMAV,TUAV,DENAIR)
      ANU=HC*AL/AKAIR
      STH=ANU/(RE*PR)
      STHH(I)=STH
      DH=STH*(PR**0.67)
      RERE(I)=RE
      HJH(I)=DH
      ANUNU(I)=ANU
C     IN KG M-1 H-1
      VISWA=0.032
      VV(I)=V(I)
C     FOR LAMINAR FLOW
        DHJL(I)=0.67*((1.0/RE)**0.5)
C     FOR TURBULANT FLOW
        DHJ(I)=0.032*((1.0/RE)**0.2)
        CALNU(I)=0.037*((RE)**0.8)*((PR)**0.43)
        CALNUL(I)=0.67*((RE)**0.5)*((PR)**0.33)
        CALNUR(I)=0.0645*((RE)**0.8)*(PR**0.33)
        CALSHR(I)=0.058*((RE)**0.8)*(SC**0.33)
        CALSH(I)=0.037*((RE)**0.8)*((SC)**0.43)
        CALSHL(I)=0.67*((RE)**0.5)*((SC)**0.33)
        CALJ(I)=0.0645*((1.0/RE)**0.2)
        CALJD(I)=0.058*((1.0/RE)**0.2)
        HHC(I)=HC
        CALHC(I)=0.0092*((DENAIR*V(I))**0.8)
        CALKP(I)=0.0302*((DENAIR*V(I))**0.8)
        FFI(I)=FI
        NUM=NUM+1
        G(I)=DENAIR*V(I)
        IF(JRHCDE(I).EQ.5)GOTO 16
        WMWM(I)=WM
        DJD(I)=DJ
        SHSH(I)=SH
        XXI(I)=B(XI(I))
        HCKP(I)=HC/AMCOEF
        PPK(I)=AMCOEF
        DELPP(I)=DELPAV
        COP(I)=ENEVAP/FI
        DELT1=T2(I)-TU2(I)
        DELT2=T13(I)-TU13(I)
        DELT3=T5(I)-TU5(I)
        DELT4=T14(I)-TU14(I)
```

```
      DELT5=T8(I)-TU8(I)
      GOTO 17
16    CONTINUE
      DELT1=T2(I)-TU(I)
      DELT2=T13(I)-TU(I)
      DELT3=T5(I)-TU(I)
      DELT4=T14(I)-TU(I)
      DELT5=T8(I)-TU(I)
      DELT6=T15(I)-TU(I)
17    CONTINUE
      F=FI-QCOND
      H1=F/DELT1
      H2=F/DELT2
      H3=F/DELT3
      H4=F/DELT4
      H5=F/DELT5
C     PRINT993,I,V(I),FI,RHAM(I),TAM(I),RH(I),TU(I)
C    +,PMM(I)*1013.25/760.0
C993  FORMAT(I2,2X,F8.2,F8.4,5F8.2,/)
C     PRINT*,B(XI(I)),SM,WM,PAMAV,DELPAV,V(I),T11(I)
C     PRINT*,HC,AMCOEF,HC/AMCOEF,DJ,DH,DENAIR*V(I)
C     PRINT*,RE,SH,ANU,CALNU(I),SC,PR
C     PRINT*,DELT1,DELT2,DELT3,DELT4,DELT5
      IF(JRHCDE(I).EQ.5)GOTO 18
      GOTO 19
18    CONTINUE
C     PRINT*,I,H1,H2,H3,H4,H5,F/DELT6,FI,HHC(I)
19    CONTINUE
C     PRINT*,DELP1,DELP2,DELP3
C     PRINT*,QCONV/FI,QRAD/FI,QCOND/FI,ENEVAP/FI,ENSEN/FI,FI
      FCONV(I)=QCONV/FI
      FCOND(I)=QCOND/FI
      FRAD(I)=QRAD/FI
      FEVAP(I)=ENEVAP/FI
      FSEN(I)=ENSEN/FI
20    CONTINUE
      CALL NARROW
      CALL A4
      CALL FGPLT(G,HHC,40,1,7,4,0,IT)
      CALL FGPLT(G,CALHC,40,20,0,4,1,IT)
C     CALL FGPLT(RERE,CALJ,31,20,0,4,1,IT)
C     CALL FGPLT(RERE,CALJD,31,20,0,4,1,IT)
C     CALL FGPLT(RERE,CALSH,39,20,0,4,1,IT)
      CALL DEVFIN
      STOP
      END
```

```
C  ROTAMETER CALIBRATION
      SUBROUTINE FMSKG(FMSR,XI,FMS)
      B1=9.2656821
      B2=-1.0816326
      B3=2.9389105E-02
      FMS=B1+B2*XI+B3*FMSR
      RETURN
      END

C  REFRECTROMETER CALIBRATIN FOR CONCENTRATION
      FUNCTION B(X)
      B1=4.33868350
      B2=-12.31684167
      B=B1*X+B2
      RETURN
```

```
      END

C  WATER VAPOUR PRESSURE CALCULATION
      FUNCTION PW(T)
      DIMENSION F(15)
      TC=374.136
      TAU=1000.0/(T+273.0)
      F(1)=-741.9242
      F(2)=-29.72100
      F(3)=-11.55286
      F(4)=-0.8685635
      F(5)=0.1094098
      F(6)=0.439993
      F(7)=0.2520658
      F(8)=0.05218684
      AA=TAU*(10.0**(-5))*(TC-T)
      SUM=0.0
      DO 1 J=1,8
      SUM=SUM+F(J)*((0.65-0.01*T)**(J-1))
1     CONTINUE
      PW=220880.*EXP(AA*SUM)
      RETURN
      END

C  SOLUTION VAPOUR PRESSURE CALCULATION
      SUBROUTINE SPR(P,TAV,XAV)
      A=0.87
      B=20.60
      C=-77.0
      PMM=A*TAV+100.0*B/XAV+C
      P=PMM*(1013.25/760.0)
      RETURN
      END

C  HEAT LOSS CALCULATION
      SUBROUTINE HTLOSS(QCOND,QRAD,TAV,T12,TAM
     C,V,SH,STD,SC,AMCOEF,PMM,JRHCDE,RE,PR,DJ,VISAIR,PAMAV,TUAV)
C     IN KWH/(KG C)
      ACPAIR=2.79E-4
C     IN KG/(M HR)
      VISAIR=6.6E-2
      AE=0.95
C     IN M
      AL=0.90
C     IN KW/(SQ M K4)
      Z=56.7E-12
C     IN KG/M3
      CALL DENSIT(PAMAV,TUAV,DENAIR)
C     IN KW/M C
      AKAIR=2.63E-5
      RE=DENAIR*V*3600.0*AL/VISAIR
      PR=ACPAIR*VISAIR/AKAIR
      QRAD=Z*AE*((TAV+273.0)**4.0-(TAM+273.0)**4.0)
CC    IN KW/MK FROM MANU CAT.(LAMELLA MAT)
      HK=4.3E-05
C     IN M
      W=0.05
      CALL COND(T12,TAM,AKAIR,AL,Z,RE,QCOND)
C     IN M2/HR
      IF(JRHCDE.EQ.5)GOTO 1
      DREF=0.22*0.3600
      D=DREF*(273.0+TUAV)/273.0
```

```
      PBAR=PMM*1013.25/760.0
      SH=AMCOEF*AL*(PBAR-PAMAV)/(D*DENAIR)
      SC=VISAIR/(D*DENAIR)
      STD=SH/(RE*SC)
      DJ=STD*(SC**0.67)
      GOTO 2
C   DUMMY STATEMENTS FOR DRY GENERATOR
1     SH=0.0
      SC=0.0
      DJ=0.0
2     CONTINUE
      RETURN
      END
```

```
C   AVERAGE VALUE CALCULATION BY SIMPSON'S RULE
      SUBROUTINE MEAN(P1,P2,P3,PAV)
      PAV=(P1+4.0*P2+P3)/6.0
      RETURN
      END
      SUBROUTINE MEAN1(P1,P2,P3,P4,P5,P6,P7,P8,P9,PAV)
      PAV1=(P1+4.0*P2+P3)/6.0
      PAV2=(P4+4.0*P5+P6)/6.0
      PAV3=(P7+4.0*P8+P9)/6.0
      PAV=(PAV1+4.0*PAV2+PAV3)/6.0
      RETURN
      END

C   AIR DENSITY CALCULATION
      SUBROUTINE DENSIT(PH2O,TG,DENAIR)
      P=PH2O*100.0
      Y=0.622*P/(1.0133E5-P)
      VH=(0.00283+0.00456*Y)*(TG+273.0)
      DENAIR=(1.0+Y)/VH
      RETURN
      END

C   LOG MEAN CALCULATION
      SUBROUTINE LMEAN(DELP1,DELP3,DELPAV)
      DELPAV=(DELP1-DELP3)/LOG(DELP1/DELP3)
      RETURN
      END

C   HEAT LOSS BY CONDUCTION
      SUBROUTINE COND(T12,TAM,AKAIR,AL,Z,RE,QCOND)
CC    KUTETALADGE'S RELATION
      HCAL=0.25*(AKAIR/AL)*0.0249*(RE**0.8)
      QCONV=HCAL*(T12-TAM)
      AE=0.67
      QRAD=Z*AE*((T12+273.0)**4.0-(TAM+273.0)**4.0)
      QCOND=QCONV+QRAD
      RETURN
      END
```

APPENDIX G (Chapter 9)

```
C       THIS IS THE MAIN PROG FOR THE SIMULATION OF THE OPEN
C       CYCLE SOLAR ABSORPTION COOLING SYSTEM
        CALL XFETC(XF,XAV,F)
        PRINT *,'END XFETC'
        STOP
        END
C       THIS SUBROUTINE CALCULATES THE PERFORMANCE OF
C       THE OPEN CYCLE SYSTEM'S GENERATOR UNIT
C       NOMENCLATURE USED IN THE ROUTINE ARE
C       A1,A2,A3,AK1,AK2 ARE DEFINED TO SIMPLIFY THE EQUATIONS
C       A11-A CONSTANT
C       AE -EMMISSIVITY FACTOR FOR HR CALCULATION
C       AKAIR -THERMAL CONDUCTIVITY OF AIR
C       AAL -LENGTH OF THE COLLECTOR-GENERATOR UNIT
C       ALPHA -ABSORBTIVITY COEF. OF THE UNIT
C       AMCOEF -MASS TRANSFER COEF
C       ANU -NUSSULT NO
C       B11 -A CONSTANT
C       B  -COEF OF VOLUM EXPANSION
C       B11 -A CONSTANT
C       C11 -A CONSTANT
C       COP -COEF OF PERFORMANCE
C       CP -HEAT CAPACITY OF THE SOLUTION
C       CPAIR -HEAT CAPACITY OF AIR
C       CPW  -HEAT CAPACITY OF WATER
C       D -DIFFUSIVITY
C       DENAIR -DENSITY OF AIR
C       F -FLOW RATIO
C       G -ACCELERATION DUE TO GRAVITY
C       GO -SOLUTION FLOW RATE
C       GX -SOLUTION FLOW DENSITY
C       GXOPT -OPTIMUM SOLUTION FLOW DENSITY
C       HC -CONVECTIVE HEAT TRANSFER COEF
C       HFG -LATENT HEAT OF VAPORISATION
C       HR -RADIATION HEAT TRANSFER COEF
C       I,J,K,L,M,M1,N,NV HAVE BEEN USED AS SUBSCRIPTS
C       PAV -AVERAGE VAPOUR PRESSURE OF WATER OVER THE SOLUTION
C       PO -VAPOUR PRESSURE OF WATER AT GENERATOR INLET
C       PR -PRENDTLE NO
C       PWA -PARTIAL PRESSURE OF WATER VAPOUR IN AMBIENT AIR
C       RE -REYNOLDS NO
C       SC -SCHMIDT NO
C       SH -SHERWOOD NO
C       SIT -TOTAL SOLAR INSOLATION
C       TDIF -TEMP DIFFERENCE FOR FREE CONV
C       TF -FINAL SOLUTION TEMP
C       TGEAV -AVERAGE SOLUTION TEMP IN THE GENERATOR
C       TI -SOLUTION TEMP AT THE GENERATOR INLET
C       TMF -MEAN TEMP FOR HFG CALCULATION
C       TM -MEAN TEMP FOR HFG CALCULATION
C       TO -AMBIENT TEMP
C       TSKY -EFFECTIVE SUROUNDING TEMP FOR RADIATION HEAT LOSS
C       CALCULATIONS
C       TSOLAV -AVERAGE SOLUTION TEMP
C       UL -OVERALL HEAT TRANSFER COEF
C       VISAIR -VISCOSITY OF AIR
C       W -WIDTH OF THE GENERATOR
C       WM -AMOUNT OF WATER EVAPORATED
C       XAV -AVERAGE SOLUTION CONCENTRATION
C       XF -FINAL SOLUTION CONCENTRATION
C       XI -INITIAL SOLUTION CONCENTRATION
```

```
C       Z -STEFAN BOLTZMAN CONSTANT
C       Z1,Z2 ARE USED TO SIMPLIFY EQUATIONS

        SUBROUTINE XFETC(XF,XAV,F)
        DIMENSION SIT(5),X(4),PWA(4),TO(5),TI(3),GO(7),AAL(10)
        DIMENSION V(4),XAV(1000)
        READ 1,(AAL(II),II=1,6)
1       FORMAT(6F10.3)
        READ 5,(SIT(I),I=1,5)
        READ 3,(X(J),J=1,4)
        READ 3,(PWA(K),K=1,4)
        READ 5,(TO(L),L=1,5)
        READ 2,(GO(M),M=1,7)
2       FORMAT(7F10.3)
        READ 4,(TI(N),N=1,3)
3       FORMAT(4F10.3)
4       FORMAT(3F10.4)
5       FORMAT(5F10.3)
        READ 6,(V(NV),NV=1,4)
6       FORMAT(4F10.3)
        ALPHA=0.95
        Z=56.7E-12
        AKAIR=2.63E-5
        G=1.27E8
        CALL DENSIT(PWA(K),TO(L),DENAIR)
        VISAIR=6.6E-2
        AE=0.95
        CPAIR=2.79E-4
        CPW=1.0*(2.9E-4)/0.25
        M1=0
        DO 20 NV=1,1
        DO 19 N=1,1
        DO 18 J=1,1
        DO 17 K=1,1
        DO 16 L=1,1
        DO 15 I=1,3
        DO 14 M=1,6
        DO 13 II=1,1
        IF(X(J).LE.0.42.AND.X(J).GE.0.30)THEN
        A11=0.87
        B11=20.60
        C11=-77.00
        ELSEIF(X(J).GE.0.41.AND.X(J).LE.0.44)THEN
        A11=2.40
        B11=63.44
        C11=-266.2
        ELSE
        GOTO 7
7       A11=1.73
        B11=38.2
        C11=-162.96
        ENDIF
        PRINT 8,AAL(II),GO(M)/0.9,V(NV),TI(N),X(J),PWA(K),TO(L),SIT(I)
8       FORMAT(8F10.4)
        PO=(A11*TI(N)+B11/X(J)+C11)/750.00
        M1=0
        XF=X(J)+0.005
        PAV=PO*750
9       M1=M1+1
        XAV(M1)=(X(J)+XF)/2.0
        TSOLAV=(PAV-C11-B11/XAV(M1))/A11
        IF(M1.LE.2)GOTO 10
```

```
      IF((XAV(M1)-XAV(M1-1)).LE.0.00001)GOTO 11
10    TM=(TO(L)+TSOLAV)/2.0
      TMF=1.8*TM+32.0
      B=1/(273.0+TM)
      RE=DENAIR*V(NV)*3600.0*AAL(II)/VISAIR
      HFG=(1049.0-0.57 *TMF)*0.000646
      PR=CPAIR*VISAIR/AKAIR
      TDIF=TSOLAV-TO(L)
      ANU=0.0695*(RE**0.794)*(PR**0.333)
      HC=AKAIR*ANU/AAL(II)
      TSKY1=0.0552*((TO(L)+273.0)**1.5)
      HR=Z*AE*((TSOLAV+273.0)**4.0-(TO(L)+273.0)**4.0)/(TSOLAV-TO(L))
      UL=HC+HR
C     AMCOEF UNIT IS KG/HR M2 MBAR
      DREF=0.22*0.3600
      D=DREF*(273.0+TO(L))/273.0
      PMBAR=1013.25
      PMM=760.0
      SC=VISAIR/(D*DENAIR)
      SH=1.876*(RE**0.508)*(SC**0.333)
      AMCOEF=SH*D*DENAIR/((PMM-PWA(K))*AAL(II))
      CP=(-3.14*X(J)+3.94)*2.7E-4
      A1=AMCOEF*B11/X(J)+A11*AMCOEF*HFG/CP+UL/CP
      A2=AMCOEF*UL*B11/(X(J)*CP)
      A3=(AMCOEF/CP)*(A11*(SIT(I)*ALPHA+UL*TO(L))+UL*(B11/X(J)+C11
C-PWA(K)*750.0))
      AK1=(-A1+((A1**2)-(4.0*A2))**0.5)/2.0
      AK2=(-A1-((A1**2)-(4.0*A2))**0.5)/2.0
      Z1=(AK1*A3/A2+AMCOEF*750.0*(PO-PWA(K)))/(AK1-AK2)
      Z2=(AK2*A3/A2+AMCOEF*750.0*(PO-PWA(K)))/(AK1-AK2)
      WM=GO(M)*Z2*EXP(AK1*AAL(II)/GO(M))-GO(M)*Z1*EXP(AK2*AAL(II)/GO(M))
C+GO(M)*A3/A2
      PAV=WM/AMCOEF+PO*750.0
      XF=X(J)*GO(M)/(GO(M)-WM)
      GOTO 9
11    F=XF/(XF-X(J))
C     0.6884KWH/KG IS THE LATENT HEAT OF EVAPORATION OF H2O AT 10C
C     COP HAS BEEN CALCULATED ASSUMING THAT ALL THE WATER EVAPORATED
C     IN THE GENERATOR CAN BE ABSORBED IN THE ABSORBER OF THE OPEN CYCLE
C     ABSORPTION COOLING SYSTEM
      COP=WM*0.6884/(SIT(I)*ALPHA)
      TGEAV=(PAV-C11-B11/XAV(M1))/A11
C     IN KW/MK
      HK=4.3E-05
      W=0.05
C     QCOND=(HK/W)*(TGEAV-TO(L))
      S=SIT(I)*ALPHA-WM*HFG-UL*(TGEAV-TO(L))
      TF=TI(N)+S/(GO(M)*CP)
      DELP=PAV-PWA(K)
      Q=ALPHA*SIT(I)
C     WMOD=0.1099*(DELP**0.566)*(Q**0.903)*(V(NV)**0.071)
      CALL GXOPT(WMOPT,GX,AK1,AK2,Z1,Z2,A2,A3,AAL(II))
      PRINT 12,GX,WM,WMOPT,COP,XF,TF,TGEAV,PAV,PO*750.,F
12    FORMAT(10F10.4)
13    CONTINUE
14    CONTINUE
15    CONTINUE
16    CONTINUE
17    CONTINUE
18    CONTINUE
19    CONTINUE
20    CONTINUE
```

```
      RETURN
      END

C     THIS SUBROUTINE CALCULATES THE OPTIMUM VALUE
C     OF GX i.e.GXOPT WHEN WM IS MAXIMUM BY USING NEWTON RAPHSON METHOD
      SUBROUTINE GXOPT(WMOPT,GX,AK1,AK2,Z1,Z2,A2,A3,AL)
      N=0
      GX=2.0
1     AA1=(1.0-(AK1*AL)/GX)*Z2
      N=N+1
      IF(N.GT.20)GOTO 2
      DAA1=(AK1*AL)*Z2/(GX**2)
      AA2=(1.0-(AK2*AL)/GX)*Z1
      DAA2=(AK2*AL)*Z1/(GX**2)
      BB1=EXP((AK1*AL)/GX)
      DBB1=-((AK1*AL)/(GX**2))*EXP((AK1*AL)/GX)
      BB2=EXP(AK2*AL/GX)
      DBB2=-((AK2*AL)/(GX**2))*EXP(AK2*AL/GX)
      ALHS=AA1*BB1-AA2*BB2+A3/A2
      DALHS=(AA1*DBB1+BB1*DAA1)-(AA2*DBB2+BB2*DAA2)
      GX=GX-ALHS/DALHS
      IF(ALHS.GT.1.0E-20)GOTO 1
2     GOX=GX
      WMOPT=GOX*Z2*BB1-GOX*Z1*BB2+GOX*A3/A2
      RETURN
      END

C  AIR DENSITY CALCULATION
      SUBROUTINE DENSIT(PH2O,TG,DENAIR)
      P=PH2O*100.0
      Y=0.622*P/(1.0133E5-P)
      VH=(0.00283+0.00456*Y)*(TG+273.0)
      DENAIR=(1.0+Y)/VH
      RETURN
      END
```